HYDROGEN CONTAMINATION IN TITANIUM AND TITANIUM ALLOYS

PART IV: THE EFFECT OF HYDROGEN ON THE MECHANICAL PROPERTIES AND CONTROL OF HYDROGEN IN TITANIUM ALLOYS

D. N. WILLIAMS
F. R. SCHWARTZBERG
P. R. WILSON
W. M. ALBRECHT
M. W. MALLETT
R. I. JAFFEE

BATTELLE MEMORIAL INSTITUTE

SEPTEMBER 1957

WRIGHT AIR DEVELOPMENT CENTER
AIR RESEARCH AND DEVELOPMENT COMMAND
UNITED STATES AIR FORCE
WRIGHT-PATTERSON AIR FORCE BASE, OHIO

FOREWORD

This report was prepared by Battelle Memorial Institute under USAF Contract No. AF 33(616)-2813. This contract was initiated under Project No. 7351, "Metallic Materials", Task No. 73510, "Titanium and Titanium Alloys". The project was administered under the direction of the Materials Laboratory, Directorate of Research, Wright Air Development Center, with Lt. Harris M. Burte and Mr. Howard J. Middendorp acting as project engineers.

This report covers the period from December 1954 to March 1957.
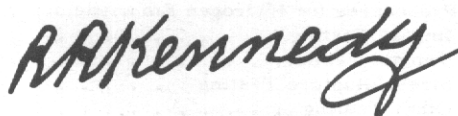
WADC TR 54-616 Pt IV

ABSTRACT

A comprehensive investigation of hydrogen in titanium alloys was carried out. Tests were conducted to gain an insight into the mechanism of the slow-strain embrittlement of titanium alloys by hydrogen, and a tentative theory is presented. Eighty titanium alloys were examined in the stabilized condition to determine the effect of composition on the tendency toward hydrogen embrittlement. The effect of microstructural variations on the tendency toward embrittlement was also studied. In addition to studying the effects of hydrogen on the properties of titanium, factors affecting hydrogen pickup by titanium and methods of removing hydrogen from titanium were investigated. Included were investigations of low pressure solubility, degassing methods, and the pickup of hydrogen from various atmospheres.
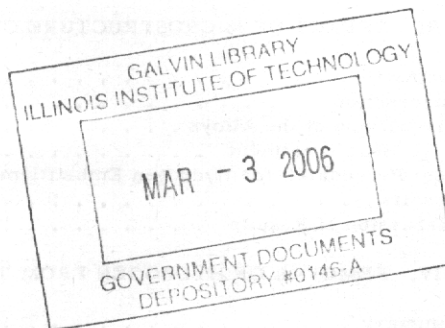
PUBLICATION REVIEW

This report has been reviewed and approved.

FOR THE COMMANDER:

R. R. Kennedy

R. R. KENNEDY
Chief, Metals Branch
Materials Laboratory

TABLE OF CONTENTS

LIST OF ILLUSTRATIONS

LIST OF TABLES

Page

Page

Page

HYDROGEN CONTAMINATION IN TITANIUM AND TITANIUM ALLOYS
Part IV: The Effect of Hydrogen on the Mechanical Properties
and Control of Hydrogen in Titanium Alloys

PHASE I. MECHANISM OF SLOW-STRAIN EMBRITTLEMENT
OF TITANIUM ALLOYS BY HYDROGEN

Summary

A number of investigations were undertaken in an effort to gain a better understanding of the mechanism of slow-strain embrittlement of titanium alloys by hydrogen. A complete picture of this mechanism was not obtained. However, a tentative explanation was possible from these investigations.

Slow-strain embrittlement is believed to be caused by precipitation under strain of titanium hydride at a suitable interface leading to nonductile failure. Thus, slow-strain embrittlement is a form of strain aging. This condition requires that a nonequilibrium condition exist in the alloy, such that precipitation will occur under strain. From tentative equilibrium relationships, either alpha or beta could develop a supersaturated condition leading to embrittlement on straining. It is believed that both phases can contribute to embrittlement when suitably alloyed.

Since precipitation is controlled by the diffusion rate of hydrogen, embrittlement of a supersaturated alloy at a given hydrogen level and strain rate would be expected to decrease as the temperature is lowered. Similarly, changes in the equilibrium solubility of hydrogen in alpha and beta titanium such that the supersaturated condition is removed result in an absence of embrittlement at elevated temperature (about 200 to 300 F in one alloy examined thoroughly). This leads to the development of a minimum in the ductility curve when ductility is plotted versus test temperature. Unfortunately, this minimum occurs quite close to room temperature in most titanium alloys.

Considerable control of the hydrogen level necessary to cause embrittlement can be exercised by alloying and by heat treatment. This control is probably due to changes brought about in hydrogen solubility and mobility, ability to develop a supersaturated condition, and distribution of hydrogen among the phases present in the alloy.

The objective of this phase of the investigation was to obtain a more complete understanding of the mechanism of slow-strain embrittlement of alpha-beta titanium alloys by hydrogen. Embrittlement of alpha-beta alloys is strain-rate sensitive in that the tendency toward embrittlement becomes more severe with decreased strain rate. This immediately suggests a diffusion-controlled process. It is now generally believed that hydrogen diffuses to preferred sites, probably alpha-beta interfaces, under the presence of plastic strain. The hydrogen then precipitates as hydride and embrittlement occurs. Several questions arise concerning this brief description of the mechanism. For example, does the hydrogen precipitate immediately as a hydride, or does it build up slowly during straining, finally precipitating catastrophically to cause failure? Also, does the hydrogen diffuse rather homogeneously to preferred sites throughout the material under stress, or does it diffuse only at localized highly stressed areas?

In this phase of the research program, several investigations were performed in order to answer the above questions and to determine more positively the nature of the mechanism of embrittlement. In several cases, the results obtained were inconclusive. In others, the results tended to disprove one theory but gave no concrete support to a competing theory. For the most part, these limited investigations were preliminary in nature and were intended to give qualitative rather than quantitative information. However, several of the methods of approaching this problem showed promise, and it is hoped that these can be further investigated in future work.

Results

The various investigations carried out during the study of the mechanism of slow-strain embrittlement are described in the following sections. The conclusions which can be drawn from each investigation are also indicated.

Effects of Strain Rate and Test Temperature

Hydrogen embrittlement of alpha-beta titanium alloys has been found to be a function of both strain rate and temperature. Embrittlement becomes more severe at lower strain rates and lower testing temperatures[1]. Some investigations[2,3] have shown a recovery in ductility at low temperatures. A shift in ductility minimum to lower temperature with decreasing testing speed has also been observed[3].

A detailed study of tensile ductility as a function of temperature and strain rate over a range of hydrogen levels was undertaken to gain a more exact understanding of the effects of temperature and strain rate on ductility in a hydrogen-containing titanium alloy. Standard 0.125-inch-diameter specimens of Ti-2Mo-2Fe-2Cr alloy were prepared at three hydrogen levels: vacuum annealed (20 ppm), 250 ppm, and 500 ppm. Hydrogenation at both hydrogen levels and vacuum annealing were carried out after final machining of the tensile specimens using the following thermal cycle: annealing at 1470 F for 1/2 hour; cooling to 1250 F, holding 1 hour; and cooling to room temperature.

Specimens were tested at platen speeds of 0.5, 0.05, and 0.005 inch per minute. Temperatures were obtained using the following liquid media: 300 F, mineral oil; 212 F, boiling water; 32 F, ice and water mixture; 10 F, ice and salt water mixture; -58 to -110 F, dry ice and methanol mixture; and -320 F, liquid nitrogen. Test results are shown in Table 1 and Figures 1, 2, and 3. Vacuum-annealed material tested at temperatures from 212 F to -320 F showed a gradual decrease in ductility with decreasing temperature, as shown in Figure 1. Specimens at the 250 ppm level tested at temperatures in the range of 212 F to -100 F showed progressive embrittlement below room temperature at all three testing speeds, as shown in Figure 2. At -100 F, specimens tested at all three speeds showed about the same degree of embrittlement. Testing at temperatures below -100 F was not carried out. Tensile testing at the 500 ppm level was performed over the temperature range of 300 to -320 F. Results of testing at this level, shown in Figure 3, indicated a ductility minimum at approximately 0 F for all tensile-test speeds (platen speeds of 0.5, 0.05, and 0.005 inch per minute). Tension-impact tests in the temperature range of 70 to -100 F showed no embrittlement.

The data obtained in this program are not complete enough for a full analysis of the effect of temperature and strain rate on the position of the ductility minimum. A more complete study in the temperature range from -100 to 100 F might show the shift in ductility minimum previously reported[3].

The time dependency of slow-strain embrittlement is shown by increased embrittlement at slower testing speeds. The recovery of ductility at faster testing speeds in the low-temperature range indicates that insufficient time is available for diffusion of hydrogen and precipitation of hydride.

The general characteristics of slow-strain embrittlement are shown quite clearly by these studies. These are:

(1) Hydrogen must be present in the alloy.

(2) Embrittlement is strain-rate sensitive. Even a highly susceptible alloy will appear ductile in impact tests,

TABLE 1. EFFECT OF TESTING SPEED AND TEMPERATURE ON TENSILE[a] DUCTILITY OF Ti-2Mo-2Fe-2Cr ALLOY AT TWO HYDROGEN LEVELS

Test Temperature, F	Test Speed Platen Speed, in./min	Test Speed Impact Speed, ft/sec	Ultimate Strength, 1000 psi	Breaking Energy, ft-lb	Elongation, per cent in 4D	Reduction in Area, per cent
			Vacuum Annealed Samples			
212	0.5	--	135.5	--	20.0	63.0
212	0.05	--	132.5	--	21.0	63.0
212	0.005	--	127.5	--	24.0	59.0
70	0.5	--	148.5	--	27.4	57.5
70	0.05	--	147.5	--	19.2	59.5
70	0.005	--	147.1	--	14.8	56.5
0	0.5	--	165.2	--	27.3	52.2
0	0.05	--	163.4	--	16.0	50.3
0	0.005	--	145.9	--	16.0	56.6
-58	0.5	--	175.0	--	--(b)	54.1
-58	0.05	--	173.0	--	--(b)	54.5
-58	0.005	--	169.2	--	--(b)	56.5
-110	0.5	--	186.5	--	13.7	29.2
-110	0.05	--	185.5	--	14.0	49.0
-110	0.005	--	180.3	--	27.3	46.8
-320	0.005	--		--	14.0	29.9
			Samples Containing 250 ppm Hydrogen			
212	0.5	--	137.6	--	24.8	59.0
212	0.05	--	133.4	--	--(b)	59.0
212	0.005	--	126.5	--	35.0	53.4
70	0.5	--	148.1	--	26.0	59.0
70	0.05	--	147.9	--	30.0	59.0

TABLE 1. EFFECT OF TESTING SPEED AND TEMPERATURE ON TENSILE[a] DUCTILITY OF Ti-2Mo-2Fe-2Cr ALLOY AT TWO HYDROGEN LEVELS (Continued)

Test Temperature, F	Test Speed		Ultimate Strength, 1000 psi	Breaking Energy, ft-lb	Elongation, per cent in 4D	Reduction in Area, per cent
	Platen Speed, in./min	Impact Speed, ft/sec				
Samples Containing 250 ppm Hydrogen (Continued)						
70	0.005	--	147.3	--	17.0	59.0
32	0.5	--	158.2	--	18.0	46.9
32	0.05	--	158.6	--	24.0(c)	24.3
32	0.005	--	148.7	--	11.0(b)	12.5
0	0.5	--	163.1	--	21.0	35.0
0	0.05	--	163.8	--	12.0	12.8
0	0.005	--	153.5	--	4.0(b)	8.1
-50	0.5	--	174.6	--	18.0	19.7
-50	0.05	--	174.6	--	11.0(d)	8.1
-50	0.005	--	165.1	--	6.0(b)	8.3
-100	0.5	--	185.1	--	7.0(b)	8.3
-100	0.05	--	187.7	--	5.0(c)	7.2
-100	0.005	--	180.5	--	5.0	8.3
-320	0.05	--	241.4	--	<1.0(e)	<1.0
-320	0.005	--	244.5	--	<1.0(b)	<1.0
Samples Containing 500 ppm Hydrogen						
300	0.5	--	128.1	--	28.0	64.0
300	0.05	--	125.9	--	20.8(b)	64.0
300	0.005	--	121.8	--	28.0	61.2
70	--	12.75	--	17	6.0	53.8
70	0.5	--	154.7	--	22.5	59.1
70	0.05	--	154.2	--	13.7	51.6
70	0.005	--	151.9	--	10.8	12.7

TABLE 1. EFFECT OF TESTING SPEED AND TEMPERATURE ON TENSILE(a) DUCTILITY OF Ti-2Mo-2Fe-2Cr ALLOY AT TWO HYDROGEN LEVELS (Continued)

Test Temperature, F	Test Speed		Ultimate Strength, 1000 psi	Breaking Energy, ft-lb	Elongation, per cent in 4D	Reduction in Area, per cent
	Platen Speed, in./min	Impact Speed, ft/sec				
Samples Containing 500 ppm Hydrogen (Continued)						
32	0.5	--	167.5	--	14.0	50.5
32	0.05	--	163.3	--	14.0	22.5
32	0.005	--	160.9	--	8.0	8.1
25	--	12.75	--	16	<1.0	61.6
10	0.5	--	170.5	--	9.0	8.0
10	0.5	--	169.4	--	8.1	9.2
10	0.05	--	166.8	--	6.0(b)	8.1
10	0.05	--	166.1	--	4.0(c)	8.1
10	0.005	--	161.2	--	4.0(c)	8.1
10	0.005	--	159.5	--	4.6	7.7
-58	0.5	--	189.0	--	--(b)	45.9
-58	0.05	--	182.3	--	14.0	21.3
-58	0.005	--	179.2	--	7.0(b)	9.4
-100	0.5	--	195.2	--	18.8	42.3
-100	0.5	--	195.3	--	13.9(c)	48.2
-100	0.05	--	191.7	--	13.7(c)	42.4
-100	0.05	--	196.5	--	12.1	21.1
-100	0.005	--	190.7	--	8.0	7.8
-100	0.005	--	189.6	--	5.9(b)	9.4
-110	--	12.75	--	17	1.9	48.2
-320	0.5	--	287.2	--	<1.0	6.4
-320	0.05	--	287.2	--	<1.0	<1.0

(a) Standard 0.125-inch-diameter tensile specimens.
(b) Failed outside of gage length.
(c) Failed through punched gage mark.

(d) Failed in two places.
(e) Failed in two places, both outside of gage length.
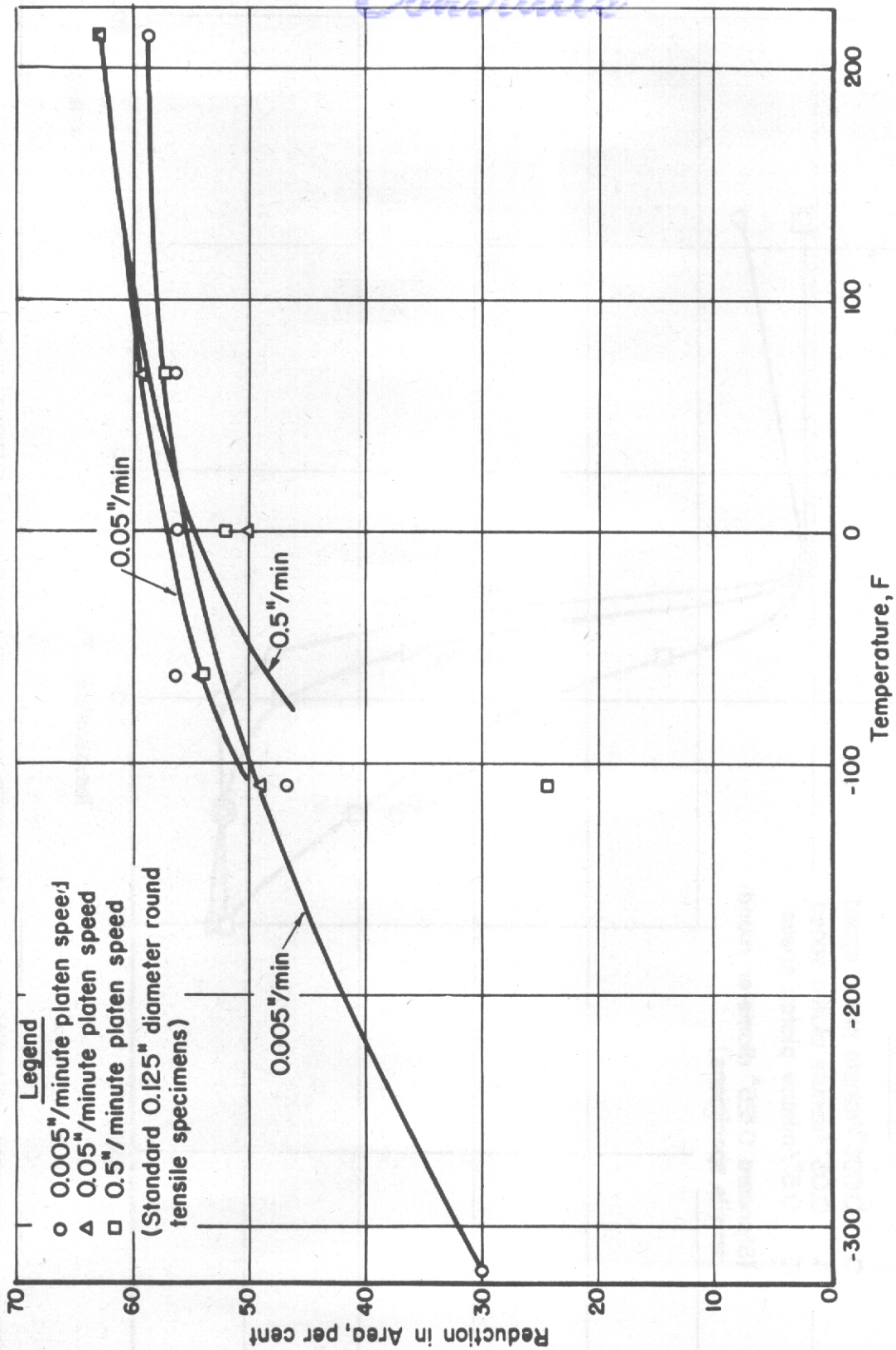
FIGURE 1. EFFECT OF TESTING SPEED AND TEMPERATURE ON TENSILE DUCTILITY OF Ti-2Mo-2Fe-2Cr ALLOY IN THE VACUUM- ANNEALED CONDITION
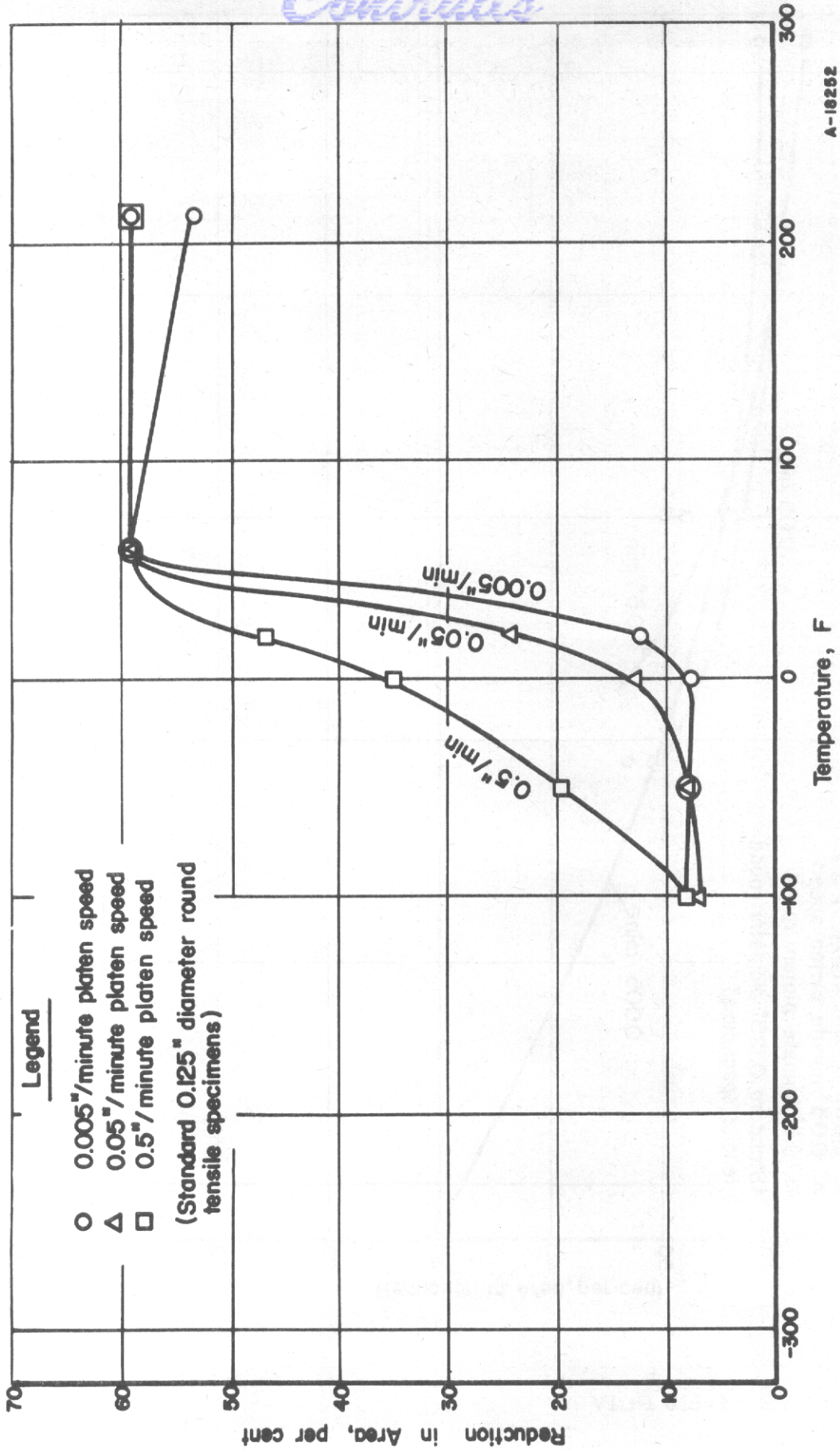
FIGURE 2. EFFECT OF TESTING SPEED AND TEMPERATURE ON TENSILE DUCTILITY OF Ti-2Mo-2Fe-2Cr ALLOY AT THE 250-PPM HYDROGEN LEVEL

A-18252
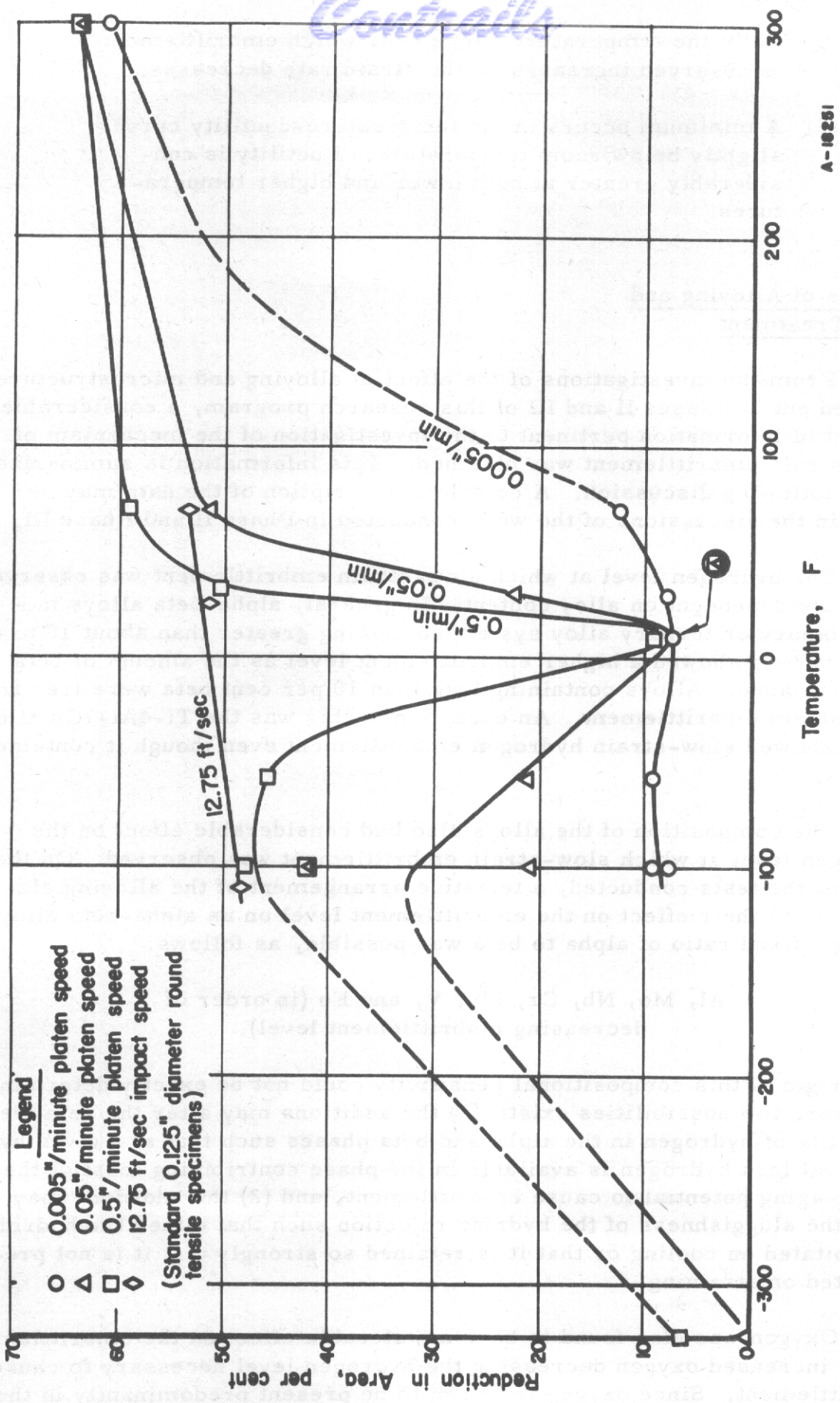
FIGURE 3. EFFECT OF TESTING SPEED AND TEMPERATURE ON TENSILE DUCTILITY OF Ti-2Mo-2Fe-2Cr ALLOY AT THE 500-PPM HYDROGEN LEVEL

A-18251

while the temperature range over which embrittlement
is observed increases as the strain rate decreases.

(3) A minimum occurs in the temperature-ductility curve
slightly below room temperature. Ductility is con-
siderably greater at both lower and higher tempera-
tures.

Effects of Alloying and Heat Treatment

From the investigations of the effect of alloying and microstructure
carried out in Phases II and III of this research program, a considerable
amount of information pertinent to the investigation of the mechanism of
slow-strain embrittlement was obtained. This information is summarized
in the following discussion. A complete description of the data may be
found in the discussions of the work conducted in Phase II and Phase III.

The hydrogen level at which slow-strain embrittlement was observed
was quite dependent on alloy content. In general, alpha-beta alloys in a
given binary or ternary alloy system containing greater than about 10 to 20
per cent beta showed a higher embrittlement level as the amount of beta
was increased. Alloys containing less than 10 per cent beta were free from
slow-strain embrittlement. An exception to this was the Ti-4Al-7Cu alloy,
which showed slow-strain hydrogen embrittlement even though it contained
no beta.

The composition of the alloys also had considerable effect on the
hydrogen level at which slow-strain embrittlement was observed. On the
basis of the tests conducted, a tentative arrangement of the alloying ele-
ments as to their effect on the embrittlement level on an alpha-beta alloy
having a fixed ratio of alpha to beta was possible, as follows:

Al, Mo, Nb, Cr, Mn, V, and Fe (in order of
decreasing embrittlement level).

The origin of this compositional sensitivity could not be exactly determined.
However, two possibilities exist: (1) the additions may alter the relative
solubility of hydrogen in the alpha and beta phases such that at a given hydro-
gen level less hydrogen is available in the phase contributing most of the
strain-aging potential to cause embrittlement, and (2) the additions may
alter the sluggishness of the hydride rejection such that either the hydride is
precipitated on cooling or that it is retained so strongly that it is not pre-
cipitated on straining.

Oxygen was also found to have a noticeable effect on the embrittlement
level, increased oxygen decreasing the hydrogen level necessary to cause
embrittlement. Since oxygen is known to be present predominantly in the

alpha phase in an alpha-beta alloy, the effect of oxygen must be either to alter the hydrogen solubility in alpha at the stabilizing temperature such that a greater amount of hydrogen is present in the beta phase at a given hydrogen level or to alter the tendency for precipitation of hydride from alpha during straining.

The studies of the effect of microstructure on hydrogen level at which slow-strain embrittlement occurred were quite interesting. Strength level appeared to have little effect. The principal observations of this study were that increasing the alpha grain size decreased the hydrogen level necessary for embrittlement and that decreasing the final annealing temperature decreased the embrittlement level.

The effect of alpha grain size is probably directly related to the amount of alpha-beta interfacial area available for nucleation of hydride. A larger grain size would result in a smaller amount of hydrogen being capable of embrittling the interfacial area, since the amount of interfacial area would be smaller. The effect of alpha grain size was most pronounced when increasing the grain size resulted in a change from an alpha to a beta matrix. This suggests that precipitation of hydride from the beta phase contributes to embrittlement.

The effect of final annealing temperature on embrittlement level did not appear to be related only to the relative amounts of alpha and beta present. Presumably, a lower annealing temperature results in a partition of the available hydrogen between the alpha and beta phases which is more favorable to the precipitation of hydride on subsequent straining at room temperature. This would also explain why some hydrogen-containing alloys which showed no slow-strain embrittlement before exposure show embrittlement following thermal exposure in stability testing[4].

Occurrence of Hydride in
Alpha-Beta Alloys

Metallographic examination of a number of the alloys tested during the studies conducted in Phases II and III resulted in the observation of a third phase tentatively identified as hydride.

The appearance of the third phase was noted at hydrogen concentrations as low as 200 ppm in some alloys. In most cases, this phase occurred at the alpha-beta interface. Figure 4 shows an excellent example of the appearance of this phase which occurred at the interface between the acicular alpha needles and the beta. A similar condition was observed for the equiaxed Ti-6Mn alloy at 600 ppm (Figure 5) and the Ti-4Fe alloy at 200 ppm (Figure 6). In all three alloys, slow-strain embrittlement was first observed at the hydrogen level of the specimens shown in the photomicrographs.

500X   N27351

FIGURE 4.   Ti-2Mo-2Fe-2Cr ALLOY CONTAINING 200 PPM HYDROGEN

Solution heat treated and aged.
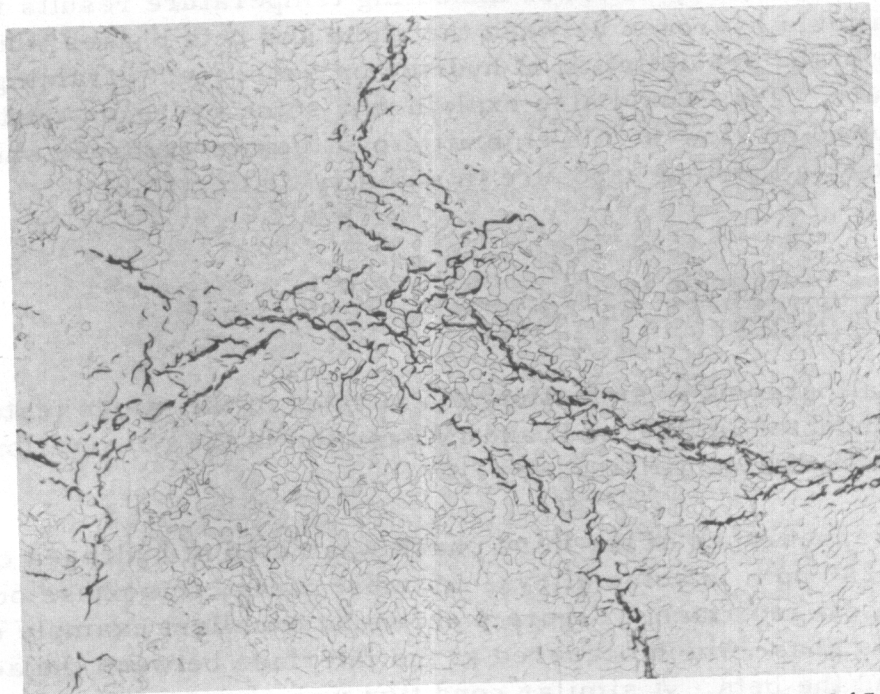
500X   N28655

FIGURE 5.   Ti-6Mn ALLOY CONTAINING 600 PPM HYDROGEN

Stabilized.
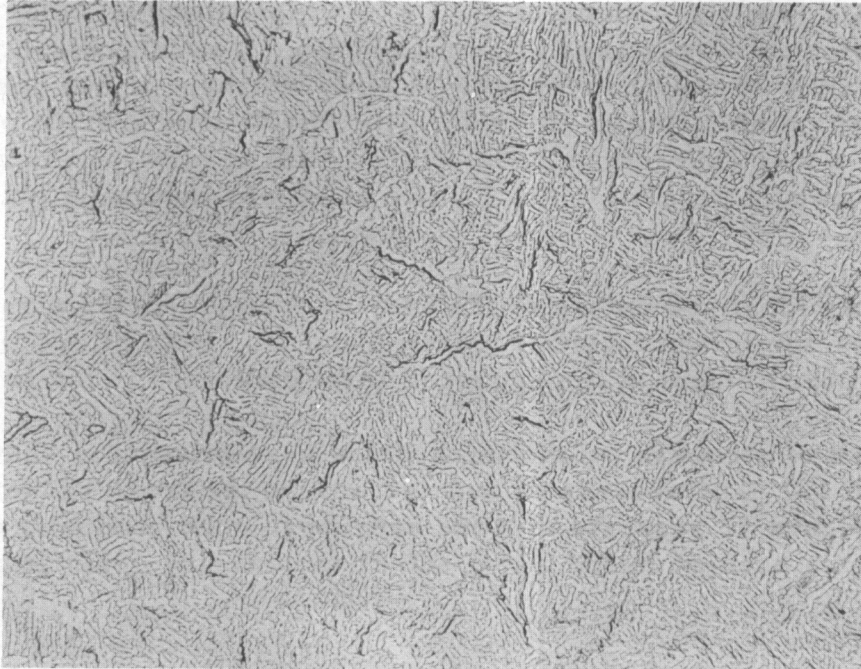
250X   N26155

FIGURE 6.   Ti-4Fe ALLOY CONTAINING 200 PPM HYDROGEN

Stabilized.

The appearance of hydride in a Ti-4Ta alloy containing 200 ppm hydrogen is shown in Figure 7. This alloy was impact embrittled, but showed no slow-strain embrittlement. The Ti-2Fe alloy shown in Figure 8 also was brittle in impact, while free from slow-strain embrittlement. The difference between the two hydride patterns is quite marked. It is interesting to note that a Ti-8Ta alloy showed no slow-strain embrittlement at 800 ppm, while a Ti-4Fe alloy was embrittled at 200 ppm. Apparently, the hydride pattern shown in Figure 8 is characteristic of alloys prone to slow-strain embrittlement, but the amount present in the Ti-2Fe alloy was not sufficient to cause embrittlement.

The highly localized nature of the hydride formed during straining is shown by the photomicrographs in Figures 9 and 10. Both alloys first showed slow-strain embrittlement at the hydrogen level contained in these samples.

The effect of strain in promoting hydride precipitation is shown in Figures 11 and 12. The absence of hydride around the fresh Vicker impressions in Figure 12 suggests that the hydride formed gradually due to residual stresses present in the metal rather than during application of the load.

Although a number of strained alloys were examined during this investigation, resulting in the observation of numerous examples of hydride formation of the type illustrated, no traces of hydride at the fracture of brittle material have yet been observed. This may be due to inadequate metallographic preparation to retain the hydride intact on the fracture surface. It is also possible that the hydride precipitating in front of a moving crack causes failure before a sufficient amount is formed to be visible microscopically.

Tests for Progressive Hydride
Precipitation During Strain

In an attempt to determine whether slow-strain embrittlement was cumulative, a series of tests was performed in which specimens were stressed at constant load to just short of fracture and then broken at high testing speeds. If a sample showed embrittlement in the high-speed test, it could be assumed that the damage occurred during stress-rupture exposure. By testing samples removed after progressively greater strains (short of fracture) it should be possible to determine whether progressive hydride precipitation was occurring during straining. It was hoped by these means to determine whether hydride precipitated continuously during straining, with embrittlement occurring when a sufficient amount was formed, or whether the time-dependent step was diffusion of hydrogen, with embrittlement occurring when the hydrogen concentration was great enough for precipitation to start.

The first series of tests was performed on Ti-2Mo-2Cr-2Fe alloy containing about 400 ppm hydrogen. The samples were exposed in stress
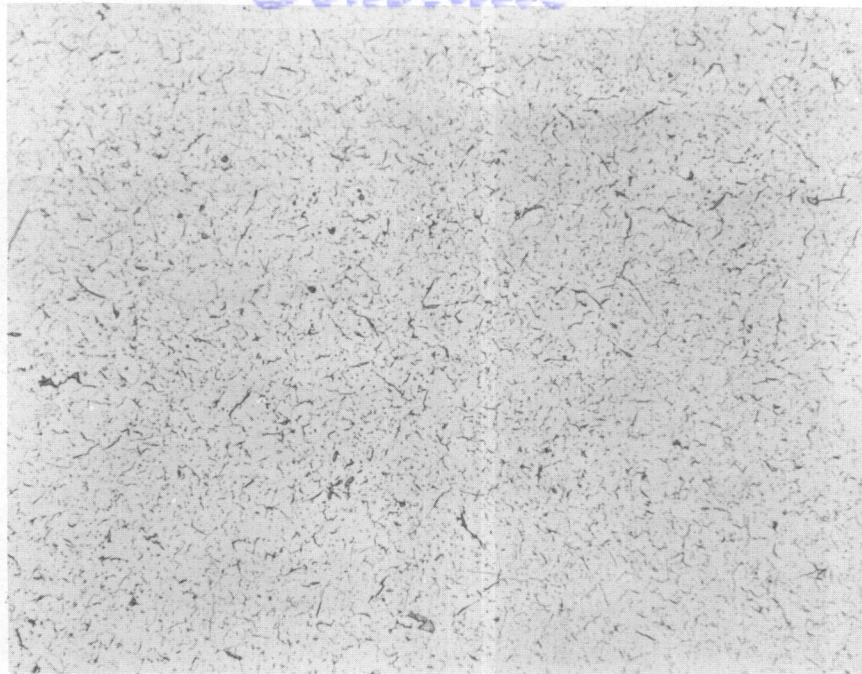
500X   N31439

FIGURE 7.   Ti-4Ta ALLOY CONTAINING 200 PPM HYDROGEN
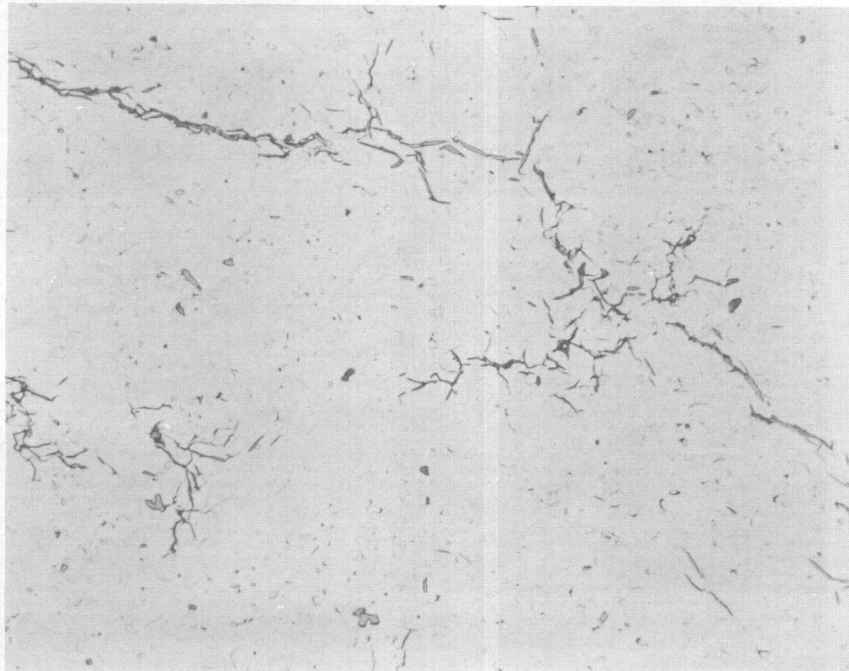
Stabilized.

500X   N31430

FIGURE 8.   Ti-2Fe ALLOY CONTAINING 200 PPM HYDROGEN
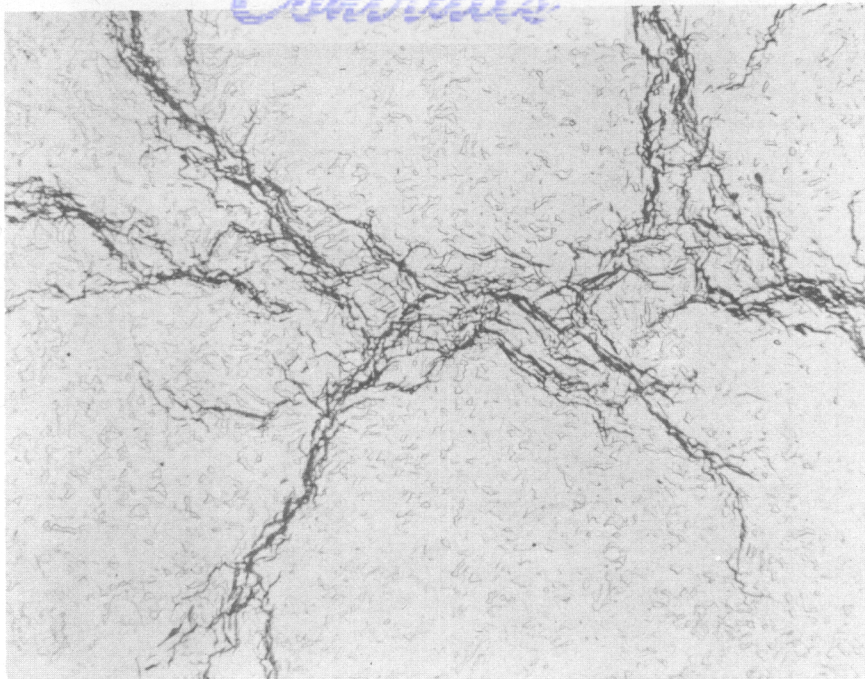
Stabilized.

500X   N31438

FIGURE 9.   Ti-2Mn-2Cr ALLOY CONTAINING 400 PPM HYDROGEN

Stabilized.
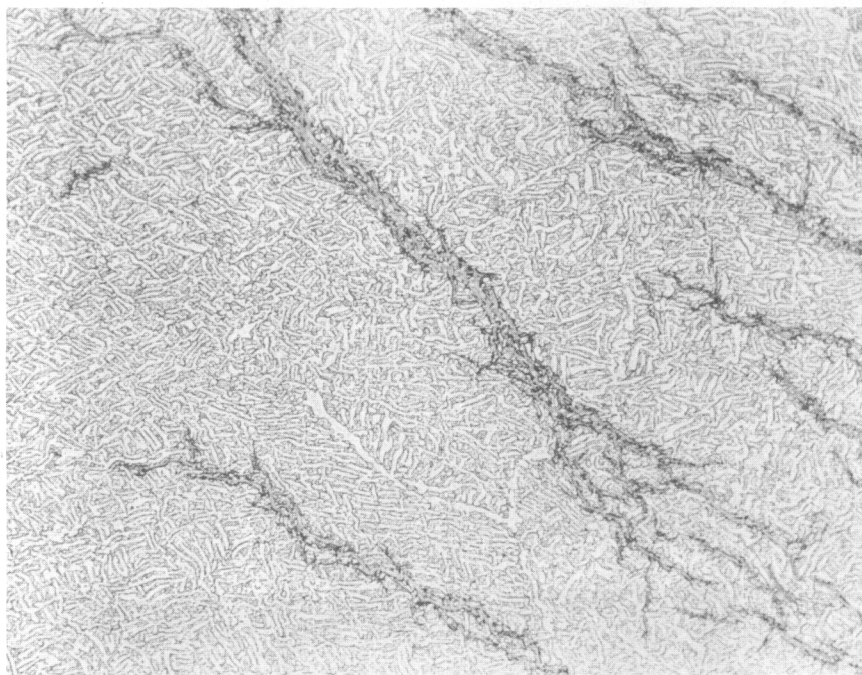
500X   N27349

FIGURE 10.   Ti-2Mo-2Fe-2Cr ALLOY CONTAINING 200 PPM HYDROGEN

Solution heat treated and aged.
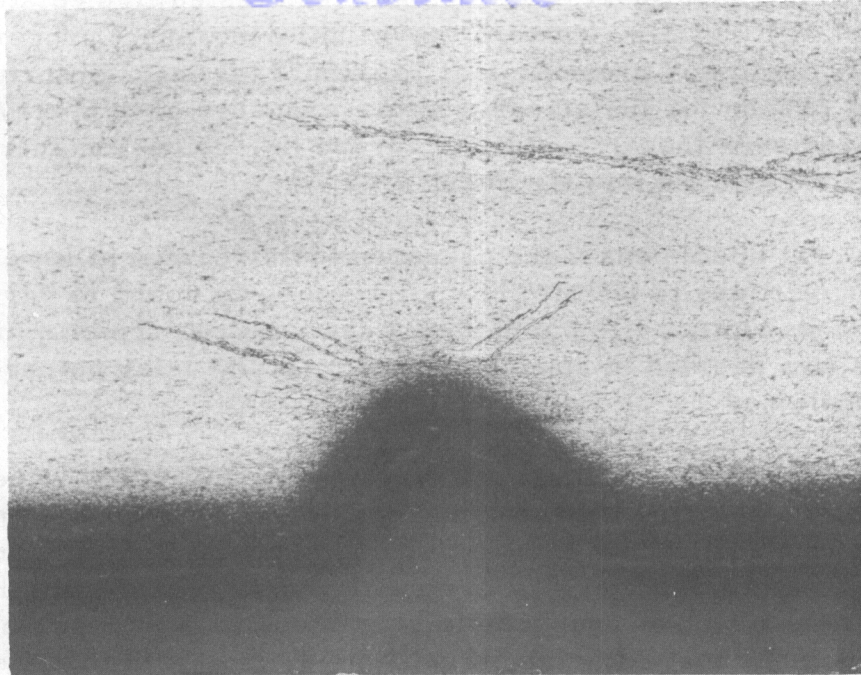
75X   N28249

FIGURE 11. HYDRIDE AROUND A NOTCH IN THE SHOULDER OF AN
UNTESTED Ti-4V ALLOY (HIGH OXYGEN) TENSILE
SPECIMEN CONTAINING 200 PPM HYDROGEN
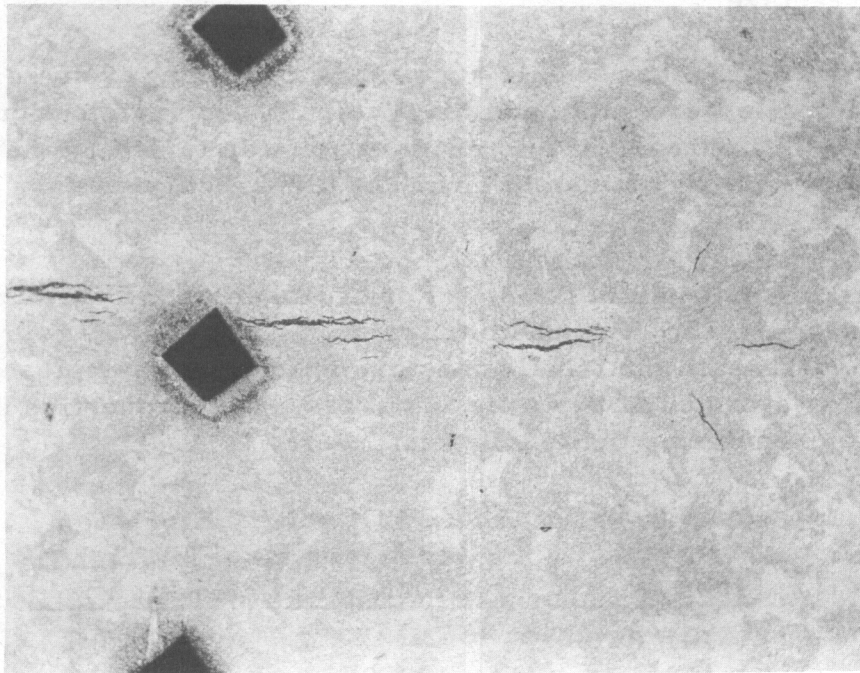
100X   N31442

FIGURE 12.   HYDRIDE AROUND A FORMER VICKERS HARDNESS
IMPRESSION (REMOVED BY POLISHING) IN A
Ti-4Mn ALLOY CONTAINING 200 PPM HYDROGEN

Stabilized.

WADC TR 54-616 Pt IV   17

rupture for times just short of failure and then tested immediately in tensile impact. The test results, Table 2, show uniform impact properties suggesting that no hydride was present prior to impact testing. Unfortunately, the stress level chosen for the stress-rupture exposure gave a very short rupture time, and even though rupture occurred in a brittle manner, an element of doubt was introduced into the results.

Additional specimens were prepared for stressing at lower loads to produce longer times to failure. Rupture time was found to vary so greatly that an average rupture life could not be determined. To eliminate this problem, it was decided to conduct a similar study using notched stress-rupture samples.

Notched rupture specimens of Ti-2Mo-2Fe-2Cr alloy were prepared in the vacuum-annealed and hydrogenated (250 ppm) conditions. Specimens were strung in series and held at constant stress until the first specimen failed. Failure of the other specimens was considered imminent, and these specimens were then tested as fast tensile specimens (0.5 inch per minute). Examination of the test data, given in Table 3, indicated that the hydrogen level selected was too low to cause embrittlement, since the stress-rupture specimen failed in a ductile manner. Due to a lack of time, this test was not rerun. Future work utilizing this technique should prove informative.

Microstructural Path
of Brittle Fracture

A number of broken tensile specimens remaining from earlier investigations at Battelle were sectioned longitudinally for examination of the fracture region. The purpose of this examination was to determine whether fracture occurred predominantly along the alpha-beta interface in hydrogen-embrittled material.

A striking example of the effect of hydrogen on the fracture mechanism is shown in Figure 13. Two photomicrographs are shown, representing the structure just beneath the tensile fracture of identical samples of Ti-2Mo-2Cr-2Fe alloy strained at two different rates. The properties of the material, measured during the tensile test, were:

Strain Rate	Ultimate Tensile Strength, 1000 psi	0.2% Offset Yield Strength, 1000 psi	Elongation, per cent in 4D	Reduction in Area, per cent
High	141.8	--	19.0	37.2
Low	138.1	132.9	15.5	15.8

The principal effect of hydrogen was to decrease the reduction in area in the slow strain test. Examination of the structures shown in Figure 13 indicated that this was accompanied by a marked change in the fracture mechanism.

WADC TR 54-616 Pt IV   18

TABLE 2. UNNOTCHED TENSILE IMPACT PROPERTIES OF Ti-2Mo-2Fe-2Cr ALLOY PRESTRAINED IN STRESS-RUPTURE

| Prestrain Conditions | | | | Tensile Impact Properties(a) | | |
Time, min	Rupture Time, per cent	Elongation, per cent	Reduction in Area, per cent	Impact Energy, ft-lbs(b)	Elongation, per cent	Reduction in Area, per cent
13.5	100	3.5	6.1	--	--	--
3.5	25	0.6	--	17.8	9.3	50.8
5.2	37.5	2.2	--	23.2	14.4	51.1
7.0	50	1.7	--	19.0	11.1	53.0
8.8	62.5	2.0	--	16.8	10.5	40.4
10.5	75	3.5	--	20.2	12.0	43.2
12.2	87.5	2.4	--	19.2	10.2	45.8

(a) Ductility based on initial specimen dimensions (before prestrain).
(b) 0.125 inch diameter samples.

TABLE 3. NOTCHED TENSILE PROPERTIES OF Ti-2Mo-2Fe-2Cr ALLOY PRESTRAINED IN STRESS-RUPTURE

Hydrogen Content, ppm	Prestrain Conditions			Subsequent Notched Tensile Properties		
	Stress, 1000 psi	Time, hours	Reduction in Area, per cent	Testing Speed	Reduction in Area, per cent(b)	Notched Tensile Strength, 1000 psi
20	205	0.6	4.6	Failed in rupture test		
250	205	0.9(a)	5.3	Failed in rupture test		
250	205	0.9(a)	1.7	0.5 in./min	5.9(c)	216
250	205	0.9(a)	2.4	0.5 in./min	5.1(c)	211
250	205	0.9(a)	3.1	0.005 in./min	6.9(c)	236
250	No prestrain			0.5 in./min	2.9	217

(a) This sample was loaded in increments from 105,000 psi to 205,000 psi. The figure given is time at 205,000 psi. Total time under stress was 225 hours.

(b) Reduction in area based on original area under notch (before prestrain).

(c) These samples showed cracks at the base of the notch after prestrain.
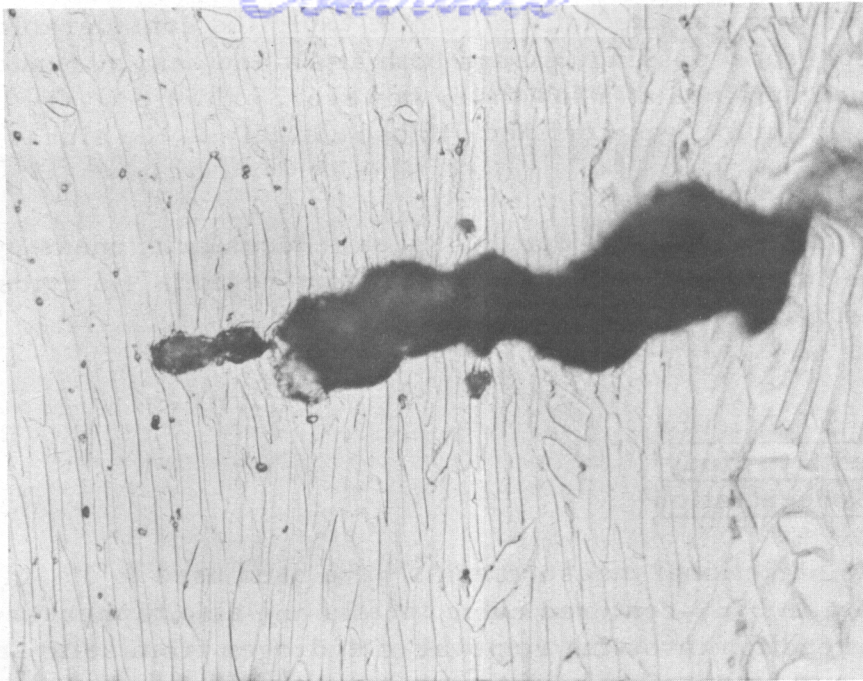
1000X   N23755

Tested With High Strain Rate (0.2 In./Min Platen Speed)
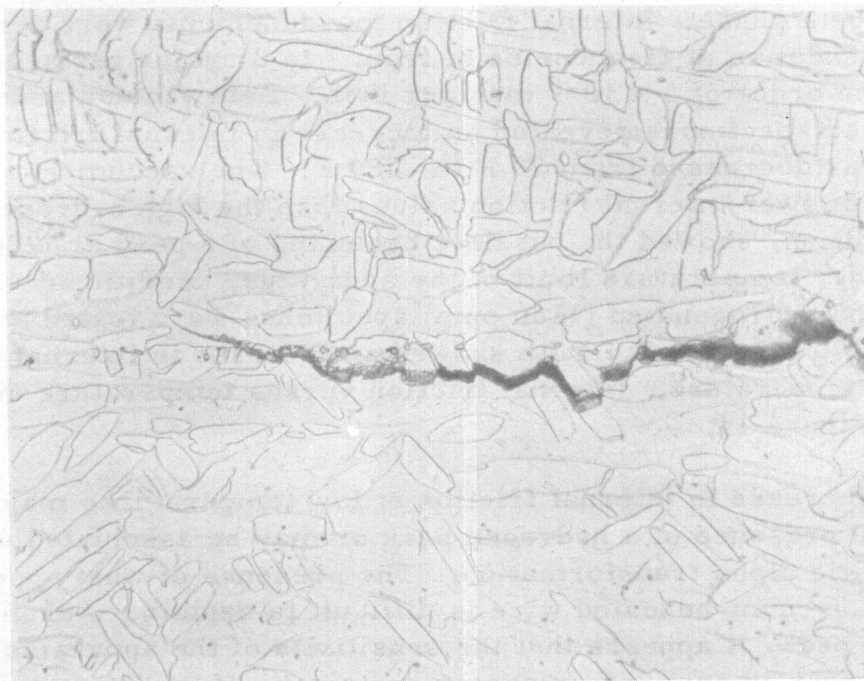
1000X   N23756

Tested With Low Strain Rate (0.02 In./Min Platen Speed)

FIGURE 13. MICROSTRUCTURE OF FRACTURE OF Ti-2Mo-2Fe-2Cr
ALLOY TENSILE SPECIMENS CONTAINING
300 PPM HYDROGEN

The test specimen strained at a high rate exhibited considerable flow with fracture apparently passing through both alpha and beta at random. The test specimen strained at a low rate, however, exhibited very little evidence of flow, and fracture was confined almost entirely to the alpha-beta interface.

These results suggest that hydrogen induces brittleness by lowering the fracture stress of the alpha-beta boundary region. No evidence of hydride was visible at the interface.

Use of Internal Friction Measurements to Study Hydrogen Concentration*

Internal frictional measurements have been used to obtain hydrogen diffusion data in body-centered cubic metals and also to measure the progress of the reaction involving removal of hydrogen from solid solution. Thus, it should be possible to determine nonequilibrium hydrogen solubility in the beta phase by internal friction measurements. It was hoped that this method of testing might also serve to detect the precipitation of hydrogen under stress if it precipitated from the beta phase.

Wire samples of Ti-8Mn, 0.080 inch in diameter, were prepared and hydrogenated to 1180 ppm. The wires were water quenched from 1400 F to retain the beta phase. Internal friction measurements were performed in a torsion pendulum at frequencies of from 1 to 2 cycles per second and strain levels of the order of 5×10^{-5} inch per inch. Both vacuum annealed and hydrogenated specimens revealed an increase in internal friction as the temperature was decreased from 70 F to -280 F. The vacuum-annealed specimen showed lower internal friction values than the high hydrogen specimen and, in addition, showed the possible beginning of a peak at -280 F, which was the lower temperature limit of the apparatus. Additional vacuum-annealed and hydrogenated (1180 ppm) specimens were tested at temperatures from 70 F to 825 F. Both showed an increase in internal friction with increased temperature. Internal friction versus temperature curves are plotted in Figure 14.

The increase in internal friction at low temperatures may be attributed to the presence of a hydrogen peak or may be associated with a beta to martensitic alpha transformation. The presence of what appears to be a peak in the vacuum-annealed wire is difficult to explain. Assuming that it is a hydrogen peak, it appears that the sensitivity of the apparatus is very great to detect a peak in such low-hydrogen material. If this is true, the peak in the high-hydrogen wire would probably be of considerable magnitude. Values of the activation energy were calculated assuming the -280 F peak was caused by hydrogen. Values of 6000 and 6200 calories/mol are obtained,

---

*Internal friction tests performed by R. E. Maringer of Battelle.
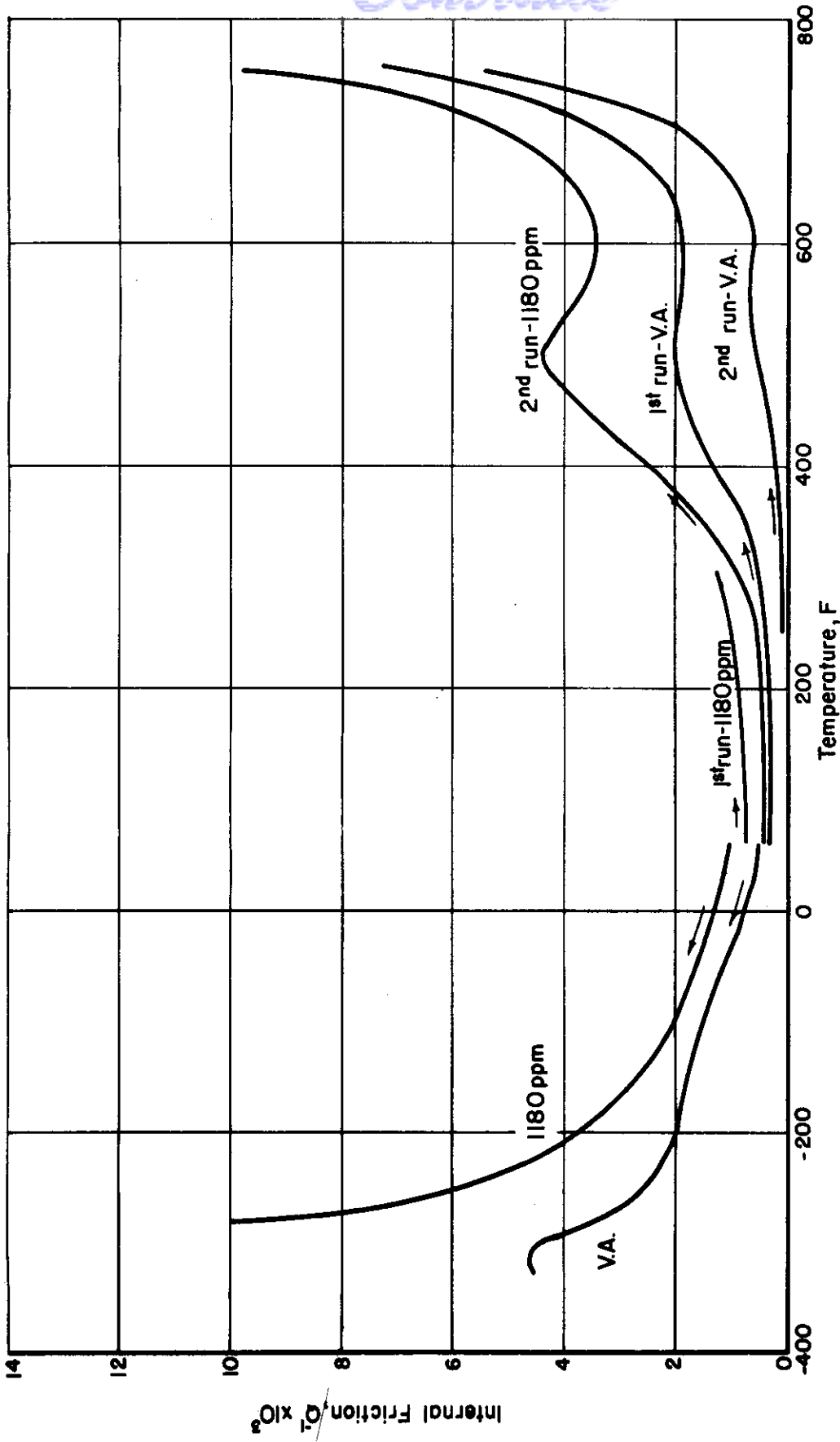
FIGURE 14. VARIATION OF INTERNAL FRICTION OF Ti-8Mn ALLOY WITH TEMPERATURE AT TWO HYDROGEN LEVELS

Arrows indicate direction of temperature change during testing.

both of which are in close agreement with the value of 6640 ± 500 calories/mol reported by Wasilewski and Kehl[5].

Since the completion of this work, the low-temperature apparatus has been modified, and a temperature of about -320 F can now be reached. This may be sufficient to determine whether a true peak exists.

One of the original aims of this investigation was to measure hydride precipitation by observing changes in internal friction brought about by a decrease in the hydrogen in solution. This aim was based on the assumption that hydride precipitation was homogeneous. Microstructure studies performed simultaneously indicated the hydride precipitation was highly localized and that diffusion was nonhomogeneous. Consequently, the use of internal friction measurements to detect changes in hydrogen solubility under stress appeared to have little likelihood of success, and work on these internal friction studies was discontinued.

Use of X-Ray Diffraction to Study Hydrogen Concentration*

X-ray diffraction studies were made in an attempt to detect differences in the lattice constants of material near the fracture of Ti-8Mn alloy tensile specimens in the vacuum-annealed and hydrogenated (400 ppm) conditions. The purpose of this investigation was to determine whether the lattice constants of material near the fracture were changed due to hydride precipitation and to determine whether hydride could be detected in the diffraction patterns.

Two hydrogen and one vacuum-annealed specimen were examined at both the fracture surface and in an unstrained portion of the test specimen. The polished surfaces of both vacuum-annealed and 400 ppm specimens were examined on the X-ray spectrometer for phase identification. Only the alpha and beta phases were observed. No hydride was apparent in the hydrogenated specimen. The same faces were coated with a thin smear of tungsten powder standard, and examined again with slow-speed traverse for the purpose of determining the lattice constants of the beta and alpha phases.

The fractured ends were examined using a Debye camera with wedge-type mounting of the sample. For these photographs, the sample was held stationary, with the edge of the "lip" from the fracture surface at the center of the camera and the X-ray beam striking the "lip" from the fracture side. With this type of sample, precise determinations of interplanar spacings are quite difficult, and the reflections were broad because of the plastic and elastic strain in the sample. However, calculations of the lattice constants of beta were made from the (211) reflections with as much precision as possible under the circumstances.

---

*X-ray tests performed by C. M. Schwartz and J. R. Doig of Battelle.

The results of the X-ray diffraction studies are shown in Table 4. It is apparent that 400 ppm hydrogen caused little change in the beta lattice, as shown by comparing the results of tests on unstrained portions of the two samples. However, straining resulted in a noticeable expansion of the lattice at the fracture surface (0.016 and 0.011 Angstrom units in the 400 ppm sample, 0.007 Angstrom units in the 10 ppm sample). This may be due to errors in measurement in examining the fracture surface. However, it is also possible that the observed change is real, indicating a very pronounced segregation of hydrogen to the beta in the fracture area. Further X-ray investigations should be conducted to check these lattice changes.

TABLE 4. DETERMINATION OF THE LATTICE CONSTANTS OF BETA PHASE IN Ti-8Mn ALLOY

Hydrogen Content, ppm	Portion Examined	Method of Examination	Lattice Constant of Beta, Å	Interplanar Spacing (10.3) of Alpha, Å
400	Unstrained end	Spectrometer	3.202	--
400	Fracture	Debye, wedge sample	3.213	1.3304
400	Fracture	Debye, wedge sample	3.218	1.3310
10	Unstrained end	Spectrometer	3.201	--
10	Fracture	Debye, wedge sample	3.208	1.3315

Permanent Damage From Hydrogen
Charging and Degassing

One of the important questions relating to the effects of hydrogen is whether a vacuum anneal can truly reclaim high-hydrogen material, with no adverse effects remaining. Tensile bars were prepared from Ti-8Mn, Ti-2Mo-2Fe-2Cr, and Ti-4Al-4Mn rods which had been swaged in the alpha-beta field. These samples were tested after (1) vacuum annealing, (2) hydrogenating to about 650 ppm, or (3) hydrogenating to about 650 ppm and vacuum annealing. Room-temperature tensile tests were carried out using a platen speed of 0.005 inch per minute and the tensile properties compared to see whether any residual effects due to hydrogen could be detected. The results of these tests, shown in Table 5, indicate that tensile properties are fully restored by vacuum annealing. Hydrogen contents given in Table 5 indicated a very effective vacuum anneal. All six samples were annealed at one time. Therefore, only one vacuum-annealed sample of each alloy was analyzed.

TABLE 5. EFFECT OF HYDROGEN CHARGING AND DEGASSING ON THE MECHANICAL PROPERTIES OF THREE TITANIUM ALLOYS

Alloy and Treatment	Hydrogen Content, ppm	Ultimate Tensile Strength, 1000 psi	0.2% Offset Yield Strength, 1000 psi	Elongation, % in 4D	Reduction in Area, %
Ti-8Mn					
Vacuum annealed	15	126.9	--	12	48
Hydrogenated	520	132.0	119.8	11	5
Hydrogenated, then vacuum annealed	--	126.0	110.8	14	46
Ti-2Mo-2Fe-2Cr					
Vacuum annealed	--	125.4	113.4	12	49
Hydrogenated	520	124.0	115.4	11	5
Hydrogenated, then vacuum annealed	12	125.6	114.2	13	45
Ti-4Al-4Mn					
Vacuum annealed	12	155.9	Defective specimen		
Hydrogenated	300	151.6	144.2	12	19
Hydrogenated, then vacuum annealed	--		135.6	12	39

Metallographic examination of the fracture region of these samples resulted in the discovery of an unusual effect not previously observed in this project. The necked portion of the ductile samples appeared to contain extensive porosity when examined as polished. This porosity was observed in both the charged and degassed and degassed-only materials. A typical example of this structure is shown in Figure 15. Porosity appeared to result from tearing around small inclusions tentatively identified as carbides. Similar strain-induced porosity has been observed by Forscher in zirconium and was attributed by him to the presence of hydride[6]. Subsequent studies have shown this phenomenon to be common to most ductile metals[7].

Effect of Cold Work on Embrittlement Tendency

Sheet tensile specimens of Ti-2Mo-2Fe-2Cr alloy, containing either 8 or 650 ppm hydrogen, were fabricated so as to contain, at 0.040-inch thickness, either 0, 5, 10, 15, or 30 per cent reduction in area by cold rolling. All samples were forged to bar in the beta field, hydrogenated or vacuum annealed, hot rolled to an intermediate thickness in the alpha-beta field, given a stabilizing heat treatment, and cold rolled as required to 0.040-inch sheet. The microstructures showed equiaxed alpha in a beta matrix with no evidence of hydride.

The results of tensile tests at a platen speed of 0.05 inch per minute are shown in Table 6. Also included in this table are bend and hardness data. The sample containing no cold work showed similar tensile properties, even though a large difference in bend ductility was observed. Cold work caused considerable embrittlement in the high-hydrogen samples. With 10 per cent reduction or greater, this material tended to form delayed cracks before testing which led to rapid failure with little ductility. The vacuum-annealed material, on the other hand, showed increased strength with increased cold reduction.

As little as 10 per cent cold reduction was sufficient to cause cracking in the high-hydrogen material before testing. The sample with 5 per cent reduction failed in a brittle manner during testing. These tests show that residual stress present in an alloy is adequate to promote slow-strain embrittlement in a susceptible alloy, confirming the identity between delayed failure in formed parts and slow-strain embrittlement during testing. The similarities between these two types of failure were pointed out shortly after the discovery of delayed failure in formed parts[8].
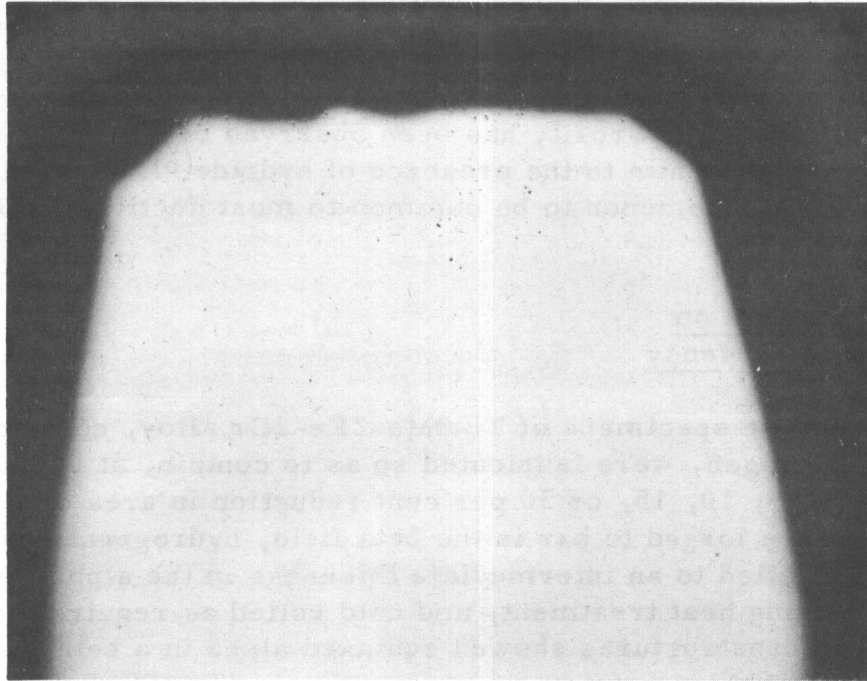
50X   As Polished   N25173

FIGURE 15.   MICROSTRUCTURE OF THE REDUCED SECTION OF A
              HYDROGEN-CHARGED AND DEGASSED Ti-2Mo-2Fe-
              2Cr ALLOY TENSILE SPECIMEN SHOWING POROSITY
              IN THE NECKED REGION

TABLE 6. EFFECT OF COLD WORK ON THE MECHANICAL PROPERTIES
OF Ti-2Mo-2Fe-2Cr ALLOY SHEET

Alloy	Prior Cold Reduction(a), per cent	Ultimate Tensile Strength, 1000 psi	0.2% Offset Yield Strength, 1000 psi	Elongation, % in 1 in.	Reduction in Area, %	Minimum Bend Radius, T	Hardness, VHN	Hydrogen Content, ppm
Vacuum annealed	0	129.1	126.0	8	12	3	357	8
Ditto	5	135.8	115.0	17	35	5	362	--
"	10	141.2	126.7	4	10	5	360	--
"	15	157.1	145.6	5	13	>10	373	--
"	30	162.6	150.4	7	32	4	361	--
Hydrogenated	0	132.8	128.0	5	10	>10	351	650
Ditto	5	141.2	133.8	1	6	>10	362	--
"	10	(b)	--	--	--	>10	383	--
"	15	(b)	--	--	--	>10	374	--
"	30	(b)	--	--	--	>10	401	--

(a) All samples cold finished to 0.040 inch after hot rolling at 1500 F, held 4 hours at 1400 F, furnace cooled to 1200 F, and held 4 hours.
(b) Brittle, failed through cracks which formed in sheet after final rolling, but before testing.

Effect of Cyclic Loading on Slow-Strain Embrittlement

It has been suggested that under conditions of cyclic loading, the damage to hydrogen-containing alpha-beta titanium alloys may not be cumulative. Delay periods between applications of load may allow removal of the embrittling condition by allowing diffusion to occur. In order to determine the effect of cyclic delay periods on stress-rupture properties, six 0.125-inch-diameter Ti-8Mn alloy stress-rupture specimens were prepared containing 370 ppm hydrogen.

Two of the specimens were tested to failure in a standard stress-rupture test at 90 per cent of the ultimate tensile strength. The remaining specimens were cyclically loaded with the time per cycle (3.5 hours) equaling one half of the average stress-rupture life obtained from the first two tests. Two of these specimens were given a one-day delay period at no stress between load cycles, and the other two were given a one-month no-load delay period. Test results are shown in Table 7. Specimens tested with no delay failed in 5.4 and 8.7 hours; those tested with a one-day delay period failed in 15.6 and 23.6 hours total time at stress; and those with one-month delay period failed in 39.7 and 45.2 hours total time at stress. All specimens failed in a brittle manner and exhibited similar per cent elongation and reduction in area values.

The results of these tests appear to substantiate the suggestion that the damage under conditions of cyclic loading may not be cumulative and that recovery may occur during no-load delay periods. However, to more positively confirm this effect, the experiment should be repeated using hydrogen-free samples.

Use of a Low-Speed Tensile Test to Detect Slow-Strain Embrittlement

Several alloys prepared in the Phase II investigation were found to be ductile in a low-speed tensile test and brittle in a stress-rupture test. A study was made of the possibility of detecting embrittlement using tensile testing speeds considerably lower than 0.005 inch per minute. A 6 per cent chromium alloy containing 300 ppm hydrogen was tested in an attempt to find the testing speed at which transition from ductile to brittle failure occurred. Test results are shown in Table 8. The tensile test at the lowest strain rate (0.0003 inch per inch per minute) showed a very slight decrease in ductility, while a stress-rupture test at a higher strain rate (0.0023 inch per inch per minute) showed considerable embrittlement. The strain rate was controlled in tensile testing by a strain pacer on the test machine which permitted head travel to be maintained constant.

From the data given in Table 8, it is apparent that an alloy is much more sensitive to hydrogen embrittlement in a stress-rupture test than in a tensile test. The reason for this difference is not apparent.

WADC TR 54-616 Pt IV   30

TABLE 7. INTERRUPTED STRESS-RUPTURE TEST RESULTS OF Ti-8Mn ALLOY
CONTAINING 370 PPM HYDROGEN

Sample(a)	Applied Stress		Number of Cycles	Delay Period(b)	Total Rupture Time, hr	Total Elongation, per cent	Total Reduction in Area, per cent
	Per Cent of UTS	1000 psi					
1	90	123.5	--	--	8.7	5.9	1.1
2	90	123.5	--	--	5.4	4.8	6.3
3	90	123.5	7	1 day	23.6	6.1	6.6
4	90	123.5	4	1 day	15.6	5.8	6.2
5	90	123.5	12	1 month	39.7	4.7	7.5
6	90	123.5	13	1 month	45.2	5.4	6.0

(a) Standard 0.125 inch diameter round specimens.
(b) One cycle of loading equaled a stress of 123,500 psi for 3.5 hours followed by a delay period as indicated at no stress.

TABLE 8. DUCTILITY VERSUS STRAIN RATE FOR THE Ti-6Cr ALLOY AT 300 PPM HYDROGEN

Type of Test(a)	Time to Failure, hours	Strain Rate(b), in./in./min	Ultimate Strength, 1000 psi	Elongation, per cent in 4D	Reduction in Area, per cent
Tensile(c)	<0.2	0.6	126.6	22	48.7
Tensile(c)	0.7	0.006	122.6	28	56.2
Tensile	2	0.0012	146.8	15	50.1
Tensile	4	0.0006	154.0	16	46.3
Tensile	8	0.0003	143.0	9(d)	45.1
Stress-rupture(c)	6.2	0.0023	--	6	6.6
Stress-rupture(c)	144.0	0.0000013	--	--	15.6

(a) Standard 0.125-inch-diameter tensile specimens used for all tests.
(b) Strain rate in tensile tests obtained by dividing the platen speed by reduced section length; strain rate in stress-rupture tests from measured second stage creep rates.
(c) Tensile and stress-rupture tests from Phase II.
(d) Failed through punched gage mark.

It has been pointed out by those familiar with stress-corrosion failures in aluminum alloys that there is a close similarity between this type of failure and the slow-strain embrittlement in titanium alloys. This similarity suggests that slow-strain embrittlement in hydrogen-containing titanium alloys might be a form of stress corrosion (and thereby preventable by proper surface protection).

In an effort to check this possibility, twelve stress-rupture specimens were prepared from Ti-8Mn alloy. Six of the specimens contained 20 ppm hydrogen. The remaining six specimens contained 370 ppm hydrogen. These specimens were tested at two stress levels (85 and 95 per cent of the ultimate tensile strength) at room temperature and in one of three atmospheres - normal, dry, or moist. No control was exercised over the normal atmosphere. The dry and moist atmospheres were prepared by enclosing the specimens with either a desiccant (Drierite) or water-soaked cotton during the test and for 24 hours prior to the test. The results of these stress-rupture tests are given in Table 9.

The high-hydrogen specimens showed embrittlement in all atmospheres, while the low-hydrogen specimens remained ductile in all atmospheres. Differences in rupture time and ductility among similarly stressed specimens in the three atmospheres are most probably due to normal variations in stress-rupture test results.

As is the case with most tests for stress corrosion, unless the test shows definite evidence for the stress-corrosion mechanism, it is indecisive. The data in Table 9 cannot be interpreted as indicating that stress corrosion was not the mechanism causing failure, since it is also possible that the test itself was inadequate.

Discussion of Results

From the investigations described in the preceding sections, it is possible to construct a tentative mechanism to explain the ability of hydrogen to cause embrittlement of titanium alloys during low speed testing.

It has been shown that failure in embrittled material occurs predominately along alpha-beta interfaces. It has also been shown that hydride (not positively identified) precipitates under strain along the alpha-beta interface in a number of alloys exhibiting slow-strain embrittlement. Therefore, it seems reasonable to assume that the direct cause of brittleness is hydride at the interface. The inability to detect hydride at the fracture surface with either metallographic or X-ray examination is not too great a block in accepting this explanation. Metallographic examination of

TABLE 9. EFFECT OF ATMOSPHERE ON STRESS-RUPTURE PROPERTIES OF Ti-8Mn ALLOY AT TWO HYDROGEN LEVELS(a)

Hydrogen Content, ppm	Test Atmosphere(b)	Applied Stress Per Cent of UTS	1000 psi	Rupture Time, hours	Elongation, per cent in 4D	Reduction in Area, per cent
20	Normal	95	128.2	4.2	23	59
20	Normal	85	114.6	>315.0(c)	--	--
20	Dry	95	128.2	25.3	22	55
20	Dry	85	114.6	>256.7(c)	--	--
20	Moist	95	128.2	0.5	25	56
20	Moist	85	114.6	>259.0(c)	--	--
370	Normal	95	130.3	1.3	7	6
370	Normal	85	116.6	39.7	1	4
370	Dry	95	130.3	3.3	1	6
370	Dry	85	116.6	>256.8(c)	--	--
370	Moist	95	130.3	16.6	11	11
370	Moist	85	116.6	255.2	3	7

(a) Standard 0.125 inch diameter specimens.

(b) Dry and moist atmospheres prepared by enclosing the sample during the test, and for 24 hours prior to the test, with either a desiccant (Drierite) or water.

(c) Test discontinued.

a number of alloys showed that the hydride formed in a highly nonhomogeneous manner and tended to form in regions of high stress. X-ray examination also suggested that a considerable buildup of hydrogen in the beta phase had occurred at the fracture surface. It is possible that failure followed so rapidly after the initial hydride formation in the fracture region that very little growth of hydride occurred.

Studies of the effect of strain rate and temperature on the slow-strain embrittlement tendency suggested that the embrittlement phenomenon is a form of strain aging, since a minimum occurred in the temperature-ductility curves at constant strain rate. This minimum is probably due to the combined effects of two factors; decreased diffusion rate of hydrogen to the interfacial region as the testing temperature is decreased and increased hydrogen solubility as the testing temperature is increased, with a resulting lessening of the tendency toward hydride precipitation. The first factor leads to decreased embrittlement at low temperature and the second to decreased embrittlement at high temperatures. The process is also strain-rate sensitive, suggesting the strain is necessary to obtain the required diffusion of hydrogen.

A process of this type requires that a state of supersaturation exist in the alloy. That is, either the alpha or the beta phase or both must contain more than the equilibrium amount of hydrogen at room temperature, such that precipitation of hydride is favored. Evidence has been obtained suggesting the supersaturation can exist in both phases when suitably alloyed. If so, both alpha and beta alloys, as well as alpha-beta alloys, should be susceptible to strain aging and possibly to embrittlement. Thus far, no evidence of strain aging in an all-beta alloy has been reported. However, as far as is known, no all-beta alloys have been thoroughly examined for hydrogen embrittlement.

Several of the investigations conducted suggested that precipitation of hydride occurs quite late in the straining process, and that the rate controlling process is the diffusion of hydrogen to a site favorable for precipitation. For example, no damage to impact properties was observed in an alloy strained to just short of brittle failure in a stress-rupture test. Also, cyclically strained material, when given long intermediate "rest" periods at no stress, showed considerably increased life, even though failure ultimately occurred in a brittle manner. The recovery process must involve the diffusion of hydrogen away from regions of high concentration since hydride, once formed, would be in equilibrium with the surrounding material. The highly localized nature of hydride precipitation in strained alpha-beta alloys also suggests that the movement of hydrogen occurs quite freely, while the formation of hydride occurs only in the most favorable (most highly stressed) region.

The effects of alloying on the hydrogen level at which embrittlement is first observed are probably due to one of two factors: their effect on the distribution of hydrogen between the alpha and beta phases or their effect on

the ability of the alloy to retain hydrogen to room temperature so as to develop a supersaturated condition favorable to strain aging. For example, aluminum in alpha titanium reduces the maximum solubility of hydrogen at elevated temperature but apparently permits the hydrogen dissolved to be retained to room temperature, where at least a part of it can precipitate under strain.

Microstructural variations also affect the tendency toward hydrogen embrittlement. Decreasing the amount of alpha-beta interface in an alloy results in a smaller amount of hydrogen being required to produce embrittlement. This is particularly evident if the interface is maintained such that it forms an almost continuous path through the alloy.

The final annealing or stabilizing temperature can also affect the hydrogen embrittlement level, a lower temperature resulting in less hydrogen being necessary to cause embrittlement. This effect is also believed due to differences in hydrogen distribution between the alpha and beta phases.

References

(1) Lenning, G. A., Craighead, C. M., and Jaffee, R. I., "The Effect of Hydrogen on the Mechanical Properties of Titanium and Titanium Alloys", Third Summary Report from Battelle Memorial Institute to Watertown Arsenal on Contract No. DA-33-019-ORD-938 (July 31, 1954).

(2) Kotfila, R. J., and Erbin, E. F., "Hydrogen Embrittlement of a Titanium Alloy", Metals Progress, 55 (4), 128 (October, 1954).

(3) Ripling, E. J., "Overcoming Rheotropic Embrittlement in Titanium and Titanium-Base Alloys", Third Quarterly Progress Report from Case Institute of Technology to Wright Air Development Center, Contract No. AF 33(616)-2223 (June 4, 1954).

(4) Schwartzberg, F. R., Rahr, W. D., Williams, D. N., and Jaffee, R. I., "The Measurement of the Thermal Stability of Titanium Alloys", TML Report No. 55 (October 5, 1956).

(5) Wasilewski, R. J., and Kehl, G. L., "Summary Report on Diffusion of Hydrogen, Nitrogen, and Oxygen in Titanium", Report No. WAL 401/149-11A (July 13, 1953).

(6) Forscher, F., "Strain-Induced Porosity and Hydrogen Embrittlement in Zirconium", Trans. AIME, 206, 537 (1956).

(7) Wood, R. A., Williams, D. N., Ogden, H. R., and Jaffee, R. I., "Porosity in Formed Unalloyed Titanium", to be published by TML.

(8) Jaffee, R. I., and Maykuth, D. J., "Survey of the Problem of Delayed Cracking in Formed Titanium Parts", TML Report No. 7 (June 20, 1955).

PHASE II. THE EFFECT OF ALLOY COMPOSITION
ON HYDROGEN EMBRITTLEMENT

Summary

To determine the effect of alloy composition on hydrogen embrittlement, eighty binary, ternary, and quaternary titanium alloys were prepared and tested to determine the hydrogen level (up to 800 ppm) necessary to cause either slow-strain or impact embrittlement. All alloys were tested in the stabilized condition after similar stabilizing heat treatments. Alloy composition was found to have a pronounced effect on the hydrogen embrittlement level. The information gained from this investigation may be summarized as follows:

1. Increasing amounts of alloy addition in a given alpha-beta alloy system increased the resistance to slow-strain embrittlement. This tendency is apparently due to the increased amounts of beta present in the alloy. However, a reversal of this trend was observed in some alloy systems such that an alloy which was predominately alpha, and showed no tendency toward slow-strain embrittlement, was made susceptible by further alloying.

2. The presence of beta was not necessary for slow-strain embrittlement to occur. A titanium aluminum-copper alloy containing alpha and a compound phase exhibited slow-strain embrittlement.

3. The hydrogen content necessary to cause slow-strain embrittlement was high in alpha-beta alloys in which aluminum, molybdenum, or niobium was the principal alloy addition.

4. The hydrogen content necessary to cause slow-strain embrittlement was low in alloys in which chromium, manganese, vanadium, or iron was the principal addition. At a constant alpha-beta ratio, the embrittlement level decreased approximately in the order shown, with iron being the most detrimental.

5. Increased amounts of oxygen lowered the hydrogen content at which slow-strain embrittlement was observed.

6. The tendency toward impact embrittlement appeared to be reduced by the presence of chromium, molybdenum, or vanadium in an alloy.

Experience has shown conclusively that some titanium alloys are much less sensitive to hydrogen embrittlement than others. This portion of the investigation was designed to determine the effects of the common alloying elements on the hydrogen embrittlement level of titanium alloys. Among the variables to be examined were:

(1) Type of beta-stabilizing addition

(2) Amount of addition

(3) Combinations of beta-stabilizing additions

(4) Aluminum or tin additions

(5) Interstitial level.

Eighty alloys were selected for study. These alloys were first heat treated to a fully stabilized condition and then tested using impact, tensile, and stress-rupture tests to determine the maximum amount of hydrogen which could be tolerated without embrittlement.

Some data have also been reported which indicate that hydrogen may adversely affect thermal stability. Therefore, thirty of the alloys were exposed to thermal stability test conditions at each of two hydrogen levels and then tested to determine whether instability was related to hydrogen content.

The results of these studies are reported in this phase of the report. Unfortunately, the hydrogen embrittlement level of all the alloys was not completely determined since the unexpectedly high tolerance of some of the alloys, as measured with unnotched stress-rupture tests, required an excessively large number of tests to be run. Time limitations prevented completion of all of these tests.

Preparation of the Alloys

All alloys were tested in the form of fully stabilized 1/4-inch-diameter rod. This rod was prepared as described in the following sections.

Alloying and Melting

All the alloys with the exception of the high-purity iodide-base alloys were prepared from 140 BHN sponge. An analysis of the sponge is given

in Table 10. High-purity metal was used to make all alloy additions except oxygen, which was added in preoxygenated sponge.

TABLE 10. ANALYSIS OF 140 BHN
TITANIUM SPONGE

Element	Weight Per Cent[a]
C	0.03
H	0.009
N	0.010
O	0.108[b]
Cl	0.010
Fe	0.018
Al	0.018
Cu	0.001
Cr	< 0.005
Mg	0.004
Mn	0.092
Mo	< 0.005
Ni	0.002
Pb	< 0.010
Si	0.004
V	< 0.002
Zr	0.110

(a) As reported by The Dow Chemical Company.
(b) From analysis of ingot K-1 (Ti-4Mo).

Two-pound ingots were made for all but four of the alloys. These ingots were double arc melted with a tungsten electrode in a water-cooled copper crucible under a static argon atmosphere of 20 inches of mercury. After melting, homogeneity was checked radiographically, and the ingots were remelted until the radiograph indicated satisfactory homogeneity.

Four of the alloys were melted as 20-pound ingots so that sufficient material would be available for the microstructural studies described under Phase III. These alloys were Ti-8Mn (K-13), Ti-4Al-4Mn (K-38), Ti-2Mo-2Cr-2Fe (K-33), and Ti-6Al-4V (K-37).

The Ti-4Al-4Mn alloy was prepared by melting two 10-pound ingots with a tungsten electrode in a water-cooled copper crucible under a static argon atmosphere of 30 to 50 microns. These ingots were then forged and rolled to sheet, descaled, cut into small pieces, mixed, and remelted as one 20-pound ingot. A static atmosphere of 25 per cent argon-75 per cent helium at 20 microns was used over this melt.

The other three alloys were consumable-electrode melted. The charge was first pressed into an electrode, then melted, the ingot forged to

electrode size, and remelted. Furnace atmospheres for these melts were as follows:

Alloy	Melt	Composition	Pressure
Ti-8Mn	First	10 per cent argon-90 per cent helium	Atmospheric
Ti-8Mn	Second	Ditto	Ditto
Ti-6Al-4V	First	50 per cent helium-50 per cent argon	200 microns
Ti-6Al-4V	Second	Ditto	Ditto
Ti-2Mo-2Cr-2Fe	First	50 per cent helium-50 per cent argon	30 microns
Ti-2Mo-2Cr-2Fe	Second	Ditto	160 microns

A number of the alloys were analyzed using chips obtained during machining of the test specimens to determine the normal recovery. Results of the analyses are given in Table 11. Unless otherwise indicated, analyses were by standard wet chemical methods. These results show excellent agreement of the actual composition with the intended composition.

The variation in oxygen content was determined only for the Ti-4Mo series of alloys. These results were as follows:

Alloy	No.	Oxygen Content, wt %
Ti-4Mo, iodide base	K-46	0.053
Ti-4Mo, sponge base	K-1	0.108
Ti-4Mo, oxidized sponge (0.15 per cent added)	K-48	0.278

Fabrication

After radiography had indicated suitable homogeneity, the ingots were ground to remove surface defects apt to cause laps and forged to 3/4-inch-round bars. The bars were then reground and swaged to 5/8-inch rod. Before further processing, the 5/8-inch bar was cut into suitable lengths for subsequent test requirements and machined to remove all surface scale. At this stage, the rods were vacuum annealed and then hydrogenated to the desired hydrogen level.

The microstructure of the rods was controlled by a final swaging operation to 1/4-inch rod at a temperature low in the alpha-beta field. This treatment insured a fine, equiaxed alpha-beta or alpha-compound structure in all two-phase alloys.

Fabrication temperatures for all three fabrication steps are included in Table 12.

TABLE 11. RESULTS OF CHEMICAL ANALYSES

Intended Addition, weight per cent	Alloy No.	Addition by Analysis, weight per cent										
		Mo	V	Nb	Ta	Mn	Cr	Fe	Cu	Ni	Al	Sn
Binary Alloys												
Beta Isomorphous, non-hydride formers												
4Mo	K-1	4.14										
8Mo	K-2	8.54										
20Mo	K-3	19.8										
Beta Isomorphous, hydride formers												
4V	K-4		3.92									
8V	K-5		7.57									
20V	K-6		19.3									
4Ta	K-7				5.1							
8Ta	K-8				8.2[a]							
4Nb	K-9			4.7[a]								
8Nb	K-10			9.0[a]								
Eutectoid, sluggish												
4Mn	K-11					3.99						
6Mn	K-12					6.01						
8Mn	K-13					7.31						
Eutectoid, relatively active												
2Fe	K-14							2.0[a]				
4Fe	K-15							3.98				
4Cr	K-16						3.53					
6Cr	K-17						5.78					
8Cr	K-18						7.08					
Eutectoid, active												
4Cu	K-19								3.47			
7Cu	K-20								6.47			
4Ni	K-68									4.70		
7Ni	K-69									7.2		
Beta Multiplicity												
2Mo-2V	K-21	1.85	1.45									
4Mo-4V	K-22	3.75	3.90									
8Mo-8V	K-23	7.74	7.91									
2Mn-2Fe	K-24					2.0[a]		2.1[a]				
2Mn-2Cr	K-25					2.0[a]	2.0[a]					
2Cr-2Fe	K-26						1.9[a]	2.1[a]				
3Cr-3Fe	K-27						2.7[a]	3.0[a]				
2Mn-2Cr-2Fe	K-28					2.1[a]	2.0[a]	2.2[a]				
2Mo-2Mn	K-29	1.96				1.72						
2Mo-2Cu	K-71	2.23							1.80			
2Mn-2Cu	K-70					1.9[a]			2.1[a]			
2Mo-2Fe	K-30	2.05						1.69				
2V-2Fe	K-31		1.93					1.87				
2Mo-2Cr	K-32	1.73					1.87					
2Mo-2Fe-2Cr	K-33	1.73					1.85	1.88				

TABLE 11. RESULTS OF CHEMICAL ANALYSES (Continued)

Intended Addition, weight per cent	Alloy No.	Addition by Analysis, weight per cent										
		Mo	V	Nb	Ta	Mn	Cr	Fe	Cu	Ni	Al	Sn
Aluminum Additions												
4Al-4Mo	K-34	4.2[a]									3.7[a]	
6Al-4Mo	K-35	4.0[a]									5.5[a]	
4Al-4V	K-36		4.4[a]								4.0[a]	
6Al-4V	K-37		4.0[a]								6.0[a]	
4Al-4Mn	K-38					4.0[a]					4.1[a]	
6Al-4Mn	K-39					3.7[a]					6.4[a]	
4Al-2Fe	K-40							2.1[a]			3.7[a]	
6Al-2Fe	K-41							2.1[a]			6.5[a]	
4Al-4Cr	K-42						3.7[a]				4.0[a]	
6Al-4Cr	K-43						3.8[a]				6.6[a]	
4Al-7Cu	K-72								6.3[a]		3.9[a]	
4Al-2Cr-2Fe	K-44						2.0[a]	2.0[a]			4.1[a]	
4Al-1.3Mo-1.3Cr-1.3Fe	K-45	1.55[a]					1.45[a]	1.45[a]			3.9[a]	
Tin Additions												
12Sn-4Mo	K-73	3.78										10.6
12Sn-4V	K-74		3.23									10.3
12Sn-4Mn	K-75					3.9[a]						13.7[a]
12Sn-2Fe	K-76							1.9[a]				13.3[a]
12Sn-4Cr	K-77						3.8[a]					13.1[a]
12Sn-7Cu	K-78								6.46			11.1
Interstitial Level												
4Mo, iodide base	K-46	4.09										
4Mo, sponge plus 0.15 O_2	K-48	3.99										
20Mo, iodide base	K-47	19.7										
20Mo, sponge plus 0.15 O_2	K-49	20.6										
4V, iodide base	K-50		3.85									
4V, sponge plus 0.15 O_2	K-52		3.94									
20V, iodide base	K-51		19.0									
20V, sponge plus 0.15 O_2	K-53		19.8									
8Mn, iodide base	K-54					7.39						
8Mn, sponge plus 0.15 O_2	K-55					7.49						
6Cr, iodide base	K-56						5.84					
6Cr, sponge plus 0.15 O_2	K-57						5.80					
7Cu, iodide base	K-80								6.49			
7Cu, sponge plus 0.15 O_2	K-79								6.47			
6Al-4Mo, iodide base	K-58	4.05									5.88	
6Al-4Mo, sponge plus 0.15 O_2	K-59	4.05									5.93	
6Al-4V, iodide base	K-60		3.71								6.03	
6Al-4V, sponge plus 0.15 O_2	K-61		4.2[a]								6.1[a]	
4Al-4Mn, iodide base	K-62					3.6[a]					3.9[a]	
4Al-4Mn, sponge plus 0.15 O_2	K-63					4.0[a]					4.0[a]	

TABLE 11. RESULTS OF CHEMICAL ANALYSES (Continued)

Intended Addition, weight per cent	Alloy No.	Addition by Analysis, weight per cent										
		Mo	V	Nb	Ta	Mn	Cr	Fe	Cu	Ni	Al	Sn
4Al-4Fe, iodide base	K-64							4.0[a]			4.0[a]	
4Al-4Fe, sponge plus 0.15 O$_2$	K-65							4.5[a]			3.9[a]	
4Al-4Cr, iodide base	K-66						3.9[a]				3.9[a]	
4Al-4Cr, sponge plus 0.15 O$_2$	K-67						3.9[a]				4.0[a]	

(a) By quantitative spectrographic analysis.

TABLE 12. FABRICATION DATA FOR ALLOYS PREPARED FOR THE STUDY OF THE EFFECT OF COMPOSITION ON HYDROGEN EMBRITTLEMENT

Intended Addition, weight per cent	Alloy No.	Forging Temperature, F	Swaging Temperature, to 5/8-Inch Round, F	Swaging Temperature, to 1/4-Inch Round, F
Binary Alloys				
Beta Isomorphous, non-hydride formers				
4Mo	K-1	1650	1500	1300
8Mo	K-2	1650	1500	1300
20Mo	K-3	1800	1700	1400
Beta Isomorphous, hydride formers				
4V	K-4	1700	1600	1300
8V	K-5	1650	1600	1300
20V	K-6	1800	1600	1300
4Ta	K-7	1650	1500	
8Ta	K-8	1700	1500	1200
4Nb	K-9	1650	1500	1300
8Nb	K-10	1800	1650	1300
Eutectoid, sluggish				
4Mn	K-11	1600	1500	1300
6Mn	K-12	1600	1500	1300
8Mn	K-13	1700	1600	1300
Eutectoid, relatively active				
2Fe	K-14	1650	1500	1300
4Fe	K-15	1650	1600	1300
4Cr	K-16	1600	1500	1300
6Cr	K-17	1800	1650	1300
8Cr	K-18	1650	1600	1300
Eutectoid, active				
4Cu	K-19	1650	1600	1300
7Cu	K-20	1800	1650	1400
4Ni	K-68	1800	1700	1300
7Ni	K-69			
Beta Multiplicity				
2Mo-2V	K-21	1700	1500	1300
4Mo-4V	K-22	1700	1500	1300
8Mo-8V	K-23	1800	1700	1300
2Mn-2Fe	K-24	1650	1600	1300
2Mn-2Cr	K-25	1650	1600	1300
2Cr-2Fe	K-26	1650	1600	1300
3Cr-3Fe	K-27	1650	1600	1300
2Mn-2Cr-2Fe	K-28	1650	1600	1300
2Mo-2Mn	K-29	1800	1650	1300
2Mo-2Cu	K-71	1650	1500	1300
2Mn-2Cu	K-70	1650	1600	1300
2Mo-2Fe	K-30	1700	1500	1300
2V-2Fe	K-31	1800	1600	1300
2Mo-2Cr	K-32	1700	1600	1300
2Mo-2Cr-2Fe	K-33	1800	1600	1300
Aluminum Additions				
4Al-4Mo	K-34	1800	1700	1400
6Al-4Mo	K-35	1900	1700	1400
4Al-4V	K-36	1800	1600	1300
6Al-4V	K-37	1900	1700	1400
4Al-4Mn	K-38	1800	1600	1400
6Al-4Mn	K-39	1800	1650	1400
4Al-2Fe	K-40	1800	1650	1400
6Al-2Fe	K-41	1800	1650	1400

TABLE 12. FABRICATION DATA FOR ALLOYS PREPARED FOR THE STUDY OF THE EFFECT
OF COMPOSITION ON HYDROGEN EMBRITTLEMENT (Continued)

Intended Addition, weight per cent	Alloy No.	Forging Temperature, F	Swaging Temperature, to 5/8-Inch Round, F	Swaging Temperature, to 1/4-Inch Round, F
4Al-4Cr	K-42	1800	1650	1400
6Al-4Cr	K-43	1800	1650	1400
4Al-7Cu	K-72	1800	1650	1400
4Al-2Cr-2Fe	K-44	1800	1600	1300
4Al-1.3Cr-1.3Fe-1.3Mo	K-45	1800	1600	1300
Tin Additions				
12Sn-4Mo	K-73	1650	1500	1300
12Sn-4V	K-74	1800	1700	1400
12Sn-4Mn	K-75	1800	1600	1400
12Sn-2Fe	K-76	1800	1700	1400
12Sn-4Cr	K-77	1800	1650	1400
12Sn-7Cu	K-78	1800	1650	1400
Interstitial Level				
4Mo, iodide base	K-46	1600	1650	1300
4Mo, sponge plus 0.15 O_2	K-48	1700	1600	1300
20Mo, iodide base	K-47	1800	1650	1300
20Mo, sponge plus 0.15 O_2	K-49	1800	1700	1400
4V, iodide base	K-50	1600	1650	1300
4V, sponge plus 0.15 O_2	K-52	1800	1600	1300
20V, iodide base	K-51	1800	1650	1300
20V, sponge plus 0.15 O_2	K-53	1800	1600	1300
8Mn, iodide base	K-54	1600	1650	1300
8Mn, sponge plus 0.15 O_2	K-55	1700	1600	1300
6Cr, iodide base	K-56	1600	1650	1300
6Cr, sponge plus 0.15 O_2	K-57	1800	1600	1300
7Cu, iodide base	K-80	1750	1600	1300
7Cu, sponge plus 0.15 O_2	K-79	1650	1600	1300
6Al-4Mo, iodide base	K-58	1800	1650	1400
6Al-4Mo, sponge plus 0.15 O_2	K-59	1900	1700	1400
6Al-4V, iodide base	K-60	1800	1650	1400
6Al-4V, sponge plus 0.15 O_2	K-61	1900	1700	1400
4Al-4Mn, iodide base	K-62	1800	1650	1400
4Al-4Mn, sponge plus 0.15 O_2	K-63	1800	1600	1400
4Al-4Fe, iodide base	K-64	1800	1650	1400
4Al-4Fe, sponge plus 0.15 O_2	K-65	1800	1600	1400
4Al-4Cr, iodide base	K-66	1800	1650	1400
4Al-4Cr, sponge plus 0.15 O_2	K-67	1800	1600	1400

Vacuum Annealing and Hydrogenation

At an intermediate position in the fabrication schedule, the rods were carefully cleaned to remove all surface scale and vacuum annealed for 6 to 8 hours at 1500 F. This resulted in a uniformly low hydrogen content of approximately 20 ppm.

The rods were then hydrogenated to the desired hydrogen level by heating at 1470 F for 40 hours in a Sieverts' apparatus. In general, analysis showed good agreement between the intended and actual hydrogen content. However, it was observed that when several alloys of different compositions were hydrogenated in one batch, some alloys showed selective absorption at the expense of the others. This is shown by the data given in Table 13. It is apparent that those alloys possessing a high beta content absorbed a larger portion of the hydrogen present. This is most easily seen in Batch No. 10460-25, where Ti-8Mo gained the most hydrogen, while Ti-7Cu gained only a small amount. Aluminum, due to its tendency to raise the beta transus and thus decrease the amount of beta present at 1470 F (the hydrogenation temperature), caused lowered hydrogen absorption when present in an alloy. On the basis of these results, individual hydrogenation was used as much as possible, and care was taken when batch hydrogenation was necessary to insure that all alloys were of equivalent alloy type to prevent unequal absorption. Analysis showed that using these precautions, the intended and actual hydrogen contents were quite close together.

Heat Treatment

Although a number of alloy types were represented, it was felt advisable to standardize on a single heat treatment to permit valid comparisons to be made between alloys. Therefore, all alloys were stabilized by annealing the 1/4-inch-round rod for 1 hour at 1300 F, furnace cooling to 1100 F, and air cooling. The stabilizing treatment was carried out in air.

Representative microstructures resulting from the low final fabrication temperature and the stabilizing treatment given above are shown in Figures 16 through 19. Except in those alloys whose compositions were such that they were in the all-beta field at 1100 to 1300 F, all alloys exhibited a fine-grained structure.

The heat treatment gave satisfactory results for all alloys except the ternary Ti-Al-Cr alloys. These alloys apparently tended to precipitate compound at 1100 F leading to extreme embrittlement which, in most cases, prevented the determination of their hydrogen tolerance.

TABLE 13. RELATIVE ABSORPTION OF ALLOYS HYDROGENATED IN A BATCH AT THE 200 PPM INTENDED HYDROGEN LEVEL

Alloy Addition, weight per cent	Alloy Number	Hydrogen Content, ppm[a]
Batch No. 10460-24		
4Nb	K-9	194
4Mn	K-11	209
2Fe	K-14	196
4Fe	K-15	229
4Cr	K-16	230
4Cu	K-19	139
2Mn-2Fe	K-24	230
2Mn-2Cr	K-25	214
2Cr-2Fe	K-26	232
Batch No. 10460-25		
4Mo	K-1	184
8Mo	K-2	233
6Mn	K-12	212
8Cr	K-18	229
7Cu	K-20	129
3Cr-3Fe	K-27	229
2Mn-2Cr-2Fe	K-28	216
Batch No. 10460-34		
8Nb	K-10	299
6Cr	K-17	331
2Mo-2Mn	K-29	304
6Al-4Mn	K-39	150
4Al-4Fe	K-40	177
6Al-2Fe	K-41	152
4Al-4Cr	K-42	205
6Al-4Cr	K-43	171
Batch No. 10460-37		
2Mo-2Cr	K-32	332
4Al-1.3Cr-1.3Fe-1.3Mo	K-45	198
8Mn-0.15O_2	K-55	323
4Al-4Mn-0.15O_2	K-63	202
4Al-4Fe-0.15O_2	K-65	195
Batch No. 10460-45		
2V-2Fe	K-31	274
4V-0.15O_2	K-52	260
6Cr-0.15O_2	K-57	296
6Al-4V-0.15O_2	K-61	140

(a) Hydrogen analysis by warm extraction method.
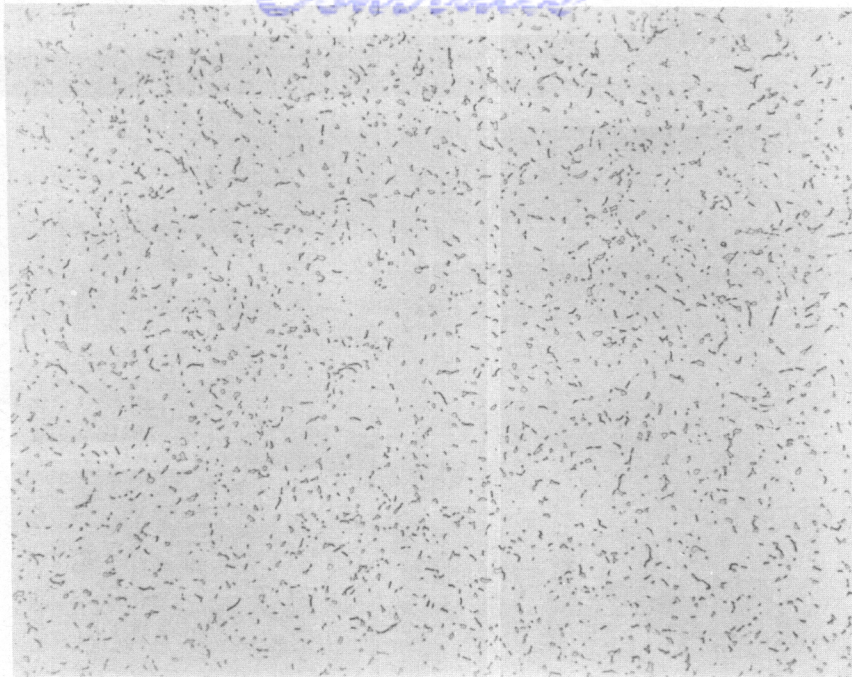
500X   N32179

FIGURE 16. MICROSTRUCTURE OF VACUUM-ANNEALED Ti-6Al-4V (K-37)
SHOWING SMALL PARTICLES OF BETA IN AN ALPHA
MATRIX
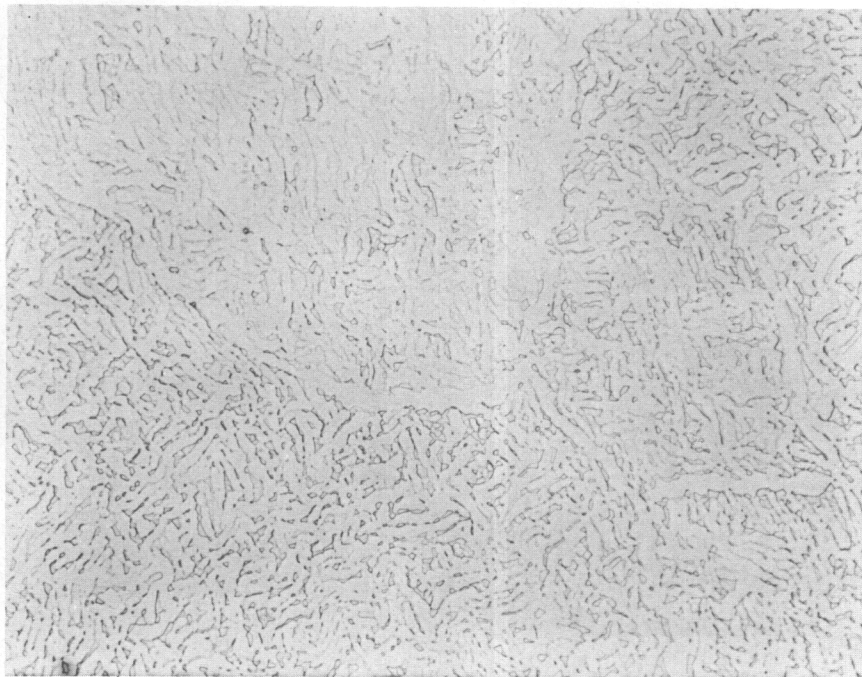
500X   N31440

FIGURE 17. MICROSTRUCTURE OF VACUUM-ANNEALED Ti-2Cr-2Fe
(K-26) SHOWING A MIXTURE OF APPROXIMATE 50 PER
CENT ALPHA (WHITE) AND BETA (GRAY)
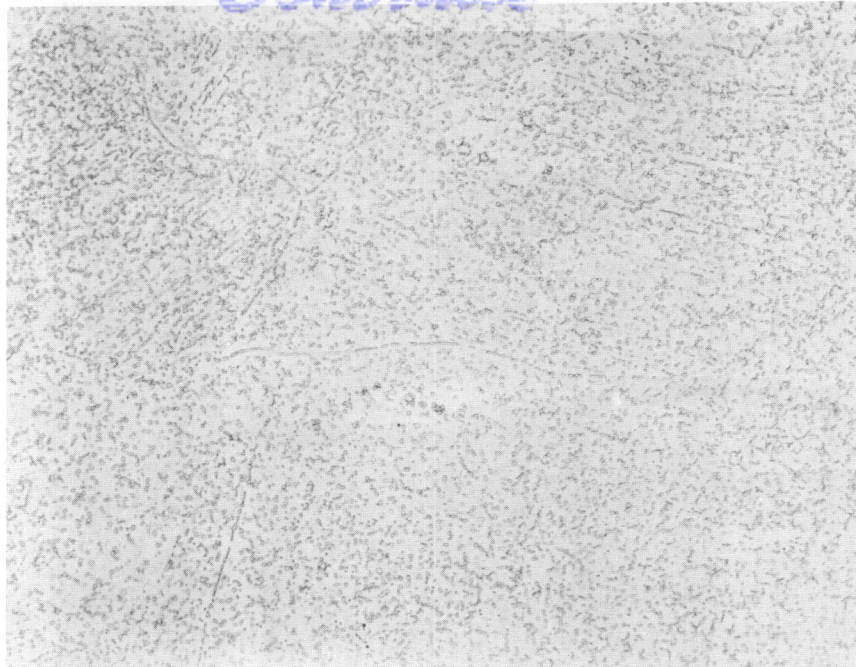
500X   N31434

FIGURE 18. MICROSTRUCTURE OF VACUUM-ANNEALED Ti-20V (K-6)
SHOWING SMALL PARTICLES OF ALPHA IN A MATRIX
OF COARSE GRAINED BETA
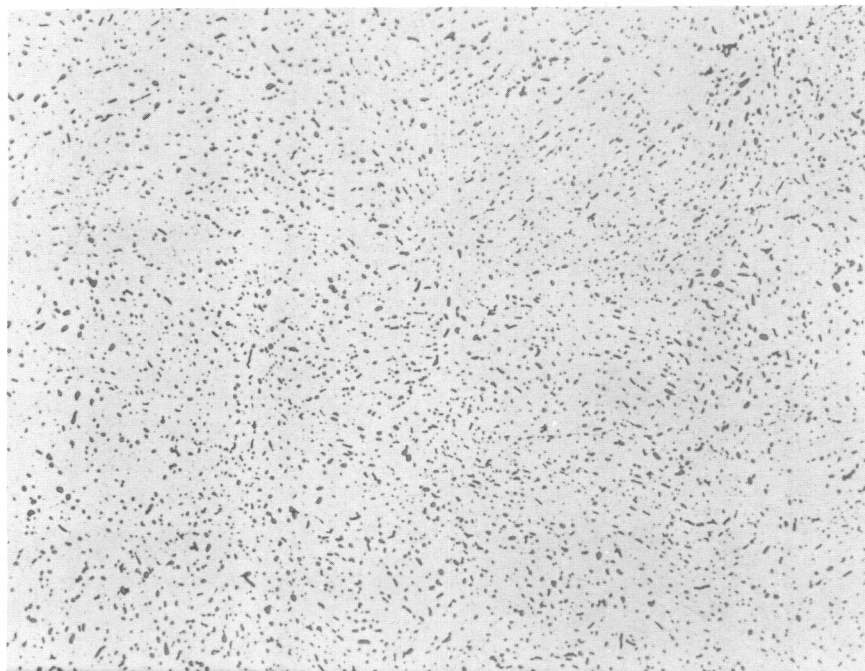
500X   N31431

FIGURE 19. MICROSTRUCTURE OF VACUUM-ANNEALED Ti-4Cu
(Ti-19) SHOWING PARTICLES OF COMPOUND
(Ti_2Cu) IN AN ALPHA MATRIX

WADC TR 54-616 Pt IV   50

Alloys were tested in notched impact, fast tension, slow tension, and unnotched stress rupture. Tests were run in the vacuum-annealed condition, and at hydrogen levels selected within 200, 300, 400, 600, and 800 ppm in order to bracket the range in which embrittlement occurred. Two types of embrittlement due to hydrogen were encountered — impact embrittlement and slow-strain embrittlement. Occasionally, both types of embrittlement were observed in the same alloy.

Impact Testing

Impact tests were conducted using the microsample illustrated in Figure 20. This specimen has been shown by extensive comparative tests to give numerical results, in in.-lb, equivalent to those from the standard charpy test, in ft-lb[9]. Impact tests were conducted at 77 F and -40 F using a Tinius-Olsen machine with an impact velocity of 11.37 feet per second. Single-specimen tests were run at each temperature.

Tensile Testing

Tensile tests were conducted using the standard specimen shown in Figure 20. Two strain rates were used, with head-travel velocities of 0.005 inch per minute and 0.5 inch per minute. Yield strengths were determined during testing at the lower speed by means of strain gages and a strain recorder. Two measurements of elongation were made; the conventional elongation between 1/2-inch gage marks was determined. In addition, marks were placed on the shoulder and an elongation measured from these points. This figure is reported as the "extension" and was used to estimate elongation when failure occurred outside the gage marks on the specimen.

Stress-Rupture Testing

Constant-load stress-rupture tests were carried out using the tensile specimen shown in Figure 20. Three specimens were prepared for testing and were loaded at a measured percentage of the ultimate strength as determined in the slow tensile test. If failure did not occur in 250 hours, the specimen was removed from test. Stress, time to failure, elongation, extension (measured as described under "Tensile Testing"), and reduction in area were determined. If a sample failed in 10 or more hours, it was assumed to give a valid indication of rupture behavior. In most cases, attempts were made to induce failures in about 150 hours. A ductile failure under these conditions was assumed to indicate an absence of slow-strain embrittlement tendencies at this hydrogen level. Similarly, a runout
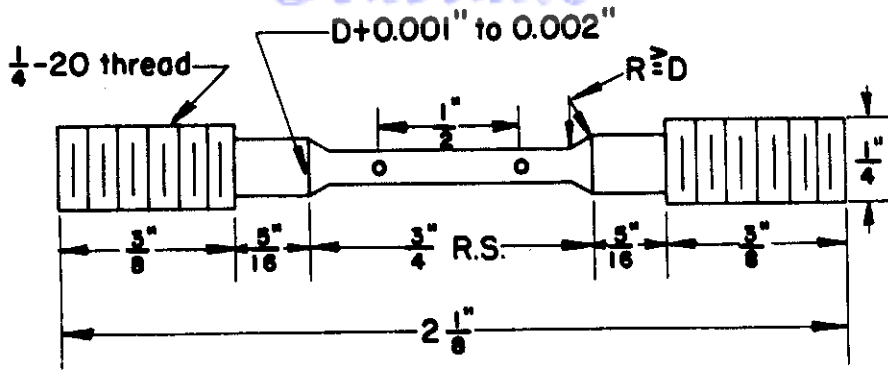
a. Tensile Specimen
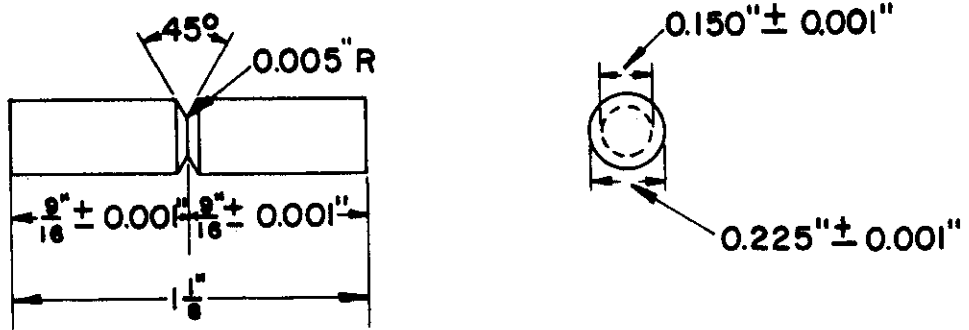
b. Notched-Bend Impact Specimen   A-15291

FIGURE 20. SPECIFICATIONS FOR TEST SPECIMENS

(> 250 hours) in which the elongation during testing exceeded 5 per cent was assumed to indicate that the alloy was not susceptible to slow-strain embrittlement at the level in question.

Other Testing

The broken ends of the impact specimens were used for chemical analysis and microstructural examination. Selected tensile and stress-rupture specimens were also sectioned for microstructural examination after failure.

Test Procedures for Thermal Stability

Thirty of the alloys were exposed to elevated temperatures at two hydrogen levels to determine the effect of hydrogen on thermal stability. The alloys tested are shown in Table 14.

Four tensile specimens of each alloy were prepared, two containing 20 ppm and two containing 200 ppm. All were prepared in the same manner as the alloys described in the previous section, except that the specimens were machined to 0.187-inch diameter. One specimen at each level was exposed in an air atmosphere for 200 hours at 800 F. The other two specimens were given identical exposures while stressed at 25,000 psi. No elongation occurred during exposure. After exposure, the specimens were ground to 0.125-inch diameter and tested in tension at room temperature using a test speed of 0.005 inch per minute. The results of these tests were then compared with those from unexposed specimens tested in the broad survey of effect of composition on embrittlement. A marked loss in ductility, especially of reduction in area, was assumed to indicate thermal instability.

Results

Hydrogen Embrittlement Level of Stabilized Titanium Alloys

Results of all tests conducted on the stabilized alloys are given in the Appendix in Tables 33 through 112. Each table completely describes one alloy, giving the results of impact, tensile, and stress-rupture tests, a concise description of the microstructure, and a conclusion regarding the hydrogen tolerance of the alloy. The tables have been arranged in order of increasing alloy designation number of the alloy being described for ease of location.

TABLE 14. ALLOYS TESTED TO DETERMINE
THE EFFECTS OF HYDROGEN ON
THERMAL STABILITY

Intended Addition, weight per cent	Alloy No.
4Mo	K-1
8Mo	K-2A[a]
4V	K-4
4Mn	K-11
8Mn	K-13
4Fe	K-15
6Cr	K-17
4Cu	K-19
7Cu	K-20
2Cr-2Fe	K-26
3Cr-3Fe	K-27
2Mo-2Cu	K-71
2Mn-2Cu	K-70
2Mo-2Fe	K-30
2Mo-2Cr	K-32
2Mo-2Fe-2Cr	K-33
4Al-4Mo	K-34
6Al-4Mo	K-35
4Al-4V	K-36
6Al-4V	K-37
4Al-4Mn	K-38
6Al-4Mn	K-39
4Al-1.3Cr-1.3Fe-1.3Mo	K-45A[a]
12Sn-4Mo	K-73
12Sn-4Mn	K-75
12Sn-4Cr	K-77
8Mn-sponge plus 0.15 O_2	K-55
7Cu-sponge plus 0.15 O_2	K-79
6Al-4V-sponge plus 0.15 O_2	K-61
4Al-4Mn-sponge plus 0.15 O_2	K-63

(a) Insufficient material was available from these two alloys to complete
the thermal stability tests. One additional 1/2 pound ingot of each
alloy was cast.

In most alloys, it was possible to determine a hydrogen embrittlement level from these tests. Two types of embrittlement were observed: slow-strain embrittlement, usually observed only in stress-rupture tests, and impact embrittlement. Inconclusive results were due either to incomplete testing or to general embrittlement of the alloys. Embrittlement was apparently produced in several alloys as a result of a stabilizing treatment at 1100 F. This was particularly troublesome in chromium-containing alloys, and was apparently a result of eutectoid decomposition of the beta phase.

A new phase, tentatively identified as hydride, was observed in a number of alloys. The hydrogen level at which this phase was observed (when found) and an estimate of the amount of alpha present in the vacuum-annealed and stabilized conditions is given in the microstructural section of the tables.

In the absence of notched-stress-rupture testing, the results reported should not be used to fix a hydrogen tolerance for slow-strain embrittlement. The hydrogen tolerance of these alloys may be 100 to 200 ppm lower in the presence of a severe notch. Notch-stress-rupture testing will be conducted in an extension of this research.

Thermal Stability of
Titanium Alloys

The results of low-speed (0.005 inch per minute) tensile tests carried out on thirty of the alloys after thermal exposure at 800 F for 200 hours are given in the Appendix in Table 113. Properties of the unexposed material may be found in the slow-tensile section in the appropriate tables describing the results of the tests to determine the hydrogen embrittlement level. One of the two alloys which were recast to obtain sufficient material for the thermal stability tests, K-45A, appeared to be considerably different from the original ingot, K-45. Analysis for aluminum, iron, and chromium showed no major differences. Presumably, the difference was due to oxygen. No analysis was made, however.

Discussion of Results

Hydrogen Embrittlement Level of
Stabilized Titanium Alloys

In order to permit comparison of the effects of hydrogen on the various titanium alloys, the data given in the Appendix in Tables 33 through 112 have been summarized in Tables 15 through 18. Two types of embrittlement were observed in these alloys. The first, slow-strain embrittlement, was generally observed in stress-rupture testing, although it was noticed occasionally in slow tensile testing, also. The hydrogen level at which

TABLE 15. HYDROGEN EMBRITTLEMENT LEVEL OF BINARY TITANIUM ALLOYS

Composition (Balance Ti), per cent	Tensile Properties[a]			Hydrogen Embrittlement Level, ppm[c]	
	UTS, 1000 psi	Elongation % in 4D[b]	Volume % Alpha[a]	Slow-Strain	Impact
Beta-Isomorphous Additions					
4Mo	94.8	28	80	800	>800
8Mo	103.4	(29)	60-70	>800	Progressive
20Mo	136.4	16	20	>800	Alloy brittle
4V	103.7	(33)	80	200	>200
8V	113.9	30	60-70	200	Progressive
20V	124.5	11	30	>800	Alloy brittle
4Ta	86.3	26	90	(>400)	200
8Ta	90.8	27	80-90	>800	200
4Nb	89.6	31	80	>800	200
8Nb	91.0	(31)	60-70	600	Progressive
Sluggish Eutectoid Additions					
4Mn	104.3	(36)	70	200	>400
6Mn	118.0	28	60	600	200
8Mn	126.5	26	50	300	200[d]
4Cr	108.3	33	70-80	200	>200
6Cr	123.2	25	60-70	300	>300
8Cr	117.2	31	60-70	600	>600
2Fe	83.8	38	70	>600	200
4Fe	104.3	32	60	200	Alloy brittle
Active Eutectoid Additions					
4Cu	82.2	(33)	90	--	200
7Cu	92.4	23	80	--	(<400)
4Ni	75.1	22	80-90	>800	Alloy brittle
7Ni	98.0	(10)	75	(>400)	Alloy brittle

(a) As measured in vacuum annealed, stabilized alloys. Tensile tests at 0.005 inch per minute.

(b) Elongation values given in parentheses estimated from the measured extension between the shoulders of the tensile specimen.

(c) Hydrogen embrittlement levels given in parentheses estimated from incomplete test results.

(d) Impact ductility recovered at 300 ppm.

Composition (Balance Ti), per cent	Tensile Properties[a]		Volume % Alpha[a]	Hydrogen Embrittlement Level, ppm[c]	
	UTS, 1000 psi	Elongation % in 4D[b]		Slow-Strain	Impact
4Mo	94.8	28	80	800	>800
4Al-4Mo	140.5	16	70-80	>800	200
6Al-4Mo	167.5	18	80	>800	200
12Sn-4Mo	140.7	15	--	(800)	>800
4V	103.7	(33)	80	200	>200
4Al-4V	141.6	18	90	200	>600
6Al-4V	145.0	13	90	>800	>800
12Sn-4V	151.5	23	70-80	(>300)	(<300)
4Mn	104.3	(36)	70	200	200
4Al-4Mn	150.0	20	60-70	(400)	200
6Al-4Mn	172.3	18	80	>800	Alloy brittle
12Sn-4Mn	150.2	26	80	300	(>300)
4Cr	108.3	33	70-80	200	>200
4Al-4Cr	141.6	(10)	80	600	Alloy brittle
6Al-4Cr	166.7	(7)	80	Alloy brittle	Alloy brittle
12Sn-4Cr	149.5	22	80	(>200)	(>200)
2Fe	83.8	38	70	>600	200
4Al-2Fe	127.8	20	80-90	200	200
6Al-2Fe	159.7	17	80-90	600	Alloy brittle
12Sn-2Fe	144.0	17	80	200	200
2Cr-2Fe	101.0	(29)	80	200	200
4Al-2Cr-2Fe	163.4	(21)	70	600	>600
2Cr-2Fe-2Mo	112.8	31	50	(>300)	>300
4Al-1.3Cr-1.3Fe-1.3Mo	171.5	21	80	(400-600)	Alloy brittle
7Cu	92.4	23	80	--	(<400)
4Al-7Cu	141.0	15	80	(300-800)	Alloy brittle
12Sn-7Cu	149.7	9	--	(>200)	Alloy brittle

(a) As measured in vacuum annealed, stabilized alloys. Tensile tests at 0.005 inch per minute.

(b) Elongation values given in parentheses estimated from the measured extension between the shoulders of the tensile specimen.

(c) Hydrogen embrittlement levels given in parentheses estimated from incomplete test results.

TABLE 17. EFFECT OF COMBINATIONS OF ALLOY ADDITIONS ON THE
HYDROGEN EMBRITTLEMENT LEVEL OF TITANIUM ALLOYS

Composition (Balance Ti), per cent	Tensile Properties[a]			Hydrogen Embrittlement Level, ppm[c]	
	UTS, 1000 psi	Elongation, % in 4D[b]	Volume % Alpha[a]	Slow-Strain	Impact
Beta-Isomorphous:Beta-Isomorphous					
20Mo	136.4	16	20	>800	Alloy brittle
8Mo-8V	133.4	(19)	30-40	>800	(<800)
20V	124.5	11	30	>800	Alloy brittle
8Mo	103.4	(29)	60-70	>800	Progressive
4Mo-4V	111.2	34	60-70	800	Progressive
8V	113.9	30	60-70	200	Progressive
4Mo	94.8	28	80	800	>800
2Mo-2V	96.1	33	80	(>400)	>400
4V	103.7	(33)	80	200	>200
Beta-Isomorphous:Sluggish-Euctectoid					
4Mo	94.8	28	80	800	>800
2Mo-2Mn	105.4	27	60	300	>300
4Mn	104.3	(36)	70	200	200
4Mo	94.8	28	80	800	>800
2Mo-2Cr	112.5	28	60-70	300	>300
4Cr	108.3	33	70-80	200	>200
4Mo	94.8	28	80	800	>800
2Mo-2Fe	116.8	31	70	300	300
4Fe	104.3	32	60	200	Alloy brittle
4V	103.7	(33)	80	200	>200
2V-2Fe	102.7	(30)	75	300	>300
4Fe	104.3	32	60	200	Alloy brittle
4Mo	94.8	28	80	800	>800
4Fe	104.3	28	60	200	Alloy brittle
6Cr	123.2	25	60-70	300	>300
2Mo-2Fe-2Cr	112.8	31		(>300)	>300
Sluggish-Eutectoid:Sluggish-Eutectoid					
4Mn	104.3	(36)	70	200	200
2Mn-2Cr	103.2	(33)	80	400	>400
4Cr	108.3	(33)	70-80	200	>200

Composition (Balance Ti), per cent	Tensile Properties[a]		Volume % Alpha[a]	Hydrogen Embrittlement Level, ppm[c]	
	UTS, 1000 psi	Elongation % in 4D[b]		Slow-Strain	Impact
4Mn	104.3	(36)	70	200	200
2Mn-2Fe	102.9	(31)	90	200	200
4Fe	104.3	32	60	200	Alloy brittle
4Cr	108.3	33	70-80	200	>200
2Cr-2Fe	101.0	(29)	80	200	200
4Fe	104.3	32	60	200	Alloy brittle
6Cr	123.2	25	60-70	300	>300
3Cr-3Fe	118.5	(33)	50-60	200	200
4Fe	104.3	32	60	200	Alloy brittle
4Fe	104.3	32	60	200	Alloy brittle
6Mn	118.0	28	60	600	200
6Cr	123.2	25	60-70	300	>300
2Fe-2Mn-2Cr	119.5	(40)	60	200	200
Beta-Isomorphous:Active-Eutectoid					
4Mo	94.8	28	80	800	>800
2Mo-2Cu	97.4	26	90	(>200)	(>200)
4Cu	82.2	(33)	90	--	200
Sluggish-Eutectoid:Active-Eutectoid					
4Mn	104.3	(36)	70	200	200
2Mn-2Cu	97.0	(29)	80-90	(800)	(300-800)
4Cu	82.2	(33)	90	--	200

(a) As measured in vacuum annealed, stabilized alloys. Tensile tests at 0.005 inch per minute.

(b) Elongation values given in parentheses estimated from the measured extension between the shoulders of the tensile specimen.

(c) Hydrogen embrittlement levels given in parentheses estimated from incomplete test results.

TABLE 18. EFFECT OF BASE METAL PURITY ON THE HYDROGEN
EMBRITTLEMENT LEVEL OF TITANIUM ALLOYS

Composition (Balance Ti), per cent	Tensile Properties[a]			Hydrogen Embrittlement Level, ppm[c]	
	UTS, 1000 psi	Elongation % in 4D[b]	Volume % Alpha[a]	Slow-Strain	Impact
4Mo					
Iodide	79.0	29	80	>800	>800
Sponge	94.8	28	80	800	>800
O$_2$ added	118.6	(28)	80	(300-400)	Progressive
20Mo					
Iodide	109.5	30	<5	>800	>800
Sponge	136.4	16	20	>800	Alloy brittle
O$_2$ added	145.4	(12)	30	600[e]	Alloy brittle
4V					
Iodide	76.4	26	80	>400	(200-400)
Sponge	103.7	(33)	80	200	>200
O$_2$ added	113.8	24	80	100	>200
20V					
Iodide	125.0	(10)	<5	>800	>800
Sponge	124.5	11	30	>800	Alloy brittle
O$_2$ added	130.8	(9)	10	(>800)	Alloy brittle
8Mn					
Iodide	117.8	22	50	400	400
Sponge	126.5	26	50	300	200[d]
O$_2$ added	153.8	(31)	60	300	200
6Cr					
Iodide	97.9	23	60-70	>400	>400
Sponge	123.2	25	60-70	300	>300
O$_2$ added	136.4	(24)	60-70	300	200
7Cu					
Iodide	75.0	32	80	>800	200
Sponge	92.4	23	80	--	(<400)
O$_2$ added	110.2	27	80	>800	Alloy brittle
6Al-4Mo					
Iodide	144.3	12	80	>800	>800
Sponge	167.5	18	80	>800	200
O$_2$ added	174.0	(14)	80	>800	Alloy brittle

Composition (Balance Ti), per cent	Tensile Properties[a]			Hydrogen Embrittlement Level, ppm[c]	
	UTS, 1000 psi	Elongation % in 4D[b]	Volume % Alpha[a]	Stress-Strain	Impact
6Al-4V					
Iodide	139.5	8	90	(>600)	>600
Sponge	145.0	13	85-90	>800	>800
O$_2$ added	178.2	(16)	90	600	Alloy brittle
4Al-4Mn					
Iodide	144.3	18	70	(>400)	(<400)
Sponge	150.0	20	60-70	(400)	200
O$_2$ added	161.0	20	80	300	Alloy brittle
4Al-4Fe					
Iodide	139.4	15	70	(300-400)	200
O$_2$ added	172.5	20	70-80	300	Alloy brittle
4Al-4Cr					
Iodide	127.8	15	80	(400)	Alloy brittle
Sponge	141.6	(10)	80	600	Alloy brittle
O$_2$ added	171.5	2	60-70	Alloy brittle	Alloy brittle

(a) As measured in vacuum annealed, stabilized alloys. Tensile tests at 0.005 inch per minute.

(b) Elongation values given in parentheses estimated from the measured extension between the shoulders of the tensile specimen.

(c) Hydrogen embrittlement levels given in parentheses estimated from incomplete test results.

(d) Impact ductility recovered at 300 ppm.

(e) This value may be in error. See Table 81.

slow-strain embrittlement occurred was generally quite obvious, with the level immediately below showing no signs of embrittlement, and the level above showing extensive embrittlement both in slow-tensile and in stress-rupture tests. The second type of embrittlement, impact embrittlement, was more difficult to locate. Three types of impact embrittlement were observed: a definite drop in impact properties at a specific hydrogen level, a gradual loss in impact properties with increasing hydrogen content, and complete impact embrittlement at all levels, including the vacuum-annealed condition. Embrittlement was assumed to have occurred whenever the alloy lost more than 50 per cent of the impact properties exhibited by the vacuum-annealed material or when the impact properties at room temperature dropped below 10 inch-pounds. The three types of embrittlement are believed to be due to hydride precipitation, hydrogen in solution, and general alloy brittleness, respectively.

In addition to designating the hydrogen level at which slow-strain embrittlement and impact embrittlement were observed, the tabulation indicates the tensile properties of the alloys (ultimate strength and elongation) and the amount of alpha present in the alloys. The values given refer to vacuum-annealed material.

The hydrogen embrittlement levels of binary titanium alloys containing molybdenum, vanadium, tantalum, niobium, manganese, iron, chromium, copper, and nickel are shown in Table 15.

Two of the beta-isomorphous alloy additions, molybdenum and niobium, formed alloys which did not show slow-strain embrittlement until large amounts of hydrogen were present. Titanium-vanadium alloys, on the other hand, showed embrittlement at 200 ppm in the alloys containing 4 and 8 per cent vanadium. No slow-strain embrittlement was observed in tantalum-containing alloys. Impact embrittlement was observed at 200 ppm in both tantalum-containing alloys and in the 4 per cent niobium alloy. Three of the alloys showed progressive embrittlement in impact with increasing hydrogen content, 8 per cent molybenum, 8 per cent vanadium, and 8 per cent niobium. This effect is probably due to solution of hydrogen in the beta phase. The 20 per cent molybdenum and vanadium alloys were brittle in impact at all levels, including the vacuum-annealed condition.

It is apparent that the beta-isomorphous additions showed three quite different behavior patterns with respect to hydrogen tolerance. Tantalum additions in the amounts studied resulted in alloys prone to impact embrittlement but apparently free from tendencies toward slow-strain embrittlement. It is possible that tantalum in greater amounts would result in an alloy susceptible to slow-strain embrittlement. Both of the alloys tested were predominately alpha. Molybdenum and niobium alloys tolerated considerable amounts of hydrogen before showing slow-strain embrittlement, but did ultimately become embrittled. Vanadium-containing alloys showed slow-strain embrittlement at quite low hydrogen levels. These latter three

alloys appeared to be relatively free from loss of impact ductility from hydride formation.

The three sluggish-eutectoid additions, manganese, iron, and chromium, also showed somewhat different resistance to hydrogen embrittlement. Increasing chromium additions resulted in progressively increased resistance to slow-strain embrittlement, while no impact embrittlement was observed. The manganese-containing alloys, however, showed a quite different trend. The maximum resistance to slow-strain embrittlement was observed at 6 per cent manganese, with both 4 and 8 per cent manganese alloys showing embrittlement at a lower hydrogen level. The two higher manganese alloys showed impact embrittlement at a low hydrogen level. The 8 per cent alloy recovered impact ductility when the hydrogen content was increased, however. Both iron-containing alloys showed impact embrittlement, and slow-strain embrittlement was observed at a low level in the 4 per cent iron alloy. Except for the low hydrogen level at which slow-strain embrittlement occurred, the behavior of the iron-containing alloys was quite similar to that of the niobium-containing alloys.

Three quite different types of behavior were developed in the sluggish-eutectoid alloys as the hydrogen content was increased. The most difficult to understand is the variation of hydrogen tolerance with composition occurring in the manganese alloys. This effect should probably be considered with some skepticism until confirmed by further work.

The active eutectoid additions, copper and nickel, behaved in a similar manner. Both showed impact embrittlement at low hydrogen levels while being free from slow-strain embrittlement. This is similar to the behavior of pure titanium[10].

Examination of the data given in Table 15 indicates that the hydrogen level at which slow-strain embrittlement is observed in a given alloy system increases as the amount of beta present in the alloy increases. However, if very little beta is present, the tendency toward slow-strain embrittlement may be absent, as shown by the 4 and 8 per cent tantalum, the 4 per cent niobium alloys, the 2 per cent iron alloy, the 4 and 7 per cent copper alloys, and the 4 and 7 per cent nickel alloys. Also, it is apparent that some compositions can retain considerably more hydrogen without ill effects than others. For example, a 4 per cent molybdenum alloy can contain up to 800 ppm hydrogen before embrittlement is observed, while a 4 per cent vanadium alloy shows embrittlement at 200 ppm. Both alloys contained approximately 20 per cent beta. This suggests that slow-strain embrittlement is affected both by the composition and the amount of the phases present.

The hydrogen embrittlement level of ternary alloys containing the alpha-strengthening additions aluminum and tin is shown in Table 16. The addition of aluminum caused the slow-strain embrittlement level to increase in every case. This effect was most apparent when 6 per cent aluminum was added. Presumably, this is due to the increased solubility of hydrogen in

alpha titanium containing aluminum[11], since the amount of beta present either remained constant or was reduced slightly by the addition of aluminum.

The addition of 12 per cent tin to the alloys, roughly equivalent to 4 per cent aluminum in strengthening effect, was less effective than 4 per cent aluminum in increasing the hydrogen tolerance of the alloys. However, a slight improvement was observed in several cases. It seems likely that a larger addition of tin might have resulted in more definite improvement in the hydrogen tolerance of the alloys.

The changes in the hydrogen embrittlement level brought about by the addition of aluminum appear to be of considerable significance. As mentioned above, aluminum is known to promote the retention of hydrogen in binary titanium-aluminum alpha alloys. The addition of aluminum to these alloys, with the resulting formation of a high-aluminum alpha phase (it should be noted that aluminum did not result in any significant increase in the amount of beta phase present in any of the alloys) would be expected to promote increased tolerance to hydrogen. However, the effect of aluminum on the copper-containing alloy was quite unexpected. Previous theories of the mechanism of slow-strain embrittlement in titanium alloys have assumed that embrittlement was due largely to changes in the hydrogen distribution in the beta phase. The fact that the 4 aluminum-7 copper alloy is susceptible to slow-strain embrittlement indicates that the source of embrittlement, at least in this alloy, is hydrogen in the alpha phase, since no beta was present in the alloy.

The results of combining two or more alloy additions on the hydrogen embrittlement level are shown in Table 17. As might be expected, the embrittlement level of a ternary or quaternary alloy fell at an intermediate level between the embrittlement levels of the component alloy additions. In most cases, the embrittlement level was closer to that of the lower of the parent additions, as shown, for example, in the 2Mo-2Fe alloy.

The results of the investigation of the effect of base-metal purity on the hydrogen embrittlement level are shown in Table 18. In every case, increasing the metal purity raised the hydrogen level at which slow-strain embrittlement was observed. Since oxygen is known to partition chiefly to the alpha phase, these data also suggest, as did the results obtained from the alloys containing aluminum, that slow-strain embrittlement can be quite strongly affected by the composition of the alpha phase.

Although it is difficult to compare all the additions since such things as amount of alpha and beta, strength level, and microstructural variations (alpha grain size, etc.) would be expected to have an important effect, it is apparent that the slow-strain embrittlement level is high when aluminum, molybdenum, and niobium are added. Chromium beta phase in sufficient amounts is beneficial. Alloys containing vanadium and iron showed quite low embrittlement levels, while manganese appeared intermediate between chromium

and vanadium in its effect on slow-strain embrittlement. Tin in the amounts added had little effect on slow-strain embrittlement level. No slow-strain embrittlement was observed in copper, nickel, or tantalum-containing alloys. However, larger amounts of tantalum might have resulted in alloys susceptible to slow-strain embrittlement.

By examining the data in Tables 15 through 18, it is possible to rank the various additions as to their effect on slow-strain embrittlement level in alpha-beta alloys somewhat as follows:

Additions which result in high level (decreasing tolerance) Al, Mo, Nb
Additions which result in lower level (decreasing tolerance) Cr, Mn, Fe, V
Additions which showed no slow-strain embrittlement   Cu, Ni
Additions for which results were inclusive   Ta, Sn

Oxygen, which is not included in the tabulation, lowered the slow-strain embrittlement level in all alloys tested.

A further ranking of the additions can be made by comparing the results in the more complex alloys, as, for example, Ti-4Al-4V, Ti-4Al-4Cr, Ti-4Al-4Mn, and Ti-4Al-2Fe, which suggest that the four beta stabilizing additions might be arranged, in order of decreasing embrittlement level, as follows: chromium, manganese, vanadium, and iron.

The effect of alloy addition on impact properties is also of interest. Binary alloys containing tantalum, niobium, manganese, iron, copper, and nickel showed definite impact embrittlement due to hydride formation. Binary alloys containing molybdenum, vanadium, and chromium did not show impact embrittlement. Ternary alloys containing these three additions also appeared to have greater resistance to impact embrittlement, as shown by comparing Ti-2Cr-2Fe with Ti-2Mn-2Fe or Ti-2Mo-2Cu with Ti-2Mn-2Cu.

The data which has been summarized in Tables 15 through 18 should be used only to compare the effects of the various alloy additions. The use of these data to set hydrogen tolerance levels for various alloys would, in most cases, result in the selection of a tolerance level from 100 to 200 ppm too high since no notched-stress-rupture tests were run. Notched testing of these alloys will be carried out in additional work with these alloys in order that the hydrogen tolerance may be determined.

The Effect of Hydrogen on
Thermal Stability

The effect of 200 ppm hydrogen on the ability of thirty of the alloys to withstand exposure at 800 F without damage to room-temperature tensile properties was determined. The results of this investigation are given in the Appendix in Table 113. These data are summarized in Table 19.

WADC TR 54-616 Pt IV   65

Composition (Balance Ti)	Exposure Condition[a]	Room Temperature Tensile Properties[c]			
		20 ppm		200 ppm	
		UTS[b]	% RA	UTS[b]	% RA
4Mo	None	94.8	61	95.6	64
	Unstressed	101.1	55	103.2	56
	Stressed	99.2	43	102.2	49
8Mo[d]	None	103.4	58	103.7	76
	Unstressed	104.9	56	109.0	39
	Stressed	104.5	54	109.0	52
4V	None	103.7	56	105.1	57
	Unstressed	110.8	50	111.2	48
	Stressed	109.7	42	110.2	47
4Mn	None	104.3	59	109.8	25
	Unstressed	104.5	42	104.7	41
	Stressed	105.4	42	104.2	41
8Mn	None	126.5	37	130.0	44
	Unstressed	121.7	47	136.3	18
	Stressed	125.8	41	126.5	30
8Mn, O_2 added	None	153.8	49	155.8	50
	Unstressed	154.2	44	150.5	11
	Stressed	155.8	42	155.5	15
4Fe	None	104.3	44	111.1	18
	Unstressed	106.0	25	110.0	24
	Stressed	108.5	15	101.2	23
6Cr	None	123.2	33	122.2	61
	Unstressed	141.2	5	139.7	5
	Stressed	142.3	8	138.7	6
4Cu	None	82.2	45	87.2	38
	Unstressed	77.8	37	79.5	39
	Stressed	77.3	37	84.5	36
7Cu	None	92.4	40	93.7	48
	Unstressed	91.6	28	91.4	43
	Stressed	90.0	42	91.6	48

| Composition (Balance Ti) | Exposure Condition[a] | Room Temperature Tensile Properties[c] | | | |
| | | 20 ppm | | 200 ppm | |
		UTS[b]	% RA	UTS[b]	% RA
7Cu, O_2 added	None	110.2	36	110.6	37
	Unstressed	109.5	34	109.6	39
	Stressed	110.3	36	109.9	27
2Cr-2Fe	None	101.0	39	106.5	50
	Unstressed	106.1	17	108.5	36
	Stressed	107.1	34	108.3	25
3Cr-3Fe	None	118.5	55	123.6	43
	Unstressed	127.5	23	130.0	25
	Stressed	128.9	46	130.7	16
2Mo-2Cu	None	97.4	54	98.0	50
	Unstressed	97.3	53	95.1	47
	Stressed	96.9	53	96.2	48
2Mn-2Cu	None	97.0	38	96.7	38
	Unstressed	93.2	45	92.8	28
	Stressed	94.9	35	97.4	35
2Mo-2Fe	None	116.8	54	117.1	45
	Unstressed	115.8	48	115.2	24
	Stressed	113.8	45	115.8	22
2Mo-2Cr	None	112.5	60	107.0	61
	Unstressed	108.7	50	108.0	45
	Stressed	109.3	50	108.5	41
2Mo-2Fe-2Cr	None	112.8	51	114.2	53
	Unstressed	110.7	48	115.0	42
	Stressed	111.7	44	116.4	34
4Al-4Mo	None	140.5	50	148.3	50
	Unstressed	144.0	49	139.3	48
	Stressed	141.2	49	138.5	50
6Al-4Mo	None	167.5	49	180.0	37
	Unstressed	168.0	45	167.5	50
	Stressed	169.5	44	169.0	49
4Al-4V	None	141.6	43	139.2	48
	Unstressed	135.0	51	139.9	33
	Stressed	134.3	46	137.8	36

| Composition (Balance Ti) | Exposure Condition[a] | Room Temperature Tensile Properties[c] | | | |
| | | 20 ppm | | 200 ppm | |
		UTS[b]	% RA	UTS[b]	% RA
6Al-4V	None	145.0	40	150.1	48
	Unstressed	147.1	45	157.0	35
	Stressed	146.8	42	154.7	37
6Al-4V, O_2 added	None	178.2	23	180.5	39
	Unstressed	174.9	35	182.7	35
	Stressed	174.1	39	183.7	38
4Al-4Mn	None	150.0	43	154.0	43
	Unstressed	151.5	25	152.9	42
	Stressed	151.6	26	153.5	40
4Al-4Mn, O_2 added	None	161.0	51	171.7	30
	Unstressed	163.1	35	171.5	36
	Stressed	162.4	41	171.7	46
6Al-4Mn	None	172.3	26	179.0	46
	Unstressed	173.9	30	176.3	45
	Stressed	175.0	41	177.2	30
4Al-1.3Mo-1.3Fe-1.3Cr[d]	None	171.5	46	172.1	47
	Unstressed	142.8	47	145.7	42
	Stressed	143.4	43	147.6	44
12Sn-4Mo	None	140.7	53	139.6	60
	Unstressed	146.5	44	145.0	50
	Stressed	146.2	53	144.8	47
12Sn-4Mn	None	150.2	48	149.5	50
	Unstressed	150.7	46	150.0	42
	Stressed	151.3	42	150.6	12
12Sn-4Cr	None	149.5	55	147.9	59
	Unstressed	158.8	13	150.6	1
	Stressed	158.0	16	156.4	6

(a) Exposure conditions used were as follows:
   Unstressed: 200 hours at 800 F, in air
   Stressed: 200 hours at 800 F stressed to 25,000 psi, in air.
(b) Ultimate tensile strength given in 1000 psi.
(c) Tested at 0.005 inch per minute head travel. One-half-inch gage length.
(d) These materials recast to obtain sufficient material for testing. The samples exposed at 800 F came from a different heat than the unexposed samples.

Previous work has shown that elevated-temperature exposure of hydrogen-containing alloys can result in increased susceptibility to slow-strain embrittlement with a resulting loss in slow-speed tensile properties after exposure[12].

Using the criterion that a 50 per cent loss in reduction in area is indicative of thermal instability, it is seen that only nine of the thirty alloys showed instability. Of these, only four alloys showed instability at 200 ppm while being stable at the vacuum-annealed hydrogen level. These alloys were Ti-8Mn (both sponge base and alloyed with oxygen), Ti-12Sn-4Mn, and Ti-2Mo-2Fe. The remaining five unstable alloys showed a loss in ductility in both the vacuum-annealed and 200 ppm samples. These alloys were Ti-6Cr, Ti-3Cr-3Fe, Ti-2Cr-2Fe, Ti-12Sn-4Cr, and Ti-4Fe. It is interesting to note that four of the five alloys contained chromium. Previous work has indicated that alloys containing chromium are particularly susceptible to instability due to eutectoid decomposition of the beta phase[13].

References

(9) Holden, F. C., Ogden, H. R., and Jaffee, R. I., "A Micro Notched-Bar Impact Test for Titanium Alloys", Paper No. 47, Presented at ASTM Pacific Area National Meeting (September 17-21, 1956).

(10) Jaffee, R. I., Lenning, G. A., and Craighead, C. M., "Effect of Testing Variables on the Hydrogen Embrittlement of Ti and a Ti-8Mn Alloy", Trans. AIME, 206, 907 (1956).

(11) Lenning, G. A., Berger, L. W., and Jaffee, R. I., "Effect of Hydrogen on the Mechanical Properties of Titanium and Titanium Alloys", Fourth Summary Report from Battelle Memorial Institute to Watertown Arsenal, Contract No. DAI-33-019-505-ORD-(P)-1 (July 31, 1955).

(12) Schwartzberg, F. R., Rahr, W. D., Williams, D. N., and Jaffee, R. I., "Measurement of the Thermal Stability of Titanium Alloys", TML Report No. 55 (October 5, 1956).

(13) Ogden, H. R., Holden, F. C., and Jaffee, R. I., "Effect of Composition and Annealing Treatment on the Thermal Stability of Ti-Cr-Mo Alloys", Paper No. 48, Presented at ASTM Pacific Area National Meeting (September 17-21, 1956).

PHASE III. EFFECT OF MICROSTRUCTURE ON HYDROGEN EMBRITTLEMENT

Summary

Four alpha-beta titanium alloys were examined after various heat treatments to determine the effect of microstructure on the hydrogen content necessary to cause slow-strain embrittlement.

Microstructural variations appeared to exert a definite influence on slow-strain embrittlement level in alpha-beta alloys containing hydrogen. The following trends were observed:

1. Increasing the alpha grain size decreased the hydrogen level at which slow-strain embrittlement was observed. This effect probably was related to the amount of alpha-beta interface present, but may have been affected, at least in part, by changes from an alpha to a beta matrix as the alpha grain size increased.

2. Increasing the final annealing temperature increased the hydrogen level at which slow-strain embrittlement was observed. This probably was the result of an increased amount of beta and to a change in the distribution of hydrogen in the alloy.

3. Acicularity did not appear to change the hydrogen level at which slow-strain embrittlement was observed. Differences in hydrogen tolerance between acicular and equiaxed material appeared to be due primarily to differences in alpha grain size (amount of interface). Since acicular structures tend to be quite coarse, an acicular structure is probably undesirable in an alloy from the standpoint of hydrogen tolerance.

4. Strength level appeared to have little effect on the hydrogen level at which slow-strain embrittlement was observed.

In contrast to the effects of microstructure on slow-strain embrittlement, only slight changes in impact embrittlement level were observed to result from changes in microstructure.

Introduction

Since the tendency toward slow-strain hydrogen embrittlement is believed to be dependent upon the precipitation of hydride in alpha-beta interfaces, microstructural variations should have considerable effect on hydrogen tolerance. That is, a fully stabilized alloy which was embrittled at 200 ppm might be ductile if the grain size was decreased (which would

increase the amount of available alpha-beta interface, and, as a result, decrease continuity of hydride precipitation). Other microstructural variations, such as alpha grain shape (acicular or equiaxed), relative amounts of alpha and beta, and continuity of the matrix phase (alpha or beta), would also be expected to exert an influence on hydrogen tolerance.

The effect of microstructure was examined by comparing the effects of the following microstructural variables on the hydrogen tolerance of four alloys:

(1) Alpha configuration – equiaxed or acicular

(2) Alpha grain size (three alloys only)

(3) Amount and composition of beta – stabilized, solution heat treated, or solution heat treated and aged.

None of these variables was checked independently of the others. In addition, the further variable of different strength level was necessarily introduced. However, several consistent trends could be observed from the test results.

The results of the microstructural study are described in this report. Unfortunately, as was the case in the survey of the effect of composition, not all the work was completed. However, sufficient data are available for fairly definite conclusions to be drawn.

Preparation of the Alloys

Four alloys were used in this investigation: Ti-8Mn, Ti-2Mo-2Cr-2Fe, Ti-6Al-4V, and Ti-4Al-4Mn. The melting and fabrication of these alloys were described in the sections on alloying and melting, fabrication, and vacuum annealing and hydrogenation in the description of work conducted in Phase II (see alloys K-13, K-33, K-37, and K-38). The final heat treatment was varied, however, to give the desired microstructural conditions.

Heat Treatment

Since the fabrication of the alloys was carried out low in the alpha-beta field, the alloys contained equiaxed alpha-beta structures unless heated into the beta field. Also, the grain size was initially quite fine and could be controlled either by length of annealing treatment in the alpha-beta field, or by cooling rate from an anneal in the beta field. Nine microstructural conditions were examined for three of the alloys (Ti-8Mn, Ti-6Al-4V, Ti-4Al-4Mn). These were:

Equiaxed alpha
Stabilized, three different alpha grain sizes
Solution heat treated
Solution heat treated and aged.

Acicular alpha
Stabilized, two different alpha grain sizes
Solution heat treated
Solution heat treated and aged.

Only six microstructural conditions were studied for the fourth alloy (Ti-2Mo-2Cr-2Fe). In this case, only two stabilized specimens were prepared, one equiaxed and one acicular. A complete description of the heat treatments used in preparing the alloys is given in Table 20.

Test Procedures for Hydrogen Embrittlement

With the exception of the addition of one new hydrogen level, 100 ppm, the test procedures used in the study of the effects of microstructure on hydrogen embrittlement were identical with those used in the previously described study of the effect of composition on hydrogen embrittlement.

Results

The heat treatments selected were found to give a wide variation in microstructure. Photomicrographs showing the structure as it appeared in vacuum-annealed material are given in Figures 21 through 24.

Both the Ti-8Mn alloy (Figure 21) and the Ti-2Mo-2Fe-2Cr alloy (Figure 22) seemed to show a tendency toward alpha grain-boundary precipitation. The other two alloys showed little evidence of this tendency (an exception is seen in Ti-4Al-4Mn in one condition, Figure 24 i).

Although all samples were etched in a 1-1/2 HF-3-1/2HNO$_3$-H$_2$O reagent, considerable variation in etch attack occurred. For example, in the Ti-2Mo-2Cr-2Fe alloy shown in Figure 22, the alpha phase etched lighter than the beta phase in c and f, darker than the beta phase in b, and about the same as the beta phase in a, d, and e. This difference in etched appearance causes no difficulty, however, since alpha is easily distinguished by its mode of precipitation. Differences in matrix phase are also apparent in these alloys. All Ti-8Mn and Ti-2Mo-2Cr-2Mn alloys possessed a beta matrix. The matrix phase was different in the various conditions in the Ti-6Al-4V and Ti-4Al-4Mn alloys, however. For example, Figure 23 a and g show an alpha matrix, while Figure 23 h has a beta matrix. A similar difference is apparent in comparing Figure 24 a and Figure 24 g and h.

TABLE 20. HEAT TREATMENTS USED IN MICROSTRUCTURAL STUDIES

| Condition No. | Heat Treatment Schedule[a] | | | |
	Ti-8Mn (K-13)	Ti-2Mo-2Cr-2Fe (K-33)	Ti-6Al-4V (K-37)	Ti-4Al-4Mn (K-38)
1. Equiaxed alpha-beta, stabilized[b]	2 hours at 1300 F, furnace cool to 1100 F, hold 1 hour	2 hours at 1300 F, furnace cool to 1100 F, hold 1 hour	2 hours at 1300 F, furnace cool to 1100 F, hold 1 hour	2 hours at 1300 F, furnace cool to 1100 F, hold 1 hour
2. Equiaxed alpha-beta solution heat treated	2 hours at 1300 F, water quench	2 hours at 1300 F, water quench	2 hours at 1300 F, water quench	2 hours at 1300 F, water quench
3. Equiaxed alpha-beta, solution heat treated and aged	2 hours at 1300 F water quench, 16 hours at 900 F	2 hours at 1300 F, water quench, 16 hours at 900 F	2 hours at 1300 F, water quench, 16 hours at 900 F	2 hours at 1300 F, water quench, 16 hours at 900 F
4. Acicular alpha-beta, stabilized	1 hour at 1520 F, furnace cool to 1100 F, hold 1/2 hour, air cool in argon	1 hour at 1560 F, furnace cool to 1100 F, hold 1/2 hour, air cool in argon	1 hour at 1900 F, furnace cool to 1300 F, hold 1 hour, furnace cool to 1100 F, hold 1 hour, air cool in argon	1 hour at 1790 F, furnace cool to 1100 F, hold 1/2 hour, air cool in argon
5. Acicular alpha-beta, solution heat treated	1 hour at 1520 F, furnace cool to 1300 F, hold 1 hour, water quench in argon	1 hour at 1560 F, furnace cool to 1300 F, hold 1 hour, water quench in argon	1 hour at 1900 F, furnace cool to 1300 F, hold 1 hour, water quench in argon	1 hour at 1790 F, furnace cool to 1300 F, hold 1 hour, water quench in argon
6. Acicular alpha-beta, solution heat treated and aged	1 hour at 1520 F, furnace cool to 1300 F, hold 1 hour, water quench, age 16 hours at 900 F, in argon	1 hour at 1560 F, furnace cool to 1300 F, hold 1 hour, water quench, age 16 hours at 900 F, in argon	1 hour at 1900 F, furnace cool to 1300 F, hold 1 hour, water quench, age 16 hours at 900 F, in argon	1 hour at 1790 F, furnace cool to 1300 F, hold 1 hour, water quench, age 16 hours at 900 F, in argon
7. Fine or medium equiaxed alpha-beta, stabilized	(Fine) 6 hours at 1200 F, furnace cool to 1100 F, hold 1 hour	--	(Medium) 1 hour at 1600 F, furnace cool to 1300 F, hold 1 hour, furnace cool to 1100 F	(Medium) 2 hours at 1700 F, furnace cool to 1300 F, hold 1 hour, furnace cool to 1100 F, hold 1 hour in argon
8. Coarse equiaxed alpha-beta, stabilized	5 hours at 1350 F, furnace cool to 1100 F, hold 1 hour	--	16 hours at 1700 F, furnace cool to 1300 F, hold 1 hour, furnace cool to 1100 F, hold 1 hour, in argon	16 hours at 1700 F, furnace cool to 1300 F, hold 1 hour, furnace cool to 1100 F, hold 1 hour, in argon
9. Fine acicular alpha-beta, stabilized	1 hour at 1520 F, furnace quench to 1200 F, hold 1 hour, furnace cool to 1100 F, in argon	--	1 hour at 1900 F, furnace quench to 1300 F, hold 1/2 hour, furnace cool to 1100 F, hold 1/2 hour, in argon	1 hour at 1790 F, furnace quench to 1300 F, hold 1/2 hour, furnace cool to 1100 F, hold 1/2 hour, in argon

(a) Unless otherwise indicated, all treatments were in air and were concluded by an air cool from the final temperature.
(b) This condition used in comparing the four alloys with the other alloys prepared in Phase II to study the effect of composition on hydrogen embrittlement.

In general, little change in the ratio of alpha to beta was observed in the microstructure. However, it can be assumed on the basis of known phase relationships that the solution heat-treated material contained a larger proportion of beta than either the stabilized or solution heat-treated and aged material. Whether the stabilized material contains a greater or lesser proportion of beta than the solution heat-treated and aged material is difficult to predict, since the approach to equilibrium at the aging temperature is slow.

The results of mechanical tests to determine the hydrogen embrittlement level of these materials are given in the Appendix in Table 114 through 146. Each table also includes a brief statement of the conclusions reached on the basis of the tests reported.

Discussion of Results

The information contained in the Appendix in Tables 114 through 146 relating to the effect of alpha grain size on the hydrogen embrittlement level is shown in Table 21. This table includes a description of the alloy, the tensile properties as vacuum annealed, and the observed hydrogen embrittlement level.

An examination of the data obtained from the nine tests on equiaxed material (as stabilized) shows some difference in effect of grain size on the various alloys, the Ti-8Mn apparently being unaffected by grain size variations, while Ti-6Al-4V and Ti-4Al-4Mn show definitely lowered resistance to slow-strain embrittlement as the alpha particle size increases. This difference might be due to the fact that the Ti-8Mn did not develop an alpha grain size comparable in coarseness to the other two alloys, or to the fact that increasing alpha grain size resulted in a change from an alpha to a beta matrix in Ti-6Al-4V and Ti-4Al-4Mn. The absence of pronounced embrittlement in the medium alpha grain size Ti-8Mn, which also showed a beta matrix, suggests the first explanation is probably correct. Comparison of the effect of alpha grain size of acicular material also suggests that alpha grain size may have an effect on slow-strain embrittlement level. Although no difference due to alpha grain size was observed in Ti-8Mn, and the Ti-6Al-4V data is not sufficiently complete to permit comparison, Ti-4Al-4Mn alloy showed a definite increase in hydrogen embrittlement level as the acicular alpha grain size decreased.

On the basis of the data given in Table 21, it can be concluded that decreasing the alpha grain size will raise the slow-strain embrittlement level. The most probable explanation of this effect on the basis of the available data is that decreasing the alpha grain size increased the amount of alpha-beta interface, which would increase the available area for hydride precipitation and thus decrease the amount of interface which a fixed amount of hydrogen could embrittle.
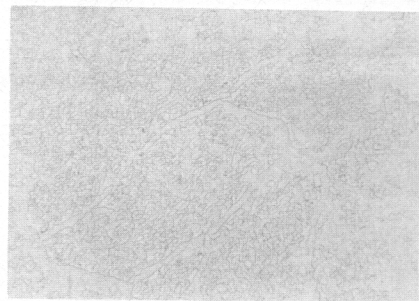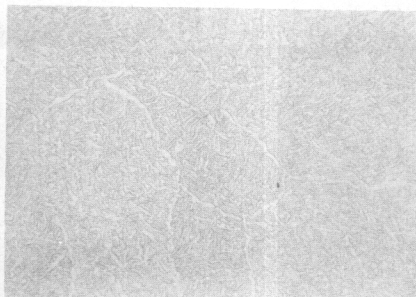
300X   N32167   300X   N32168   300X   N32169

a. Medium Equiaxed Alpha, Stabilized   b. Medium Equiaxed Alpha, Solution Heat Treated   c. Medium Equiaxed Alpha, Solution Heat Treated and Aged
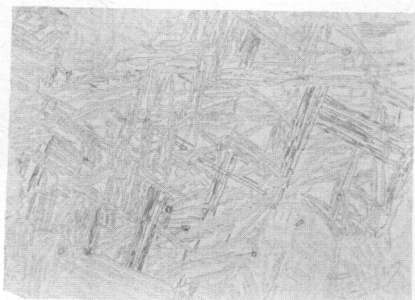
300X   N32170   300X   N32171   300X   N32172
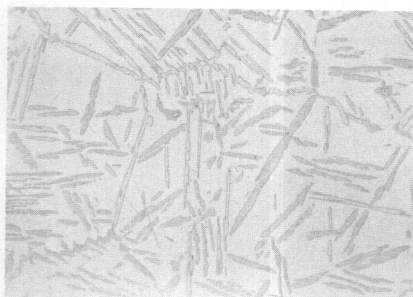
d. Coarse Acicular Alpha, Stabilized   e. Coarse Acicular Alpha, Solution Heat Treated   f. Coarse Acicular Alpha, Solution Heat Treated and Aged

300X   N32153   300X   N32158   300X   N32152
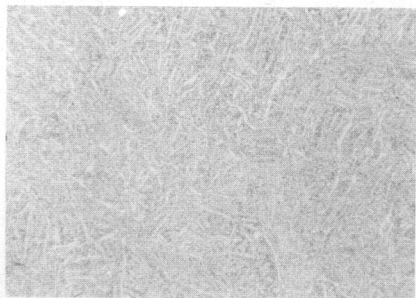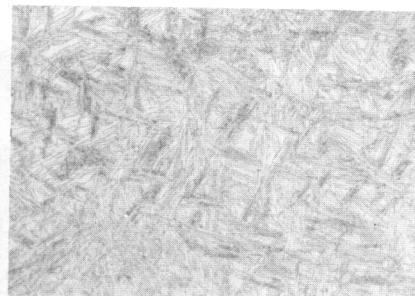
g. Fine Equiaxed Alpha, Stabilized   h. Coarse Equiaxed Alpha, Stabilized   i. Medium Acicular Alpha, Stabilized

FIGURE 21. MICROSTRUCTURES OF Ti-8Mn ALLOY (K-13) IN VARIOUS CONDITIONS

Nominal hydrogen content 20 ppm.
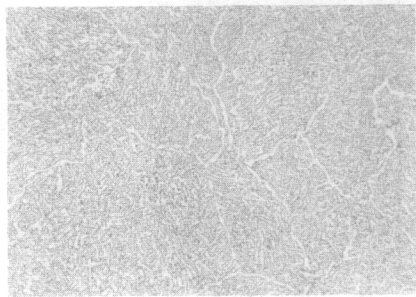
300X   N32173

a. Medium Equiaxed Alpha,
    Stabilized
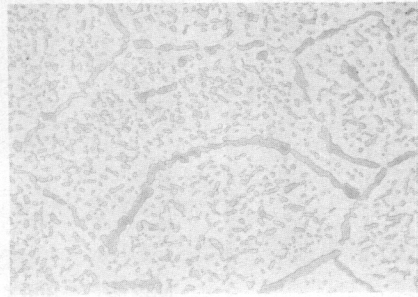
300X   N32174

b. Medium Equiaxed Alpha,
    Solution Heat Treated
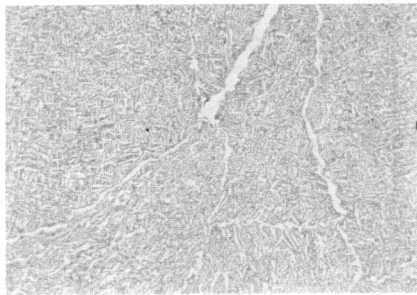
300X   N32175

c. Medium Equiaxed Alpha,
    Solution Heat Treated And Aged

300X   N32176

d. Medium Acicular Alpha,
    Stabilized

300X   N32177

e. Medium Acicular Alpha,
    Solution Heat Treated
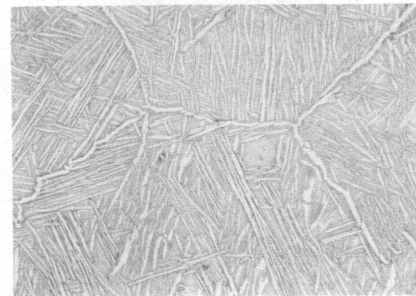
300X   N32178

f. Medium Acicular Alpha,
    Solution Heat Treated and Aged

FIGURE 22.   MICROSTRUCTURES OF Ti-2Mo-2Fe-2Cr ALLOY (K-33) IN VARIOUS CONDITIONS

Nominal hydrogen content 20 ppm.
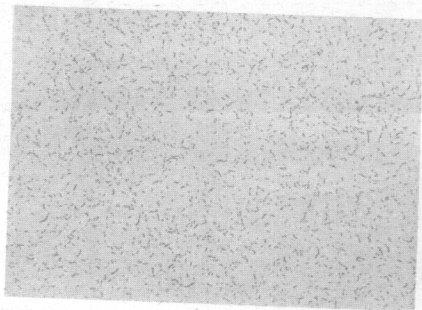
300X   N32179

a. Fine Equiaxed Alpha,
Stabilized
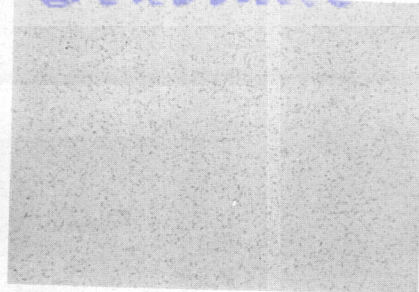
300X   N32180

b. Fine Equiaxed Alpha,
Solution Heat Treated

300X   N32181

c. Fine Equiaxed Alpha,
Solution Heat Treated and Aged
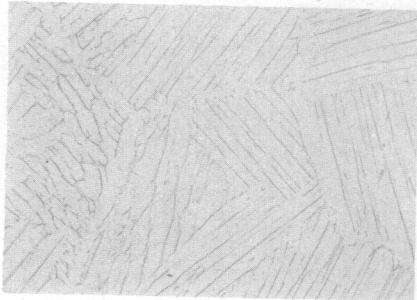
300X   N32182

d. Coarse Acicular Alpha,
Stabilized
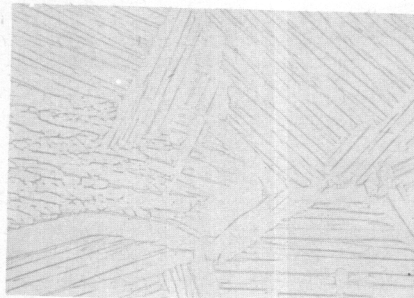
300X   N32183

e. Coarse Acicular Alpha,
Solution Heat Treated
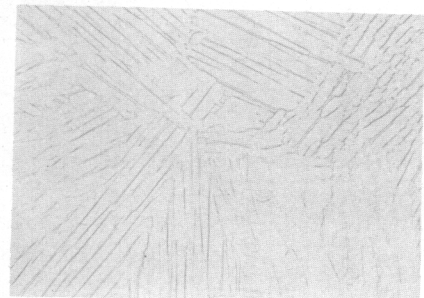
300X   N39356

f. Coarse Acicular Alpha,
Solution Heat Treated and Aged
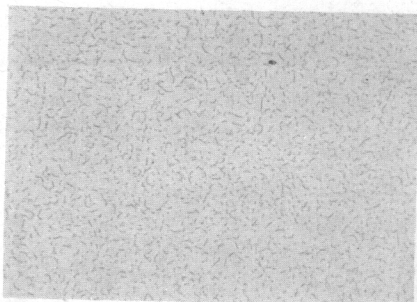
300X   N32157

g. Medium Equiaxed Alpha,
Stabilized
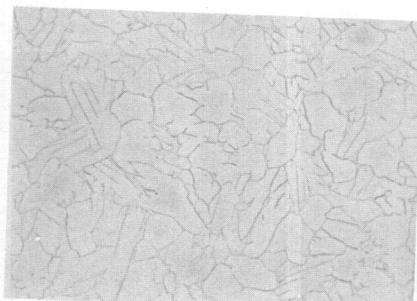
300X   N32159

h. Coarse Equiaxed Alpha,
Stabilized
(Some Areas Very Coarse Acicular Alpha)
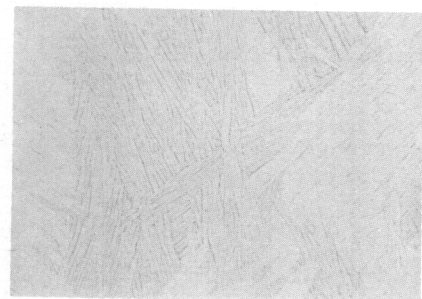
300X   N32154

i. Medium Acicular Alpha,
Stabilized

FIGURE 23. MICROSTRUCTURES OF Ti-6Al-4V ALLOY (K-37) IN VARIOUS CONDITIONS

Nominal hydrogen content 20 ppm.

300X   N32161
a. Fine Equiaxed Alpha,
Stabilized

300X   N32162
b. Fine Equiaxed Alpha,
Solution Heat Treated
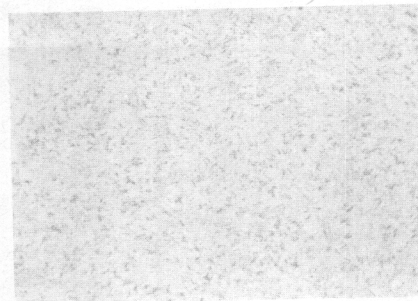
300X   N32163
c. Fine Equiaxed Alpha,
Solution Heat Treated and Aged
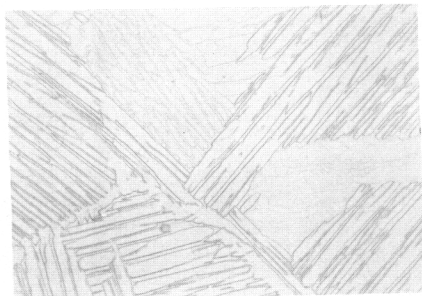
300X   N32164
d. Coarse Acicular Alpha,
Stabilized
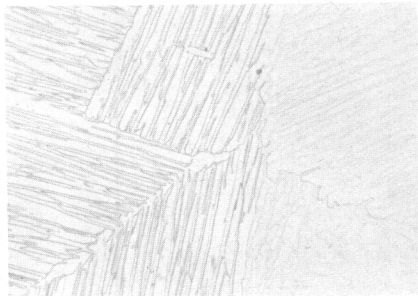
300X   N32165
e. Coarse Acicular Alpha,
Solution Heat Treated
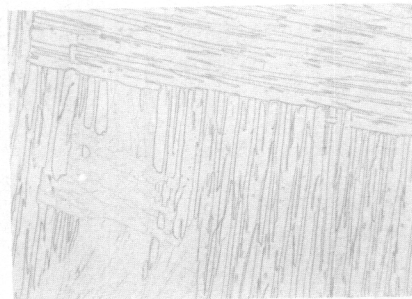
300X   N32166
f. Coarse Acicular Alpha,
Solution Heat Treated and Aged
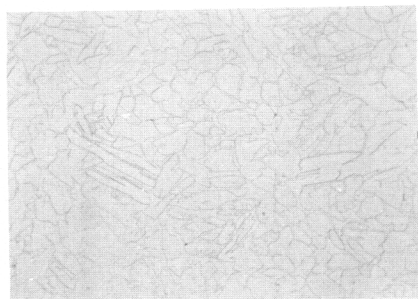
300X   N32155
g. Medium Equiaxed Alpha,
Stabilized

300X   N32160
h. Coarse Equiaxed Alpha,
Stabilized

300X   N32156
i. Fine Acicular Alpha,
Stabilized

FIGURE 24. MICROSTRUCTURES OF Ti-4Al-4Mn ALLOY (K-38) IN VARIOUS CONDITIONS

Nominal hydrogen content 20 ppm.

TABLE 21. EFFECT OF ALPHA GRAIN SIZE ON THE HYDROGEN EMBRITTLEMENT LEVEL OF THREE ALPHA-BETA TITANIUM ALLOYS AS STABILIZED AT 1100 F

Description of Alpha Grain Size[a] Type	Tensile Properties[b]		Volume % Alpha[b]	Hydrogen Embrittlement Level, ppm	
	UTS, 1000 psi	Elongation, % in 4D		Slow Strain[c]	Impact[c]
Titanium-8 Manganese					
Fine (4μ) equiaxed	130.0	32	60	(>200)	200
Medium (6μ) equiaxed	126.5	26	50	300	200[d]
Coarse (8μ) equiaxed	122.4	31	50	300	>300
Medium acicular	123.9	28	50	300	>300
Coarse acicular	120.7	30	50	300	>300
Titanium-6 Aluminum-4 Vanadium					
Fine (6μ) equiaxed	145.0	13	90	>800	>800
Medium (12μ) equiaxed	130.9	(17)	90	(>400)	(>400)
Coarse (24μ) equiaxed[e]	149.9	9	90	200	>200
Medium acicular	139.4	13	95	(>400)	(>200)
Coarse acicular	139.0	12	90	(800)	(>600)
Titanium-4 Aluminum-4 Manganese					
Fine (4μ) equiaxed	150.0	20	60-70	600	>600
Medium (16μ) equiaxed	134.5	24	60	(>300)	(>300)
Coarse (24μ) equiaxed	132.8	(21)	60	(100-200)	(>200)
Fine acicular	148.7	13	--	(>300)	(>300)
Coarse acicular	143.5	10	60-70	200	>200

(a) Grain diameter, in microns, given for equiaxed alpha.
(b) Tensile properties and per cent alpha determined from vacuum annealed material. Low speed (0.005 inch per minute) tensile test. Elongation values in parentheses estimated from extension between shoulders of specimen.
(c) Values in parentheses from incompleted tests.
(d) Impact ductility recovered at 300 ppm.
(e) Some regions in this material showed very coarse acicular alpha.

The information given in the Appendix in Tables 112 through 146 relating to the effect of amount and composition of beta, with both equiaxed and acicular alpha grain shapes, is summarized in Table 22. A pronounced tendency for the solution heat-treated material to show the greatest resistance to slow-strain embrittlement, while the solution heat treated and aged showed the least, was observed in all the alloys. The impact embrittlement also appeared to be slightly sensitive to heat treatment, with the solution heat treated and aged material showing impact embrittlement at a lower hydrogen level than the other material.

The tendency toward slow-strain embrittlement apparently increases as the final annealing temperature is decreased. This suggests that heat treatment affects embrittlement either by altering the alpha-beta ratio or by altering the hydrogen distribution between alpha and beta. The high tolerance of the solution heat-treated material is probably due chiefly to the increased amount of beta present. However, it is unlikely that the same reasoning would apply to the difference between fully stabilized and solution heat-treated and aged materials. This difference may be due to a tendency toward an increasingly unfavorable distribution of hydrogen between alpha and beta as the final annealing temperature is decreased or to a tendency toward microsegregation of hydrogen as the temperature is decreased. Thermal exposure at moderately low temperatures is also capable of altering the susceptibility to slow-strain embrittlement.

With the exception of the equiaxed Ti-2Mo-2Fe-2Cr samples, the strength variations showed the expected trend, with the solution heat-treated and aged material being strongest and the stabilized material weakest. No consistent effect of strength level on embrittlement tendencies is apparent. However, it is possible that the difference in slow-strain embrittlement level between stabilized and solution heat-treated and aged material is due at least in part to the difference in tensile properties.

A comparison of the embrittlement level of acicular material with that of equiaxed material in equivalent conditions suggests that acicularity lowers the hydrogen tolerance of these alloys. However, this is probably an incorrect interpretation of the data, since in every case the acicular material had a considerably coarser alpha grain size than the corresponding equiaxed material. Comparison of the acicular with the coarse equiaxed material in the stabilized condition (see Table 21) shows that acicularity in itself is probably not detrimental except insofar as it tends to result in a coarser alpha structure.

As was pointed out in the previous discussion of the Phase II work, data included in this report should not be used to set hydrogen tolerance levels for the various heat-treated conditions. Notch stress-rupture testing will be carried out to determine the hydrogen tolerance of all materials.

TABLE 22. EFFECT OF HEAT TREATMENT ON THE HYDROGEN EMBRITTLEMENT LEVEL
OF FOUR ALPHA-BETA TITANIUM ALLOYS

Description of Heat Treatment			Tensile Properties[a]		Volume % Alpha[a]	Hydrogen Embrittlement Level, ppm	
Type	Final Temperature, F	Type of Alpha	UTS, 1000 psi	Elongation % in 4D		Slow-Strain[b]	Impact[b]
Titanium-8 Manganese							
Solution heat treated	1300	Equiaxed	140.6	16	50	(400-600)	200
Stabilized	1100	Equiaxed	126.5	26	50	300	200[c]
Solution heat treated and aged	900	Equiaxed	162.5	(18)	50	200	Alloy brittle
Solution heat treated	1300	Acicular	144.5	26	30	(>400)	200
Stabilized	1100	Acicular	123.9	28	50	300	>300
Solution heat treated and aged	900	Acicular	154.4	(19)	30	100	Alloy brittle
Titanium-2 Molybdenum-2 Iron-2 Chromium							
Solution heat treated	1300	Equiaxed	159.5	20	40	(300-600)	(<600)
Stabilized	1100	Equiaxed	112.8	(31)	50	(>300)	(>300)
Solution heat treated and aged	900	Equiaxed	123.5	24	30	300	200
Solution heat treated	1300	Acicular	124.5	(24)	40	400	>400
Stabilized	1100	Acicular	107.4	(30)	60	400	>400
Solution heat treated and aged	900	Acicular	131.8	(14)	50	200	100
Titanium-6 Aluminum-4 Vanadium							
Solution heat treated	1300	Equiaxed	144.5	14	90	800	800
Stabilized	1100	Equiaxed	145.0	13	85-90	>800	>800
Solution heat treated and aged	900	Equiaxed	152.7	(14)	90	(>400)	(>400)
Solution heat treated	1300	Acicular	133.3	(12)	90	800	>800
Stabilized	1100	Acicular	139.0	12	90	(800)	(>600)
Solution heat treated and aged	900	Acicular	135.5[d]	21[d]	90	(300-400)	(>400)
Titanium-4 Aluminum-4 Manganese							
Solution heat treated	1300	Equiaxed	152.0	(21)	60	(>800)	>800
Stabilized	1100	Equiaxed	150.0	20	60-70	600	>600
Solution heat treated and aged	900	Equiaxed	162.1	(16)	--	200	Alloy brittle
Solution heat treated	1300	Acicular	148.8	12	60	>800	>800
Stabilized	1100	Acicular	143.5	10	60-70	200	>200
Solution heat treated and aged	900	Acicular	159.3	10	60	200	100

(a) Tensile properties and per cent alpha from vacuum annealed material. Low speed tensile tests. Elongation values in parentheses estimated from extension between shoulders of specimen.
(b) Values in parentheses from incomplete tests.
(c) Impact ductility recovered at 300 ppm.
(d) Tensile properties from sample showing equiaxed structure (see Table 134).

PHASE IV. REMOVAL OF HYDROGEN FROM TITANIUM
AND TITANIUM ALLOYS

Summary

The degassing of alpha titanium in the range 1110 to 1560 F is not a true diffusion process. The degassing coefficients are lower than the diffusion coefficients for hydrogen. Probably desorption of hydrogen from the metal surface is the controlling process during degassing. Apparently surface effects are negligible in degassing beta titanium at 1650 and 1870 F since the degassing and diffusion coefficients are in good agreement. Degassing rates of the titanium alloys investigated were less than those for titanium.

Factors which were found to affect the degassing rate of titanium and its alloys are (1) specimen size and (2) thick oxide films. Degassing rates at 1290 F of specimens of commercial titanium (high interstitial) with diameters equal to or less than 0.12 inch varied directly with the diameter (probably desorption controlled) while degassing rates of specimens greater than 0.12 inch in diameter varied inversely as the square of the diameter (diffusion controlled). Oxide films about 0.0001 inch thick decrease the degassing rate at 1290 F of iodide and commercial titanium (high interstitial) and Ti-8Mn alloy.

The solubility of hydrogen in titanium and its alloys in the range 1110 to 1830 F at pressures of 0.05 to 10 microns of mercury follows the square root or Sieverts' law. For the titanium alloys the solubility increases with increasing amount of beta phase present from alloy to alloy at the same temperature and pressure.

The removal of hydrogen from commercial titanium (low interstitial) at 1290 F using an argon sweep requires rapid flow rates to lower the hydrogen content to a reasonable level. Therefore, the technique is not feasible for degassing large amounts of titanium because of the large volume of argon required.

Introduction

The presence of hydrogen in titanium and titanium alloys has detrimental effects on the mechanical properties of the metal[14, 15, 16]. The hydrogen content of commercial titanium is often of the order of 200 ppm by weight[17] and varies with alloy composition. As a consequence, titanium and some titanium alloys as normally processed are not ductile unless treated to lower the hydrogen content. The best known hydrogen removal treatment is heating the material in a vacuum. The rate of

WADC TR 54-616 Pt IV   82

removal (degassing) at a given time determines the duration of the treatment required to attain a satisfactory low hydrogen level. The partial pressure of hydrogen in the system during this treatment determines the lowest hydrogen content that can be obtained at equilibrium at the given temperature.

The present investigation was made to determine the rates of degassing and the low-pressure, equilibrium solubility of hydrogen in titanium and its alloys. The temperature range 1110 to 1832 F was investigated.

Consideration was also given to an inert gas sweep method for the removal of hydrogen.

Materials

Materials used in this investigation were annealed 5/8-inch-diameter rods of commercial titanium and various commercial titanium alloys, and a 3/8-inch-diameter rod of arc-melted iodide titanium. A list of the materials is given in Table 23 along with the producer's analysis.

Rods 3/8 and 3/16 inch in diameter were swaged from some of the stock material. The rods were machined to remove any oxide film and then cut into specimens 1 inch (2.5 cm) long. All specimens were given a final dry abrasion with 240-grit silicon carbide paper and washed in ACS Reagent-grade acetone.

Degassing Rates

Method

The method to measure degassing rates has been previously described[17]. Essentially it consists of heating a cylindrical specimen in a vacuum furnace attached to a gas-analysis apparatus. The hydrogen evolved is collected, measured, and analyzed periodically. Degassing is continued until the gas evolution ceases. The residual hydrogen content amounts to about three parts per million (ppm) or one to two per cent of the initial hydrogen content.

Degassing rate data were used to calculate the degassing coefficient of hydrogen in the specimen under specific degassing conditions. The method is based upon the general solution of Fick's diffusion law for round wires[18]. From the general solution, an equation was derived for the

TABLE 23. ANALYSIS OF TITANIUM AND TITANIUM ALLOYS

Material Nominal Composition, weight per cent	Element, weight per cent							
	C	N	Mn	Al	Sn	Fe	Cr	Mo
Iodide titanium(a)	0.011	0.003	0.007	<0.005	0.005	0.001	<0.01	0.005
Commercial titanium (low-interstitial)	0.04	0.02	--	--	--	--	--	--
Commercial titanium (high-interstitial)	0.03	0.05	--	--	--	--	--	--
Ti-4Mn-4Al	0.03	0.03	3.0	3.0	--	--	--	--
Ti-8Mn	0.12	0.03	7.1	--	--	--	--	--
Ti-5Al-2.5Sn	0.06	0.02	--	4.7	2.8	--	--	--
Ti-3Al-5Cr	0.05	0.036	--	3.47	--	0.31	4.94	--
Ti-2Fe-2Mo-2Cr	0.025	0.025	--	--	--	2.47	2.12	2.11

(a) Other elements present: Zr 0.1, Si 0.005, Ni 0.006, Cu 0.005, and O_2 0.018.

conditions where the radius and length of a wire are not equal. For long times of degassing in vacuum the solution may be simplified to

$$\log C/C_O = -0.252 - \left(\frac{4.28}{\ell^2} + \frac{2.52}{R^2} \right) Dt \qquad (1)$$

where

C/C_O = fraction of initial hydrogen content, (C_O), remaining at any time, t

t = time in seconds

R = radius, cm

ℓ = length, cm

D = degassing coefficient, cm^2/sec.

The logarithm of C/C_O, the fraction of hydrogen remaining, was plotted against t, time. The slope of this plot is $(4.28/\ell^2 + 2.52/R^2) D$ from which D, the degassing coefficient, can be calculated.

Results and Discussion

Iodide Titanium. Initial studies were made with iodide titanium. The degassing rates for this material were to serve as reference points to determine the effect of alloy composition on the degassing rates of the alloys. Cylindrical specimens 0.36 inch (0.92 cm) in diameter were used. Data for alpha iodide titanium were obtained in the range 1110 to 1560 F. Degassing coefficients for beta iodide titanium were determined at 1650 and 1870 F. The results are given in Table 24. The diffusion coefficients obtained from concentration gradients by Wasilewski and Kehl[19] are also given for comparison.

The degassing coefficient of hydrogen in alpha iodide titanium varied with temperature in the range from 1200 to 1560 F according to the equation

$$\log D = \frac{-2790}{T\ (K)} - 1.84. \qquad (2)$$

TABLE 24. DEGASSING AND DIFFUSION COEFFICIENTS FOR HYDROGEN IN ALPHA AND BETA IODIDE TITANIUM

Temperature, F	Phase	Degassing Coefficient, 10^{-5} cm^2/sec	Diffusion Coefficient[a], 10^{-5} cm^2/sec
1200	Alpha	1.3	2.0
1290	Alpha	2.0	3.0
1380	Alpha	2.7	4.0
1470	Alpha	3.5	5.2
1560	Alpha	4.8	7.0
1650	Beta	10.	11.
1870	Beta	14.	15.

(a) From work of Wasilewski and Kehl[19].

At temperatures below about 1200 F, the experimental degassing rates were slower than those calculated from an extrapolation of Equation (2). The degassing rates determined at 1110 and 1150 F and the extrapolated values are compared below.

Temperature, F	Degassing Coefficient, 10^{-5} cm^2/sec	
	Experimental	Calculated
1110	0.4	0.9
1150	0.7	1.1

In addition, all the degassing coefficients are somewhat lower than the diffusion coefficients obtained by Wasilewski and Kehl. Theoretically, the degassing and diffusion coefficients should be the same unless a boundary condition existing at the metal surface slows removal of hydrogen. In other studies it was found that very thin oxide films inhibited certain surface reactions. Resulting induction periods for reaction were eliminated by dissolving the films in the specimen at 1470 F. To determine the effect of extremely thin invisible oxide films on degassing, a clean abraded speci- men was heated to 1470 F in less than two minutes and held there for three minutes which time should have been sufficient to dissolve any oxide film which may have formed subsequent to abrasion. The specimen then was cooled to 1112 F and the degassing rate determined at that temperature. The rate was found to be the same as that for similar specimens heated to 1110 F only. These data suggest that the slow degassing was not caused by an extremely thin surface oxide film. However, the probability remains that other surface effects regulate the degassing process. Thus, desorption of hydrogen from the metal surface may be the controlling step and not diffusion in the metal. As an example, very little or no hydrogen can be

extracted from a zirconium cylinder at temperatures below 1165 F at pressures of the order of 10^{-5} mm of mercury, while it is known that hydrogen can diffuse into the metal at lower temperatures as is shown by the gradient method[20].

It is seen in Table 24, that the degassing and diffusion coefficients of hydrogen in beta-iodide titanium determined by the two methods are in good agreement. It is likely that surface effects are negligible in the degassing of iodide titanium at temperatures in the beta range.

Commercial Titanium and Alloys. The degassing coefficients of hydrogen in the commercial titanium (high interstitial), Ti-8Mn, and Ti-4Mn-4Al alloys were determined in the range 1110 to 1470 F. Coefficients were obtained for the commercial titanium (low interstitial), Ti-5Al-2.5Sn, Ti-2Fe-2Mo-2Cr, and Ti-3Al-5Cr alloys at 1290 F. The results are given in Table 25. For comparison, the degassing coefficients of iodide titanium are included.

TABLE 25. DEGASSING COEFFICIENTS OF
HYDROGEN IN TITANIUM ALLOYS

Alloy Designation	Degassing Coefficient, 10^{-5} cm^2/sec, at Indicated Temperature			
	1110 F	1290 F[a]	1470 F	1650 F
Iodide titanium	0.4	2.0	3.5	10
Commercial titanium (high interstitial)	0.7	1.4	2.6	7.2
Ti-4Mn-4Al	1.0	1.6	2.6	--
Ti-5Al-2.5Sn	0.8	1.7	--	--
Ti-8Mn	0.7	0.9	1.5	--
Commercial titanium (low interstitial)	--	1.0	--	--
Ti-2Fe-2Mo-2Cr	--	1.2	--	--
Ti-3Al-5Cr	--	1.0	--	--

(a) Duplicate determinations at 1290 F agree to about $\pm 0.2 \times 10^{-5}$ cm^2/sec.

It is seen that all of the commercial titanium and titanium alloys degas more slowly than does iodide titanium, except at 1110 F where iodide titanium has an abnormally low degassing rate. Since all of the alloys investigated were solid solutions, equiaxed alpha-beta type, the alloying constituents would be expected to block interstitial sites in the titanium structure. This slows the movement of the interstitial hydrogen atoms through the lattice which in turn decreases the degassing rate.

The equations for the variation of degassing coefficient with temperature for the alloys covering the range 1110 to 1470 F were calculated by the method of least squares. The equations for degassing coefficient, D, in cm^2/sec are:

for commercial titanium (high interstitial)

$$\log D = -2700/T(^\circ K) - 2.03, \tag{3}$$

for Ti-8Mn alloy,

$$\log D = 1510/T(^\circ K) - 3.44, \tag{4}$$

and for Ti-4Mn-4Al alloy,

$$\log D = 1970/T(^\circ K) - 2.74. \tag{5}$$

To determine if microstructure affected the degassing rate, a specimen of Ti-8Mn alloy was heat treated to produce an acicular microstructure and then degassed. The degassing rate of this specimen at 1290 F was the same as that of specimens of the same alloy having an equiaxed alpha-beta structure. Thus, microstructure had no observable effect on the rate of removal of hydrogen from titanium. This would be expected since volume diffusion is dependent only upon temperature and the phase constitution of the material. Concentration of one phase in the grain boundaries may, of course, lead to different results.

Further experiments were made with commercial titanium (high interstitial) to determine whether there is an effect of specimen dimension on the degassing coefficient. Coefficients were obtained from cylinders of various diameters at 1290 F. The results are given in Table 26. Degassing coefficients for specimens having diameters of 0.36 inch (0.92 cm) and 0.24 inch (0.61 cm) are the same. Also the degassing rates varied inversely with the square of the diameter. These results indicate that the degassing is diffusion controlled for specimens in this size range. However, it is seen from Table 26 that the degassing coefficients for small-diameter specimens decrease with decreasing specimen diameter. The degassing coefficient appears to vary directly with the diameter of the specimen. Since the diameter of a long cylinder (thereby the degassing coefficient) varies inversely with the surface area to mass ratio, it appears that surface effects (probably desorption) are important in controlling degassing. Apparently for specimens with diameters equal to or less than 0.12 inch (0.30 cm), diffusion in the metal is not rate controlling. This result is not unique. Studies of the diffusion of hydrogen in iron summarized by Johnson and Hill[21] showed that the controlling step in degassing was a function of diameter. Reactions occurring at the surface of iron are rate controlling for diameters of less than 3/8 inch but a true diffusion process is rate controlling for diameters larger than 3/8 inch. It is likely that the degassing of titanium and its alloys is a similar phenomenon.

Specimen Diameter, inch (cm)	Degassing Coefficients, 10^{-5} cm^2/sec
0.36 (0.92)	1.4
0.24 (0.61)	1.3
0.12 (0.30)	0.60
0.059 (0.15)	0.33

The presence of an oxide film on titanium alloys could also hinder the rate of removal of hydrogen from the metal. It was shown above that extremely thin invisible oxide films which may be present on clean abraded specimens did not affect the degassing rate of alpha-iodide titanium at 1110 F. However, it was suspected that thick visible oxide films might decrease the degassing rate. Therefore, the effects of such films on the degassing of iodide titanium, commercial titanium (high interstitial), and Ti-8Mn alloys were investigated. Specimens were heated in air under various conditions to form surface films of different thicknesses. Actual thicknesses of some of the films were not determined since they were too thin to be measured by the usual metallographic techniques.

The degassing rates at 1290 F were determined. It is seen from Table 27 that the degassing coefficients for iodide titanium and commercial titanium (high interstitial) specimens having no oxide film, are not significantly different from those for similar specimens with thin films. However, for specimens having thick films, the degassing coefficient is appreciably smaller. In fact, no measurable degassing was observed for iodide titanium having a thick oxide film. On the basis of these results, it appears that only comparatively thick films, 0.0001 inch (0.0003 cm) or greater, appreciably decrease the degassing rate.

Practical Degassing Curves

As an aid to the solution of practical degassing problems of titanium and titanium alloys, families of curves applicable to the degassing of cylinders and sheets are given in Figures 25 and 26, respectively. The fraction of hydrogen remaining, C/C_o, is plotted versus time. Each line represents a value of the parameter D/a^2 where D is the degassing coefficient in cm^2/sec and "a" is the radius or half-thickness of a cylinder or sheet, respectively.

TABLE 27. THE EFFECT OF SURFACE FILMS ON THE DEGASSING OF TITANIUM AND TITANIUM ALLOYS AT 1290 F

Material	Condition for Film Formation			Degassing Coefficient, 10^{-5} cm^2/sec
	Time, hours	Temperature, F	Oxide Film	
Iodide titanium	0	--	None	2.0
	0.5	750	Very thin	1.8
	1.0	1245	Thin	2.1
	3.0	1455	Thick (0.0001 in.)	None[a]
Commercial titanium (high interstitial)	0	--	None	1.4
	1	1245	Thin	1.9
	3	1455	Thick (0.0001 in.)	0.29
Ti-8Mn	0	--	None	0.90
	3	1455	Thick (0.0001 in.)	0.41

(a) No hydrogen was evolved from the specimen during three hours at temperature.
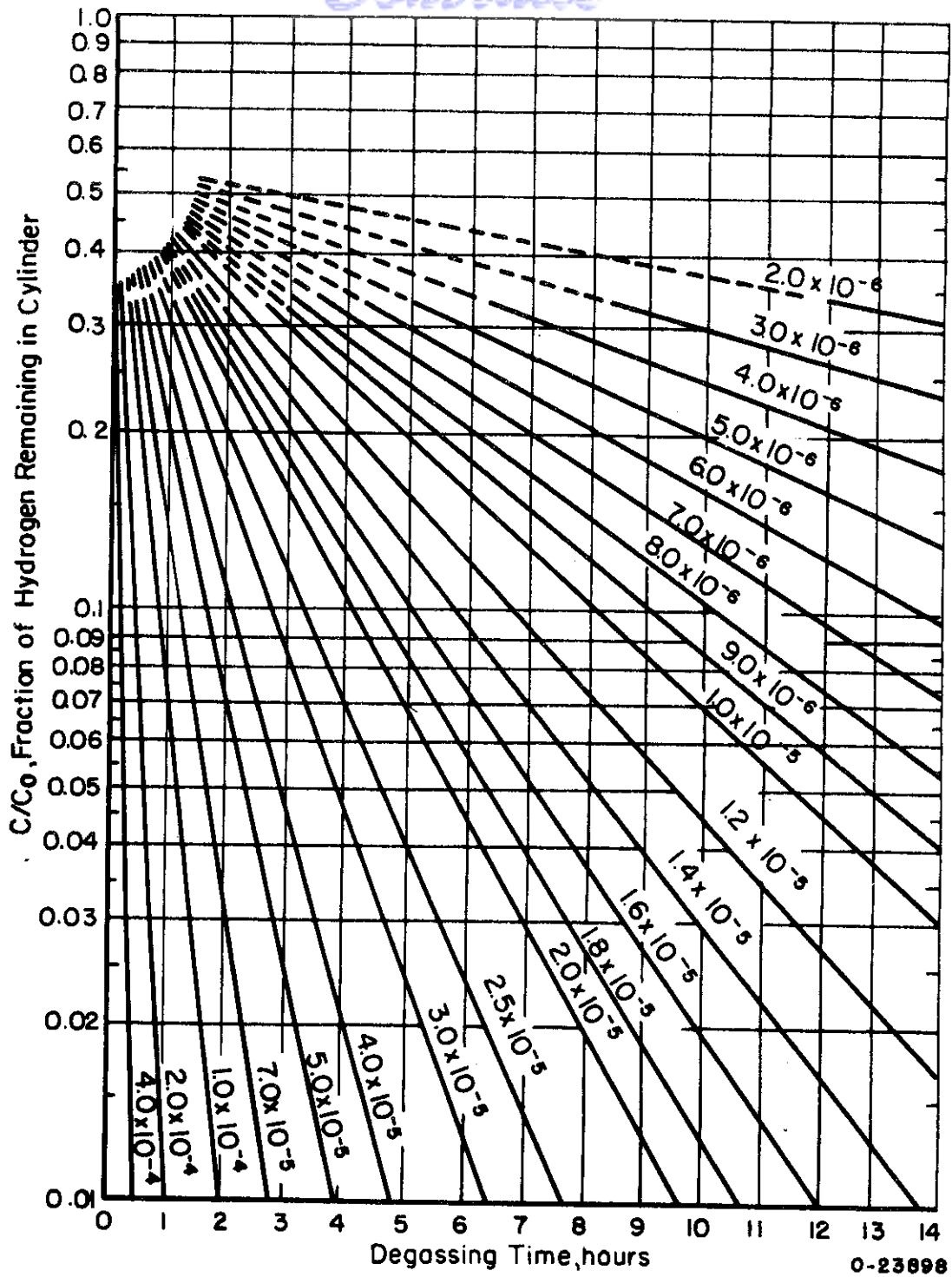
FIGURE 25. VARIATION OF FRACTION OF HYDROGEN REMAINING
WITH TIME FOR CYLINDERS OF VARIOUS RADII

The numbers on the lines are values of D/a^2.
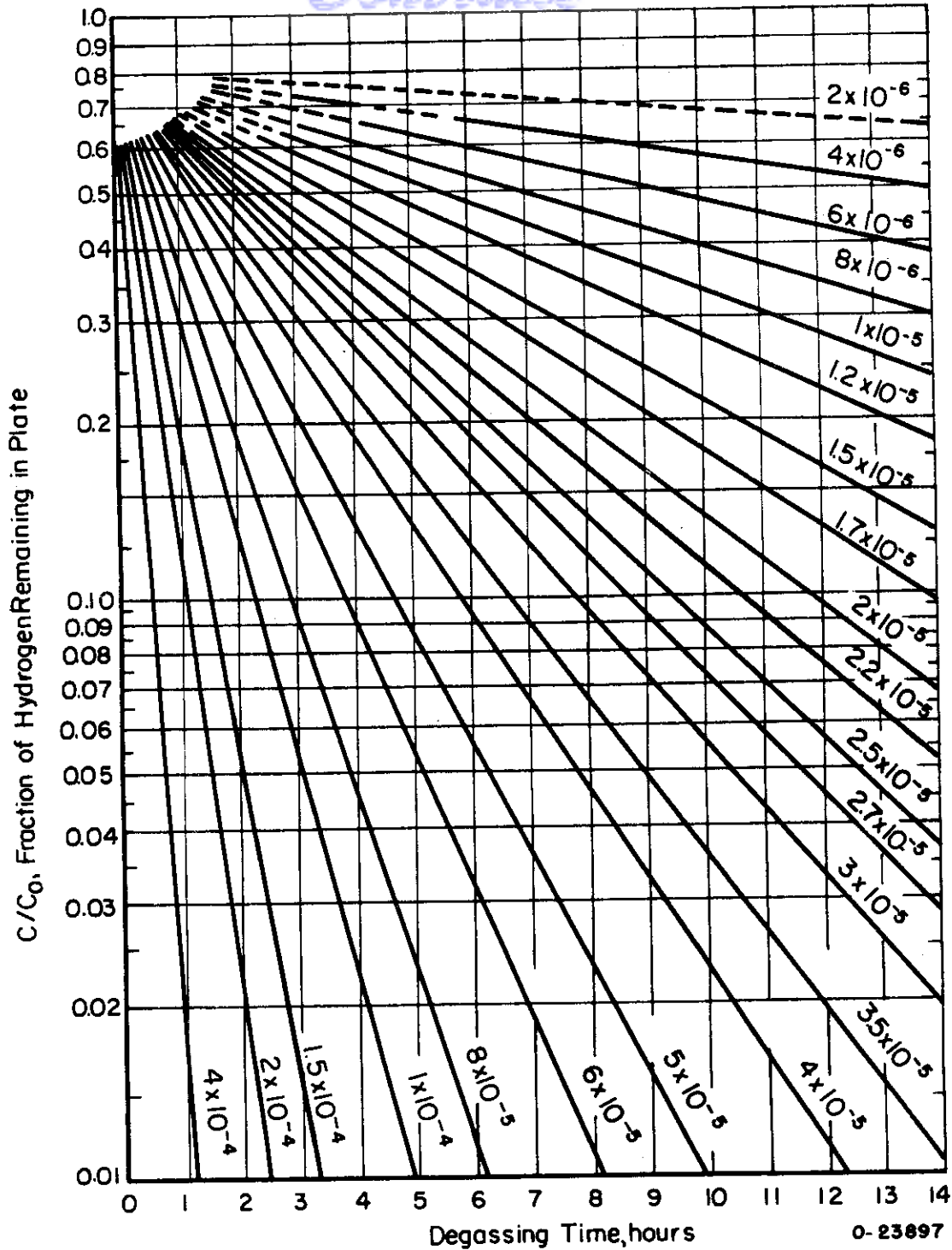
FIGURE 26. VARIATION OF FRACTION OF HYDROGEN REMAINING WITH TIME FOR PLATES OF VARIOUS HALF-THICKNESSES, a

The numbers on the lines are values of D/a^2.

The curves in Figure 25 were derived from Equation (1) for the de-gassing of cylinders. For cylinders with lengths at least seven times their diameters, the error in predicted values of C/C_O is one per cent or less. Shorter lengths require shorter degassing times.

The curves in Figure 26 were derived from the following (approximate) equation for vacuum degassing of sheets[22]:

$$\log (1-f) = \log \left(\frac{8}{\pi^2}\right) - \frac{\pi^2}{4 \times 2.303} \frac{Dt}{a^2} \qquad (6)$$

where

f = fraction of initial hydrogen removed at any time

$(1-f) = C/C_O$ = fraction of initial hydrogen content (C_O) remaining at any time

t = time, seconds

D = degassing coefficient, cm^2/sec

a = half thickness of sheet, cm

The dashed portions of the lines yield values of C/C_O having errors of two per cent or more. This results from the use of the approximate degassing equation. The range of degassing coefficients used to calculate values of D/a^2 was that obtained from this study.

To use these curves, the value of D/a^2 is calculated from the de-gassing coefficient for a given material at a given temperature and the value of "a" which is being considered. From the curve which corresponds to the value of D/a^2, the fraction, C/C_O remaining at any given time is determined.

Low-Pressure Hydrogen Solubility

Method

Studies of low-pressure hydrogen solubility were carried out in an apparatus[17], consisting of a high-purity hydrogen source, heated specimen chambers and a vacuum pumping system. The high-purity hydrogen was obtained from the thermal decomposition of uranium hydride and diffused into the apparatus through a palladium tube. The flow of hydrogen through the apparatus at the desired pressure level was controlled by proper manipulation of the temperatures of the uranium hydride and palladium tube.

For the present work, the manifold of the apparatus was modified to connect four specimen chambers, each having its own furnace. With this change, specimens could be run simultaneously at the same pressure but at four different temperatures.

The pressure in the apparatus could be regulated to any desired value in the range 0.01 to 10 microns of mercury pressure and maintained within ±5 per cent of the value for several hours. Specimen temperatures were controlled to a ±10 F.

Specimens 1/8 inch in diameter by 1/2-inch long were used. These were abraded with 240-grit silicon carbide paper, washed with ACS Reagent-grade acetone, and placed in the furnace tube of the apparatus.

All solubility determinations were carried out for a period of six hours at constant temperature and pressure. This time apparently was adequate to obtain equilibrium since specimens heated for twelve hours did not show significantly different results. At the end of an experiment, the furnace tubes containing the specimens were quenched in cold water. The specimens were then analyzed for their hydrogen contents by the vacuum-fusion method.

Results and Discussions

The low-pressure solubilities of hydrogen in commercial titanium and several titanium alloys were determined at 1110, 1290, 1470, and 1830 F in the pressure range 0.05 to 10 microns of mercury pressure. A rather extensive study was made of the hydrogen solubility in Ti-8Mn, Ti-4Mn-4Al, and Ti-5Al-2.5Sn alloys and commercial titanium (high interstitial). Single values only (at 1290 F and 10 microns of mercury pressure) were obtained to determine the order of magnitude of solubilities for Ti-3Al-5Cr and Ti-2Fe-2Mo-2Cr alloys. A summary of the experimental results is given in Table 28. Included are the hydrogen solubilities for iodide titanium and commercial titanium (low interstitial) which were derived from extrapolation of previous Battelle work using the same method[17].

Metallographic examination of the specimens after heat treatment indicated that, in general, hydrogen solubility increased with increasing amount of beta phase present (at the same temperature and pressure). For example, the Ti-8Mn alloy, which is, predominantly beta phase in the low temperature range, has the greatest equilibrium hydrogen solubilities of all alloys investigated. For alloys predominantly alpha phase at lower temperatures, an abrupt break to higher solubilities is noted in going above the temperature where the alpha to beta transformation occurs. The experimental data at 1830 F represents alloys which were entirely beta phase.

TABLE 28. LOW-PRESSURE SOLUBILITY OF HYDROGEN IN COMMERCIAL TITANIUM AND ITS ALLOYS

Temperature, F	Pressure, microns of mercury	Hydrogen, parts per million by weight							
		Iodide Titanium	Ti-5Al-2.5Sn	Ti-4Mn-4Al	Ti-3Al-5Cr	Commercial Titanium (High Interstitial)	Commercial Titanium (Low Interstitial)	Ti-2Fe-2Mo-2Cr	Ti-8Mn
1110	0.05	--	10	12.3	--	22.4	--	--	--
	0.5	--	--	26.5	--	49.3	--	--	35.8
	2.0	--	32.2	43.8	--	54.6	--	--	62.8
	10.0	110(a)	81.8	93.0	--	122	186(b)	--	141
1290	0.05	--	3.8	3.5	--	7.2	--	--	--
	0.5	--	--	12.6	--	17.8	--	--	21.4
	2.0	--	24.3	26.1	--	33.6	--	--	45.8
	10.0	57(a)	47.7	56.6	62.8	66.4	78(b)	82.0	92.5
1470	0.05	--	2.2	2.7	--	4.5	--	--	--
	0.5	--	--	8.0	--	10.0	--	--	14.9
	2.0	--	12.1	18.4	--	18.8	--	--	30.7
	10.0	34(a)	28.8	35.2	--	46.7	52(b)	--	62.6
1830	0.05	--	0.9	1.2	--	3.1	--	--	--
	0.5	--	--	5.5	--	7.6	--	--	8.4
	2.0	--	11.3	12.9	--	14.0	--	--	14.6
	10.0	--	24.8	29.3	--	33.4	--	--	39.6

(a) Extrapolated from Reference (23).
(b) Extrapolated from Reference (17).

It was found that the data followed the square root or Sieverts' law for a diatomic gas, $S = kp^{1/2}$, where S is the solubility, p is the pressure, and k is the proportionality constant or Sieverts' constant in units of $S/p^{1/2}$. In Figure 27, the solubility of hydrogen in parts per million is plotted versus the square root of pressure for the Ti-8Mn alloy. It is seen that straight-line isotherms are obtained which pass through the origin. Similar plots for the Ti-4Mn-4Al and Ti-5Al-2.5Sn alloys and commercial titanium (high interstitial) also follow Sieverts' law.

The variation of Sieverts' constant K with temperature in degrees Kelvin is given by the equation,

$$\log K = \log (S/p^{1/2}) = A/T + B, \tag{7}$$

where T is absolute temperature and A and B are constants. In Figure 28, the logarithm of K is plotted versus the reciprocal of absolute temperature for all the materials used in this investigation and for iodide titanium and commercial titanium (low interstitial). Equations for the best straight lines in Figure 28 were calculated by the method of least squares for the Ti-4Mn-4Al, Ti-5Al-2.5Sn, and Ti-4Mn-4Al alloys and for commercial titanium (high interstitial). These equations for Sieverts' constant, K, in units of $Sppm/p^{1/2}$ ($microns^{1/2}$) in the range 1110 to 1470 F are for commercial titanium (high interstitial),

$$\log K = 2020/T - 0.723, \tag{8}$$

for Ti-4Mn-4Al,

$$\log K = 1880/T - 0.674, \tag{9}$$

and for Ti-5Al-2.5Sn,

$$\log K = 2000/T - 0.895. \tag{10}$$

The equation of the Ti-8Mn alloy in the range 1110 to 1832 F is

$$\log K = 1640/T - 0.209. \tag{11}$$

Since Sieverts' plots go through the origin, the constant, K, may be estimated from a single determination. Thus, only single points are given for the Ti-3Al-5Cr and Ti-2Fe-2Mo-2Cr alloys in Figure 28.

It is seen from the data that optimum vacuum-degassing conditions observed for the titanium alloys were obtained at 1832 F and 0.05 micron of mercury. Therefore, treatment of titanium alloys at the lowest pressure that can be obtained and at the highest practical temperature would be the best for lowering the hydrogen content of the material. Also it should be noted that the solubilities given in this paper are based on the pressure of
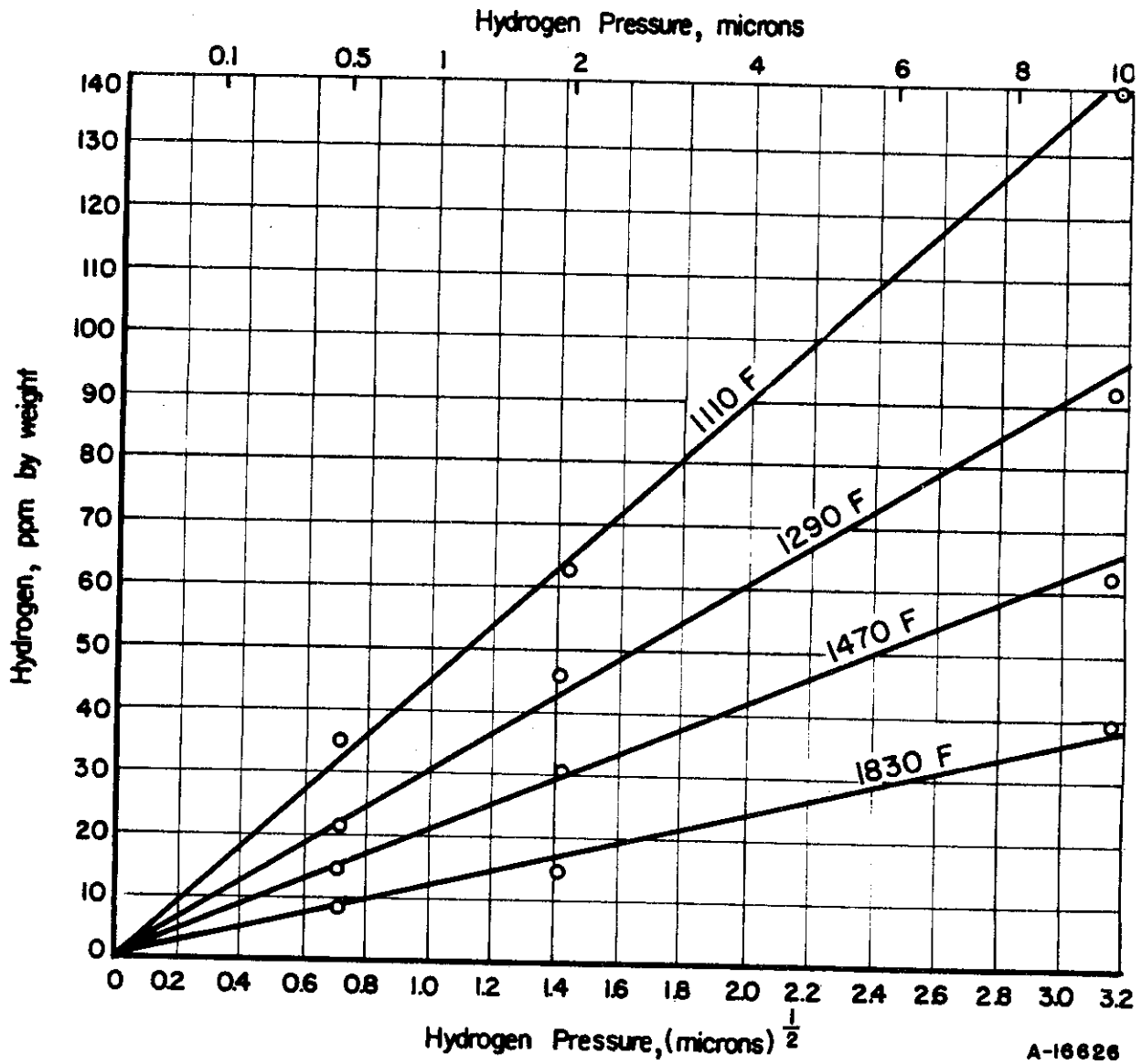
FIGURE 27. SIEVERT'S PLOT FOR HYDROGEN SOLUBILITY IN
Ti-8Mn ALLOY
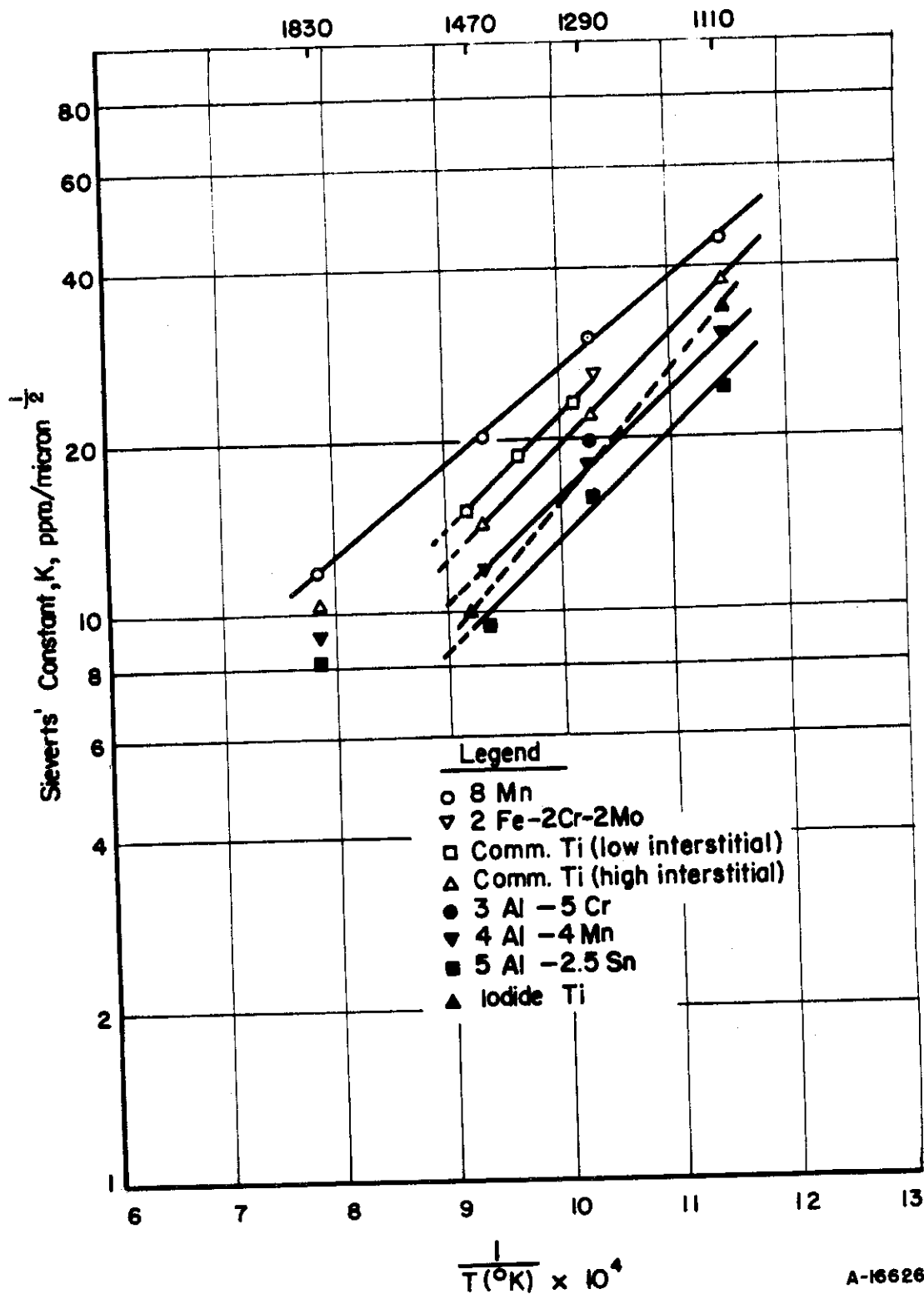
FIGURE 28.   VARIATION OF SIEVERTS' CONSTANT WITH TEMPERATURE
FOR TITANIUM ALLOYS

hydrogen in the system. Consequently, in applying these data to actual vacuum furnace conditions, the partial pressure of hydrogen in the system must be used and not the total pressure of the system.

Hydrogen Removal by Inert Gas Sweep

In addition to vacuum heating, a method employing an inert gas sweep has been investigated for hydrogen removal from titanium and titanium alloys. As shown in the section on low-pressure hydrogen solubility, the equilibrium solubility of hydrogen in titanium and its alloys is dependent upon the partial pressure of hydrogen above the sample. If the partial pressure of hydrogen is lower than the equilibrium solubility pressure, hydrogen diffuses from the specimen. A low partial pressure of hydrogen may be maintained either with a vacuum or with an inert gas sweep maintained at a proper flow rate.

Calculations were made to determine the order of magnitude of flow rates required. The calculations were based on the low-pressure equilibrium solubility and the degassing rate at 1290 F of commercial titanium (low interstitial) for a 100-gram sample (3/8 inch in diameter by 1 inch long) with an initial hydrogen concentration of 300 ppm by weight. From Equation (1), the fraction of hydrogen remaining at a given time was calculated. Then the instantaneous rate of hydrogen removal into a vacuum was determined. The minimum flow rate of argon to permit maximum hydrogen removal was calculated from the rate of removal of hydrogen and the low-pressure equilibrium solubility for the fraction of hydrogen remaining at the given time. A summary of the calculations is given in Table 29.

TABLE 29.   SUMMARY OF CALCULATIONS TO DETERMINE ARGON FLOW FOR DEGASSING COMMERCIAL TITANIUM (LOW INTERSTITIAL)[a]

Time, minutes	Fraction of H_2 Remaining	Rate of H_2 Removal, ml (STP)/min	Minimum Required Argon Flow[b], liters (STP)/min
20	0.39	0.17	6
60	0.18	0.083	13
120	0.060	0.026	36
240	0.0065	0.0028	1800

(a) Calculations based on a specimen 3/8 inch in diameter by 1 inch long.

(b) Instantaneous flow rate at time indicated.

It is seen that the flow rate of argon must increase as the fraction of hydrogen remaining in the specimen decreases. This is because the equilibrium partial pressure of hydrogen decreases as the solubility is lowered. Therefore, a larger amount (flow) of argon is necessary to maintain a sufficiently low partial pressure of hydrogen for degassing.

The above calculations of flow rates are based upon the assumption that there is instantaneous mixing of the carrier gas, argon, with the evolved hydrogen. This condition can be approximated by the use of narrow furnace tubes where the carrier gas passes directly over the specimen and where turbulent mixing of the gases occurs.

Several experiments were made in an apparatus which consisted essentially of a Vycor tube heated by a resistance furnace. A Flowrator was used to meter tank-grade argon through the apparatus. A narrow exit tube was used to minimize back diffusion of air into the apparatus. Temperature was measured by means of a thermocouple spot-welded to the sample.

Results and Discussion

Specimens (3/8 inch in diameter by 1 inch long) of commercial titanium (low interstitial) having an initial hydrogen concentration of 300 ppm were heated at 1290 F for 1 and 4 hours in an argon atmosphere. Argon flow rates from 10 to 35 liters per minute were used. Hydrogen analyses of experimental specimens were made by the vacuum-fusion method.

The results of the experiments are shown in Table 30. It is seen that the amount of hydrogen remaining at any given time is a function of the flow rate. For the size of sample used, 3/8 inch in diameter by 1 inch long, flow rates of 22 and 35 liters per minute were adequate to reduce the hydrogen content to a reasonable level. However, for samples of different geometric dimensions and weight, other flow rates would be required. For example, for a cylinder 1 inch in diameter and 3 feet long, the minimum required argon flow would be 150 liters per minute to remove one-half the hydrogen content in one hour at 1290 F. If a constant flow rate is maintained and the diameter and/or length of specimen is increased, longer times would be required to remove one-half of the hydrogen. Since large quantities of argon are required, it appears that the method would not be feasible to degas large amounts of titanium.

TABLE 30. REMOVAL OF HYDROGEN FROM COMMERCIAL
TITANIUM (HIGH INTERSTITIAL)[a] AT 1290 F
IN FLOWING ARGON ATMOSPHERES

Time, hours	Argon Flow, liters (STP)/min	H_2 Remaining, ppm
1	10	132
4	10	67
1	22	87
1	35	67
4	35	40

(a) Data were obtained on specimens 3/8 inch in diameter by 1 inch long.

References

14. Jaffee, R. I., and Campbell, I. E., Trans. Am. Inst. Mining Met. Engrs., 185, 646-655 (1949).

15. Lenning, G. A., Craighead, C. M., and Jaffee, R. I., Ibid., 200, 367-376 (1954).

16. Kotfila, R. J., and Erbin, E. F., Metal Progress, 66, 128-131 (1954).

17. Griffith, C. B., and Mallett, M. W., "Vacuum Metallurgy", 147, The Electrochemical Society, Inc., New York (1955).

18. Demerez, A., Hock, A. G., and Meunier, F. A., Acta Metallurgica, 2 (2), 214 (1954).

19. Wasilewski, R. J., and Kehl, G. L., Metallurgia, 50, 225-230 (1954).

20. Mallett, M. W., and Albrecht, W. M., J. Electrochemical Soc., 104, 142-146 (1957).

21. Johnson, E. W., and Hill, M. L., Acta Metallurgica, 3, 99 (1955).

22. Dushman, S., "Vacuum Technique", John Wiley and Sons, Inc., New York, 619 (1949).

23. McQuillan, A. D., Proc. Royal Soc., 204, 309 (1950).

PHASE V. FACTORS AFFECTING PICKUP OF HYDROGEN

Summary

The effects of surface films, alloy composition, and furnace atmospheres on the pickup of hydrogen by titanium were studied. An oxide film on titanium was found, in sufficient thicknesses, to be an effective barrier to hydrogen absorption at 1290 F provided the film was not cooled to room temperature before exposure to hydrogen. The rate of absorption of hydrogen by four titanium alloys at 1290 F and 100 mm Hg pressure was found to vary in roughly the same order as their low pressure solubility (determined in Phase IV). The maximum solubility at 1290 F and 100 mm Hg was also found to vary, but not in the same order. The pickup of hydrogen by commercial-purity titanium at 1290 F in an oxidizing atmosphere (air) and in a gas-fired furnace neutral atmosphere was negligible in four hours. In a reducing atmosphere having a partial pressure of hydrogen of about 15 mm of Hg significant pickup occurred.

Introduction

An investigation of the factors affecting the pickup of hydrogen by titanium and titanium alloys has been made. The effects of surface films, alloy composition and furnace atmospheres were studied.

Results and Discussion

The Effect of Surface Films

The rates of absorption of hydrogen were obtained with iodide titanium having films of various thicknesses. The films were prepared by heating specimens in air at 1290 F for various lengths of time as follows:

Time, hours	Description of Film
1/4	Very thin, black
1	Thin, grayish-blue
3	Thick (0.0003 cm), pearl gray

Rate measurements for the absorption of hydrogen were made at 1290 F and 100 mm mercury pressure. Data for the rate of absorption of hydrogen by iodide titanium having no film were also obtained at the same temperature and pressure as a standard of comparison. Rates were obtained

for specimens with films that either were cooled or were not cooled before reaction. The results are summarized in Figures 29 and 30.

Figure 29 is a plot of hydrogen consumed, ml (STP) per cm^2 of surface area, versus time for specimens cooled to room temperature after forming oxide films and reheated to 1290 F for reaction with hydrogen. The initial rates of absorption decreased with increasing film thickness; however, at the end of the initial reactions, the rates approached that of iodide titanium having no oxide film.

Figure 30 is a plot of hydrogen consumed versus time for the reaction of hydrogen with specimens having oxide films which were not cooled to room temperature prior to reaction. Again the initial rates of absorption generally were slower for thicker films. After an initial slower reaction, the rate of absorption of hydrogen by the specimen with the very thin film approached that of iodide titanium having no oxide film. The rate for the specimen with the thin film was rapid initially but did not approach the rate for iodide titanium in 8000 seconds. No absorption of hydrogen by the specimen with the thick film occurred in 11,000 seconds.

A comparison of Figures 29 and 30 shows that the over-all rate of absorption is faster for titanium which was oxidized and cooled before hydrogenation than for titanium which was oxidized and reacted with hydrogen isothermally. Presumably this is the result of cracking of the oxide skin during cooling.

The Effect of Alloy Composition

A study was made of the effect of alloy composition upon the rate of absorption of hydrogen by titanium and titanium alloys. The reaction of hydrogen with high-purity titanium and the alloys Ti-8Mn, commercial titanium (low interstitial), and Ti-4Al-4Mn was studied at 1290 F and 100 mm of mercury pressure. The results are given in Figure 31, which is a plot of hydrogen consumed versus time. The initial reaction of hydrogen with the alloys follows the same trend as the low-pressure hydrogen solubility. The Ti-8Mn alloy has the fastest initial reaction rate and the greatest low-pressure hydrogen solubility.

It is seen from Figure 31, that the amount of hydrogen absorbed reaches a plateau, indicating that the rate of absorption has become nearly zero. These plateaus represent the maximum solubilities of hydrogen for the alloys and iodide titanium at 1290 F and 100 mm of mercury pressure. Since all specimen weights are approximately the same, the relative position of the plateaus represents the order of solubilities. Solubilities calculated from the total amount of hydrogen absorbed are summarized in Table 31.
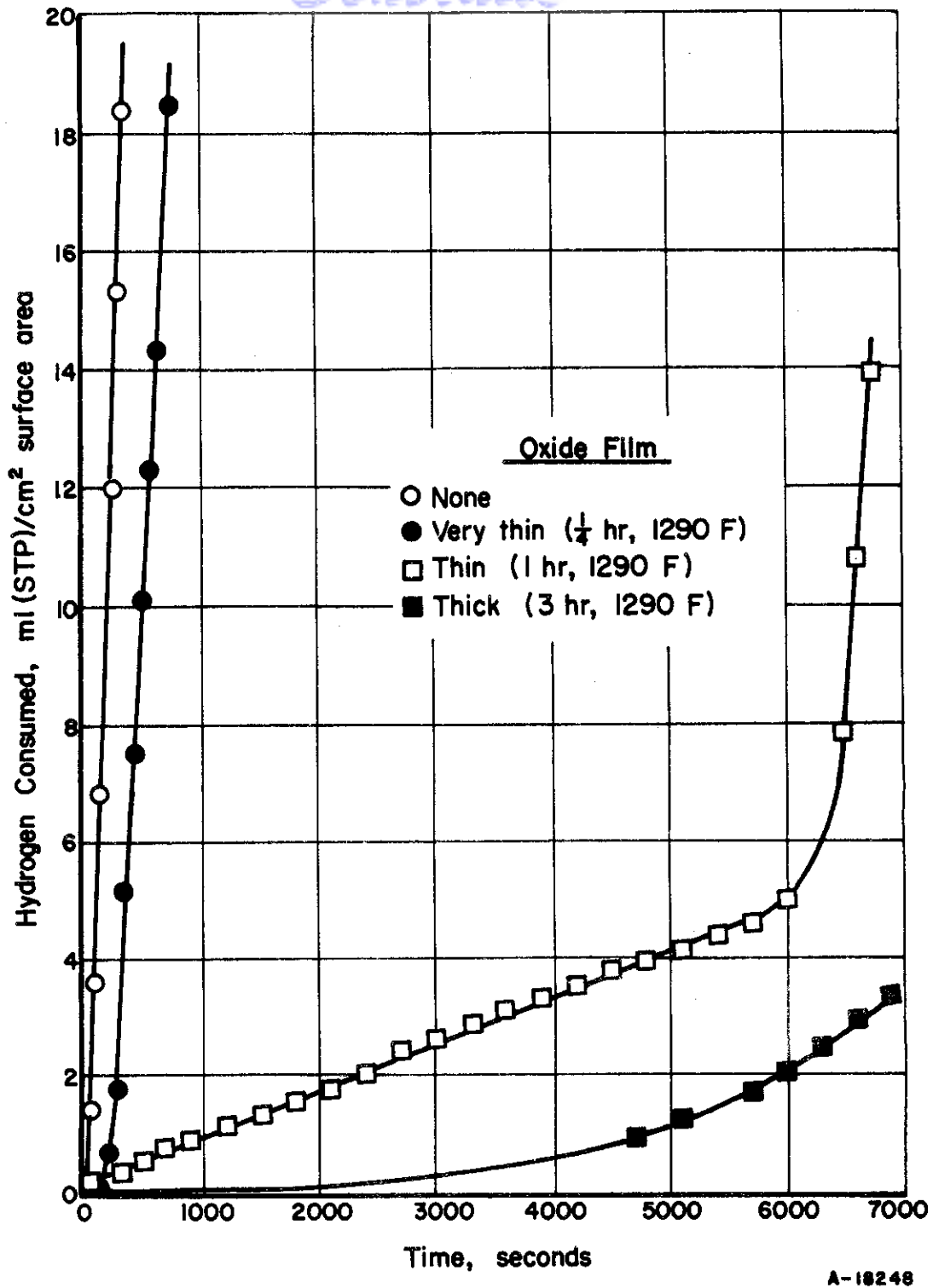
FIGURE 29. REACTIONS RATES AT 1290 F AND 100 MM Hg PRESSURE
OF HYDROGEN WITH HIGH-PURITY TITANIUM HAVING
VARIOUS OXIDE FILM THICKNESSES

Specimens cooled before reaction.
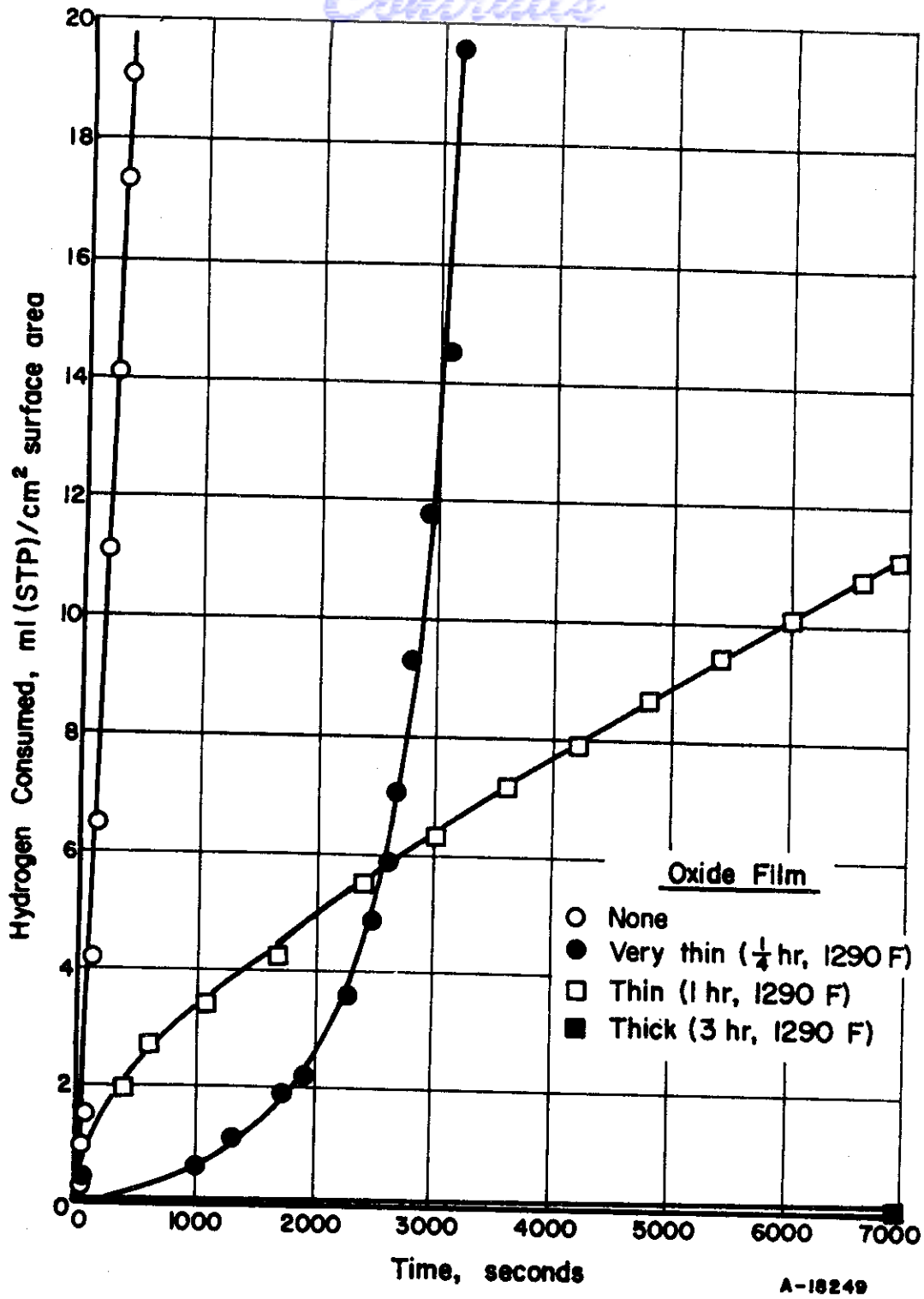
FIGURE 30.   REACTION RATES AT 1290 F AND 100 MM Hg PRESSURE
OF HYDROGEN WITH HIGH-PURITY TITANIUM HAVING
VARIOUS OXIDE FILM THICKNESSES

Specimens not cooled before reaction.

WADC TR 54-616 Pt IV   105
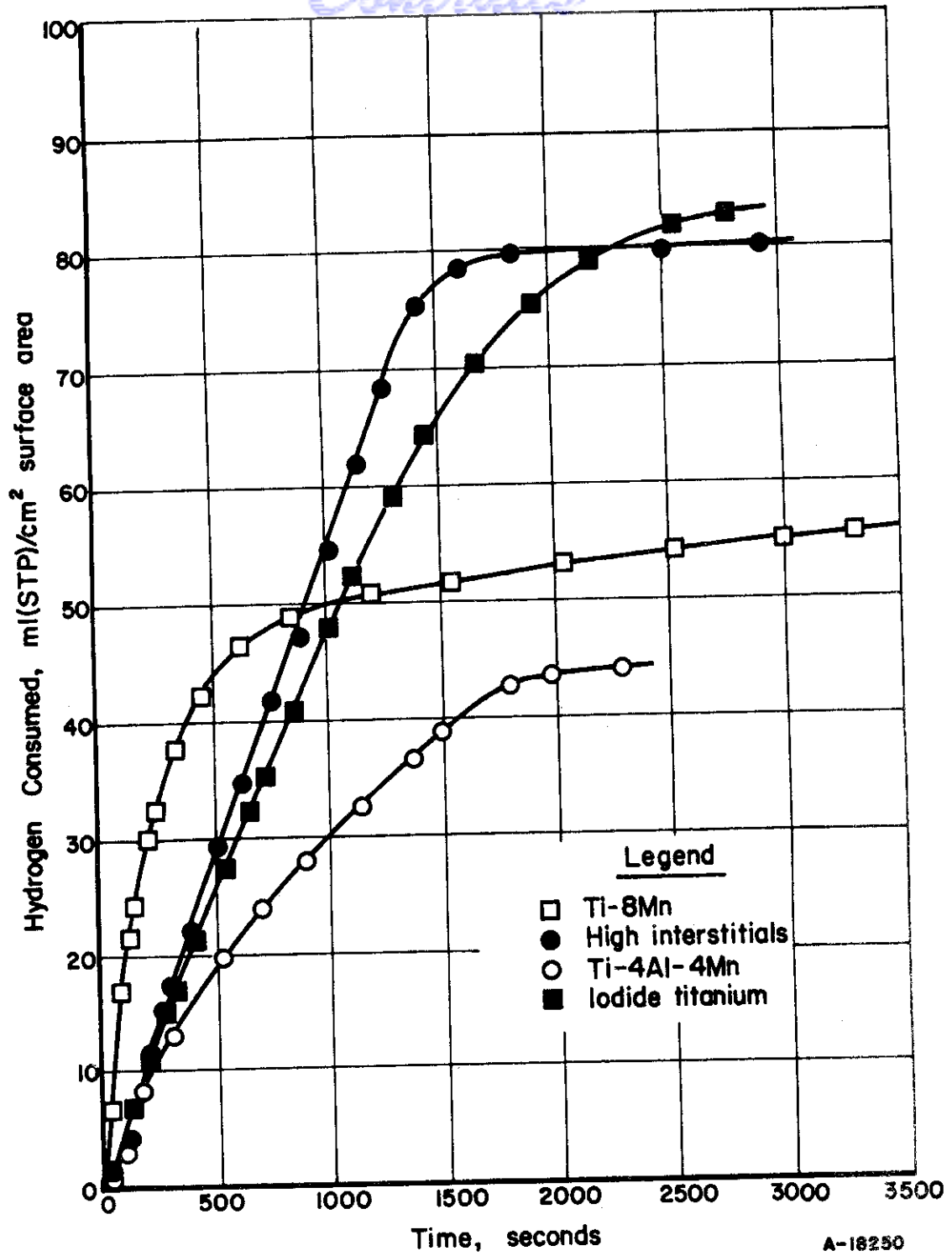
FIGURE 31. REACTION RATES OF TITANIUM ALLOYS WITH H_2 AT 1290 F AND 100 MM Hg PRESSURE

TABLE 31. SOLUBILITY OF HYDROGEN IN TITANIUM AND TITANIUM ALLOYS AT 1290 F AND 100 MM OF MERCURY PRESSURE

Nominal Composition, weight per cent	Hydrogen Content, weight per cent
Iodide Ti	1.3[a]
Commercial titanium (high interstitial)	1.2
Ti-8Mn	0.93
Ti-4Al-4Mn	0.81

(a) This is in good agreement with the solubility, 1.2 weight per cent interpolated from the work of McQuillan[24].

The Effect of Furnace Atmospheres

A study was made of the effect of oxidizing and reducing furnace atmospheres upon the pickup of hydrogen by commercial titanium (low interstitial). Oxidizing conditions are normally used in commercial heat treatment of titanium and its alloys. In this work, the effect of reducing atmospheres was investigated also. Both cylinders and plates were used.

Specimens with clean surfaces were heated at 1290 F for various times in electric muffle furnaces having either an oxidizing or a reducing atmosphere. The oxidizing atmosphere was air and the reducing mixture was a gas mixture having a typical composition as follows:

Constituent	Nominal Composition, volume per cent
CO_2	1.0
CO	32.0
H_2	2.0
CH_4	0.5
N_2	64.5
	100.0

The results for 3/8-in. cylinders and 2 in. by 2 in. by 0.060 in. sheet are listed in Table 32. After treatment, the samples were analyzed for hydrogen by the vacuum-fusion method.

TABLE 32. HYDROGEN CONTENT OF COMMERCIAL TITANIUM (LOW INTERSTITIAL) CYLINDERS AND SHEET HEATED AT 1290 F IN OXIDIZING AND REDUCING ATMOSPHERES

Sample Geometry	Time, hours	Heat Treating Atmosphere	Hydrogen Content, ppm by weight
Cylinder	0	None (control)	10
"	1	Oxidizing	11
"	2	"	10
"	4	"	10
"	1	Reducing	11
"	2	"	13
"	4	"	26
Sheet	0	None (control)	8
"	1	Oxidizing	8
"	4	"	8
"	1	Reducing	30
"	4	"	60

The results show that there was no pickup of hydrogen by samples heated in the oxidizing atmosphere for four hours. However, there was significant pickup in specimens heated in the reducing atmosphere. This is to be expected in view of the fact that the reducing atmosphere contains a partial pressure of hydrogen of about 15 mm of mercury (2 volume per cent). There was a much greater pickup of hydrogen in the sheet material than in the cylindrical specimens. Since sheet material has a higher surface to mass ratio, a greater initial hydrogen pickup would be expected.

An additional experiment was carried out in a typical gas-fired furnace having a neutral atmosphere. In normal operation the atmosphere of this furnace fluctuates between a slightly oxidizing and a slightly reducing composition. There was no hydrogen pickup in a 3/8-in. diameter cylinder of commercial titanium (low interstitial) after four hours at 1290 F.

From these experiments, it is concluded that there is no hydrogen pickup by commercial titanium (low interstitial) which is heat treated in an electric muffle furnace having an oxidizing atmosphere and a gas-fired furnace having a neutral atmosphere. However, there is hydrogen pickup in electric muffle furnaces having a reducing atmosphere.

Reference

24. McQuillan, A. D., Proc. Royal Soc., 204, 309 (1950).

The Materials Laboratory, WADC, requested that various amounts of titanium alloys be hydrogenated for Armour Research Foundation for use under their contract No. AF 33(616)- 206 with WADC. The materials were submitted by Armour to Battelle for hydrogenation.

Ten, one-pound lots of Ti-5Al, two, one-pound lots of Ti-7Al-3Mo, two, one-pound lots of Ti-25V, and eleven, one-pound lots of Ti-6Al-4V were hydrogenated. The processed materials were returned to Armour.

One-half the lots of each of the alloys, Ti-5Al and Ti-7Al-3Mo, were hydrogenated to 100 ppm and the other half to 200 ppm. Since the initial hydrogen content, 100 ppm of the Ti-7Al-3Mo alloy was the same as one of the desired levels, no hydrogen was added to one lot of this alloy. This batch was heated in an evacuated sealed chamber using the same heating cycle as that used for the other lots after hydrogenation. Thus, all lots should be in the same heat-treated condition.

Before hydrogenation, the other lots were vacuum degassed at 1300 F. Hydrogen was added at 1300 F and the specimens held at this temperature for 20 hours in the residual gases in the sealed off hydrogenation chamber.

Eleven, one-pound lots of Ti-6Al-4V were hydrogenated to 150 ppm. One lot of Ti-25V was hydrogenated to a level of 100 ppm and one lot to a level of 200 ppm. The procedure for adding hydrogen was the same as described above.

Two lots of Ti-6Al-4V alloy and two lots of iodide titanium were hydrogenated to 350 ppm for the Materials Laboratory, WADC. The lots weighed in the range of 12 to 25 grams. Hydrogen was added at 1560 F and all lots were homogenized at 1560 F for 4 to 8 hours.

The data given in this report may be found in the following Battelle Memorial Institute laboratory record books: No. 9818, pages 1 through 100; No. 10447, pages 1 through 57; No. 10720, pages 1 through 23; No. 8868, pages 75 through 81; No. 10316, pages 1 through 100; No. 10465, pages 1 through 100; No. 10562, pages 1 through 100; No. 10785, pages 7 through 17; No. 10805, pages 1 through 100; No. 10980, pages 1 through 21; and No. 11172, pages 1 through 40.

APPENDIX I

COMPLETE TEST DATA FROM PHASES II AND III

Hydrogen Content, ppm		VHN (10-Kg Load)		Metallographic Structure, 20 ppm
Nominal	By Analysis	Hydrogen Content	VHN	
20	22	20	216	Structure: equiaxed α-β
200	180	200	217	Third phase: --
600	--	600	212	Vol % α: 80
800	--	800	212	α grain size: 2 μ

Unnotched Stress-Rupture Tests Using 0.125-In. Round Samples

Nominal Hydrogen	Applied Stress		Rupture Time, hours	Extension, % Between Shoulders	Elongation, % in 4D	Reduction in Area, %
	Psi	% of Ultimate Tensile Strength				
20	90,000	95	14.4	24	28(c)	59
20	85,300	90	264(a)	10	13	12
20	85,300	90	153	19	--(c)	59
200	86,000	90	246	20	--(c)	65
200	86,000	90	240	19	--(c)	62
600	89,600	93	14.4	20	36	52
600	86,800	90	54.2	17	28	54
800	87,600	93	80.9	18	19	31

(a) Test discontinued before failure; (b) Broke outside gage mark; (c) Broke on gage mark.

Unnotched Tensile Tests Using 0.125-In. Round Samples

Nominal Hydrogen	Ultimate Tensile Strength, psi	Yield Strength, psi			Proportional Limit, psi	Extension, % Between Shoulders	Elongation, % in 4D	Reduction in Area, %
		0.2% Offset	0.1% Offset	0.01% Offset				
		Low Testing Speed - 0.005 In./Min						
20	94,800	73,400	69,400	62,400	59,800	18	28	61
200	95,600	75,200	70,700	62,000	59,300	18	15(b)	64
600	96,400	64,400	57,700	42,900	36,400	18	30	57
800	94,200	61,900	55,400	41,700	37,200	18	33	55
		High Testing Speed - 0.5 In./Min						
20	98,800					19	31	58
200	100,000					19	35	67
600	102,400					17	31	61
800	99,200					17	32	61

(a) Broke on gage mark; (b) Broke outside gage mark.

Notch-Bend Impact Tests Using Micro Sample

Nominal Hydrogen	Energy Absorbed, in-lb		Conclusion
	At 77 F	At -40 F	
20	54	43	Slow-strain embrittlement at 800 ppm; no impact embrittlement
200	44	36	
600	53	40	
800	65	37	

TABLE 34.   RESULTS OF TESTS TO DETERMINE THE HYDROGEN SENSITIVITY
OF THE Ti-8Mo ALLOY (K-2)

Hydrogen Content, ppm		VHN (10-Kg Load)		Metallographic Structure, 20 ppm
Nominal	By Analysis	Hydrogen Content	VHN	
20	15	20	226	Structure: equiaxed α+β
200	230	200	243	Third phase: --
600	--	600	240	Vol % α: 60-70
800	--	800	--	α grain size: 2 μ

Unnotched Stress-Rupture Tests Using 0.125-In. Round Samples

Nominal Hydrogen	Applied Stress		Rupture Time, hours	Extension, % Between Shoulders	Elonga- tion, % in 4D	Reduction in Area, %
	Psi	% of Ultimate Tensile Strength				
20	98,200	95	7.9	25	--(c)	69
20	96,000	93	35.6	18	31	64
200	98,500	95	95.2	18	17	71
200	96,300	93	256.1(a)	11	14	--
600	100,900	95	6.6	15	--(b)	69
600	98,600	93	70.7	16	--(c)	68
800	104,200	95	35.4	16	--(c)	51

(a) Test discontinued before failure; (b) Broke outside gage mark; (c) Broke on gage mark.

Unnotched Tensile Tests Using 0.125-In. Round Samples

Nominal Hydrogen	Ultimate Tensile Strength, psi	Yield Strength, psi			Propor- tional Limit, psi	Extension, % Between Shoulders	Elonga- tion, % in 4D	Reduction in Area, %
		0.2% Offset	0.1% Offset	0.01% Offset				
Low Testing Speed - 0.005 In./Min								
20	103,400	91,000	83,700	73,800	70,500	17	22(a)	58
200	103,700	99,800	89,600	72,000	67,200	17	27	76
600	106,100	100,000	90,200	68,600	61,400	18	33	69
800	109,600	97,100	85,600	65,000	56,100	13	16(b)	60
High Testing Speed - 0.5 In./Min								
20	108,900					15	29	68
200	113,500					14	28	67
600	110,600					15	31	79
800	115,300					14	27	69

(a) Broke on gage mark; (b) Broke outside gage mark.

Notch-Bend Impact Tests Using Micro Sample

Nominal Hydrogen	Energy Absorbed, in-lb		Conclusion
	At 77 F	At -40 F	
20	66	47	No slow-strain embrittlement; progressive loss
200	52	35	of impact properties as the hydrogen content
600	40	26	increased
800	37	21	

Hydrogen Content, ppm		VHN (10-Kg Load)		Metallographic Structure, 20 ppm
Nominal	By Analysis	Hydrogen Content	VHN	
20	--	20	292	Structure: β + fine spheroidal α
200	200	200	292	Third phase: --
600	593	600	294	Vol % α: 20
800	--	800	--	α grain size: $2~\mu$

Unnotched Stress-Rupture Tests Using 0.125-In. Round Samples

Nominal Hydrogen	Applied Stress		Rupture Time, hours	Extension, % Between Shoulders	Elongation, % in 4D	Reduction in Area, %
	Psi	% of Ultimate Tensile Strength				
20	126,800	93	256.3[a]	2.2	3	--
200	125,500	93	216.4	10	14	40
600	128,300	95	15.6	9	15	35
600	126,900	94	263.0[a]	6	8	--
800	132,600	97	3.3	11	18	39
800	130,000	95	257.0[a]	4	0	--

(a) Test discontinued before failure; (b) Broke outside gage mark; (c) Broke on gage mark.

Unnotched Tensile Tests Using 0.125-In. Round Samples

Nominal Hydrogen	Ultimate Tensile Strength, psi	Yield Strength, psi			Proportional Limit, psi	Extension, % Between Shoulders	Elongation, % in 4D	Reduction in Area, %
		0.2% Offset	0.1% Offset	0.01% Offset				
Low Testing Speed - 0.005 In./Min								
20	136,400	129,300	128,800	124,900	119,500	8	16	37
200	135,000	128,400	127,700	121,500	114,500	11	16[a]	23
600	135,000	132,700	132,200	125,000	122,500	10	18	35
800	136,800	135,800	135,600	130,600	125,800	8	10[b]	36
High Testing Speed - 0.5 In./Min								
20	142,100					8	20	43
200	140,800					7	13	36
600	145,500					8	18	34
800	143,400					7	10	38

(a) Broke on gage mark; (b) Broke outside gage mark.

Notch-Bend Impact Tests Using Micro Sample

Nominal Hydrogen	Energy Absorbed, in-lb		Conclusion
	At 77 F	At -40 F	
20	8	6	No slow-strain embrittlement; alloy brittle in impact testing
200	3	5	
600	5	4	
800	6	6	

Hydrogen Content, ppm		VHN (10-Kg Load)		Metallographic Structure, 20 ppm
Nominal	By Analysis	Hydrogen Content	VHN	
20	--	20	242	Structure: α + fine spheroidal β
200	200	200	236	Third phase: --
				Vol % α: 80
				α grain size: 3 μ

Unnotched Stress-Rupture Tests Using 0.125-In. Round Samples

Nominal Hydrogen	Applied Stress		Rupture Time, hours	Extension, % Between Shoulders	Elongation, % in 4D	Reduction in Area, %
	Psi	% of Ultimate Tensile Strength				
20	96,400	93	145.8	19	20	57
200	97,700	93	41.0	11	18[b]	11
200	95,700	91	45.5	9	8[b]	11

(a) Test discontinued before failure; (b) Broke outside gage mark; (c) Broke on gage mark.

Unnotched Tensile Tests Using 0.125-In. Round Samples

Nominal Hydrogen	Ultimate Tensile Strength, psi	Yield Strength, psi			Proportional Limit, psi	Extension, % Between Shoulders	Elongation, % in 4D	Reduction in Area, %
		0.2% Offset	0.1% Offset	0.01% Offset				
			Low Testing Speed - 0.005 In./Min					
20	103,700	87,200	85,900	77,400	73,100	19	24[a]	56
200	105,100	89,600	88,400	80,400	75,900	19	34	57
			High Testing Speed - 0.5 In./Min					
20	107,900					15	28	59
200	108,000					16	30	62

(a) Broke on gage mark; (b) Broke outside gage mark.

Notch-Bend Impact Tests Using Micro Sample

Nominal Hydrogen	Energy Absorbed, in-lb		Conclusion
	At 77 F	At -40 F	
20	50	42	Slow-strain embrittlement at 200 ppm; no impact embrittlement
200	47	38	

Hydrogen Content, ppm		VHN (10-Kg Load)		Metallographic Structure, 20 ppm
Nominal	By Analysis	Hydrogen Content	VHN	
20				Structure: equiaxed $\alpha + \beta$
200				Third phase: --
400				Vol % α: 60-70
600				α grain size: 3 μ

Unnotched Stress-Rupture Tests Using 0.125-In. Round Samples

Nominal Hydrogen	Applied Stress		Rupture Time, hours	Extension, % Between Shoulders	Elonga-tion, % in 4D	Reduction in Area, %
	Psi	% of Ultimate Tensile Strength				
200	113,600	97	2.7	13	--(c)	56
200	111,300	95	202.1	10	14	18
200	111,300	95	471.8	8	12	12
400	117,400	97	1.9	9	9	13
600	120,800	97	2.1	4	6	7

(a) Test discontinued before failure; (b) Broke outside gage mark; (c) Broke on gage mark.

Unnotched Tensile Tests Using 0.125-In. Round Samples

Nominal Hydrogen	Ultimate Tensile Strength, psi	Yield Strength, psi			Propor-tional Limit, psi	Extension, % Between Shoulders	Elonga-tion, % in 4D	Reduction in Area, %
		0.2% Offset	0.1% Offset	0.01% Offset				
Low Testing Speed - 0.005 In./Min								
20	113,900	100,200	99,500	89,600	83,200	17	30	66
200	117,100	102,400	100,300	93,300	89,000	16	26	54
400	121,000	110,000	108,000	99,100	93,300	13	16	26
600	124,500	112,600	108,700	94,600	75,200	7	10	21
High Testing Speed - 0.5 In./Min								
20	114,800					14	24	64
200	118,600					13	24	62
400	119,000					13	18	57
600	126,800					8	14	46

(a) Broke on gage mark; (b) Broke outside gage mark.

Notch-Bend Impact Tests Using Micro Sample

Nominal Hydrogen	Energy Absorbed, in-lb	
	At 77 F	At -40 F
20	44	32
200	36	24
400	34	22
600	28	14

Conclusion

Slow-strain embrittlement at 200 ppm; progressive loss of impact properties as the hydrogen content increased

Hydrogen Content, ppm		VHN (10-Kg Load)		Metallographic Structure, 20 ppm
Nominal	By Analysis	Hydrogen Content	VHN	
20	--			Structure: β + fine spheroidal α
200	360			Third phase: --
600				Vol % α: 30
800				α grain size: $2\ \mu$

Unnotched Stress-Rupture Tests Using 0.125-In. Round Samples

Nominal Hydrogen	Applied Stress		Rupture Time, hours	Extension, % Between Shoulders	Elonga- tion, % in 4D	Reduction in Area, %
	Psi	% of Ultimate Tensile Strength				
20	118,300	95	262.1[a]	3	--	--
20	115,800	93	257.4[a]	2	3	--
200	116,000	97	On loading	9	18	43
200	113,700	95	263.7[a]	3	4	--
200	111,200	93	264.5[a]	2	--	--
600	121,000	95	0.1	6	15	37
600	118,500	93	261.7[a]	2	2	--
800	122,500	99	250.0[a]	3	--	--
800	120,000	97	262.7	2	2	--
800	117,600	95	257.0	2	2	--

(a) Test discontinued before failure; (b) Broke outside gage mark; (c) Broke on gage mark.

Unnotched Tensile Tests Using 0.125-In. Round Samples

Nominal Hydrogen	Ultimate Tensile Strength, psi	Yield Strength, psi			Propor- tional Limit, psi	Extension, % Between Shoulders	Elonga- tion, % in 4D	Reduction in Area, %
		0.2% Offset	0.1% Offset	0.01% Offset				
Low Testing Speed - 0.005 In./Min								
20	124,500	--	105,700	99,100	96,300	6	6[b]	18
200	119,700	--	98,000	91,100	88,200	7	10[a]	24
600	127,400	113,800	110,000	96,600	84,300	9	14	35
800	123,800	111,900	108,400	97,500	91,400	8	10	35
High Testing Speed - 0.5 In./Min								
20	116,400					3	10	34
200	113,800					9	18	49
600	119,800					8	14	37
800	118,500					7	13	35

(a) Broke on gage mark; (b) Broke outside gage mark.

Notch-Bend Impact Tests Using Micro Sample

Nominal Hydrogen	Energy Absorbed, in-lb		Conclusion
	At 77 F	At -40 F	
20	11	5	No slow-strain embrittlement; alloy brittle in impact testing
200	13	7	
600	6	10	
800	8	3	

Hydrogen Content, ppm		VHN (10-Kg Load)		Metallographic Structure, 20 ppm
Nominal	By Analysis	Hydrogen Content	VHN	
20				Structure: α + fine spheroidal β
200				Third phase: occurring at 200 ppm
400				Vol % α: 90
				α grain size: 4 μ

Unnotched Stress-Rupture Tests Using 0.125-In. Round Samples

Nominal Hydrogen	Applied Stress		Rupture Time, hours	Extension, % Between Shoulders	Elonga-tion, % in 4D	Reduction in Area, %
	Psi	% of Ultimate Tensile Strength				
200	83,100	95	3.9	14	16	47
200	81,400	93	1.1	13	--(b)	48
400	85,200	95	4.2	15	--(c)	52

(a) Test discontinued before failure; (b) Broke outside gage mark; (c) Broke on gage mark.

Unnotched Tensile Tests Using 0.125-In. Round Samples

Nominal Hydrogen	Ultimate Tensile Strength, psi	Yield Strength, psi			Propor-tional Limit, psi	Extension, % Between Shoulders	Elonga-tion, % in 4D	Reduction in Area, %
		0.2% Offset	0.1% Offset	0.01% Offset				
Low Testing Speed - 0.005 In./Min								
20	86,300	68,000	67,000	61,000	53,200	16	26	48
200	87,500	65,800	62,800	54,800	49,750	14	16(b)	48
400	91,600	69,400	64,800	46,000	37,000	16	26	56
High Testing Speed - 0.5 In./Min								
20	92,800					16	28	52
200	92,200					16	26	45
400	95,100					12	22	48

(a) Broke on gage mark; (b) Broke outside gage mark.

Notch-Bend Impact Tests Using Micro Sample

Nominal Hydrogen	Energy Absorbed, in-lb		Conclusion
	At 77 F	At -40 F	
20	35	23	No slow-strain embrittlement; impact embrittle-ment at 200 ppm
200	7	8	
400	6	5	

Hydrogen Content, ppm		VHN (10-Kg Load)		Metallographic Structure, 20 ppm
Nominal	By Analysis	Hydrogen Content	VHN	
20	--	20	--	Structure: α + fine spheroidal β
200	160	200	--	Third phase: occurring at 200 ppm
800	--	800	--	Vol % α: 80-90
				α grain size: 2 μ

Unnotched Stress-Rupture Tests Using 0.125-In. Round Samples

Nominal Hydrogen	Applied Stress		Rupture Time, hours	Extension, % Between Shoulders	Elongation, % in 4D	Reduction in Area, %
	Psi	% of Ultimate Tensile Strength				
800	91,900	93	13.9	15	--(c)	48

(a) Test discontinued before failure; (b) Broke outside gage mark; (c) Broke on gage mark.

Unnotched Tensile Tests Using 0.125-In. Round Samples

Nominal Hydrogen	Ultimate Tensile Strength, psi	Yield Strength, psi			Proportional Limit, psi	Extension, % Between Shoulders	Elongation, % in 4D	Reduction in Area, %
		0.2% Offset	0.1% Offset	0.01% Offset				
		Low Testing Speed - 0.005 In./Min						
20	90,800	72,600	69,100	60,400	54,800	17	27	54
200	93,000	70,000	67,300	56,800	51,000	18	21	57
800	98,800	71,400	65,700	53,000	47,500	15	24	48
		High Testing Speed - 0.5 In./Min						
20	96,400					15	27	55
200	97,000					14	31	54
800	103,700					14	24	49

(a) Broke on gage mark; (b) Broke outside gage mark.

Notch-Bend Impact Tests Using Micro Sample

Nominal Hydrogen	Energy Absorbed, in-lb		Conclusion
	At 77 F	At -40 F	
20	30	28	No slow-strain embrittlement; impact embrittle-
200	10	7	ment at 200 ppm
800	4	2	

TABLE 41. RESULTS OF TESTS TO DETERMINE THE HYDROGEN SENSITIVITY OF THE Ti-4Nb ALLOY (K-9)

Hydrogen Content, ppm		VHN (10-Kg Load)		Metallographic Structure, 20 ppm
Nominal	By Analysis	Hydrogen Content	VHN	
20				
200				Structure: equiaxed $\alpha + \beta$
600				Third phase: occurring at 200 ppm
800				Vol % α: 80
				α grain size: 5 μ

Unnotched Stress-Rupture Tests Using 0.125-In. Round Samples

Nominal Hydrogen	Applied Stress		Rupture Time, hours	Extension, % Between Shoulders	Elonga-tion, % in 4D	Reduction in Area, %
	Psi	% of Ultimate Tensile Strength				
20	84,900	95	1.5	20	31	59
20	80,600	90	69.8	20	--(c)	58
20	80,600	90	67.1	20	--(c)	59
200	80,500	93	73.9	17	26	63
200	78,000	90	218.4	18	--(c)	60
200	73,000	90	4.5	16	27	57
600	82,800	93	13.6	18	--(c)	51
800	80,900	93	285.9(a)	14	19	--

(a) Test discontinued before failure; (b) Broke outside gage mark; (c) Broke on gage mark.

Unnotched Tensile Tests Using 0.125-In. Round Samples

Nominal Hydrogen	Ultimate Tensile Strength, psi	Yield Strength, psi			Propor-tional Limit, psi	Extension, % Between Shoulders	Elonga-tion, % in 4D	Reduction in Area, %
		0.2% Offset	0.1% Offset	0.01% Offset				
Low Testing Speed – 0.005 In./Min								
20	89,600	68,400	66,600	60,200	56,600	20	31	61
200	86,600	63,800	60,800	52,700	49,750	18	30	57
600	89,000	62,100	56,900	43,050	36,500	20	33	53
800	87,000	59,800	52,600	33,300	23,550	20	24	49
High Testing Speed – 0.5 In./Min								
20	91,600					18	31	58
200	95,000					15	27	56
600	93,900					15	27	53
800	94,200					16	30	50

(a) Broke on gage mark; (b) Broke outside gage mark.

Notch-Bend Impact Tests Using Micro Sample

Nominal Hydrogen	Energy Absorbed, in-lb		Conclusion
	At 77 F	At -40 F	
20	54	58	No slow-strain embrittlement; impact embrittle-ment at 200 ppm
200	14	9	
600	7	5	
800	12	11	

TABLE 42. RESULTS OF TESTS TO DETERMINE THE HYDROGEN SENSITIVITY OF THE Ti-8Nb ALLOY (K-10)

Hydrogen Content, ppm		VHN (10-Kg Load)		Metallographic Structure, 20 ppm
Nominal	By Analysis	Hydrogen Content	VHN	
20	14	20	213	Structure: equiaxed $\alpha + \beta$
200	299	200	--	Third phase: occurring at 300 ppm
400	--	400	--	Vol %α: 60-70
600	--	600	227	α grain size: 2 μ

Unnotched Stress-Rupture Tests Using 0.125-In. Round Samples

Nominal Hydrogen	Applied Stress		Rupture Time, hours	Extension, % Between Shoulders	Elonga-tion, % in 4D	Reduction in Area, %
	Psi	% of Ultimate Tensile Strength				
20	84,500	93	25.7	18	--(c)	69
20	81,900	90	169.1	16	--(c)	62
20	81,900	90	178.5	20	34	69
200	85,000	93	59.9	17	26	59
200	82,400	90	105.4	8	--(b)	16
200	82,400	90	100.8	20	--(c)	60
400	83,600	90	64.0	18	--(c)	56
600	83,600	90	162.4	10	--(c)	13

(a) Test discontinued before failure; (b) Broke outside gage mark; (c) Broke on gage mark.

Unnotched Tensile Tests Using 0.125-In. Round Samples

Nominal Hydrogen	Ultimate Tensile Strength, psi	Yield Strength, psi			Propor-tional Limit, psi	Extension, % Between Shoulders	Elonga-tion, % in 4D	Reduction in Area, %
		0.2% Offset	0.1% Offset	0.01% Offset				
Low Testing Speed - 0.005 In./Min								
20	91,000	73,500	69,600	61,500	59,300	18	16(b)	65
200	91,500	75,000	69,400	57,600	54,000	21	20(b)	57
400	92,900	74,100	69,300	58,400	51,600	19	31	55
600	92,900	75,000	69,800	56,600	50,500	18	28	55
High Testing Speed - 0.5 In./Min								
20	93,800					16	27	63
200	93,700					16	29	59
400	96,200					16	28	57
600	96,900					16	29	58

(a) Broke on gage mark; (b) Broke outside gage mark.

Notch-Bend Impact Tests Using Micro Sample

Nominal Hydrogen	Energy Absorbed, in-lb		Conclusion
	At 77 F	At -40 F	
20	48	47	Slow-strain embrittlement at 600 ppm; progres-sive loss of impact properties as the hydrogen content increased.
200	56	47	
400	30	26	
600	24	26	

TABLE 43. RESULTS OF TESTS TO DETERMINE THE HYDROGEN SENSITIVITY OF THE Ti-4Mn ALLOY (K-11)

Hydrogen Content, ppm		VHN (10-Kg Load)		Metallographic Structure, 20 ppm
Nominal	By Analysis	Hydrogen Content	VHN	
20	33	20	233	Structure: equiaxed α + β
200	209	200	238	Third phase: occurring at 400 ppm(a)
400	394	400	233	Vol %α: 70
				α grain size: 4 μ

(a) Third phase observed around Vhn impressions at 200 ppm.

Unnotched Stress-Rupture Tests Using 0.125-In. Round Samples

Nominal Hydrogen	Applied Stress		Rupture Time, hours	Extension, % Between Shoulders	Elongation, % in 4D	Reduction in Area, %
	Psi	% of Ultimate Tensile Strength				
20	99,100	95	95.8	17	24(c)	52
20	97,000	93	285.5(a)	12	16	--
20	93,900	90	264.0(a)	5.7	6	--
200	104,100	95	6.7	9	14(c)	17
200	102,000	93	97.3	16	--(c)	45
200	102,000	93	257.7	11	--(b)	11
400	104,300	95	7.4	18	30	43

(a) Test discontinued before failure; (b) Broke outside gage mark; (c) Broke on gage mark.

Unnotched Tensile Tests Using 0.125-In. Round Samples

Nominal Hydrogen	Ultimate Tensile Strength, psi	Yield Strength, psi			Proportional Limit, psi	Extension, % Between Shoulders	Elongation, % in 4D	Reduction in Area, %
		0.2% Offset	0.1% Offset	0.01% Offset				
			Low Testing Speed - 0.005 In./Min					
20	104,300	81,000	80,600	76,700	74,000	21	27(b)	59
200	109,800	84,400	83,600	79,200	77,100	16	25(a)	25
400	109,800	80,400	78,100	68,000	62,200	16	21(b)	43
			High Testing Speed - 0.5 In./Min					
20	107,000					16	28	56
200	111,000					15	28	44
400	111,000					15	28	43

(a) Broke on gage mark; (b) Broke outside gage mark.

Notch-Bend Impact Tests Using Micro Sample

Nominal Hydrogen	Energy Absorbed, in-lb	
	At 77 F	At -40 F
20	30	21
200	22	9
400	20	17

Conclusion

Slow-strain embrittlement at 200 ppm in stress-rupture tests; the lack of embrittlement in. 400 ppm material is difficult to understand; no impact embrittlement

TABLE 44.   RESULTS OF TESTS TO DETERMINE THE HYDROGEN SENSITIVITY
OF THE Ti-6Mn ALLOY (K-12)

Hydrogen Content, ppm		VHN (10-Kg Load)		Metallographic Structure, 20 ppm
Nominal	By Analysis	Hydrogen Content	VHN	
20	16	20	260	Structure: equiaxed $\alpha + \beta$
200	2.2	200	272	Third phase: occurring at 600 ppm
400	--	400	274	Vol % α: 60
600	592	600	270	α grain size: 3 μ

Unnotched Stress-Rupture Tests Using 0.125-In. Round Samples

Nominal Hydrogen	Applied Stress		Rupture Time, hours	Extension, % Between Shoulders	Elongation, % in 4D	Reduction in Area, %
	Psi	% of Ultimate Tensile Strength				
20	114,400	97	13.3	14	23	44
20	112,000	95	262.1[a]	6	7	--
20	111,000	93	286.8[a]	10	14	--
200	117,800	97	16.3	17	--[c]	43
200	115,300	95	257.9[a]	10	--	--
200	113,000	93	263.7[a]	8	11	--
400	117,200	97	10.8	16	25	42
600	118,000	97	54.5	9	--[b]	8

(a) Test discontinued before failure; (b) Broke outside gage mark; (c) Broke on gage mark.

Unnotched Tensile Tests Using 0.125-In. Round Samples

Nominal Hydrogen	Ultimate Tensile Strength, psi	Yield Strength, psi			Proportional Limit, psi	Extension, % Between Shoulders	Elongation, % in 4D	Reduction in Area, %
		0.2% Offset	0.1% Offset	0.01% Offset				
Low Testing Speed - 0.005 In./Min								
20	118,000	97,500	96,000	90,200	86,100	17	28	51
200	121,500	100,300	98,600	91,400	88,900	20	30	46
400	120,800	93,800	85,600	69,600	64,700	16	24	42
600	121,800	95,000	88,200	72,100	65,600	14	20[a]	36
High Testing Speed - 0.5 In./Min								
20	118,600					14	25	54
200	125,000					15	22	52
400	124,000					16	30	48
600	123,300					15	28	48

(a) Broke on gage mark; (b) Broke outside gage mark.

Notch-Bend Impact Tests Using Micro Sample

Nominal Hydrogen	Energy Absorbed, in-lb		Conclusion
	At 77 F	At -40 F	
20	34	12	Slow-strain embrittlement at 600 ppm; impact
200	13	9	embrittlement was observed at 200 ppm
400	14	10	
600	18	13	

Hydrogen Content, ppm		VHN (10-Kg Load)		Metallographic Structure, 20 ppm
Nominal	By Analysis	Hydrogen Content	VHN	
20				
200				Structure: equiaxed $\alpha + \beta$
300				Third phase: --
				Vol % α: 50
				α grain size: 6 μ

Unnotched Stress-Rupture Tests Using 0.125-In. Round Samples

Nominal Hydrogen	Applied Stress		Rupture Time, hours	Extension, % Between Shoulders	Elonga- tion, % in 4D	Reduction in Area, %
	Psi	% of Ultimate Tensile Strength				
20	120,100	95	22.1	16	28	46
200	126,000	97	2.3	11	21	32
200	123,500	95	235.0	14	--(c)	36
300	124,000	99	0.7	15	25	40
300	121,500	97	1.7	14	--(c)	31
300	119,000	95	4.6	10	--(c)	20

(a) Test discontinued before failure; (b) Broke outside gage mark; (c) Broke on gage mark.

Unnotched Tensile Tests Using 0.125-In. Round Samples

Nominal Hydrogen	Ultimate Tensile Strength, psi	Yield Strength, psi			Propor- tional Limit, psi	Extension, % Between Shoulders	Elonga- tion, % in 4D	Reduction in Area, %
		0.2% Offset	0.1% Offset	0.01% Offset				
			Low Testing Speed - 0.005 In./Min					
20	126,500	107,800	106,600	96,400	88,400	17	26	37
200	130,000	110,600	110,800	105,600	99,200	17	24	44
300	125,300	110,400	110,000	98,700	92,400	14.7	22(c)	40
			High Testing Speed - 0.5 In./Min					
20	125,300					15	29	51
200	127,400					15	27	49
300	126,600					15	27	58

(a) Broke on gage mark; (b) Broke outside gage mark.

Notch-Bend Impact Tests Using Micro Sample

Nominal Hydrogen	Energy Absorbed, in-lb	
	At 77 F	At -40 F
20	33	12
200	14	10
300	31	10

Conclusion
Slow-strain embrittlement at 300 ppm; impact embrittlement at 200 ppm, with recovery of impact ductility

TABLE 46. RESULTS OF TESTS TO DETERMINE THE HYDROGEN SENSITIVITY
OF THE Ti-2Fe ALLOY (K-14)

Hydrogen Content, ppm		VHN (10-Kg Load)		Metallographic Structure, 20 ppm
Nominal	By Analysis	Hydrogen Content	VHN	
20	31	20	196	Structure: equiaxed $\alpha + \beta$
200	192	200	199	Third phase: occurring at 200 ppm
600	595	600	202	Vol % α: 70
				α grain size: 20 μ

Unnotched Stress-Rupture Tests Using 0.125-In. Round Samples

Nominal Hydrogen	Applied Stress		Rupture Time, hours	Extension, % Between Shoulders	Elonga-tion, % in 4D	Reduction in Area, %
	Psi	% of Ultimate Tensile Strength				
20	79,500	95	17.1	22	32	40
20	75,500	90	64.2	21	--[b]	45
20	71,300	85	258.0[a]	8	14	--
200	80,900	93	71.9	25	29	45
200	73,900	85	194.1	20	--[c]	44
200	73,900	85	257.4[a]	8	12	--
600	80,800	93	26.7	20	26[c]	44

(a) Test discontinued before failure; (b) Broke outside gage mark; (c) Broke on gage mark.

Unnotched Tensile Tests Using 0.125-In. Round Samples

Nominal Hydrogen	Ultimate Tensile Strength, psi	Yield Strength, psi			Propor-tional Limit, psi	Extension, % Between Shoulders	Elonga-tion, % in 4D	Reduction in Area, %
		0.2% Offset	0.1% Offset	0.01% Offset				
Low Testing Speed - 0.005 In./Min								
20	83,800	56,900	57,200	53,300	50,600	22	28[b]	47
200	87,000	58,400	56,000	48,150	44,800	17	27	43
600	86,900	53,900	46,900	30,600	25,500	17	31	40
High Testing Speed - 0.5 In./Min								
20	88,700					12	17	20
200	91,700					16	27	40
600	93,300					13	26	40

(a) Broke on gage mark; (b) Broke outside gage mark.

Notch-Bend Impact Tests Using Micro Sample

Nominal Hydrogen	Energy Absorbed, in-lb		Conclusion
	At 77 F	At -40 F	
20	13	12	No slow-strain embrittlement; impact embrittle-ment at 200 ppm
200	7	7	
600	5	4	

TABLE 47. RESULTS OF TESTS TO DETERMINE THE HYDROGEN SENSITIVITY OF THE Ti-4Fe ALLOY (K-15)

Hydrogen Content, ppm		VHN (10-Kg Load)		Metallographic Structure, 20 ppm
Nominal	By Analysis	Hydrogen Content	VHN	
20	14	20	245	Structure: equiaxed $\alpha + \beta$
200	229	200	243	Third phase: occurring at 200 ppm
				Vol %α: 60
				α grain size: 9-13 μ

Unnotched Stress-Rupture Tests Using 0.125-In. Round Samples

Nominal Hydrogen	Applied Stress		Rupture Time, hours	Extension, % Between Shoulders	Elonga- tion, % in 4D	Reduction in Area, %
	Psi	% of Ultimate Tensile Strength				
20	97,000	93	31.9	17	__(c)	48
20	93,900	90	256.7[a]	10	--	--
200	103,300	93	64.1	17	__(b)	34
200	103,300	93	1.2	10	12	18
200	100,000	90	8.3	7	__(c)	9

(a) Test discontinued before failure; (b) Broke outside gage mark; (c) Broke on gage mark.

Unnotched Tensile Tests Using 0.125-In. Round Samples

Nominal Hydrogen	Ultimate Tensile Strength, psi	Yield Strength, psi			Propor- tional Limit, psi	Extension, % Between Shoulders	Elonga- tion, % in 4D	Reduction in Area, %
		0.2% Offset	0.1% Offset	0.01% Offset				
		Low Testing Speed - 0.005 In./Min						
20	104,300	76,200	74,600	66,700	62,200	19	32	44
200	111,100	78,500	75,400	65,100	59,200	12	19[a]	18
		High Testing Speed - 0.5 In./Min						
20	109,800					14	25	62
200	114,500					12	21	39

(a) Broke on gage mark; (b) Broke outside gage mark.

Notch-Bend Impact Tests Using Micro Sample

Nominal Hydrogen	Energy Absorbed, in-lb		Conclusion
	At 77 F	At -40 F	
20	7	5	Slow strain embrittlement at 200 ppm; alloy brittle in impact testing
200	6	5	

TABLE 48. RESULTS OF TESTS TO DETERMINE THE HYDROGEN SENSITIVITY
OF THE Ti-4Cr ALLOY (K-16)

Hydrogen Content, ppm		VHN (10-Kg Load)		Metallographic Structure, 20 ppm
Nominal	By Analysis	Hydrogen Content	VHN	
20	--	20	243	Structure: equiaxed $\alpha + \beta$
200	230	200	245	Third phase: --
				Vol % α: 70-80
				α grain size: $2\ \mu$

Unnotched Stress-Rupture Tests Using 0.125-In. Round Samples

Nominal Hydrogen	Applied Stress		Rupture Time, hours	Extension, % Between Shoulders	Elongation, % in 4D	Reduction in Area, %
	Psi	% of Ultimate Tensile Strength				
20	103,000	95	29.8	20	28	49
20	97,500	90	258.0[a]	8	10	--
20	97,500	90	285.4[a]	7	8	--
200	103,200	93	8.9	19	--[c]	49
200	99,400	90	108.2	8	--[b]	11
200	99,900	90	102.1	11	14[b]	9

(a) Test discontinued before failure; (b) Broke outside gage mark; (c) Broke on gage mark.

Unnotched Tensile Tests Using 0.125-In. Round Samples

Nominal Hydrogen	Ultimate Tensile Strength, psi	Yield Strength, psi			Proportional Limit, psi	Extension, % Between Shoulders	Elongation, % in 4D	Reduction in Area, %
		0.2% Offset	0.1% Offset	0.01% Offset				
		Low Testing Speed – 0.005 In./Min						
20	108,300	90,200	90,000	87,400	84,400	19	33	60
200	111,000	87,600	86,000	80,000	77,700	17	22[a]	37
		High Testing Speed – 0.5 In./Min						
20	111,300					15	28	58
200	111,800					16	28	51

(a) Broke on gage mark; (b) Broke outside gage mark.

Notch-Bend Impact Tests Using Micro Sample

Nominal Hydrogen	Energy Absorbed, in-lb		Conclusion
	At 77 F	At -40 F	
20	22	10	Slow strain embrittlement at 200 ppm; no impact embrittlement
200	30	21	

Hydrogen Content, ppm		VHN (10-Kg Load)		Metallographic Structure, 20 ppm
Nominal	By Analysis	Hydrogen Content	VHN	
20	20	20	270	Structure: equiaxed $\alpha + \beta$
200	229	200	270	Third phase: --
300	331	300	281	Vol % α: 60-70
				α grain size: 2 μ

Unnotched Stress-Rupture Tests Using 0.125-In. Round Samples

Nominal Hydrogen	Applied Stress		Rupture Time, hours	Extension, % Between Shoulders	Elongation, % in 4D	Reduction in Area, %
	Psi	% of Ultimate Tensile Strength				
20	114,500	93	258.9[a]	9	12	--
20	110,900	90	258.9[a]	7	--	--
200	113,800	93	96.2	17	28	61
300	114,000	93	6.2	7	6	7
300	110,300	90	144.0	7	--[b]	16

(a) Test discontinued before failure; (b) Broke outside gage mark; (c) Broke on gage mark.

Unnotched Tensile Tests Using 0.125-In. Round Samples

Nominal Hydrogen	Ultimate Tensile Strength, psi	Yield Strength, psi			Proportional Limit, psi	Extension, % Between Shoulders	Elongation, % in 4D	Reduction in Area, %
		0.2% Offset	0.1% Offset	0.01% Offset				
			Low Testing Speed - 0.005 In./Min					
20	123,200	107,500	107,000	103,000	98,800	14	18[b]	33
200	122,200	107,300	107,200	102,000	97,300	17	27	61
300	122,600	109,200	109,500	110,000	109,800	18	28	56
			High Testing Speed - 0.5 In./Min					
20	122,500					17	28	60
200	123,000					13	29	62
300	126,600					14	22	49

(a) Broke on gage mark; (b) Broke outside gage mark.

Notch-Bend Impact Tests Using Micro Sample

Nominal Hydrogen	Energy Absorbed, in-lb		Conclusion
	At 77 F	At -40 F	
20	31	21	Slow-strain embrittlement at 300 ppm; no impact embrittlement
200	42	13	
330	44	22	

Hydrogen Content, ppm		VHN (10-Kg Load)		Metallographic Structure, 20 ppm
Nominal	By Analysis	Hydrogen Content	VHN	
20	20	20	271	Structure: equiaxed $\alpha + \beta$
200	229	200	275	Third phase: --
400	--	400	--	Vol % α: 60-70
600	--	600	276	α grain size: 2 μ

Unnotched Stress-Rupture Tests Using 0.125-In. Round Samples

Nominal Hydrogen	Applied Stress		Rupture Time, hours	Extension, % Between Shoulders	Elonga-tion, % in 4D	Reduction in Area, %
	Psi	% of Ultimate Tensile Strength				
20	111,200	95	308.9[a]	12	18	--
20	109,000	93	283.3[a]	5	5	--
200	115,500	97	30.3	14	--[c]	44
200	113,000	95	308.9[a]	8	10	--
200	110,800	93	260.8[a]	5	7	--
400	118,700	97	111.3	14	--[c]	46
400	116,300	95	253.2	15	25	50
600	119,500	100	0.6	15	30	58
600	115,900	97	8.0	6	16	14

(a) Test discontinued before failure; (b) Broke outside gage mark; (c) Broke on gage mark.

Unnotched Tensile Tests Using 0.125-In. Round Samples

Nominal Hydrogen	Ultimate Tensile Strength, psi	Yield Strength, psi			Propor-tional Limit, psi	Extension, % Between Shoulders	Elonga-tion, % in 4D	Reduction in Area, %
		0.2% Offset	0.1% Offset	0.01% Offset				
Low Testing Speed - 0.005 In./Min								
20	117,200	102,700	102,700	101,100	98,800	20	31	60
200	119,000	--	--	--	--	16	22[a]	60
400	122,400	107,400	106,200	95,500	88,800	14	18[b]	54
600	119,500	--	--	--	--	12	18	26
High Testing Speed - 0.5 In./Min								
20	121,000					16	26	56
200	125,200					21	20	48
400	124,700					15	29	64
600	123;300					14	27	61

(a) Broke on gage mark; (b) Broke outside gage mark.

Notch-Bend Impact Tests Using Micro Sample

Nominal Hydrogen	Energy Absorbed, in-lb		Conclusion
	At 77 F	At -40 F	
20	38	20	Slow-strain embrittlement at 600 ppm; no impact
200	38	30	embrittlement
400	45	30	
600	54	35	

TABLE 51.   RESULTS OF TESTS TO DETERMINE THE HYDROGEN SENSITIVITY
OF THE Ti-4Cu ALLOY (K-19)

Hydrogen Content, ppm		VHN (10-Kg Load)		Metallographic Structure, 20 ppm
Nominal	By Analysis	Hydrogen Content	VHN	
20	--	20	--	Structure: α + fine spheroidal compound
200	139	200	--	Third phase: --
				Vol % α: 90
				α grain size: 9-13 μ

Unnotched Stress-Rupture Tests Using 0.125-In. Round Samples

Nominal Hydrogen	Applied Stress		Rupture Time, hours	Extension, % Between Shoulders	Elonga-tion, % in 4D	Reduction in Area, %
	Psi	% of Ultimate Tensile Strength				
20	78,000	95	20.7	19	28	39
20	74,000	90	262.0[a]	13	18	23
20	71,500	87	258.1[a]	10	12	--
200	78,500	90	21.2	11	--[b]	36
200	75,800	87	127.4	13	--[b]	36

(a) Test discontinued before failure; (b) Broke outside gage mark; (c) Broke on gage mark.

Unnotched Tensile Tests Using 0.125-In. Round Samples

Nominal Hydrogen	Ultimate Tensile Strength, psi	Yield Strength, psi			Propor-tional Limit, psi	Extension, % Between Shoulders	Elonga-tion, % in 4D	Reduction in Area, %
		0.2% Offset	0.1% Offset	0.01% Offset				
			Low Testing Speed - 0.005 In./Min					
20	82,200	57,400	56,600	49,200	44,850	19	21[b]	45
200	87,200	61,700	57,300	45,500	42,500	15	26	38
			High Testing Speed - 0.5 In./Min					
20	86,200					15	25	46
200	91,200					16	24	33

(a) Broke on gage mark; (b) Broke outside gage mark.

Notch-Bend Impact Tests Using Micro Sample

Nominal Hydrogen	Energy Absorbed, in-lb		Conclusion
	At 77 F	At -40 F	
20	28	29	No slow strain embrittlement; impact embrittle-ment at 200 ppm
200	7	5	

Hydrogen Content, ppm		VHN (10-Kg Load)		Metallographic Structure, 20 ppm
Nominal	By Analysis	Hydrogen Content	VHN	
20	--	20	--	Structure: α + fine spheroidal comp.
200	--	200	--	Third phase: --
400	--	400	--	Vol % α: 80
				α grain size: --

Unnotched Stress-Rupture Tests Using 0.125-In. Round Samples

Nominal Hydrogen	Applied Stress		Rupture Time, hours	Extension, % Between Shoulders	Elongation, % in 4D	Reduction in Area, %
	Psi	% of Ultimate Tensile Strength				
20	87,800	95	4.6	18	26	41

(a) Test discontinued before failure; (b) Broke outside gage mark; (c) Broke on gage mark.

Unnotched Tensile Tests Using 0.125-In. Round Samples

Nominal Hydrogen	Ultimate Tensile Strength, psi	Yield Strength, psi			Proportional Limit, psi	Extension, % Between Shoulders	Elongation, % in 4D	Reduction in Area, %
		0.2% Offset	0.1% Offset	0.01% Offset				
Low Testing Speed - 0.005 In./Min								
20	92,400	67,400	63,400	34,700	25,300	14	23	40
200	93,700	68,800	64,600	53,200	47,000	22	33	48
400(c)	102,500	76,000	69,600	44,000	35,000	2	4	8
High Testing Speed - 0.5 In./Min								
20	95,800					14	26	44
400	99,900					16	29	42

(a) Broke on gage mark; (b) Broke outside gage mark; (c) This sample contained an inclusion which resulted in low ductility.

Notch-Bend Impact Tests Using Micro Sample

Nominal Hydrogen	Energy Absorbed, in-lb		Conclusion
	At 77 F	At -40 F	
20	20	12	No slow-strain embrittlement; impact embrittlement at 400 ppm or less; testing was not completed
400	5	4	

Hydrogen Content, ppm		VHN (10-Kg Load)		Metallographic Structure, 20 ppm
Nominal	By Analysis	Hydrogen Content	VHN	
20	--	20	--	Structure: equiaxed α - β
200	--	200	--	Third phase: --
400	--	400	--	Vol % α: 80
				α grain size: 2 μ

Unnotched Stress-Rupture Tests Using 0.125-In. Round Samples

Nominal Hydrogen	Applied Stress		Rupture Time, hours	Extension, % Between Shoulders	Elongation, % in 4D	Reduction in Area, %
	Psi	% of Ultimate Tensile Strength				
20	89,400	93	110.7	17	30	56
200	88,400	93	101.8	17	15[b]	57
400	90,600	95	8.0	16	17	50
400	87,400	92	115.8	13	15	--[d]

(a) Test discontinued before failure; (b) Broke outside gage mark; (c) Broke on gage mark; (d) Broke around inclusion in shoulder, R·A not measured.

Unnotched Tensile Tests Using 0.125-In. Round Samples

Nominal Hydrogen	Ultimate Tensile Strength, psi	Yield Strength, psi			Proportional Limit, psi	Extension, % Between Shoulders	Elongation, % in 4D	Reduction in Area, %
		0.2% Offset	0.1% Offset	0.01% Offset				
			Low Testing Speed - 0.005 In./Min					
20	96,100	77,200	75,200	69,900	67,400	18	33	62
200	95,000	72,300	69,600	57,000	46,500	18	20[b]	60
400	95,400	68,800	65,200	56,000	52,800	16	18	55
			High Testing Speed - 0.5 In./Min					
20	98,900					16	29	61
200	97,800					17	32	62
400	83,300					16	30	58

(a) Broke on gage mark; (b) Broke outside gage mark.

Notch-Bend Impact Tests Using Micro Sample

Nominal Hydrogen	Energy Absorbed, in-lb		Conclusion
	At 77 F	At -40 F	
20	46	38	Testing on this alloy was not completed; no embrittlement up to 400 ppm
200	43	43	
400	42	48	

Hydrogen Content, ppm		VHN (10-Kg Load)		Metallographic Structure, 20 ppm
Nominal	By Analysis	Hydrogen Content	VHN	
20	--	20	--	Structure: equiaxed $\alpha + \beta$
200	--	200	--	Third phase: --
600	--	600	--	Vol % α: 60-70
800	--	800	--	α grain size: 2 μ

Unnotched Stress-Rupture Tests Using 0.125-In. Round Samples

Nominal Hydrogen	Applied Stress		Rupture Time, hours	Extension, % Between Shoulders	Elonga-tion, % in 4D	Reduction in Area, %
	Psi	% of Ultimate Tensile Strength				
200	109,600	97	2.8	17	30	67
200	107,300	95	14.8	14	--(c)	58
200	105,000	93	312.0(a)	8	--	--
800	108,100	95	9.1	8	--(c)	16

(a) Test discontinued before failure; (b) Broke outside gage mark; (c) Broke on gage mark.

Unnotched Tensile Tests Using 0.125-In. Round Samples

Nominal Hydrogen	Ultimate Tensile Strength, psi	Yield Strength, psi			Propor-tional Limit, psi	Extension, % Between Shoulders	Elonga-tion, % in 4D	Reduction in Area, %
		0.2% Offset	0.1% Offset	0.01% Offset				
			Low Testing Speed - 0.005 In./Min					
20	111,200	99,200	96,600	88,000	81,000	19	34	69
200	113,000	98,500	94,500	83,100	79,200	16	21(a)	67
600	107,500	101,800	97,500	81,400	73,200	17	30	64
800	113,800	102,600	95,800	80,400	75,300	15	25	50
			High Testing Speed - 0.5 In./Min					
20	113,600					15	30	69
200	114,600					16	32	76
600	112,700					14	30	73
800	118,800					11	22	66

(a) Broke on gage mark; (b) Broke outside gage mark.

Notch-Bend Impact Tests Using Micro Sample

Nominal Hydrogen	Energy Absorbed, in-lb		Conclusion
	At 77 F	At -40 F	
20	56	43	Slow-strain embrittlement at 800 ppm; progress-ing loss of impact properties with increasing hydrogen content
200	46	30	
600	35	25	
800	35	20	

TABLE 55. RESULTS OF TESTS TO DETERMINE THE HYDROGEN SENSITIVITY
OF THE Ti-8Mo-8V ALLOY (K-23)

Hydrogen Content, ppm		VHN (10-Kg Load)		Metallographic Structure, 20 ppm
Nominal	By Analysis	Hydrogen Content	VHN	
20	--	20	--	Structure: β + fine spheroidal α
200	--	200	--	Third phase: --
800	--	800	--	Vol % α: 30-40
				α grain size: 2 μ

Unnotched Stress-Rupture Tests Using 0.125-In. Round Samples

Nominal Hydrogen	Applied Stress		Rupture Time, hours	Extension, % Between Shoulders	Elonga- tion, % in 4D	Reduction in Area, %
	Psi	% of Ultimate Tensile Strength				
20	124,000	93	263.9	3	7	--
200	126,300	97	259.8	11	20	39
200	121,000	93	261.9[a]	1	1	--
800	140,200	105	47.3[d]	7	11	28
800	132,200	99	258.1[a]	0	0	--
800	129,500	97	260.7[a]	1	1	--

(a) Test discontinued before failure; (b) Broke outside gage mark; (c) Broke on gage mark; (d) This sample loaded 250 hr at 134,600 psi (101%) and 250 hr at 137,300 psi (103%) before final loading at 140,200 psi (105%).

Unnotched Tensile Tests Using 0.125-In. Round Samples

Nominal Hydrogen	Ultimate Tensile Strength, psi	Yield Strength, psi			Propor- tional Limit, psi	Extension, % Between Shoulders	Elonga- tion, % in 4D	Reduction in Area, %
		0.2% Offset	0.1% Offset	0.01% Offset				
			Low Testing Speed - 0.005 In./Min					
20	133,400	126,500	125,700	121,800	117,800	11	16[a]	49
200	130,200	123,000	122,200	118,300	112,800	9	17	53
800	133,500	131,400	128,700	115,500	102,500	7	12	29
			High Testing Speed - 0.5 In./Min					
20	137,300					12	24	59
200	133,500					11	22	59
800	130,100					6	12	39

(a) Broke on gage mark; (b) Broke outside gage mark.

Notch-Bend Impact Tests Using Micro Sample

Nominal Hydrogen	Energy Absorbed, in-lb		Conclusion
	At 77 F	At -40 F	
20	12	7	No evidence of slow strain embrittlement; impact
200	15	3	embrittlement at 800 ppm; probably progressive
800	6	2	loss of impact properties occurs as hydrogen content is increased

TABLE 56. RESULTS OF TESTS TO DETERMINE THE HYDROGEN SENSITIVITY
OF THE Ti-2Mn-2Fe ALLOY (K-24)

| Hydrogen Content, ppm | | VHN (10-Kg Load) | | Metallographic |
Nominal	By Analysis	Hydrogen Content	VHN	Structure, 20 ppm
20	--	20	171	Structure: α + fine spheroidal β
200	230	200	240	Third phase: occurring at 200 ppm
				Vol % α: 90
				α grain size: 13-20 μ

Unnotched Stress-Rupture Tests Using 0.125-In. Round Samples

| Nominal Hydrogen | Applied Stress | | Rupture Time, hours | Extension, % Between Shoulders | Elonga-tion, % in 4D | Reduction in Area, % |
	Psi	% of Ultimate Tensile Strength				
20	97,500	95	46.9	20	30	49
20	95,600	93	47.6	19	--[c]	49
20	92,600	90	264.0[a]	11	--	--
200	100,100	95	21.4	10	13[c]	16
200	98,200	93	257.1[a]	9	--	--
200	94,800	90	256.9[a]	5	8	--

(a) Test discontinued before failure; (b) Broke outside gage mark; (c) Broke on gage mark.

Unnotched Tensile Tests Using 0.125-In. Round Samples

| Nominal Hydrogen | Ultimate Tensile Strength, psi | Yield Strength, psi | | | Propor-tional Limit, psi | Extension, % Between Shoulders | Elonga-tion, % in 4D | Reduction in Area, % |
		0.2% Offset	0.1% Offset	0.01% Offset				
			Low Testing Speed - 0.005 In./Min					
20	102,900	75,800	75,000	69,800	66,300	18	25[a]	43
200	105,400	84,800	74,900	68,000	64,800	16	19[a]	29
			High Testing Speed - 0.5 In./Min					
20	106,200					17	28	48
200	109,200					16	28	45

(a) Broke on gage mark; (b) Broke outside gage mark.

Notch-Bend Impact Tests Using Micro Sample

| Nominal Hydrogen | Energy Absorbed, in-lb | | | Conclusion |
	At 77 F	At -40 F		
20	54	9		Both slow-strain embrittlement and impact em-
200	10	9		brittling at 200 ppm

Hydrogen Content, ppm		VHN (10-Kg Load)		Metallographic Structure, 20 ppm
Nominal	By Analysis	Hydrogen Content	VHN	
20	--	20	--	Structure: equiaxed $\alpha + \beta$
200	230	200	--	Third phase: occurring at 400 ppm
300	--	300	--	Vol % α: 80
400	394	400	--	α grain size: 4 μ

Unnotched Stress-Rupture Tests Using 0.125-In. Round Samples

Nominal Hydrogen	Applied Stress		Rupture Time, hours	Extension, % Between Shoulders	Elongation, % in 4D	Reduction in Area, %
	Psi	% of Ultimate Tensile Strength				
20	98,000	95	263.0[a]	13	21	--
20	96,000	93	78.1	19	--[c]	59
20	93,000	90	264.0[a]	9	11	--
200	100,000	95	31.1	16	--[c]	54
200	98,100	93	56.2	17	--[c]	52
200	95,100	90	261.8[a]	10	14	--
300	98,200	95	48.9	18	31	55
400	97,500	93	76.8	10	--[b]	6

(a) Test discontinued before failure; (b) Broke outside gage mark; (c) Broke on gage mark.

Unnotched Tensile Tests Using 0.125-In. Round Samples

Nominal Hydrogen	Ultimate Tensile Strength, psi	Yield Strength, psi			Proportional Limit, psi	Extension, % Between Shoulders	Elongation, % in 4D	Reduction in Area, %
		0.2% Offset	0.1% Offset	0.01% Offset				
Low Testing Speed - 0.005 In./Min								
20	103,200	83,400	83,100	81,000	77,000	19	27[a]	61
200	105,700	84,200	83,800	77,800	75,400	17	27	49
300	103,300	80,200	78,200	71,200	65,800	20	28[b]	52
400	104,800	80,000	78,600	72,200	65,200	11	27[a]	50
High Testing Speed - 0.5 In./Min								
20	107,300					16	30	61
200	106,900					17	30	52
300	106,900					15	29	53
400	109,000					15	28	50

(a) Broke on gage mark; (b) Broke outside gage mark.

Notch-Bend Impact Tests Using Micro Sample

Nominal Hydrogen	Energy Absorbed, in-lb		Conclusion
	At 77 F	At -40 F	
20	44	34	Slow-strain embrittlement at 400 ppm; no impact embrittlement
200	32	19	
300	42	26	
400	40	21	

TABLE 58. RESULTS OF TESTS TO DETERMINE THE HYDROGEN SENSITIVITY
OF THE Ti-2Cr-2Fe ALLOY (K-26)

Hydrogen Content, ppm		VHN (10-Kg Load)		Metallographic Structure, 20 ppm
Nominal	By Analysis	Hydrogen Content	VHN	
20	15	20	--	Structure: equiaxed $\alpha + \beta$
200	232	200	--	Third phase: occurring at 200 ppm
				Vol % α: 80
				α grain size: 5 μ

Unnotched Stress-Rupture Tests Using 0.125-In. Round Samples

Nominal Hydrogen	Applied Stress		Rupture Time, hours	Extension, % Between Shoulders	Elongation, % in 4D	Reduction in Area, %
	Psi	% of Ultimate Tensile Strength				
20	96,000	95	86.3	14	--[c]	44
20	94,000	93	255.9[a]	8	11	--
200	101,100	95	22.6	10	12[c]	17
200	99,000	93	257.1[a]	13	15	--
200	95,900	90	261.3[a]	6	10	--

(a) Test discontinued before failure; (b) Broke outside gage mark; (c) Broke on gage mark.

Unnotched Tensile Tests Using 0.125-In. Round Samples

Nominal Hydrogen	Ultimate Tensile Strength, psi	Yield Strength, psi			Proportional Limit, psi	Extension, % Between Shoulders	Elongation, % in 4D	Reduction in Area, %
		0.2% Offset	0.1% Offset	0.01% Offset				
Low Testing Speed - 0.005 In./Min								
20	101,000	74,400	73,400	67,400	65,400	17	21[a]	39
200	106,500	79,500	76,900	69,000	66,700	18	30	50
High Testing Speed - 0.5 In./Min								
20	106,200					17	31	54
200	109,800					13	22[a]	37

(a) Broke on gage mark; (b) Broke outside gage mark.

Notch-Bend Impact Tests Using Micro Sample

Nominal Hydrogen	Energy Absorbed, in-lb		Conclusion
	At 77 F	At -40 F	
20	32	21	Both slow-strain and impact embrittlement at 200 ppm
200	13	10	

TABLE 59. RESULTS OF TESTS TO DETERMINE THE HYDROGEN SENSITIVITY OF THE Ti-3Cr-3Fe ALLOY (K-27)

Hydrogen Content, ppm		VHN (10-Kg Load)		Metallographic Structure, 20 ppm
Nominal	By Analysis	Hydrogen Content	VHN	
20	16	20	—	Structure: equiaxed $\alpha + \beta$
200	230	200	—	Third phase: --
				Vol % α: 50-60
				α grain size: 4 μ

Unnotched Stress-Rupture Tests Using 0.125-In. Round Samples

Nominal Hydrogen	Applied Stress		Rupture Time, hours	Extension, % Between Shoulders	Elonga-tion, % in 4D	Reduction in Area, %
	Psi	% of Ultimate Tensile Strength				
20	110,000	93	188.1	15	13	56
20	106,600	90	257.3[a]	4	4	--
200	115,000	93	153.9	11	--[c]	20
200	114,900	93	263	8	10[b]	11
200	111,100	90	219.4	6	--[b]	10

(a) Test discontinued before failure; (b) Broke outside gage mark; (c) Broke on gage mark.

Unnotched Tensile Tests Using 0.125-In. Round Samples

Nominal Hydrogen	Ultimate Tensile Strength, psi	Yield Strength, psi			Propor-tional Limit, psi	Extension, % Between Shoulders	Elonga-tion, % in 4D	Reduction in Area, %
		0.2% Offset	0.1% Offset	0.01% Offset				
			Low Testing Speed - 0.005 In./Min					
20	118,500	98,200	92,400	80,400	77,000	19	19[a]	55
200	123,600	97,800	89,600	77,400	74,200	10	17[a]	43
			High Testing Speed - 0.5 In./Min					
20	119,700					15	25	57
200	124,000					17	25	43

(a) Broke on gage mark; (b) Broke outside gage mark.

Notch-Bend Impact Tests Using Micro Sample

Nominal Hydrogen	Energy Absorbed, in-lb		Conclusion
	At 77 F	At -40 F	
20	38	15	Both slow-strain and impact embrittlement at 200 ppm
200	14	10	

Hydrogen Content, ppm		VHN (10-Kg Load)		Metallographic Structure, 20 ppm
Nominal	By Analysis	Hydrogen Content	VHN	
20	18	20	—	Structure: equiaxed $\alpha + \beta$
200	216	200	—	Third phase: --
				Vol % α: 60
				α grain size: 4 μ

Unnotched Stress-Rupture Tests Using 0.125-In. Round Samples

Nominal Hydrogen	Applied Stress		Rupture Time, hours	Extension, % Between Shoulders	Elonga-tion, % in 4D	Reduction in Area, %
	Psi	% of Ultimate Tensile Strength				
20	111,000	93	242.8	18	26	59
20	107,500	90	258.8[a]	10	8	--
200	116,500	93	46.0	15	16	49
200	113,000	90	31.5	5	6[c]	13
200	113,000	90	262.5[a]	6	7	--

(a) Test discontinued before failure; (b) Broke outside gage mark; (c) Broke on gage mark.

Unnotched Tensile Tests Using 0.125-In. Round Samples

Nominal Hydrogen	Ultimate Tensile Strength, psi	Yield Strength, psi			Propor-tional Limit, psi	Extension, % Between Shoulders	Elonga-tion, % in 4D	Reduction in Area, %
		0.2% Offset	0.1% Offset	0.01% Offset				
				Low Testing Speed - 0.005 In./Min				
20	119,500	98,700	94,000	81,700	77,800	23	21[b]	56
200	125,500	101,100	96,300	83,400	80,300	12	15[a]	24
				High Testing Speed - 0.5 In./Min				
20	121,500					14	20[a]	52
200	126,300					15	24	51

(a) Broke on gage mark; (b) Broke outside gage mark.

Notch-Bend Impact Tests Using Micro Sample

Nominal Hydrogen	Energy Absorbed, in-lb		Conclusion
	At 77 F	At -40 F	
20	38	15	Both slow-strain and impact embrittlement at
200	18	10	200 ppm

TABLE 61.   RESULTS OF TESTS TO DETERMINE THE HYDROGEN SENSITIVITY
OF THE Ti-2Mo-2Mn ALLOY (K-29)

Hydrogen Content, ppm		VHN (10-Kg Load)		Metallographic Structure, 20 ppm
Nominal	By Analysis	Hydrogen Content	VHN	
20	14	20	—	Structure: equiaxed $\alpha + \beta$
200	194	200	—	Third phase: --
300	304	300	—	Vol % α: 60
				α grain size: 4 μ

Unnotched Stress-Rupture Tests Using 0.125-In. Round Samples

Nominal Hydrogen	Applied Stress		Rupture Time, hours	Extension, % Between Shoulders	Elonga-tion, % in 4D	Reduction in Area, %
	Psi	% of Ultimate Tensile Strength				
20	98,100	93	17.5	16	26	59
20	95,000	90	168.6	18	30	50
200	98,700	93	30.0	18	28[c]	52
300	99,000	93	58.2	9	10[b]	11
300	95,800	90	74.3	10	11[b]	11

(a) Test discontinued before failure; (b) Broke outside gage mark; (c) Broke on gage mark.

Unnotched Tensile Tests Using 0.125-In. Round Samples

Nominal Hydrogen	Ultimate Tensile Strength, psi	Yield Strength, psi			Propor-tional Limit, psi	Extension, % Between Shoulders	Elonga-tion, % in 4D	Reduction in Area, %
		0.2% Offset	0.1% Offset	0.01% Offset				
		Low Testing Speed - 0.005 In./Min						
20	105,400	88,600	87,100	81,400	78,200	19	27	54
200	106,200	83,600	81,500	72,800	67,500	18	33	59
300	106,300	87,900	85,600	76,200	72,600	17	19[b]	55
		High Testing Speed - 0.5 In./Min						
20	106,400					15	29	59
200	110,200					16	32	63
300	110,300					17	30	56

(a) Broke on gage mark; (b) Broke outside gage mark.

Notch-Bend Impact Tests Using Micro Sample

Nominal Hydrogen	Energy Absorbed, in-lb		Conclusion
	At 77 F	At -40 F	
20	35	26	Slow-strain embrittlement at 300 ppm; no impact embrittlement
200	31	16	
300	28	17	

TABLE 62. RESULTS OF TESTS TO DETERMINE THE HYDROGEN SENSITIVITY OF THE Ti-2Mo-2Fe ALLOY (K-30)

Hydrogen Content, ppm		VHN (10-Kg Load)		Metallographic Structure, 20 ppm
Nominal	By Analysis	Hydrogen Content	VHN	
20	--	20	—	Structure: equiaxed α + β
200	194	200	—	Third phase: occurring at 300 ppm
300	--	300	—	Vol % α: 70
				α grain size: 2 μ

Unnotched Stress-Rupture Tests Using 0.125-In. Round Samples

Nominal Hydrogen	Applied Stress		Rupture Time, hours	Extension, % Between Shoulders	Elonga-tion, % in 4D	Reduction in Area, %
	Psi	% of Ultimate Tensile Strength				
20	--	--	--	--	--	--
200	109,000	93	20.1	16	--(c)	52
200	105,300	90	263.6[a]	11	17	--
300	110,000	95	9.4	10	27	52
300	107,700	93	65.8	6	12[b]	14

(a) Test discontinued before failure; (b) Broke outside gage mark; (c) Broke on gage mark.

Unnotched Tensile Tests Using 0.125-In. Round Samples

Nominal Hydrogen	Ultimate Tensile Strength, psi	Yield Strength, psi			Propor-tional Limit, psi	Extension, % Between Shoulders	Elonga-tion, % in 4D	Reduction in Area, %
		0.2% Offset	0.1% Offset	0.01% Offset				
			Low Testing Speed - 0.005 In./Min					
20	116,800	94,800	91,300	82,200	78,100	19	31	54
200	117,100	94,500	90,700	82,900	78,400	18	28	45
300	115,800	91,400	87,500	75,200	68,700	15	27	49
			High Testing Speed - 0.5 In./Min					
20	118,500					17	32	57
200	117,500					15	31	54
300	119,700					15	27	52

(a) Broke on gage mark; (b) Broke outside gage mark.

Notch-Bend Impact Tests Using Micro Sample

Nominal Hydrogen	Energy Absorbed, in-lb		Conclusion
	At 77 F	At -40 F	
20	14	6	Both slow-strain and impact embrittlement at
200	11	7	300 ppm
300	9	8	

TABLE 63.   RESULTS OF TESTS TO DETERMINE THE HYDROGEN SENSITIVITY OF THE Ti-2V-2Fe ALLOY (K-31)

Hydrogen Content, ppm		VHN (10-Kg Load)		Metallographic Structure, 20 ppm
Nominal	By Analysis	Hydrogen Content	VHN	
20	17	20	—	Structure: equiaxed $\alpha + \beta$
200	193	200	—	Third phase: occurring at 200 ppm
300	274	300	—	Vol % α: 75
				α grain size: 4 μ

Unnotched Stress-Rupture Tests Using 0.125-In. Round Samples

Nominal Hydrogen	Applied Stress		Rupture Time, hours	Extension, % Between Shoulders	Elongation, % in 4D	Reduction in Area, %
	Psi	% of Ultimate Tensile Strength				
20	95,500	93	47.5	19	--(c)	56
200	93,900	95	155.0	11	19	11
300	99,000	93	154.8	9	--(b)	16
300	99,000	93	32.1	11	36	48

(a) Test discontinued before failure; (b) Broke outside gage mark; (c) Broke on gage mark.

Unnotched Tensile Tests Using 0.125-In. Round Samples

Nominal Hydrogen	Ultimate Tensile Strength, psi	Yield Strength, psi			Proportional Limit, psi	Extension, % Between Shoulders	Elongation, % in 4D	Reduction in Area, %
		0.2% Offset	0.1% Offset	0.01% Offset				
		Low Testing Speed - 0.005 In./Min						
20	102,700	--	--	76,000	73,400	17	24(a)	56
200	106,300	82,300	79,300	70,000	65,300	19	24(a)	44
200	101,000	75,300	73,100	65,000	50,000	15	20(a)	51
		High Testing Speed - 0.5 In./Min						
20	105,600					16	26	61
200	108,900					15	27	49
200	85,000					16	32	52

(a) Broke on gage mark; (b) Broke outside gage mark.

Notch-Bend Impact Tests Using Micro Sample

Nominal Hydrogen	Energy Absorbed, in-lb		Conclusion
	At 77 F	At -40 F	
20	32	25	Slow-strain embrittlement at 300 ppm; no impact embrittlement
200	17	17	
300	22	17	

TABLE 64. RESULTS OF TESTS TO DETERMINE THE HYDROGEN SENSITIVITY
OF THE Ti-2Mo-2Cr ALLOY (K-32)

| Hydrogen Content, ppm | | VHN (10-Kg Load) | | Metallographic Structure, 20 ppm |
Nominal	By Analysis	Hydrogen Content	VHN	
24	192	20	—	Structure: equiaxed α + β
200	332	200	—	Third phase: --
300	--	300	—	Vol % α: 60-70
				α grain size: 2 μ

Unnotched Stress-Rupture Tests Using 0.125-In. Round Samples

| Nominal Hydrogen | Applied Stress | | Rupture Time, hours | Extension, % Between Shoulders | Elonga-tion, % in 4D | Reduction in Area, % |
	Psi	% of Ultimate Tensile Strength				
20	104,600	93	2.6	17	--(c)	60
20	101,100	90	44.1	15	--(c)	57
20	101,100	90	57.6	20	26	62
200	96,300	90	207.9	17	20	61
300	102,800	93	52.4	18	--(c)	53
300	99,500	90	73.5	8	--(b)	9
300	99,500	90	70.4	10	12	20

(a) Test discontinued before failure; (b) Broke outside gage mark; (c) Broke on gage mark.

Unnotched Tensile Tests Using 0.125-In. Round Samples

| Nominal Hydrogen | Ultimate Tensile Strength, psi | Yield Strength, psi | | | Propor-tional Limit, psi | Extension, % Between Shoulders | Elonga-tion, % in 4D | Reduction in Area, % |
		0.2% Offset	0.1% Offset	0.01% Offset				
Low Testing Speed - 0.005 In./Min								
20	112,500	98,700	96,300	90,500	88,300	16	28	60
200	107,000	89,000	86,400	79,100	75,400	16	31	61
300	110,600	--	--	89,400	83,600	15	22(a)	46
High Testing Speed - 0.5 In./Min								
20	111,300					16	28	67
200	110,000					16	31	63
300	112,300					15	36	64

(a) Broke on gage mark; (b) Broke outside gage mark.

Notch-Bend Impact Tests Using Micro Sample

| Nominal Hydrogen | Energy Absorbed, in-lb | | Conclusion |
	At 77 F	At -40 F	
20	52	47	Slow-strain embrittlement at 300 ppm; no impact embrittlement
200	41	35	
300	50	40	

TABLE 65.   RESULTS OF TESTS TO DETERMINE THE HYDROGEN SENSITIVITY
OF THE Ti-2Mo-2Cr-2Fe ALLOY (K-33)

Hydrogen Content, ppm		VHN (10-Kg Load)		Metallographic Structure, 20 ppm
Nominal	By Analysis	Hydrogen Content	VHN	
20	—	20	—	Structure: equiaxed α-β
200	—	200	—	Third phase: --
300	—	300	—	Vol % α: 50
				α grain size: 2 μ

Unnotched Stress-Rupture Tests Using 0.125-In. Round Samples

Nominal Hydrogen	Applied Stress		Rupture Time, hours	Extension, % Between Shoulders	Elonga-tion, % in 4D	Reduction in Area, %
	Psi	% of Ultimate Tensile Strength				
20	107,100	95	39.4	15	--[c]	54
20	112,800	93	262.8[a]	8	16	--
200	108,500	95	3.7	16	--[c]	52
200	106,200	93	58.3	16	28	50
300	101,900	93	258.5[a]	10	14	--

(a) Test discontinued before failure; (b) Broke outside gage mark; (c) Broke on gage mark.

Unnotched Tensile Tests Using 0.125-In. Round Samples

Nominal Hydrogen	Ultimate Tensile Strength, psi	Yield Strength, psi			Propor-tional Limit, psi	Extension, % Between Shoulders	Elonga-tion, % in 4D	Reduction in Area, %
		0.2% Offset	0.1% Offset	0.01% Offset				
			Low Testing Speed - 0.005 In./Min					
20	112,800	92,200	87,300	71,500	62,200	18	20[b]	51
200	114,200	89,400	84,300	64,600	41,200	19	35	53
300	109,600	82,800	76,400	63,800	57,800	17	25	55
			High Testing Speed - 0.5 In./Min					
20	115,100					13	26	58
200	113,500					17	29	56
300	112,000					15	29	57

(a) Broke on gage mark; (b) Broke outside gage mark.

Notch-Bend Impact Tests Using Micro Sample

Nominal Hydrogen	Energy Absorbed, in-lb		Conclusion
	At 77 F	At -40 F	
20	21	12	Testing of this alloy was not completed; no
200	13	9	embrittlement was observed at 300 ppm
300	18	8	

TABLE 66. RESULTS OF TESTS TO DETERMINE THE HYDROGEN SENSITIVITY
OF THE Ti-4Al-4Mo ALLOY (K-34)

Hydrogen Content, ppm		VHN (10-Kg Load)		Metallographic
Nominal	By Analysis	Hydrogen Content	VHN	Structure, 20 ppm
20	—	20	—	Structure: equiaxed $\alpha + \beta$
200	—	200	—	Third phase: --
600	—	600	—	Vol % α: 70-80
800	—	800	—	α grain size: 3 μ

Unnotched Stress-Rupture Tests Using 0.125-In. Round Samples

Nominal Hydrogen	Applied Stress		Rupture Time, hours	Extension, % Between Shoulders	Elongation, % in 4D	Reduction in Area, %
	Psi	% of Ultimate Tensile Strength				
20	130,600	93	262.4[a]	3	4	--
200	141,000	95	5.0	11	18	48
200	138,100	93	104.6	8	10	50
600	135,500	95	7.0	11	--[c]	52
600	132,700	93	258.2[a]	7	10	--
800	134,000	95	127.4	13	23	52

(a) Test discontinued before failure; (b) Broke outside gage mark; (c) Broke on gage mark.

Unnotched Tensile Tests Using 0.125-In. Round Samples

Nominal Hydrogen	Ultimate Tensile Strength, psi	Yield Strength, psi			Proportional Limit, psi	Extension, % Between Shoulders	Elongation, % in 4D	Reduction in Area, %
		0.2% Offset	0.1% Offset	0.01% Offset				
			Low Testing Speed - 0.005 In./Min					
20	140,500	122,000	119,700	110,000	104,400	10	16	50
200	148,300	128,900	124,800	116,500	109,200	11	22	50
600	142,700	119,900	115,800	103,000	97,200	11	15[a]	58
800	141,000	115,800	110,300	93,000	84,100	11	12	52
			High Testing Speed - 0.5 In./Min					
20	145,500					10	18	54
200	149,600					10	20	58
600	148,800					11	20	55
800	146,500					10	18	52

(a) Broke on gage mark; (b) Broke outside gage mark.

Notch-Bend Impact Tests Using Micro Sample

Nominal Hydrogen	Energy Absorbed, in-lb		Conclusion
	At 77 F	At -40 F	
20	39	29	No slow-strain embrittlement; impact embrittle-
200	16	10	ment at 200 ppm
600	19	16	
800	19	14	

Hydrogen Content, ppm		VHN (10-Kg Load)		Metallographic Structure, 20 ppm
Nominal	By Analysis	Hydrogen Content	VHN	
20	—	20	—	
200	—	200	—	Structure: equiaxed $\alpha + \beta$
600	—	600	—	Third phase: --
800	—	800	—	Vol % α: 80
				α grain size: 2 μ

Unnotched Stress-Rupture Tests Using 0.125-In. Round Samples

Nominal Hydrogen	Applied Stress		Rupture Time, hours	Extension, % Between Shoulders	Elonga-tion, % in 4D	Reduction in Area, %
	Psi	% of Ultimate Tensile Strength				
20	155,800	93	262.3[a]	3	5	--
200	174,700	97	3.4	8	8	48
200	171,000	95	15.3	9	14	49
200	167,200	93	183.7	8	--[c]	38
600	164,200	95	140.6	19	--[c]	50
800	162,500	93	83.7	12	22	53

(a) Test discontinued before failure; (b) Broke outside gage mark; (c) Broke on gage mark.

Unnotched Tensile Tests Using 0.125-In. Round Samples

Nominal Hydrogen	Ultimate Tensile Strength, psi	Yield Strength, psi			Propor-tional Limit, psi	Extension, % Between Shoulders	Elonga-tion, % in 4D	Reduction in Area, %
		0.2% Offset	0.1% Offset	0.01% Offset				
		Low Testing Speed - 0.005 In./Min						
20	167,500	150,600	149,500	142,900	138,100	11	18	49
200	180,000	--	--	--	--	7	10[a]	37
600	172,900	154,500	150,600	139,000	131,800	8	19	54
800	171,300	150,500	145,800	130,800	106,000	12	22	50
		High Testing Speed - 0.5 In./Min						
20	172,800					9	18	49
200	182,200					7	10[a]	34
600	180,500					8	18	54
800	175,300					8	16	53

(a) Broke on gage mark; (b) Broke outside gage mark.

Notch-Bend Impact Tests Using Micro Sample

Nominal Hydrogen	Energy Absorbed, in-lb		Conclusion
	At 77 F	At -40 F	
20	18	16	No evidence of slow-strain embrittlement; impact embrittlement at 200 ppm
200	8	7	
600	10	8	
800	14	10	

TABLE 68.   RESULTS OF TESTS TO DETERMINE THE HYDROGEN SENSITIVITY
OF THE Ti-4Al-4V ALLOY (K-36)

Hydrogen Content, ppm		VHN (10-Kg Load)		Metallographic Structure, 20 ppm
Nominal	By Analysis	Hydrogen Content	VHN	
20	--	20	--	
200	--	200	--	Structure: equiaxed $\alpha + \beta$
400	--	400	--	Third phase: --
600	--	600	--	Vol % α: 90
				α grain size: 5 μ

Unnotched Stress-Rupture Tests Using 0.125-In. Round Samples

Nominal Hydrogen	Applied Stress		Rupture Time, hours	Extension, % Between Shoulders	Elongation, % in 4D	Reduction in Area, %
	Psi	% of Ultimate Tensile Strength				
20	131,500	93	257.4[a]	6	--	--
200	128,600	93	80	9	--[c]	49
200	125,400	90	261.1[a]	3	5	--
400	126,500	93	171.8	10	15	37
600	128,300	95	225.8	9	12[c]	47

(a) Test discontinued before failure; (b) Broke outside gage mark; (c) Broke on gage mark.

Unnotched Tensile Tests Using 0.125-In. Round Samples

Nominal Hydrogen	Ultimate Tensile Strength, psi	Yield Strength, psi			Proportional Limit, psi	Extension, % Between Shoulders	Elongation, % in 4D	Reduction in Area, %
		0.2% Offset	0.1% Offset	0.01% Offset				
Low Testing Speed - 0.005 In./Min								
20	141,600	123,900	123,700	119,700	116,500	10	18	43
200	139,200	124,600	123,000	117,400	113,700	13	20	48
400	136,000	118,000	115,000	102,000	95,000	10	16	38
600	135,000	116,400	113,600	103,000	92,800	12	20	44
High Testing Speed - 0.5 In./Min								
20	147,800					8	16	44
200	141,400					12	24	49
400	138,800					10	19	46
600	136,800					10	19	47

(a) Broke on gage mark; (b) Broke outside gage mark.

Notch-Bend Impact Tests Using Micro Sample

Nominal Hydrogen	Energy Absorbed, in-lb		Conclusion
	At 77 F	At -40 F	
20	23	27	Testing was not completed; no embrittlement at 600 ppm
200	30	25	
400	34	30	
600	38	28	

Hydrogen Content, ppm		VHN (10-Kg Load)		Metallographic Structure, 20 ppm
Nominal	By Analysis	Hydrogen Content	VHN	
20	--	20	--	Structure: spheroidal β in α
200	--	200	--	Third phase: --
600	--	600	--	Vol % α: 90
800	--	800	--	α grain size: 6μ

Unnotched Stress-Rupture Tests Using 0.125-In. Round Samples

Nominal Hydrogen	Applied Stress		Rupture Time, hours	Extension, % Between Shoulders	Elongation, % in 4D	Reduction in Area, %
	Psi	% of Ultimate Tensile Strength				
20	134,800	93	260.7[a]	2.5	3	--
200	145,500	97	1.1	9	--[b]	44
200	142,500	95	203.5	5.1	17	47
200	139,500	93	260.7[a]	4.7	6	--
600	144,300	95	1.1	7	8[b]	43
600	141,200	93	25.0	8	16	43
800	146,300	95	20.8	10	14	43

(a) Test discontinued before failure; (b) Broke outside gage mark; (c) Broke on gage mark.

Unnotched Tensile Tests Using 0.125-In. Round Samples

Nominal Hydrogen	Ultimate Tensile Strength, psi	Yield Strength, psi			Proportional Limit, psi	Extension, % Between Shoulders	Elongation, % in 4D	Reduction in Area, %
		0.2% Offset	0.1% Offset	0.01% Offset				
			Low Testing Speed - 0.005 In./Min					
20	145,000	127,200	126,300	125,400	123,200	8	13	40
200	150,100	132,200	130,000	120,000	100,500	10	17	48
600	151,900	132,000	127,300	108,900	90,600	9	13	42
800	154,000	138,000	133,000	110,000	97,900	10	18	45
			High Testing Speed - 0.5 In./Min					
20	146,600					7	10[a]	41
200	150,800					9	17	45
600	152,000					6	8[a]	49
800	156,000					10	20	50

(a) Broke on gage mark; (b) Broke outside gage mark.

Notch-Bend Impact Tests Using Micro Sample

Nominal Hydrogen	Energy Absorbed, in-lb		Conclusion
	At 77 F	At -40 F	
20	36	30	No evidence of embrittlement
200	32	26	
600	33	28	
800	28	20	

Hydrogen Content, ppm		VHN (10-Kg Load)		Metallographic Structure, 20 ppm
Nominal	By Analysis	Hydrogen Content	VHN	
20	--	20	--	Structure: spheroidal β in α
200	--	200	--	Third phase: --
300	--	300	--	Vol % α: 60-70
400	--	400	--	α grain size: 4μ
600	--	600	--	

Unnotched Stress-Rupture Tests Using 0.125-In. Round Samples

Nominal Hydrogen	Applied Stress		Rupture Time, hours	Extension, % Between Shoulders	Elonga-tion, % in 4D	Reduction in Area, %
	Psi	% of Ultimate Tensile Strength				
20	142,500	95	60.5	11.0	19	44
20	139,500	93	262.3[a]	5.2	6	--
200	146,300	95	30.1	11.2	--[c]	43
200	143,300	93	259.8[a]	4.4	7	--
300	141,200	95	134.0	12	(c)	42

(a) Test discontinued before failure; (b) Broke outside gage mark; (c) Broke on gage mark.

Unnotched Tensile Tests Using 0.125-In. Round Samples

Nominal Hydrogen	Ultimate Tensile Strength, psi	Yield Strength, psi			Propor-tional Limit, psi	Extension, % Between Shoulders	Elonga-tion, % in 4D	Reduction in Area, %
		0.2% Offset	0.1% Offset	0.01% Offset				
Low Testing Speed - 0.005 In./Min								
20	150,000	128,000	127,900	122,900	119,500	12	20	43
200	154,000	135,900	135,500	134,000	131,700	13	16[b]	43
300	148,700	136,100	133,000	125,200	123,500	13	19	47
400	156,000	145,000	132,000	111,000	96,200	10	14	31
600	153,000	138,300	136,200	125,900	116,300	10	15	11
High Testing Speed - 0.5 In./Min								
20	152,000					11	21	46
200	154,800					11	20	45
300	149,100					10	19	33
400	160,000					9	14	44
600	155,000					7	15	22

(a) Broke on gage mark; (b) Broke outside gage mark.

Notch-Bend Impact Tests Using Micro Sample

Nominal Hydrogen	Energy Absorbed, in-lb		Conclusion
	At 77 F	At -40 F	
20	22	12	Slow strain embrittlement at 400 ppm; impact
200	13	10	embrittlement at 200 ppm
300	14	11	
400	26	18	
600	11	10	

Hydrogen Content, ppm		VHN (10-Kg Load)		Metallographic Structure, 20 ppm
Nominal	By Analysis	Hydrogen Content	VHN	
20	10	20	--	Structure: equiaxed $\alpha + \beta$
200	150	200	--	Third phase: --
600	560	600	--	Vol % α: 80
800	--	800	--	α grain size: 4μ

Unnotched Stress-Rupture Tests Using 0.125-In. Round Samples

Nominal Hydrogen	Applied Stress		Rupture Time, hours	Extension, % Between Shoulders	Elonga-tion, % in 4D	Reduction in Area, %
	Psi	% of Ultimate Tensile Strength				
20	167,100	97	258.6[a]	6	8	--
20	163,800	95	263.2[a]	2	2	--
20	160,000	93	283.5[a]	1	2	--
200	173,600	97	263.6[a]	4	5	--
200	170,000	95	256.8[a]	4.0	--	--
200	162,000	93	261.4[a]	2	1	--
600	179,900	97	4.2	10	16	43
600	178,000	96	270.5[a]	3	4	--
600	176,100	95	261.7[a]	6	12	--
800	180,800	97	19.6	9	16	41

(a) Test discontinued before failure; (b) Broke outside gage mark; (c) Broke on gage mark.

Unnotched Tensile Tests Using 0.125-In. Round Samples

Nominal Hydrogen	Ultimate Tensile Strength, psi	Yield Strength, psi			Propor-tional Limit, psi	Extension, % Between Shoulders	Elonga-tion, % in 4D	Reduction in Area, %
		0.2% Offset	0.1% Offset	0.01% Offset				
Low Testing Speed - 0.005 In./Min								
20	172,300	157,500	157,500	160,000[a]	160,800	10	18	26
200	179,000	168,000	168,000	169,500[a]	169,600	10	19	46
600	185,500	175,600	175,400	172,700	170,000	10	19	45
800	186,400	175,900	175,900	168,300	158,000	11	13	47
High Testing Speed - 0.5 In./Min								
20	176,100					10	20	49
200	186,200					9	15	43
600	188,000					9	18	43
800	184,200					10	20	48

(a) Broke on gage mark; (b) Broke outside gage mark.

Notch-Bend Impact Tests Using Micro Sample

Nominal Hydrogen	Energy Absorbed, in-lb		Conclusion
	At 77 F	At -40 F	
20	14	8	No evidence of slow-strain embrittlement; alloy
200	10	8	brittle in impact testing.
600	10	9	
800	12	6	

TABLE 72. RESULTS OF TESTS TO DETERMINE THE HYDROGEN SENSITIVITY OF THE Ti-4Al-2Fe ALLOY (K-40)

Hydrogen Content, ppm		VHN (10-Kg Load)		Metallographic Structure, 20 ppm
Nominal	By Analysis	Hydrogen Content	VHN	
20	9	20	--	Structure: equiaxed $\alpha + \beta$
200	177	200	--	Third phase: --
				Vol % α: 80-90
				α grain size: 5μ

Unnotched Stress-Rupture Tests Using 0.125-In. Round Samples

Nominal Hydrogen	Applied Stress		Rupture Time, hours	Extension, % Between Shoulders	Elonga-tion, % in 4D	Reduction in Area, %
	Psi	% of Ultimate Tensile Strength				
20	119,000	93	272.2[a]	7	8	--
20	115,000	90	257.3[a]	2	--	--
200	127,800	93	20.4	10	--[c]	30
200	123,500	90	235.8	4	--[b]	8
200	123,500	90	80.8	4	4	9

(a) Test discontinued before failure; (b) Broke outside gage mark; (c) Broke on gage mark.

Unnotched Tensile Tests Using 0.125-In. Round Samples

Nominal Hydrogen	Ultimate Tensile Strength, psi	Yield Strength, psi			Propor-tional Limit, psi	Extension, % Between Shoulders	Elonga-tion, % in 4D	Reduction in Area, %
		0.2% Offset	0.1% Offset	0.01% Offset				
			Low Testing Speed - 0.005 In./Min					
20	127,800	103,600	103,300	102,200	101,900	13	20	36
200	137,100	116,500	115,000	109,000	104,900	11	17	35
			High Testing Speed - 0.5 In./Min					
20	130,300					12	22	44
200	138,500					10	19	44

(a) Broke on gage mark; (b) Broke outside gage mark.

Notch-Bend Impact Tests Using Micro Sample

Nominal Hydrogen	Energy Absorbed, in-lb		Conclusion
	At 77 F	At -40 F	
20	15	9	Both slow-strain and impact embrittlement
200	10	8	at 200 ppm.

TABLE 73. RESULTS OF TESTS TO DETERMINE THE HYDROGEN SENSITIVITY
OF THE Ti-6Al-2Fe ALLOY (K-41)

Hydrogen Content, ppm		VHN (10-Kg Load)		Metallographic Structure, 20 ppm
Nominal	By Analysis	Hydrogen Content	VHN	
20	9	20	--	Structure: equiaxed $\alpha + \beta$
200	152	200	--	Third phase: --
400	395	400	--	Vol % α: 80-90
600	607	600	--	α grain size: 5μ

Unnotched Stress-Rupture Tests Using 0.125-In. Round Samples

Nominal Hydrogen	Applied Stress		Rupture Time, hours	Extension, % Between Shoulders	Elonga-tion, % in 4D	Reduction in Area, %
	Psi	% of Ultimate Tensile Strength				
20	154,800	97	258.3[a]	4	--	--
20	151,800	95	260.0[a]	4	--	--
20	148,800	93	69.8	8	--[c]	40
20	148,800	93	256.6[a]	3	7	--
200	161,400	97	258.0[a]	5	8	--
200	158,100	95	259.4[a]	4	--	--
200	154,000	93	308.5[a]	2	5	--
400	170,600	98	1.6	10	10	36
400	169,000	97	286.8[a]	2	--	--

(a) Test discontinued before failure; (b) Broke outside gage mark; (c) Broke on gage mark.

Unnotched Tensile Tests Using 0.125-In. Round Samples

Nominal Hydrogen	Ultimate Tensile Strength, psi	Yield Strength, psi			Propor-tional Limit, psi	Extension, % Between Shoulders	Elonga-tion, % in 4D	Reduction in Area, %
		0.2% Offset	0.1% Offset	0.01% Offset				
			Low Testing Speed - 0.005 In./Min					
20	159,700	138,500	137,800	137,500	136,600	10	9[b]	32
200	166,300	150,800	150,200	148,600	146,500	9	17	38
400	174,200	163,000	161,400	157,600	154,500	10	20	33
600	181,200	169,300	167,500	161,300	155,500	4	6[a]	8
			High Testing Speed - 0.5 In./Min					
20	161,500					10	17	40
200	172,500					8	12[a]	19
400	184,700					9	48	47
600	184,800					7	16	41

(a) Broke on gage mark; (b) Broke outside gage mark.

Notch-Bend Impact Tests Using Micro Sample

Nominal Hydrogen	Energy Absorbed, in-lb		Conclusion
	At 77 F	At -40 F	
20	13	10	Slow-strain embrittlement at 600 ppm; alloy
200	9	7	brittle in impact testing
400	10	7	
600	9	7	

TABLE 74.   RESULTS OF TESTS TO DETERMINE THE HYDROGEN SENSITIVITY
OF THE Ti-4Al-4Cr ALLOY (K-42)

Hydrogen Content, ppm		VHN (10-Kg Load)		Metallographic Structure, 20 ppm
Nominal	By Analysis	Hydrogen Content	VHN	
20	--	20	--	Structure: equiaxed $\alpha + \beta$ + fine compound
200	205	200	--	Third phase: --
400	590	400	--	Vol % α: 80
600	--	600	--	α grain size: 4μ

Unnotched Stress-Rupture Tests Using 0.125-In. Round Samples

Nominal Hydrogen	Applied Stress		Rupture Time, hours	Extension, % Between Shoulders	Elongation, % in 4D	Reduction in Area, %
	Psi	% of Ultimate Tensile Strength				
20	137,300	97	6.8	8	--(c)	26
20	134,500	95	286.2(a)	4	--	--
20	132,000	93	287.6(a)	4	5	--
200	138,800	97	6.8	8	14	26
200	136,000	95	261.0(a)	6	--	--
200	133,100	93	308.4(a)	5	5	--
400	140,800	97	0.7	12	--(b)	40
400	137,900	95	7.8	7	8	30
400	135,000	93	267.6(a)	6	9	--
600	140,500	97	8.3	3	--(b)	7

(a) Test discontinued before failure; (b) Broke outside gage mark; (c) Broke on gage mark.

Unnotched Tensile Tests Using 0.125-In. Round Samples

Nominal Hydrogen	Ultimate Tensile Strength, psi	Yield Strength, psi			Proportional Limit, psi	Extension, % Between Shoulders	Elongation, % in 4D	Reduction in Area, %
		0.2% Offset	0.1% Offset	0.01% Offset				
			Low Testing Speed - 0.005 In./Min					
20	141,600	117,900	115,600	105,000	97,700	6	8(b)	6
200	143,100	--	124,600	119,600	116,500	10	11(b)	30
400	145,200	126,000	124,000	112,100	105,600	10	16(a)	42
600	144,800	124,800	122,800	114,900	109,200	16	26	45
			High Testing Speed - 0.5 In./Min					
20	148,400					6	8	11
200	146,300					10	16	32
400	146,200					10	19	44
600	147,800					10	20	47

(a) Broke on gage mark; (b) Broke outside gage mark.

Notch-Bend Impact Tests Using Micro Sample

Nominal Hydrogen	Energy Absorbed, in-lb			Conclusion
	At 77 F	At -40 F		
20	5	6		Slow-strain embrittlement at 600 ppm; alloy brittle
200	4	3		in impact testing
400	9	8		
600	14	10		

Hydrogen Content, ppm		VHN (10-Kg Load)		Metallographic Structure, 20 ppm
Nominal	By Analysis	Hydrogen Content	VHN	
20	--	20	--	Structure: equiaxed $\alpha + \beta$
200	171	200	--	Third phase: --
				Vol %α : 80
				α grain size: 2μ

Unnotched Stress-Rupture Tests Using 0.125-In. Round Samples

Nominal Hydrogen	Applied Stress		Rupture Time, hours	Extension, % Between Shoulders	Elonga-tion, % in 4D	Reduction in Area, %
	Psi	% of Ultimate Tensile Strength				
20	158,100	95	167.6	5	--(c)	10
20	158,100	95	75.2	4	--(c)	8
20	155,000	93	262.6(a)	31	3	--
200	160,000	95	22.4	3	5	13
200	160,000	95	23.6	4	--(c)	8
200	156,500	93	308.0(a)	3	2	--

(a) Test discontinued before failure; (b) Broke outside gage mark; (c) Broke on gage mark.

Unnotched Tensile Tests Using 0.125-In. Round Samples

Nominal Hydrogen	Ultimate Tensile Strength, psi	Yield Strength, psi			Propor-tional Limit, psi	Extension, % Between Shoulders	Elonga-tion, % in 4D	Reduction in Area, %
		0.2% Offset	0.1% Offset	0.01% Offset				
				Low Testing Speed - 0.005 In./Min.				
20	166,700	146,700	145,300	137,500	132,700	4	5(a)	4
200	168,300	157,100	154,400	141,200	136,600	1	3(a)	2
				High Testing Speed - 0.5 In./Min				
20	171,400					4	5	13
200	174,600					4	6(a)	10

(a) Broke on gage mark; (b) Broke outside gage mark.

Notch-Bend Impact Tests Using Micro Sample

Nominal Hydrogen	Energy Absorbed, in-lb		Conclusion
	At 77 F	At -40 F	
20	4	4	Alloy brittle in all conditions, possibly due to
200	4	4	eutectoid decomposition during heat treating

| Hydrogen Content, ppm | | VHN (10-Kg Load) | | Metallographic |
Nominal	By Analysis	Hydrogen Content	VHN	Structure, 20 ppm
20	--	20	--	Structure: equiaxed $\alpha + \beta$
200	--	200	--	Third phase: --
400	--	400	--	Vol % α: 70
600	--	600	--	α grain size: 3μ

Unnotched Stress-Rupture Tests Using 0.125-In. Round Samples

| Nominal Hydrogen | Applied Stress | | Rupture Time, hours | Extension, % Between Shoulders | Elonga-tion, % in 4D | Reduction in Area, % |
	Psi	% of Ultimate Tensile Strength				
200	156,100	97	17.1	12	16	48
200	152,800	95	152.3	12	20	47
400	160,000	97	0.8	7	--(b)	11
400	156,500	95	11.9	14	24	52
400	153,200	93	159.3	12	--(c)	50

(a) Test discontinued before failure; (b) Broke outside gage mark; (c) Broke on gage mark.

Unnotched Tensile Tests Using 0.125-In. Round Samples

| Nominal Hydrogen | Ultimate Tensile Strength, psi | Yield Strength, psi | | | Propor-tional Limit, psi | Extension, % Between Shoulders | Elonga-tion, % in 4D | Reduction in Area, % |
		0.2% Offset	0.1% Offset	0.01% Offset				
			Low Testing Speed - 0.005 In./Min.					
20	163,400	147,200	146,100	144,300	139,600	12	16(a)	42
200	161,000	146,500	145,800	139,000	133,200	11	14(b)	48
400	164,900	148,600	146,700	140,500	136,000	14	18(b)	60
600	166,000	151,700	148,300	140,000	134,000	7	11	14
			High Testing Speed - 0.5 In./Min					
20	163,000					11	21	46
200	166,000					11	23	53
400	166,000					11	22	60
600	178,000					8	16	52

(a) Broke on gage mark; (b) Broke outside gage mark.

Notch-Bend Impact Tests Using Micro Sample

| Nominal Hydrogen | Energy Absorbed, in-lb | | | Conclusion |
	At 77 F	At -40 F		
20	13	9		Slow-strain embrittlement at 600 ppm; no impact
200	11	5		embrittlement
400	12	8		
600	--	--		

Hydrogen Content, ppm		VHN (10-Kg Load)		Metallographic Structure, 20 ppm
Nominal	By Analysis	Hydrogen Content	VHN	
20	--	20	--	Structure: equiaxed $\alpha + \beta$
300	--	300	--	Third phase: --
600	--	600	--	Vol % α: 80
				α grain size: 3μ

Unnotched Stress-Rupture Tests Using 0.125-In. Round Samples

Nominal Hydrogen	Applied Stress		Rupture Time, hours	Extension, % Between Shoulders	Elonga-tion, % in 4D	Reduction in Area, %
	Psi	% of Ultimate Tensile Strength				
300	167,000	97	7.1	11	--(c)	48
300	163,500	95	47.3	12	--(c)	46
600	166,700	97	5.7	7	10	13

(a) Test discontinued before failure; (b) Broke outside gage mark; (c) Broke on gage mark.

Unnotched Tensile Tests Using 0.125-In. Round Samples

Nominal Hydrogen	Ultimate Tensile Strength, psi	Yield Strength, psi			Propor-tional Limit, psi	Extension, % Between Shoulders	Elonga-tion, % in 4D	Reduction in Area, %
		0.2% Offset	0.1% Offset	0.01% Offset				
		Low Testing Speed - 0.005 In./Min.						
20	171,500	154,800	154,000	145,900	137,500	12	21	46
300	172,100	157,800	156,500	152,600	149,300	12	14(b)	47
600	171,800	158,500	156,000	146,000	138,000	14	18	47
		High Testing Speed - 0.5 In./Min						
20	173,900					10	20	49
300	176,500					10	17	48
600	173,500					11	22	51

(a) Broke on gage mark; (b) Broke outside gage mark.

Notch-Bend Impact Tests Using Micro Sample

Nominal Hydrogen	Energy Absorbed, in-lb		Conclusion
	At 77 F	At -40 F	
20	12	8	Testing was not completed; slow-strain
300	9	8	embrittlement at 400-600 ppm, alloy brittle in
600	9	4	impact testing

TABLE 78. RESULTS OF TESTS TO DETERMINE THE HYDROGEN SENSITIVITY
OF THE Ti-4Mo(IODIDE) ALLOY (K-46)

Hydrogen Content, ppm		VHN (10-Kg Load)		Metallographic Structure, 20 ppm
Nominal	By Analysis	Hydrogen Content	VHN	
20	29	20	--	Structure: equiaxed $\alpha + \beta$
800	--	800	--	Third phase: --
				Vol % α: 80
				α grain size: $<2\mu$

Unnotched Stress-Rupture Tests Using 0.125-In. Round Samples

Nominal Hydrogen	Applied Stress		Rupture Time, hours	Extension, % Between Shoulders	Elonga-tion, % in 4D	Reduction in Area, %
	Psi	% of Ultimate Tensile Strength				
20	75,100	95	9.7	19	--(c)	60
800	75,500	95	21.7	19	30	57

(a) Test discontinued before failure; (b) Broke outside gage mark; (c) Broke on gage mark.

Unnotched Tensile Tests Using 0.125-In. Round Samples

Nominal Hydrogen	Ultimate Tensile Strength, psi	Yield Strength, psi			Propor-tional Limit, psi	Extension, % Between Shoulders	Elonga-tion, % in 4D	Reduction in Area, %
		0.2% Offset	0.1% Offset	0.01% Offset				
		Low Testing Speed - 0.005 In./Min.						
20	79,000	60,400	56,600	47,600	41,750	18	29	62
800	79,400	50,200	43,600	30,500	25,000	18	22(a)	63
		High Testing Speed - 0.5 In./Min						
20	82,700					18	33	61
800	83,700					18	33	59

(a) Broke on gage mark; (b) Broke outside gage mark.

Notch-Bend Impact Tests Using Micro Sample

Nominal Hydrogen	Energy Absorbed, in-lb		Conclusion
	At 77 F	At -40 F	
20	55	55	No slow-strain embrittlement; some loss in
800	32	24	impact properties.

Hydrogen Content, ppm		VHN (10-Kg Load)		Metallographic Structure, 20 ppm
Nominal	By Analysis	Hydrogen Content	VHN	
20	--	20	--	Structure: β + fine spheriodal
800	--	800	--	Third phase: --
				Vol %α: <5%
				α grain size: --

Unnotched Stress-Rupture Tests Using 0.125-In. Round Samples

Nominal Hydrogen	Applied Stress		Rupture Time, hours	Extension, % Between Shoulders	Elongation, % in 4D	Reduction in Area, %
	Psi	% of Ultimate Tensile Strength				
20	106,200	97	1.6	14.0	--(c)	59
20	104,000	95	309.3(a)	5.2	9	--
800	102,700	97	4.8	11.0	--(c)	56
800	101,700	96	39.9	9.0	30	62

(a) Test discontinued before failure; (b) Broke outside gage mark; (c) Broke on gage mark.

Unnotched Tensile Tests Using 0.125-In. Round Samples

Nominal Hydrogen	Ultimate Tensile Strength, psi	Yield Strength, psi			Proportional Limit, psi	Extension, % Between Shoulders	Elongation, % in 4D	Reduction in Area, %
		0.2% Offset	0.1% Offset	0.01% Offset				
Low Testing Speed - 0.005 In./Min.								
20	109,500	107,000	106,500	101,800	98,200	15	30	69
800	105,900	105,500	105,100	100,900	97,400	11	12(b)	62
High Testing Speed - 0.5 In./Min								
20	115,200					10	20	69
800	110,000					10	22	70

(a) Broke on gage mark; (b) Broke outside gage mark.

Notch-Bend Impact Tests Using Micro Sample

Nominal Hydrogen	Energy Absorbed, in-lb		Conclusion
	At 77 F	At -40 F	
20	22	22	No embrittlement
800	22	--	

TABLE 80.   RESULTS OF TESTS TO DETERMINE THE HYDROGEN SENSITIVITY
OF THE Ti-4Mo-.15O$_2$ ALLOY (K-48)

Hydrogen Content, ppm		VHN (10-Kg Load)		Metallographic Structure, 20 ppm
Nominal	By Analysis	Hydrogen Content	VHN	
20	11	20	--	Structure: equiaxed α + β
200	--	200	--	Third phase: --
400	--	400	--	Vol %α : 80
600	--	600	--	α grain size: 2μ

Unnotched Stress-Rupture Tests Using 0.125-In. Round Samples

Nominal Hydrogen	Applied Stress		Rupture Time, hours	Extension, % Between Shoulders	Elongation, % in 4D	Reduction in Area, %
	Psi	% of Ultimate Tensile Strength				
20	110,300	93	16.7	18	--(c)	59
200	112,400	93	31.9	20	25(b)	60
200	108,800	90	105.9	9	--(c)	59
400	111,700	93	19.7	9	14	16
400	109,400	91	34.3	8	8	13
600	112,800	93	6.0	10	14	9
600	110,500	91	12.9	8	12(b)	9

(a) Test discontinued before failure; (b) Broke outside gage mark; (c) Broke on gage mark.

Unnotched Tensile Tests Using 0.125-In. Round Samples

Nominal Hydrogen	Ultimate Tensile Strength, psi	Yield Strength, psi			Proportional Limit, psi	Extension, % Between Shoulders	Elongation, % in 4D	Reduction in Area, %
		0.2% Offset	0.1% Offset	0.01% Offset				
Low Testing Speed - 0.005 In./Min.								
20	118,600	105,500	102,600	95,400	91,800	16	20(a)	59
200	120,900	105,100	100,500	90,500	86,500	19	24	54
400	120,200	100,200	95,100	82,500	73,900	15	22(a)	56
600	121,300	95,800	89,000	75,200	70,100	15	20(a)	46
High Testing Speed - 0.5 In./Min								
20	122,500					14	29	64
200	126,500					16	30	64
400	124,500					16	33	60
600	125,600					15	27	64

(a) Broke on gage mark; (b) Broke outside gage mark.

Notch-Bend Impact Tests Using Micro Sample

Nominal Hydrogen	Energy Absorbed, in-lb		Conclusion
	At 77 F	At -40 F	
20	42	18	Testing was not completed; slow-strain
200	36	12	embrittlement 300-400 ppm., no impact
400	34	10	embrittlement
600	24	7	

Hydrogen Content, ppm		VHN (10-Kg Load)		Metallographic Structure, 20 ppm
Nominal	By Analysis	Hydrogen Content	VHN	
20	--	20	--	Structure: β + fine speroidal
200	--	200	--	Third phase: --
400	--	400	--	Vol %α: 30
600	--	600	--	α grain size: 2μ

Unnotched Stress-Rupture Tests Using 0.125-In. Round Samples

Nominal Hydrogen	Applied Stress		Rupture Time, hours	Extension, % Between Shoulders	Elonga- tion, % in 4D	Reduction in Area, %
	Psi	% of Ultimate Tensile Strength				
20	135,200	93	287.7[a]	4	5	--
200	137,200	97	32.6	9	14	30
200	134,500	95	256.9[a]	--	2	--
200	131,500	93	287.7[a]	4	8	--
400	141,600	97	7.8	11	20	35
400	138,700	95	24.3	8	2	34
600	118,100	97	4.6	16	--[b]	46
600	115,600	95	3.5	10	16	17
600	113,300	93	4.0	6	10	11

(a) Test discontinued before failure; (b) Broke outside gage mark; (c) Broke on gage mark.

Unnotched Tensile Tests Using 0.125-In. Round Samples

Nominal Hydrogen	Ultimate Tensile Strength, psi	Yield Strength, psi			Propor- tional Limit, psi	Extension, % Between Shoulders	Elonga- tion, % in 4D	Reduction in Area, %
		0.2% Offset	0.1% Offset	0.01% Offset				
Low Testing Speed - 0.005 In./Min.								
20	145,400	--	135,600	133,400	130,400	7	10[a]	21
200	141,500	132,000	131,700	126,900	122,800	7	10[a]	23
400	146,000	140,000	139,000	134,000	130,000	6	8	26
600	121,800	97,000	90,800	76,500	68,400	15	25	53
High Testing Speed - 0.5 In./Min								
20	152,000					8	16	37
200	147,400					8	15	37
400	151,000					6	6	24
600	124,900					14	26	60

(a) Broke on gage mark; (b) Broke outside gage mark.

Notch-Bend Impact Tests Using Micro Sample

Nominal Hydrogen	Energy Absorbed, in-lb		Conclusion
	At 77 F	At -40 F	
20	6	6	This alloy is apparently embrittled in stress-rupture at 600 ppm. The high tensile ductility at 600 ppm as compared with 400, 200, and vacuum annealed material leads to some doubt regarding these results. Alloy brittle in impact except at 600 ppm
200	3	2	
400	6	4	
600	33	12	

Hydrogen Content, ppm		VHN (10-Kg Load)		Metallographic Structure, 20 ppm
Nominal	By Analysis	Hydrogen Content	VHN	
20	--	20	--	Structure: equiaxed $\alpha + \beta$
200	--	200	--	Third phase: occurring at 200 ppm
400	--	400	--	Vol % α: 80
				α grain size: 3μ

Unnotched Stress-Rupture Tests Using 0.125-In. Round Samples

Nominal Hydrogen	Applied Stress		Rupture Time, hours	Extension, % Between Shoulders	Elonga-tion, % in 4D	Reduction in Area, %
	Psi	% of Ultimate Tensile Strength				
20	72,600	95	19.3	15	--(c)	68
200	75,800	95	140.6	16	--(b)	59
400	79,800	98	2.0	14	22	51
400	79,000	97	254.3(a)	5	6	--
400	77,300	95	260.7(a)	9	13	--

(a) Test discontinued before failure; (b) Broke outside gage mark; (c) Broke on gage mark.

Unnotched Tensile Tests Using 0.125-In. Round Samples

Nominal Hydrogen	Ultimate Tensile Strength, psi	Yield Strength, psi			Propor-tional Limit, psi	Extension, % Between Shoulders	Elonga-tion, % in 4D	Reduction in Area, %
		0.2% Offset	0.1% Offset	0.01% Offset				
			Low Testing Speed - 0.005 In./Min.					
20	76,400	53,800	52,300	43,800	38,300	17	26	70
200	79,600	56,500	55,800	51,150	48,700	17	29	60
400	81,400	58,300	55,200	42,100	34,500	14	14(b)	57
			High Testing Speed - 0.5 In./Min					
20	77,700					17	31	71
200	80,700					17	28	59
400	85,300					13	23	53

(a) Broke on gage mark; (b) Broke outside gage mark.

Notch-Bend Impact Tests Using Micro Sample

Nominal Hydrogen	Energy Absorbed, in-lb		Conclusion
	At 77 F	At -40 F	
20	80	89	No evidence of slow-strain embrittlement at 400
200	24	22	ppm; a progressive loss of impact properties is
400	14	10	apparent, however

TABLE 83. RESULTS OF TESTS TO DETERMINE THE HYDROGEN SENSITIVITY OF THE Ti-20V (IODIDE) ALLOY (K-51)

Hydrogen Content, ppm		VHN (10-Kg Load)		Metallographic Structure, 20 ppm
Nominal	By Analysis	Hydrogen Content	VHN	
20	--	20	--	Structure: β+ fine spheroidal α
				Third phase: --
800	--	800	--	Vol % α: < 5
				α grain size: —

Unnotched Stress-Rupture Tests Using 0.125-In. Round Samples

Nominal Hydrogen	Applied Stress		Rupture Time, hours	Extension, % Between Shoulders	Elongation, % in 4D	Reduction in Area, %
	Psi	% of Ultimate Tensile Strength				
20	123,800	99	on loading	5	_(b)	56
20	121,200	97	256.9(a)	1	2	-
20	118,800	95	261.1(a)	1	1	-
800	100,200	101	on loading	13	22	62
800	98,200	99	336.0(a)	8	12	-

(a) Test discontinued before failure; (b) Broke outside gage mark; (c) Broke on gage mark.

Unnotched Tensile Tests Using 0.125-In. Round Samples

Nominal Hydrogen	Ultimate Tensile Strength, psi	Yield Strength, psi			Proportional Limit, psi	Extension, % Between Shoulders	Elongation, % in 4D	Reduction in Area, %
		0.2% Offset	0.1% Offset	0.01% Offset				
			Low Testing Speed - 0.005 In./Min.					
20	125,000	115,200	111,500	100,100	94,700	6	_(b)	54
800	99,200	73,300	71,700	64,500	55,200	14	26	60
			High Testing Speed - 0.5 In./Min					
20	121,800					5	_(b)	54
800	90,600					15	28	66

(a) Broke on gage mark; (b) Broke outside gage mark.

Notch-Bend Impact Tests Using Micro Sample

Nominal Hydrogen	Energy Absorbed, in-lb		Conclusion
	At 77 F	At -40 F	
20	51	38	No embrittlement.
800	56	35	

TABLE 84.   RESULTS OF TESTS TO DETERMINE THE HYDROGEN SENSITIVITY
OF THE Ti-4V-.15O$_2$ ALLOY (K-52)

Hydrogen Content, ppm		VHN (10-Kg Load)		Metallographic Structure, 20 ppm
Nominal	By Analysis	Hydrogen Content	VHN	
20	--	20	--	Structure: α + fine spheroidal β
100	114	100	--	Third phase: --
200	260	200	--	Vol % α: 80
				α grain size: 3μ

Unnotched Stress-Rupture Tests Using 0.125-In. Round Samples

Nominal Hydrogen	Applied Stress		Rupture Time, hours	Extension, % Between Shoulders	Elonga- tion, % in 4D	Reduction in Area, %
	Psi	% of Ultimate Tensile Strength				
20	105,900	93	21.0	15	--(c)	59
20	102,300	90	145.6	18	--(c)	60
100	99,900	90	78.6	8	13	7
200	106,000	93	14	12	--(b)	52
200	102,600	90	18.4	7	--(b)	9

(a) Test discontinued before failure; (b) Broke outside gage mark; (c) Broke on gage mark.

Unnotched Tensile Tests Using 0.125-In. Round Samples

Nominal Hydrogen	Ultimate Tensile Strength, psi	Yield Strength, psi			Propor- tional Limit, psi	Extension, % Between Shoulders	Elonga- tion, % in 4D	Reduction in Area, %
		0.2% Offset	0.1% Offset	0.01% Offset				
			Low Testing Speed - 0.005 In./Min.					
20	113,800	99,800	98,800	91,500	87,000	15	24	69
100	111,000	95,000	94,600	89,300	85,700	16	25	51
200	114,000	99,200	98,200	90,400	83,800	18	26	48
			High Testing Speed - 0.5 In./Min					
20	114,700					12	8(b)	60
100	115,000					14	26	57
200	116,900					14	26	54

(a) Broke on gage mark; (b) Broke outside gage mark.

Notch-Bend Impact Tests Using Micro Sample

Nominal Hydrogen	Energy Absorbed, in-lb		Conclusion
	At 77 F	At -40 F	
20	34	26	Slow strain embrittlement at 100 ppm. No impact
200	28	26	embrittlement.

| Hydrogen Content, ppm | | VHN (10-Kg Load) | | Metallographic Structure, 20 ppm |
Nominal	By Analysis	Hydrogen Content	VHN	
20	--	20	--	Structure: β + fine spheroidal α
200	--	200	--	Third phase: --
600	--	600	--	Vol % α: 10
800	--	800	--	α grain size: 2μ

Unnotched Stress-Rupture Tests Using 0.125-In. Round Samples

| Nominal Hydrogen | Applied Stress | | Rupture Time, hours | Extension, % Between Shoulders | Elongation, % in 4D | Reduction in Area, % |
	Psi	% of Ultimate Tensile Strength				
20	126,800	97	On loading	6	8[b]	31
20	124,200	95	262.1[a]	2	2	--
20	121,500	93	257[a]	2	--	--
200	117,700	97	258.3[a]	4	4	--
200	115,300	95	261[a]	3	5	--
200	113,000	93	281.7[a]	1	--	--
600	121,300	99	On loading	6	--[c]	30
600	120,000	98	On loading	6	--[c]	30
600	119,500	97.5	258.9[a]	--	--	--
600	118,700	97	258.8[a]	4	6	--
800	108,500	101	263.5[a]	1	1	--
800	106,300	99	281.0[a]	1	2	--

(a) Test discontinued before failure; (b) Broke outside gage mark; (c) Broke on gage mark.

Unnotched Tensile Tests Using 0.125-In. Round Samples

| Nominal Hydrogen | Ultimate Tensile Strength, psi | Yield Strength, psi | | | Proportional Limit, psi | Extension, % Between Shoulders | Elongation, % in 4D | Reduction in Area, % |
		0.2% Offset	0.1% Offset	0.01% Offset				
				Low Testing Speed - 0.005 In./Min.				
20	130,800	107,300	103,300	95,000	89,700	5	6[b]	17
200	121,400	101,500	99,200	95,000	92,100	8	8[b]	34
600	122,500	102,000	98,700	96,100	87,200	8	15	24
800	107,400	98,300	94,600	88,200	83,800	7	8	33
				High Testing Speed - 0.5 In./Min				
20	123,800					6	14	30
200	116,900					7	8	36
600	121,500					7	12	36
800	114,000					8	16	39

(a) Broke on gage mark; (b) Broke outside gage mark.

Notch-Bend Impact Tests Using Micro Sample

| Nominal Hydrogen | Energy Absorbed, in-lb | | Conclusion |
	At 77 F	At -40 F	
20	8	5	No slow strain embrittlement; alloy brittle in impact testing
200	11	8	
600	7	4	
800	4	5	

Hydrogen Content, ppm		VHN (10-Kg Load)		Metallographic Structure, 20 ppm
Nominal	By Analysis	Hydrogen Content	VHN	
20	--	20	--	Structure: equiaxed $\alpha + \beta$
300	--	300	--	Third phase: --
400	--	400	--	Vol % α: 50
				α grain size: 2μ

Unnotched Stress-Rupture Tests Using 0.125-In. Round Samples

Nominal Hydrogen	Applied Stress		Rupture Time, hours	Extension, % Between Shoulders	Elonga-tion, % in 4D	Reduction in Area, %
	Psi	% of Ultimate Tensile Strength				
20	114,200	97	310.0[a]	6	10	--
20	111,900	95	258.8[a]	6	8	--
300	117,700	97	5.6	14	22	23
300	115,300	95	55.7	12	17[b]	22

(a) Test discontinued before failure; (b) Broke outside gage mark; (c) Broke on gage mark.

Unnotched Tensile Tests Using 0.125-In. Round Samples

Nominal Hydrogen	Ultimate Tensile Strength, psi	Yield Strength, psi			Propor-tional Limit, psi	Extension, % Between Shoulders	Elonga-tion, % in 4D	Reduction in Area, %
		0.2% Offset	0.1% Offset	0.01% Offset				
			Low Testing Speed - 0.005 In./Min.					
20	117,800	93,400	92,300	85,300	77,500	16	22	39
300	121,400	106,400[a]	107,000	96,700	90,200	14	21	31
400	123,000	112,000	107,000	88,000	77,000	8	14	14
			High Testing Speed - 0.5 In./Min					
20	119,600					17	31	48
300	119,500					14	27	44
400	126,000					14	24	34

(a) Broke on gage mark; (b) Broke outside gage mark.

Notch-Bend Impact Tests Using Micro Sample

Nominal Hydrogen	Energy Absorbed, in-lb		Conclusion
	At 77 F	At -40 F	
20	36	15	Both slow strain and impact embrittlement at
300	20	10	400 ppm.
400	8	6	

Hydrogen Content, ppm		VHN (10-Kg Load)		Metallographic Structure, 20 ppm
Nominal	By Analysis	Hydrogen Content	VHN	
20	--	20	--	Structure: equiaxed $\alpha + \beta$
200	--	200	--	Third phase: --
300	323	300	--	Vol % α: 60
				α grain size: 5 μ

Unnotched Stress-Rupture Tests Using 0.125-In. Round Samples

Nominal Hydrogen	Applied Stress		Rupture Time, hours	Extension, % Between Shoulders	Elonga-tion, % in 4D	Reduction in Area, %
	Psi	% of Ultimate Tensile Strength				
20	143,000	93	77.1	15	--[c]	45
200	144,900	93	107.6	15	--[c]	59
300	140,700	93	29.5	4	--[b]	11

(a) Test discontinued before failure; (b) Broke outside gage mark; (c) Broke on gage mark.

Unnotched Tensile Tests Using 0.125-In. Round Samples

Nominal Hydrogen	Ultimate Tensile Strength, psi	Yield Strength, psi			Propor-tional Limit, psi	Extension, % Between Shoulders	Elonga-tion, % in 4D	Reduction in Area, %
		0.2% Offset	0.1% Offset	0.01% Offset				
			Low Testing Speed - 0.005 In./Min					
20	153,800	--	140,500	137,000	133,200	18	28[a]	49
200	155,800	142,500	142,700	136,000	131,200	16	24[a]	50
300	151,200	--	--	--	--	12	12[a]	41
			High Testing Speed - 0.5 In./Min					
20	150,800					15	28	55
200	154,000					14	30	54
300	153,000					16	30	59

(a) Broke on gage mark; (b) Broke outside gage mark.

Notch-Bend Impact Tests Using Micro Sample

Nominal Hydrogen	Energy Absorbed, in-lb		Conclusion
	At 77 F	At -40 F	
20	21	5	Slow-strain embrittlement at 300 ppm; impact
200	8	6	embrittlement at 200 ppm
300	7	5	

Hydrogen Content, ppm		VHN (10-Kg Load)		Metallographic Structure, 20 ppm
Nominal	By Analysis	Hydrogen Content	VHN	
20	--	20	--	Structure: equiaxed $\alpha + \beta$
300	--	300	--	Third phase: --
400	--	400	--	Vol % α: 60-70
				α grain size: 2 μ

Unnotched Stress-Rupture Tests Using 0.125-In. Round Samples

Nominal Hydrogen	Applied Stress		Rupture Time, hours	Extension, % Between Shoulders	Elonga-tion, % in 4D	Reduction in Area, %
	Psi	% of Ultimate Tensile Strength				
20	95,000	97	2.9	9	26	59
20	93,000	95	255.5[a]	9	14	--
300	97,400	97	3.0	15	--[c]	56
300	95,400	95	258.1[a]	7	11	--
300	93,300	93	264.9[a]	8	9	--
400	94,300	97	25.2	15	26	47
400	92,300	95	261.4[a]	8	10	--

(a) Test discontinued before failure; (b) Broke outside gage mark; (c) Broke on gage mark.

Unnotched Tensile Tests Using 0.125-In. Round Samples

Nominal Hydrogen	Ultimate Tensile Strength, psi	Yield Strength, psi			Propor-tional Limit, psi	Extension, % Between Shoulders	Elonga-tion, % in 4D	Reduction in Area, %
		0.2% Offset	0.1% Offset	0.01% Offset				
Low Testing Speed - 0.005 In./Min								
20	97,900	77,400	77,000	74,600	67,200	16	23	57
300	100,400	79,000	76,800	68,800	61,000	18	30	52
400	97,200	77,200	75,600	68,400	62,500	16	20[a]	53
High Testing Speed - 0.5 In./Min								
20	98,600					16	30	58
300	102,800					16	24	59
400	99,700					16	30	54

(a) Broke on gage mark; (b) Broke outside gage mark.

Notch-Bend Impact Tests Using Micro Sample

Nominal Hydrogen	Energy Absorbed, in-lb		Conclusion
	At 77 F	At -40 F	
20	53	48	No embrittlement at 400 ppm
300	47	51	
400	58	--	

Hydrogen Content, ppm		VHN (10-Kg Load)		Metallographic Structure, 20 ppm
Nominal	By Analysis	Hydrogen Content	VHN	
20	--	20	--	Structure: equiaxed $\alpha + \beta$
200	195	200	--	Third phase: --
300	296	300	--	Vol % α: 60-70
				α grain size: 4 μ

Unnotched Stress-Rupture Tests Using 0.125-In. Round Samples

Nominal Hydrogen	Applied Stress		Rupture Time, hours	Extension, % Between Shoulders	Elonga- tion, % in 4D	Reduction in Area, %
	Psi	% of Ultimate Tensile Strength				
20	126,900	93	71.2	16	--(c)	59
20	122,800	90	285.1(a)	5	7	--
200	129,800	93	33.2	17	--(c)	58
300	128,200	93	92.3	9	--(b)	17
300	124,200	90	261.3(a)	6	8	--

(a) Test discontinued before failure; (b) Broke outside gage mark; (c) Broke on gage mark.

Unnotched Tensile Tests Using 0.125-In. Round Samples

Nominal Hydrogen	Ultimate Tensile Strength, psi	Yield Strength, psi			Propor- tional Limit, psi	Extension, % Between Shoulders	Elonga- tion, % in 4D	Reduction in Area, %
		0.2% Offset	0.1% Offset	0.01% Offset				
			Low Testing Speed - 0.005 In./Min					
20	136,400	124,400	124,800	120,600	116,200	14	20(a)	57
200	139,300	127,000	126,800	123,300	119,000	14	22(a)	39
300	138,000	129,000	128,100	122,400	116,000	15	20(a)	40
			High Testing Speed - 0.5 In./Min					
20	137,600					13	24	65
200	140,000					15	28	54
300	142,200					14	25	52

(a) Broke on gage mark; (b) Broke outside gage mark.

Notch-Bend Impact Tests Using Micro Sample

Nominal Hydrogen	Energy Absorbed, in-lb		Conclusion
	At 77 F	At -40 F	
20	32	16	Slow-strain embrittlement at 300 ppm; impact
200	12	12	embrittlement at 200 ppm
300	9	10	

TABLE 90. RESULTS OF TESTS TO DETERMINE THE HYDROGEN SENSITIVITY OF THE Ti-6Al-4Mo (IODIDE) ALLOY (K-58)

Hydrogen Content, ppm		VHN (10-Kg Load)		Metallographic Structure, 20 ppm
Nominal	By Analysis	Hydrogen Content	VHN	
20	--	20	--	Structure: α + fine spheroidal β
800	--	800	--	Third phase: --
				Vol % α: 80
				α grain size: <2 μ

Unnotched Stress-Rupture Tests Using 0.125-In. Round Samples

Nominal Hydrogen	Applied Stress		Rupture Time, hours	Extension, % Between Shoulders	Elonga-tion, % in 4D	Reduction in Area, %
	Psi	% of Ultimate Tensile Strength				
20	140,000	97	59.8	8	16	44
800	145,000	97	75.1	10	8(c)	54

(a) Test discontinued before failure; (b) Broke outside gage mark; (c) Broke on gage mark.

Unnotched Tensile Tests Using 0.125-In. Round Samples

Nominal Hydrogen	Ultimate Tensile Strength, psi	Yield Strength, psi			Propor-tional Limit, psi	Extension, % Between Shoulders	Elonga-tion, % in 4D	Reduction in Area, %
		0.2% Offset	0.1% Offset	0.01% Offset				
			Low Testing Speed - 0.005 In./Min					
20	144,300	129,900	128,500	124,800	119,500	8	12	47
800	149,500	132,500	127,600	112,100	101,500	9	14(a)	54
			High Testing Speed - 0.5 In./Min					
20	150,000					7	14	49
800	156,400					9	19	56

(a) Broke on gage mark; (b) Broke outside gage mark.

Notch-Bend Impact Tests Using Micro Sample

Nominal Hydrogen	Energy Absorbed, in-lb		Conclusion
	At 77 F	At -40 F	
20	34	--	No embrittlement
800	25	14	

| Hydrogen Content, ppm | | VHN (10-Kg Load) | | Metallographic |
Nominal	By Analysis	Hydrogen Content	VHN	Structure, 20 ppm
20	--	20	--	Structure: equiaxed $\alpha + \beta$
800	--	800	--	Third phase: --
				Vol % α: 80
				α grain size: 2 μ

Unnotched Stress-Rupture Tests Using 0.125-In. Round Samples

| Nominal Hydrogen | Applied Stress | | Rupture Time, hours | Extension, % Between Shoulders | Elongation, % in 4D | Reduction in Area, % |
	Psi	% of Ultimate Tensile Strength				
20	168,800	97	70.8	9	--(c)	44
800	171,700	97	30.0	9	9	51

(a) Test discontinued before failure; (b) Broke outside gage mark; (c) Broke on gage mark.

Unnotched Tensile Tests Using 0.125-In. Round Samples

| Nominal Hydrogen | Ultimate Tensile Strength, psi | Yield Strength, psi | | | Proportional Limit, psi | Extension, % Between Shoulders | Elongation, % in 4D | Reduction in Area, % |
		0.2% Offset	0.1% Offset	0.01% Offset				
			Low Testing Speed - 0.005 In./Min					
20	174,000	160,300	159,500	156,500	154,000	8	--(a)	42
800	177,000	162,000	157,000	145,000	136,000	10	12	42
			High Testing Speed - 0.5 In./Min					
20	176,600					7	7	49
800	187,000					9	18	36

(a) Broke on gage mark; (b) Broke outside gage mark.

Notch-Bend Impact Tests Using Micro Sample

| Nominal Hydrogen | Energy Absorbed, in-lb | | Conclusion |
	At 77 F	At -40 F	
20	14	12	No slow-strain embrittlement; alloy brittle in
800	10	10	impact testing

TABLE 92. RESULTS OF TESTS TO DETERMINE THE HYDROGEN SENSITIVITY
OF THE Ti-6Al-4V (IODIDE) ALLOY (K-60)

Hydrogen Content, ppm		VHN (10-Kg Load)		Metallographic Structure, 20 ppm
Nominal	By Analysis	Hydrogen Content	VHN	
20	--	20	--	Structure: α + fine spheroidal β
600	--	600	--	Third phase: --
				Vol % α: 85-90
				α grain size: 2 μ

Unnotched Stress-Rupture Tests Using 0.125-In. Round Samples

Nominal Hydrogen	Applied Stress		Rupture Time, hours	Extension, % Between Shoulders	Elonga- tion, % in 4D	Reduction in Area, %
	Psi	% of Ultimate Tensile Strength				
20	135,300	97	73.1	7	--(c)	36
600	143,500	97	13	8	--(c)	45

(a) Test discontinued before failure; (b) Broke outside gage mark; (c) Broke on gage mark.

Unnotched Tensile Tests Using 0.125-In. Round Samples

Nominal Hydrogen	Ultimate Tensile Strength, psi	Yield Strength, psi			Propor- tional Limit, psi	Extension, % Between Shoulders	Elonga- tion, % in 4D	Reduction in Area, %
		0.2% Offset	0.1% Offset	0.01% Offset				
				Low Testing Speed - 0.005 In./Min				
20	139,500	121,900	120,800	116,600	110,800	6	8	34
600	148,000	130,900	127,000	99,000	85,300	8	7(b)	45
				High Testing Speed - 0.5 In./Min				
20	141,900					9	14	40
600	153,600					7	16	47

(a) Broke on gage mark; (b) Broke outside gage mark.

Notch-Bend Impact Tests Using Micro Sample

Nominal Hydrogen	Energy Absorbed, in-lb		Conclusion
	At 77 F	At -40 F	
20	37	--	Testing was not completed; no embrittlement at 600 ppm
600	34	32	

Hydrogen Content, ppm		VHN (10-Kg Load)		Metallographic Structure, 20 ppm
Nominal	By Analysis	Hydrogen Content	VHN	
20	--	20	--	Structure: equiaxed $\alpha + \beta$
200	140	200	--	Third phase: --
400	--	400	--	Vol % α: 90
600	595	600	--	α grain size: 5 μ

Unnotched Stress-Rupture Tests Using 0.125-In. Round Samples

Nominal Hydrogen	Applied Stress		Rupture Time, hours	Extension, % Between Shoulders	Elonga-tion, % in 4D	Reduction in Area, %
	Psi	% of Ultimate Tensile Strength				
20	169,300	95	0.1	9	15	35
20	169,300	95	7.3	10	--(c)	41
20	165,900	93	260.8(a)	2	4	--
200	171,500	95	282.5(a)	2	2	--
200	171,500	95	77.9	8	14	34
200	168,000	93	260.1(a)	4	--	--
400	181,800	97	0.1	8	--(c)	46
400	178,000	95	4.2	10	16	40
600	178,500	97	7.8	4	13	6

(a) Test discontinued before failure; (b) Broke outside gage mark; (c) Broke on gage mark.

Unnotched Tensile Tests Using 0.125-In. Round Samples

Nominal Hydrogen	Ultimate Tensile Strength, psi	Yield Strength, psi			Propor-tional Limit, psi	Extension, % Between Shoulders	Elonga-tion, % in 4D	Reduction in Area, %
		0.2% Offset	0.1% Offset	0.01% Offset				
Low Testing Speed – 0.005 In./Min								
20	178,200	162,800	162,500	161,000	156,700	9	8(b)	23
200	180,500	169,000	167,200	165,200	163,900	8	8	39
400	187,500	168,400	165,900	153,300	144,300	9	14	40
600	184,000	169,000	165,500	153,000	144,800	6	9	34
High Testing Speed – 0.5 In./Min								
20	179,000					6	6(b)	27
200	186,900					7	12	40
400	184,500					7	14	42
600	191,000					7	11	37

(a) Broke on gage mark; (b) Broke outside gage mark.

Notch-Bend Impact Tests Using Micro Sample

Nominal Hydrogen	Energy Absorbed, in-lb		Conclusion
	At 77 F	At -40 F	
20	12	8	Slow-strain embrittlement at 600 ppm; alloy brittle in impact testing
200	9	10	
400	10	12	
600	7	5	

TABLE 94. RESULTS OF TESTS TO DETERMINE THE HYDROGEN SENSITIVITY
OF THE Ti-4Al-4Mn (IODIDE) ALLOY (K-62)

Hydrogen Content, ppm		VHN (10-Kg Load)		Metallographic Structure, 20 ppm
Nominal	By Analysis	Hydrogen Content	VHN	
20	--	20	--	Structure: equiaxed $\alpha + \beta$
400	--	400	--	Third phase: --
				Vol % α: 70
				α grain size: 3 μ

Unnotched Stress-Rupture Tests Using 0.125-In. Round Samples

Nominal Hydrogen	Applied Stress		Rupture Time, hours	Extension, % Between Shoulders	Elonga- tion, % in 4D	Reduction in Area, %
	Psi	% of Ultimate Tensile Strength				
20	140,000	97	On loading	10	18	42
400	142,400	99	0.8	8	16	42
400	139,500	97	335.0	6	10	--

(a) Test discontinued before failure; (b) Broke outside gage mark; (c) Broke on gage mark.

Unnotched Tensile Tests Using 0.125-In. Round Samples

Nominal Hydrogen	Ultimate Tensile Strength, psi	Yield Strength, psi			Propor- tional Limit, psi	Extension, % Between Shoulders	Elonga- tion, % in 4D	Reduction in Area, %
		0.2% Offset	0.1% Offset	0.01% Offset				
				Low Testing Speed - 0.005 In./Min				
20	144,300	--	--	110,400	106,900	10	18	39
400	143,800	128,900	128,000	127,200	127,000	10	13	40
				High Testing Speed - 0.5 In./Min				
20	142,000					10	20	46
400	144,800					11	21	46

(a) Broke on gage mark; (b) Broke outside gage mark.

Notch-Bend Impact Tests Using Micro Sample

Nominal Hydrogen	Energy Absorbed, in-lb		Conclusion
	At 77 F	At -40 F	
20	39	13	Testing was not completed; no slow-strain
400	17	10	embrittlement at 400 ppm; impact embrittlement at 400 ppm

Hydrogen Content, ppm		VHN (10-Kg Load)		Metallographic Structure, 20 ppm
Nominal	By Analysis	Hydrogen Content	VHN	
20	--	20	--	Structure: equiaxed $\alpha + \beta$
200	202	200	--	Third phase: --
300	295	300	--	Vol % α: 80
600	598	600	--	α grain size: 5 μ

Unnotched Stress-Rupture Tests Using 0.125-In. Round Samples

Nominal Hydrogen	Applied Stress		Rupture Time, hours	Extension, % Between Shoulders	Elonga-tion, % in 4D	Reduction in Area, %
	Psi	% of Ultimate Tensile Strength				
20	156,100	97	261.8[a]	1	2	--
20	153,000	95	259.0[a]	4	--	--
20	149,900	93	261.9[a]	3	3	--
200	166,500	97	75.5	12	--	39
200	163,000	95	259.4[a]	5	--	--
200	159,800	93	282.1[a]	4	--	--
300	167,300	97	25.6	7	8	10

(a) Test discontinued before failure; (b) Broke outside gage mark; (c) Broke on gage mark.

Unnotched Tensile Tests Using 0.125-In. Round Samples

Nominal Hydrogen	Ultimate Tensile Strength, psi	Yield Strength, psi			Propor-tional Limit, psi	Extension, % Between Shoulders	Elonga-tion, % in 4D	Reduction in Area, %
		0.2% Offset	0.1% Offset	0.01% Offset				
			Low Testing Speed – 0.005 In./Min					
20	161,000	151,500	151,700	150,200	147,200	11	20	51
200	171,700	159,800	159,300	158,900	157,000	13	20[a]	30
300	172,500	162,100	161,000	159,400	156,700	14	20[a]	48
600	175,500	165,300	162,800	151,600	154,200	1	12[a]	13
			High Testing Speed – 0.5 In./Min					
20	175,000					10	20	49
200	173,300					11	20	49
300	176,100					11	20	49
600	177,500					11	21[a]	50

(a) Broke on gage mark; (b) Broke outside gage mark.

Notch-Bend Impact Tests Using Micro Sample

Nominal Hydrogen	Energy Absorbed, in-lb		Conclusion
	At 77 F	At -40 F	
20	12	9	Slow-strain embrittlement at 300 ppm; alloy brittle in impact tests
200	9	7	
300	9	8	
600	7	7	

Hydrogen Content, ppm		VHN (10-Kg Load)		Metallographic Structure, 20 ppm
Nominal	By Analysis	Hydrogen Content	VHN	
20	--	20	--	Structure: equiaxed $\alpha + \beta$
200	--	200	--	Third phase: --
400	--	400	--	Vol % α: 60-70
				α grain size: 2-3 μ

Unnotched Stress-Rupture Tests Using 0.125-In. Round Samples

Nominal Hydrogen	Applied Stress		Rupture Time, hours	Extension, % Between Shoulders	Elonga-tion, % in 4D	Reduction in Area, %
	Psi	% of Ultimate Tensile Strength				
20	135,200	97	63.2	7	9	32
200	141,800	97	69.8	8	17	36
200	138,900	95	261.3[a]	3	4	--
400	143,300	97	4.9	4	8	5

(a) Test discontinued before failure; (b) Broke outside gage mark; (c) Broke on gage mark.

Unnotched Tensile Tests Using 0.125-In. Round Samples

Nominal Hydrogen	Ultimate Tensile Strength, psi	Yield Strength, psi			Propor-tional Limit, psi	Extension, % Between Shoulders	Elonga-tion, % in 4D	Reduction in Area, %
		0.2% Offset	0.1% Offset	0.01% Offset				
Low Testing Speed - 0.005 In./Min								
20	139,400	114,000	111,200	108,700	107,500	9	15	33
200	146,300	125,000	123,500	115,100	99,800	11	13[b]	37
400	147,700	127,700	123,800	118,500	113,800	7	10	24
High Testing Speed - 0.5 In./Min								
20	141,500					8	12[a]	38
200	151,400					9	17	37
400	151,100					8	17	35

(a) Broke on gage mark; (b) Broke outside gage mark.

Notch-Bend Impact Tests Using Micro Sample

Nominal Hydrogen	Energy Absorbed, in-lb		Conclusion
	At 77 F	At -40 F	
20	13	10	Slow-strain embrittlement at 400 ppm; impact embrittlement at 200 ppm
200	8	4	
400	6	--	

Hydrogen Content, ppm		VHN (10-Kg Load)		Metallographic Structure, 20 ppm
Nominal	By Analysis	Hydrogen Content	VHN	
20	--	20	--	Structure: equiaxed $\alpha + \beta$
200	--	200	--	Third phase: none
300	--	300	--	Vol % α: 70-80
				α grain size: 5 μ

Unnotched Stress-Rupture Tests Using 0.125-In. Round Samples

Nominal Hydrogen	Applied Stress		Rupture Time, hours	Extension, % Between Shoulders	Elonga-tion, % in 4D	Reduction in Area, %
	Psi	% of Ultimate Tensile Strength				
20	164,000	95	43.4	11	--(c)	53
20	160,500	93	256.1(a)	5	--	--
200	168,800	95	261.2(a)	7	8	--
200	168,800	95	149.7	12	--(c)	36
200	165,200	93	261.3(a)	4	--	--
300	167,300	95	78.7	4	6(b)	8

(a) Test discontinued before failure; (b) Broke outside gage mark; (c) Broke on gage mark.

Unnotched Tensile Tests Using 0.125-In. Round Samples

Nominal Hydrogen	Ultimate Tensile Strength, psi	Yield Strength, psi			Propor-tional Limit, psi	Extension, % Between Shoulders	Elonga-tion, % in 4D	Reduction in Area, %
		0.2% Offset	0.1% Offset	0.01% Offset				
			Low Testing Speed - 0.005 In./Min					
20	172,500	162,400	157,800	153,100	152,000	12	20	46
200	177,600	--	--	--	--	9	17	23
300	176,100	165,900	163,700	158,800	154,400	6	10	16
			High Testing Speed - 0.5 In./Min					
20	176,400					9	16	44
200	180,700					2	2	6
300	178,200					8	18	44

(a) Broke on gage mark; (b) Broke outside gage mark.

Notch-Bend Impact Tests Using Micro Sample

Nominal Hydrogen	Energy Absorbed, in-lb		Conclusion
	At 77 F	At -40 F	
20	10	6	Slow-strain embrittlement at 300 ppm; alloy
200	6	5	brittle in impact testing
300	4	2	

Hydrogen Content, ppm		VHN (10-Kg Load)		Metallographic Structure, 20 ppm
Nominal	By Analysis	Hydrogen Content	VHN	
20	--	20	--	Structure: equiaxed α + β + fine sph.
400	--	400	--	compound

Third phase: --
Vol % α: 80
α grain size: 2 μ

Unnotched Stress-Rupture Tests Using 0.125-In. Round Samples

Nominal Hydrogen	Applied Stress		Rupture Time, hours	Extension, % Between Shoulders	Elonga- tion, % in 4D	Reduction in Area, %
	Psi	% of Ultimate Tensile Strength				
20	126,500	99	0.6	6	10	23
20	124,000	97	263.0[a]	3	6	--
400	132,100	99	0.3	8	15	29
400	129,400	97	4.3	9	10	35
400	126,700	95	287.6[a]	4	8	--

(a) Test discontinued before failure; (b) Broke outside gage mark; (c) Broke on gage mark.

Unnotched Tensile Tests Using 0.125-In. Round Samples

Nominal Hydrogen	Ultimate Tensile Strength, psi	Yield Strength, psi			Propor- tional Limit, psi	Extension, % Between Shoulders	Elonga- tion, % in 4D	Reduction in Area, %
		0.2% Offset	0.1% Offset	0.01% Offset				
Low Testing Speed - 0.005 In./Min								
20	127,800	105,600	104,000	96,200	90,200	9	15	28
400	133,400	116,500	113,900	104,000	96,600	10	14[a]	35
High Testing Speed - 0.5 In./Min								
20	130,500					9	15	33
400	137,000					9	18	37

(a) Broke on gage mark; (b) Broke outside gage mark.

Notch-Bend Impact Tests Using Micro Sample

Nominal Hydrogen	Energy Absorbed, in-lb		Conclusion
	At 77 F	At -40 F	
20	5	7	Testing was not completed; no slow-strain
400	6	3	embrittlement was apparent at 400 ppm; alloy brittle in impact testing

Hydrogen Content, ppm		VHN (10-Kg Load)		Metallographic Structure, 20 ppm
Nominal	By Analysis	Hydrogen Content	VHN	
20	--	20	--	Structure: equiaxed $\alpha + \beta$ + fine sph. comp.
200	--	200	--	Third phase: --
				Vol % α: 60-70
				α grain size: 3 μ

Unnotched Stress-Rupture Tests Using 0.125-In. Round Samples

Nominal Hydrogen	Applied Stress		Rupture Time, hours	Extension, % Between Shoulders	Elonga-tion, % in 4D	Reduction in Area, %
	Psi	% of Ultimate Tensile Strength				

(a) Test discontinued before failure; (b) Broke outside gage mark; (c) Broke on gage mark.

Unnotched Tensile Tests Using 0.125-In. Round Samples

Nominal Hydrogen	Ultimate Tensile Strength, psi	Yield Strength, psi			Propor-tional Limit, psi	Extension, % Between Shoulders	Elonga-tion, % in 4D	Reduction in Area, %
		0.2% Offset	0.1% Offset	0.01% Offset				
			Low Testing Speed - 0.005 In./Min					
20	171,500	155,500	153,500	143,300	133,500	1	2[a]	17
200	180,000	165,900	163,200	154,200	150,700	2	4[a]	5
			High Testing Speed - 0.5 In./Min					
20	173,200					1	2[a]	1
200	177,200					1	2[a]	3

(a) Broke on gage mark; (b) Broke outside gage mark.

Notch-Bend Impact Tests Using Micro Sample

Nominal Hydrogen	Energy Absorbed, in-lb		Conclusion
	At 77 F	At -40 F	
20	3	3	This alloy was brittle as stabilized; apparently
200	3	4	the stabilization temperature was too low permitting eutectoid decomposition

TABLE 100. RESULTS OF TESTS TO DETERMINE THE HYDROGEN SENSITIVITY OF THE Ti-4Ni ALLOY (K-68)

Hydrogen Content, ppm		VHN (10-Kg Load)		Metallographic
Nominal	By Analysis	Hydrogen Content	VHN	Structure, 20 ppm
20	--	20	--	Structure: α + fine sph. comp.
200	--	200	--	Third phase: --
800	--	800	--	Vol % α: 80-90
				α grain size: --

Unnotched Stress-Rupture Tests Using 0.125-In. Round Samples

Nominal Hydrogen	Applied Stress		Rupture Time, hours	Extension, % Between Shoulders	Elonga-tion, % in 4D	Reduction in Area, %
	Psi	% of Ultimate Tensile Strength				
20	69,900	93	23.9	14	22	31
200	73,000	97	3.1	14	--(c)	36
800	74,100	97	1.3	16	29	37
800	72,600	95	5.8	14	20	37
800	71,000	--	21.1	19	--(c)	29

(a) Test discontinued before failure; (b) Broke outside gage mark; (c) Broke on gage mark.

Unnotched Tensile Tests Using 0.125-In. Round Samples

Nominal Hydrogen	Ultimate Tensile Strength, psi	Yield Strength, psi			Propor-tional Limit, psi	Extension, % Between Shoulders	Elonga-tion, % in 4D	Reduction in Area, %
		0.2% Offset	0.1% Offset	0.01% Offset				
			Low Testing Speed - 0.005 In./Min					
20	75,100	48,200	46,700	38,150	32,300	13	22	33
200	75,300	44,700	38,500	23,550	18,800	12	21	29
800	76,400	52,600	47,900	35,750	26,000	17	21	38
			High Testing Speed - 0.5 In./Min					
20	80,300					11	15	27
200	81,300					13	22	28
800	81,400					14	22	34

(a) Broke on gage mark; (b) Broke outside gage mark.

Notch-Bend Impact Tests Using Micro Sample

Nominal Hydrogen	Energy Absorbed, in-lb		Conclusion
	At 77 F	At -40 F	
20	8	10	No slow-strain embrittlement; alloy brittle in
200	4	4	impact testing
800	2	2	

Hydrogen Content, ppm		VHN (10-Kg Load)		Metallographic Structure, 20 ppm
Nominal	By Analysis	Hydrogen Content	VHN	
20	--	20	--	Structure: α + coarse comp.
400	--	400	--	Third phase: --
				Vol % α: 75%
				α grain size: --

Unnotched Stress-Rupture Tests Using 0.125-In. Round Samples

Nominal Hydrogen	Applied Stress		Rupture Time, hours	Extension, % Between Shoulders	Elongation, % in 4D	Reduction in Area, %
	Psi	% of Ultimate Tensile Strength				
20	93,100	95	0.4	7	--(c)	12
400	97,900	95	3.2	9	12	15

(a) Test discontinued before failure; (b) Broke outside gage mark; (c) Broke on gage mark.

Unnotched Tensile Tests Using 0.125-In. Round Samples

Nominal Hydrogen	Ultimate Tensile Strength, psi	Yield Strength, psi			Proportional Limit, psi	Extension, % Between Shoulders	Elongation, % in 4D	Reduction in Area, %
		0.2% Offset	0.1% Offset	0.01% Offset				
Low Testing Speed - 0.005 In./Min								
20	98,000	69,900	68,100	63,700	58,800	6	10(a)	15
400	103,000	70,900	64,500	51,000	46,200	7	9	12
High Testing Speed - 0.5 In./Min								
20	103,000					7	10	16
400	108,500					4	14	7

(a) Broke on gage mark; (b) Broke outside gage mark.

Notch-Bend Impact Tests Using Micro Sample

Nominal Hydrogen	Energy Absorbed, in-lb		Conclusion
	At 77 F	At -40 F	
20	2	3	No slow-strain embrittlement; alloy brittle
400	4	4	in impact testing

Hydrogen Content, ppm		VHN (10-Kg Load)		Metallographic Structure, 20 ppm
Nominal	By Analysis	Hydrogen Content	VHN	
20	--	20	--	Structure: equiaxed $\alpha + \beta$ + comp.
200	--	200	--	Third phase: --
800	--	800	--	Vol % α: 80-90
				α grain size: 5 μ

Unnotched Stress-Rupture Tests Using 0.125-In. Round Samples

Nominal Hydrogen	Applied Stress		Rupture Time, hours	Extension, % Between Shoulders	Elongation, % in 4D	Reduction in Area, %
	Psi	% of Ultimate Tensile Strength				
20	92,200	95	0.6	16[b]	16[b]	43
200	91,800	95	3.4	14	--[c]	36
200	89,900	93	17.6	18	--[c]	37
200	88,000	91	262.8[a]	8	11	--
800	91,600	93	61.5	10	14	17

(a) Test discontinued before failure; (b) Broke outside gage mark; (c) Broke on gage mark.

Unnotched Tensile Tests Using 0.125-In. Round Samples

Nominal Hydrogen	Ultimate Tensile Strength, psi	Yield Strength, psi			Proportional Limit, psi	Extension, % Between Shoulders	Elongation, % in 4D	Reduction in Area, %
		0.2% Offset	0.1% Offset	0.01% Offset				
				Low Testing Speed - 0.005 In./Min				
20	97,000	71,200	70,100	61,100	55,400	17	23[b]	38
200	96,700	73,000	62,800	51,500	45,000	17	28	38
800	98,500	66,600	61,800	48,700	33,500	15	18	31
				High Testing Speed - 0.5 In./Min				
20	96,800					14	22	43
200	95,900					14	16[b]	41
800	102,000					14	19	39

(a) Broke on gage mark; (b) Broke outside gage mark.

Notch-Bend Impact Tests Using Micro Sample

Nominal Hydrogen	Energy Absorbed, in-lb		Conclusion
	At 77 F	At -40 F	
20	22	20	Testing was not completed; slow-strain embrittle-
200	16	12	ment at 300-800 ppm; impact embrittlement at
800	10	10	300-800 ppm

TABLE 103. RESULTS OF TESTS TO DETERMINE THE HYDROGEN SENSITIVITY
OF THE Ti-2Mo-2Cu ALLOY (K-71)

Hydrogen Content, ppm		VHN (10-Kg Load)		Metallographic Structure, 20 ppm
Nominal	By Analysis	Hydrogen Content	VHN	
20	--	20	--	Structure: equiaxed $\alpha + \beta$
200	--	200	--	Third phase: --
				Vol % α: 90
				α grain size: $< 2\,\mu$

Unnotched Stress-Rupture Tests Using 0.125-In. Round Samples

Nominal Hydrogen	Applied Stress		Rupture Time, hours	Extension, % Between Shoulders	Elongation, % in 4D	Reduction in Area, %
	Psi	% of Ultimate Tensile Strength				
20	92,500	95	4.5	15	--(c)	55
200	91,100	93	28.7	15	--(c)	54

(a) Test discontinued before failure; (b) Broke outside gage mark; (c) Broke on gage mark.

Unnotched Tensile Tests Using 0.125-In. Round Samples

Nominal Hydrogen	Ultimate Tensile Strength, psi	Yield Strength, psi			Proportional Limit, psi	Extension, % Between Shoulders	Elongation, % in 4D	Reduction in Area, %
		0.2% Offset	0.1% Offset	0.01% Offset				
				Low Testing Speed - 0.005 In./Min				
20	97,400	79,600	78,300	58,300	47,700	21	26	54
200	98,000	75,200	73,800	68,100	64,400	15	24	50
				High Testing Speed - 0.5 In./Min				
20	101,500					15	29	47
200	100,500					15	28	49

(a) Broke on gage mark; (b) Broke outside gage mark.

Notch-Bend Impact Tests Using Micro Sample

Nominal Hydrogen	Energy Absorbed, in-lb		Conclusion
	At 77 F	At -40 F	
20	30	22	Testing was not completed; no embrittlement at 200 ppm
200	24	12	

TABLE 104. RESULTS OF TESTS TO DETERMINE THE HYDROGEN SENSITIVITY OF THE Ti-4Al-7Cu ALLOY (K-72)

Hydrogen Content, ppm		VHN (10-Kg Load)		Metallographic Structure, 20 ppm
Nominal	By Analysis	Hydrogen Content	VHN	
20	--	20	--	Structure: α + fine spheroidal comp.
200	--	200	--	Third phase: --
800	--	800	--	Vol % α: 80
				α grain size: --

Unnotched Stress-Rupture Tests Using 0.125-In. Round Samples

Nominal Hydrogen	Applied Stress		Rupture Time, hours	Extension, % Between Shoulders	Elongation, % in 4D	Reduction in Area, %
	Psi	% of Ultimate Tensile Strength				
20	136,700	97	5.6	9	12	25
200	139,500	95	310.9(a)	4	--	--
800	145,500	95	26.5	5	--(c)	8
800	145,500	95	9.1	4	6	7

(a) Test discontinued before failure; (b) Broke outside gage mark; (c) Broke on gage mark.

Unnotched Tensile Tests Using 0.125-In. Round Samples

Nominal Hydrogen	Ultimate Tensile Strength, psi	Yield Strength, psi			Proportional Limit, psi	Extension, % Between Shoulders	Elongation, % in 4D	Reduction in Area, %
		0.2% Offset	0.1% Offset	0.01% Offset				
			Low Testing Speed - 0.005 In./Min					
20	141,000	123,100	121,500	112,800	106,600	9	15	23
200	146,800	133,500	131,600	121,300	115,200	10	12(b)	35
800	153,200	133,400	126,000	96,200	82,000	8	10(a)	24
			High Testing Speed - 0.5 In./Min					
20	145,100					7	15	22
200	148,500					7	15	41
800	156,000					8	16	34

(a) Broke on gage mark; (b) Broke outside gage mark.

Notch-Bend Impact Tests Using Micro Sample

Nominal Hydrogen	Energy Absorbed, in-lb		Conclusion
	At 77 F	At -40 F	
20	6	6	Testing was not completed; slow-strain embrittlement at 300-800 ppm; alloy brittle in impact testing
200	10	7	
800	4	1	

Hydrogen Content, ppm		VHN (10-Kg Load)		Metallographic Structure, 20 ppm
Nominal	By Analysis	Hydrogen Content	VHN	
20	--	20	--	Structure: equiaxed $\alpha + \beta$
200	--	200	--	Third phase: --
800	--	800	--	Vol % α: --
				α grain size: $< 1 \mu$

Unnotched Stress-Rupture Tests Using 0.125-In. Round Samples

Nominal Hydrogen	Applied Stress		Rupture Time, hours	Extension, % Between Shoulders	Elongation, % in 4D	Reduction in Area, %
	Psi	% of Ultimate Tensile Strength				
20	130,900	93	255.6[a]	1	3	--
200	135,400	97	12.1	11	23	57
800	135,000	97	0.1	10	21	61
800	132,300	95	2.2	10	17	57

(a) Test discontinued before failure; (b) Broke outside gage mark; (c) Broke on gage mark.

Unnotched Tensile Tests Using 0.125-In. Round Samples

Nominal Hydrogen	Ultimate Tensile Strength, psi	Yield Strength, psi			Proportional Limit, psi	Extension, % Between Shoulders	Elongation, % in 4D	Reduction in Area, %
		0.2% Offset	0.1% Offset	0.01% Offset				
				Low Testing Speed - 0.005 In./Min				
20	140,700	128,400	126,000	115,300	110,500	9	15	53
200	139,600	125,900	122,500	114,800	109,000	10	8[b]	60
800	139,200	118,400	112,300	97,400	87,500	12	20	56
				High Testing Speed - 0.5 In./Min				
20	145,500					9	19	39
200	145,800					10	18	59
800	138,600					12	24	69

(a) Broke on gage mark; (b) Broke outside gage mark.

Notch-Bend Impact Tests Using Micro Sample

Nominal Hydrogen	Energy Absorbed, in-lb		Conclusion
	At 77 F	At -40 F	
20	34	14	No evidence of embrittlement
200	19	12	
800	33	14	

Hydrogen Content, ppm		VHN (10-Kg Load)		Metallographic Structure, 20 ppm
Nominal	By Analysis	Hydrogen Content	VHN	
20	--	20	--	Structure: equiaxed $\alpha + \beta$
300	--	300	--	Third phase: --
				Vol % α: 70-80
				α grain size: $< 2 \mu$

Unnotched Stress-Rupture Tests Using 0.125-In. Round Samples

Nominal Hydrogen	Applied Stress		Rupture Time, hours	Extension, % Between Shoulders	Elonga- tion, % in 4D	Reduction in Area, %
	Psi	% of Ultimate Tensile Strength				
20	143,900	95	78.8	--	--[c]	60
300	143,500	95	6.0	12	20	50
300	140,400	93	252.8[a]	7	8	--

(a) Test discontinued before failure; (b) Broke outside gage mark; (c) Broke on gage mark.

Unnotched Tensile Tests Using 0.125-In. Round Samples

Nominal Hydrogen	Ultimate Tensile Strength, psi	Yield Strength, psi			Propor- tional Limit, psi	Extension, % Between Shoulders	Elonga- tion, % in 4D	Reduction in Area, %
		0.2% Offset	0.1% Offset	0.01% Offset				
Low Testing Speed - 0.005 In./Min								
20	151,500	144,000	143,800	137,000	125,500	12	23	57
300	151,000	143,000	142,000	135,000	129,000	12	21	56
High Testing Speed - 0.5 In./Min								
20	154,700					10	20	64
300	157,000					10	20	57

(a) Broke on gage mark; (b) Broke outside gage mark.

Notch-Bend Impact Tests Using Micro Sample

Nominal Hydrogen	Energy Absorbed, in-lb		Conclusion
	At 77 F	At -40 F	
20	32	16	Testing was not completed; no slow-strain
300	16	18	embrittlement at 300 ppm; some loss in
			impact strength at 300 ppm

| Hydrogen Content, ppm | | VHN (10-Kg Load) | | Metallographic |
Nominal	By Analysis	Hydrogen Content	VHN	Structure, 20 ppm
20	--	20	--	Structure: equiaxed $\alpha + \beta$
200	--	200	--	Third phase: --
300	--	300	--	Vol % α: 80
				α grain size: 2 μ

Unnotched Stress-Rupture Tests Using 0.125-In. Round Samples

| Nominal Hydrogen | Applied Stress | | Rupture Time, hours | Extension, % Between Shoulders | Elonga-tion, % in 4D | Reduction in Area, % |
	Psi	% of Ultimate Tensile Strength				
200	145,000	97	2	13	--(c)	54
200	142,000	95	262.6(a)	4	6	--
300	145,500	97	0.8	8	15	27
300	142,500	95	4.7	6	2	13
300	139,500	93	13.5	5	4	10

(a) Test discontinued before failure; (b) Broke outside gage mark; (c) Broke on gage mark.

Unnotched Tensile Tests Using 0.125-In. Round Samples

| Nominal Hydrogen | Ultimate Tensile Strength, psi | Yield Strength, psi | | | Propor-tional Limit, psi | Extension, % Between Shoulders | Elonga-tion, % in 4D | Reduction in Area, % |
		0.2% Offset	0.1% Offset	0.01% Offset				
			Low Testing Speed - 0.005 In./Min					
20	150,200	134,900	135,000	132,400	123,900	13	26	48
200	149,500	140,400	139,800	125,500	106,000	12	20	50
300	150,000	143,000	142,000	134,000	128,000	9	14	45
			High Testing Speed - 0.5 In./Min					
20	153,000					11	22	53
200	152,500					11	19	57
300	146,300					9	16	55

(a) Broke on gage mark; (b) Broke outside gage mark.

Notch-Bend Impact Tests Using Micro Sample

| Nominal Hydrogen | Energy Absorbed, in-lb | | Conclusion |
	At 77 F	At -40 F	
20	29	18	Slow-strain embrittlement at 300 ppm; no impact
200	23	16	embrittlement
300	24	14	

Hydrogen Content, ppm		VHN (10-Kg Load)		Metallographic Structure, 20 ppm
Nominal	By Analysis	Hydrogen Content	VHN	
20	--	20	--	Structure: platelet α + fine β
200	--	200	--	Third phase: --
				Vol % α: 80
				α grain size: < 25 μ

Unnotched Stress-Rupture Tests Using 0.125-In. Round Samples

Nominal Hydrogen	Applied Stress		Rupture Time, hours	Extension, % Between Shoulders	Elonga-tion, % in 4D	Reduction in Area, %
	Psi	% of Ultimate Tensile Strength				
20	136,800	95	66.0	11	18	44
200	141,600	97	4.1	3	--(c)	8
200	138,700	95	5.7	6	--(c)	10

(a) Test discontinued before failure; (b) Broke outside gage mark; (c) Broke on gage mark.

Unnotched Tensile Tests Using 0.125-In. Round Samples

Nominal Hydrogen	Ultimate Tensile Strength, psi	Yield Strength, psi			Propor-tional Limit, psi	Extension, % Between Shoulders	Elonga-tion, % in 4D	Reduction in Area, %
		0.2% Offset	0.1% Offset	0.01% Offset				
			Low Testing Speed - 0.005 In./Min					
20	144,000	127,500	127,000	124,500	121,300	12	17	44
200	146,000	134,400	133,900	127,700	123,600	10	17	34
			High Testing Speed - 0.5 In./Min					
20	147,200					10	19	46
200	149,700					10	21	46

(a) Broke on gage mark; (b) Broke outside gage mark.

Notch-Bend Impact Tests Using Micro Sample

Nominal Hydrogen	Energy Absorbed, in-lb		Conclusion
	At 77 F	At -40 F	
20	24	14	Both slow-strain and impact embrittlement at
200	14	9	200 ppm

Hydrogen Content, ppm		VHN (10-Kg Load)		Metallographic Structure, 20 ppm
Nominal	By Analysis	Hydrogen Content	VHN	
20	--	20	--	Structure: equiaxed $\alpha + \beta$
200	--	200	--	Third phase: --
				Vol % α: 80
				α grain size: 3 μ

Unnotched Stress-Rupture Tests Using 0.125-In. Round Samples

Nominal Hydrogen	Applied Stress		Rupture Time, hours	Extension, % Between Shoulders	Elongation, % in 4D	Reduction in Area, %
	Psi	% of Ultimate Tensile Strength				
20	141,900	95	51.3	11	--(c)	49
200	140,500	95	225.0	9	--(c)	36

(a) Test discontinued before failure; (b) Broke outside gage mark; (c) Broke on gage mark.

Unnotched Tensile Tests Using 0.125-In. Round Samples

Nominal Hydrogen	Ultimate Tensile Strength, psi	Yield Strength, psi			Proportional Limit, psi	Extension, % Between Shoulders	Elongation, % in 4D	Reduction in Area, %
		0.2% Offset	0.1% Offset	0.01% Offset				
Low Testing Speed - 0.005 In./Min								
20	149,500	139,500	139,500	136,500	133,300	10	22	55
200	147,900	139,000	139,300	135,000	130,800	12	23	59
High Testing Speed - 0.5 In./Min								
20	149,500					13	25	59
200	148,500					11	25	66

(a) Broke on gage mark; (b) Broke outside gage mark.

Notch-Bend Impact Tests Using Micro Sample

Nominal Hydrogen	Energy Absorbed, in-lb		Conclusion
	At 77 F	At -40 F	
20	30	18	Testing was not completed; no embrittlement was observed at 200 ppm
200	26	22	

TABLE 110. RESULTS OF TESTS TO DETERMINE THE HYDROGEN SENSITIVITY OF THE Ti-12Sn-7Cu ALLOY (K-78)

Hydrogen Content, ppm		VHN (10-Kg Load)		Metallographic Structure, 20 ppm
Nominal	By Analysis	Hydrogen Content	VHN	
20	--	20	--	Structure: α + fine sph. comp.
200	--	200	--	Third phase: --
				Vol % α: --
				α grain size: --

Unnotched Stress-Rupture Tests Using 0.125-In. Round Samples

Nominal Hydrogen	Applied Stress		Rupture Time, hours	Extension, % Between Shoulders	Elonga-tion, % in 4D	Reduction in Area, %
	Psi	% of Ultimate Tensile Strength				
20	142,200	95	1.1	9	--(c)	33
200	140,700	97	29.2	8	11	34
200	137,700	95	316.8(a)	5	8	--

(a) Test discontinued before failure; (b) Broke outside gage mark; (c) Broke on gage mark.

Unnotched Tensile Tests Using 0.125-In. Round Samples

Nominal Hydrogen	Ultimate Tensile Strength, psi	Yield Strength, psi			Propor-tional Limit, psi	Extension, % Between Shoulders	Elonga-tion, % in 4D	Reduction in Area, %
		0.2% Offset	0.1% Offset	0.01% Offset				
Low Testing Speed - 0.005 In./Min								
20	149,700	137,100	135,900	128,700	121,700	7	9	36
200	145,000	132,300	130,000	114,900	106,000	7	10	30
High Testing Speed - 0.5 In./Min								
20	150,800					7	13	29
200	150,400					7	14	36

(a) Broke on gage mark; (b) Broke outside gage mark.

Notch-Bend Impact Tests Using Micro Sample

Nominal Hydrogen	Energy Absorbed, in-lb		Conclusion
	At 77 F	At -40 F	
20	8	8	Testing was not completed; no slow-strain embrittlement at 200 ppm; alloy brittle in impact testing
200	8	5	

TABLE 111. RESULTS OF TESTS TO DETERMINE THE HYDROGEN SENSITIVITY
OF THE Ti-7Cu-.15O$_2$ ALLOY (K-79)

Hydrogen Content, ppm		VHN (10-Kg Load)		Metallographic
Nominal	By Analysis	Hydrogen Content	VHN	Structure, 20 ppm
20	--	20	--	Structure: α + fine spheroidal comp.
200	--	200	--	Third phase: --
800	--	800	--	Vol % α: --
				α grain size: --

Unnotched Stress-Rupture Tests Using 0.125-In. Round Samples

Nominal Hydrogen	Applied Stress		Rupture Time, hours	Extension, % Between Shoulders	Elongation, % in 4D	Reduction in Area, %
	Psi	% of Ultimate Tensile Strength				
200	105,100	95	6.3	17	--(c)	36
800	109,000	95	1.9	13	--(c)	34

(a) Test discontinued before failure; (b) Broke outside gage mark; (c) Broke on gage mark.

Unnotched Tensile Tests Using 0.125-In. Round Samples

Nominal Hydrogen	Ultimate Tensile Strength, psi	Yield Strength, psi			Proportional Limit, psi	Extension, % Between Shoulders	Elongation, % in 4D	Reduction in Area, %
		0.2% Offset	0.1% Offset	0.01% Offset				
Low Testing Speed - 0.005 In./Min								
20	110,200	92,000	89,900	79,000	74,400	16	27	36
200	110,600	84,600	79,800	64,000	55,500	14	23	37
800	114,800	88,700	82,300	62,800	50,200	14	24	28
High Testing Speed - 0.5 In./Min								
20	115,000					10	17	18
200	115,100					13	19	39
800	116,900					13	24	37

(a) Broke on gage mark; (b) Broke outside gage mark.

Notch-Bend Impact Tests Using Micro Sample

Nominal Hydrogen	Energy Absorbed, in-lb		Conclusion
	At 77 F	At -40 F	
20	8	8	No slow-strain embrittlement; alloy brittle in impact testing
200	6	6	
800	3	3	

Hydrogen Content, ppm		VHN (10-Kg Load)		Metallographic Structure, 20 ppm
Nominal	By Analysis	Hydrogen Content	VHN	
20	--	20	--	Structure: α + fine spheriodal comp.
200	--	200	--	Third phase: --
800	--	800	--	Vol % α: 80
				α grain size: --

Unnotched Stress-Rupture Tests Using 0.125-In. Round Samples

Nominal Hydrogen	Applied Stress		Rupture Time, hours	Extension, % Between Shoulders	Elonga-tion, % in 4D	Reduction in Area, %
	Psi	% of Ultimate Tensile Strength				
20	69,700	93	256.2[a]	11	--	--
200	77,700	93	250.0[a]	6	--	--
800	70,000	95	260.7[a]	10	21	--

(a) Test discontinued before failure; (b) Broke outside gage mark; (c) Broke on gage mark.

Unnotched Tensile Tests Using 0.125-In. Round Samples

Nominal Hydrogen	Ultimate Tensile Strength, psi	Yield Strength, psi			Propor-tional Limit, psi	Extension, % Between Shoulders	Elonga-tion, % in 4D	Reduction in Area, %
		0.2% Offset	0.1% Offset	0.01% Offset				
		Low Testing Speed - 0.005 In./Min						
20	75,000	48,100	44,900	34,200	30,100	19	32	40
200	83,600	57,000	46,200	26,850	22,000	14	16	44
800	73,700	44,100	38,100	24,700	20,200	17	30	42
		High Testing Speed - 0.5 In./Min						
20	77,400					16	28	44
200	88,900					15	25	38
800	75,200					14	16	42

(a) Broke on gage mark; (b) Broke outside gage mark.

Notch-Bend Impact Tests Using Micro Sample

Nominal Hydrogen	Energy Absorbed, in-lb		Conclusion
	At 77 F	At -40 F	
20	22	--	No slow-strain embrittlement; impact embrittle-ment at 200 ppm
200	10	10	
800	4	--	

TABLE 113. TENSILE PROPERTIES OF TITANIUM ALLOYS AFTER EXPOSURE AT 800 F IN AIR

Alloy No.	Composition Balance Ti	Hydrogen Content, ppm	Thermal Exposure Time, hrs	Temp, F	Stress, 1000 psi	Ultimate Strength, psi	Yield Strength, psi 0.2% Offset	0.1% Offset	0.01% Offset	Proportional Limit, psi	Extension, per cent	Elongation, per cent in 4D	Reduction in Area, per cent
K-1	4Mo	20	200	800	25.0	99,200	77,200	71,500	56,700	49,300	15	18[a]	43
		20	200	800	0	101,100	77,600	73,100	61,600	55,200	16	30	55
		200	200	800	25.0	102,200	77,400	72,300	57,000	49,100	15	22[b]	49
		200	200	800	0	103,700	77,900	73,000	61,200	52,300	13	22	56
K-2A	8Mo	20	200	800	25.0	104,500	85,100	79,200	63,000	57,200	13	14[a]	54
		20	200	800	0	104,900	87,200	82,400	69,000	64,200	12	16[b]	56
		200	200	800	25.0	109,000	78,600	72,200	54,500	47,850	15	23[b]	52
		200	200	800	0	109,000	86,700	81,900	67,400	59,500	11	14[b]	39
K-4	4V	20	200	800	25.0	109,700	91,400	91,700	90,000	87,000	18	28	42
		20	200	800	0	110,800	95,300	95,400	90,600	84,800	14	17[a]	50
		200	200	800	25.0	110,300	84,400	80,700	62,800	54,200	15	19[a]	47
		200	200	800	0	111,200	87,600	83,200	64,700	57,000	17	23[b]	48
K-11	4Mn	20	200	800	25.0	105,400	76,600	71,800	52,100	39,100	19	24	42
		20	200	800	0	104,500	78,100	75,800	67,200	60,800	14	25	42
		200	200	800	25.0	104,200	71,300	64,600	43,900	36,600	18	24	41
		200	200	800	0	104,700	76,300	72,600	60,900	52,900	15	26	41
K-13	8Mn	20	200	800	25.0	125,800	95,300	88,100	73,500	66,500	12	27	41
		20	200	800	0	121,700	101,000	95,300	80,300	74,600	18	29	47
		200	200	800	25.0	126,500	102,100	88,500	78,300	74,300	13	21[b]	30
		200	200	800	0	136,300	110,000	104,700	86,150	77,200	10	14[b]	18
K-15	4Fe	20	200	800	25.0	108,500	77,300	58,500	35,150	28,200	10	13[a]	15
		20	200	800	0	106,000	72,700	67,880	50,300	40,150	13	16	25
		200	200	800	25.0	101,150	70,300	60,700	30,550	25,000	11	14	23
		200	200	800	0	110,000	70,200	63,600	41,600	29,200	10	22	24
K-17	6Cr	20	200	800	25.0	142,300	98,400	90,800	81,200	70,800	4	7	8
		20	200	800	0	141,200	102,100	95,800	80,350	73,100	4	8[a]	5
		200	200	800	25.0	138,700	98,700	91,200	76,500	66,300	3	3[a]	6
		200	200	800	0	139,700	103,100	95,200	78,835	64,000	4	6[a]	5
K-19	4Cu	20	200	800	25.0	77,300	56,600	52,200	31,900	21,200	10	12[a]	37
		20	200	800	0	77,800	57,400	54,600	37,400	30,800	11	23	37
		200	200	800	25.0	84,500	59,000	54,200	40,800	31,800	10	15	36
		200	200	800	0	79,500	51,800	44,700	24,700	17,550	11	22	39
K-20	7Cu	20	200	800	25.0	90,000	67,800	64,600	46,700	38,500	17	16[a]	42
		20	200	800	0	91,600	72,200	71,000	65,900	61,500	17	26	28
		200	200	800	25.0	91,600	69,000	63,200	39,500	29,200	19	28	48
		200	200	800	0	91,400	69,700	64,500	41,600	32,100	16	26	43
K-26	2Cr-2Fe	20	200	800	25.0	107,100	71,200	66,400	44,000	33,000	12	16[a]	34
		20	200	800	0	106,100	73,300	69,700	59,300	49,100	9	14	17
		200	200	800	25.0	108,300	70,000	47,100	45,700	38,300	13	16[a]	25
		200	200	800	0	108,500	73,600	68,000	51,500	42,300	13	23	36
K-27	3Cr-3Fe	20	200	800	25.0	128,900	84,500	77,400	67,200	60,200	10	18	46
		20	200	800	0	127,500	90,000	84,600	67,800	59,800	12	20[b]	23
		200	200	800	25.0	130,700	86,500	77,700	61,200	54,800	8	16	16
		200	200	800	0	130,000	90,350	82,000	63,100	52,300	10	20[a]	25
K30	2Mo-2Fe	20	200	800	25.0	113,800	91,200	89,500	83,400	77,300	18	30	45
		20	200	800	0	115,800	95,400	93,600	82,800	78,000	14	24[a]	48
		200	200	800	25.0	115,800	88,400	86,800	80,700	76,200	12	20[a]	22
		200	200	800	0	115,200	90,200	88,000	78,600	72,600	13	19	24
K-32	2Mo-2Cr	20	200	800	25.0	109,300	87,500	85,600	77,200	73,200	16	17[a]	50
		20	200	800	0	108,700	86,700	85,000	77,800	70,800	13	21[b]	50
		200	200	800	25.0	108,500	89,100	86,900	78,600	71,700	17	22[a]	41
		200	200	800	0	108,000	87,200	85,100	76,600	72,800	17	28	45
K-33	2Mo-2Fe-2Cr	20	200	800	25.0	111,700	81,900	78,300	63,900	54,200	17	22[a]	44
		20	200	800	0	110,700	85,800	83,200	73,700	69,200	16	20[a]	48
		200	200	800	25.0	116,400	79,600	75,000	60,800	53,600	14	18[a]	34
		200	200	800	0	115,000	86,100	81,600	68,200	61,900	19	23[a]	42
K-34	4Al-4Mo	20	200	800	25.0	141,200	123,400	120,400	111,200	105,700	10	18	49
		20	200	800	0	144,000	121,500	119,200	112,200	106,800	11	20	49
		200	200	800	25.0	138,500	118,500	115,300	104,600	94,600	12	22	50
		200	200	800	0	139,300	121,200	119,100	108,800	101,200	10	18	48

Alloy No.	Composition Balance Ti	Hydrogen Content, ppm	Thermal Exposure Time, hrs	Temp, F	Stress, 1000 psi	Ultimate Strength, psi	Yield Strength, psi 0.2% Offset	0.1% Offset	0.01% Offset	Proportional Limit, psi	Extension, per cent	Elongation, per cent in 4D	Reduction in Area, per cent
K-35	6Al-4Mo	20	200	800	25.0	169,500	153,000	151,500	142,400	134,300	9	15	44
		20	200	800	0	168,000	151,500	150,000	146,200	143,000	9	17	45
		200	200	800	25.0	169,000	153,000	152,900	146,900	142,400	9	13	49
		200	200	800	0	167,500	153,800	152,700	148,600	145,800	9	20	50
K-36	4Al-4V	20	200	800	25.0	134,300	119,600	119,200	114,200	109,600	10	15	46
		20	200	800	0	135,000	118,500	118,000	113,800	108,700	11	21	51
		200	200	800	25.0	137,800	123,500	120,000	110,000	101,000	9	18[b]	36
		200	200	800	0	139,900	126,000	124,500	111,100	102,700	10	17	33
K-37	6Al-4V	20	200	800	25.0	146,800	131,000	130,600	127,800	124,000	9	11[a]	42
		20	200	800	0	147,100	131,800	131,200	127,000	122,700	9	13	45
		200	200	800	25.0	154,700	143,300	142,100	134,500	126,900	7	14	37
		200	200	800	0	157,000	145,000	143,800	138,400	133,500	6	8[b]	35
K-38	4Al-4Mn	20	200	800	25.0	151,600	133,500	132,500	127,700	122,500	10	14[a]	26
		20	200	800	0	151,500	134,600	134,100	130,000	125,100	10	16	25
		200	200	800	25.0	153,500	139,000	137,400	133,500	128,500	11	13[a]	40
		200	200	800	0	152,900	139,100	138,000	129,500	124,200	13	17[b]	42
K-39	6Al-4Mn	20	200	800	25.0	175,000	162,400	160,400	162,400	164,000	11	18	41
		20	200	800	0	173,900	159,500	159,500	158,600	154,900	13	13[b]	30
		200	200	800	25.0	177,200	167,500	167,900	167,600	167,500	9	12[b]	30
		200	200	800	0	176,300	168,100	168,500	166,600	163,200	11	20	45
K-45A	4Al-1.3Mo-1.3Fe-1.3Cr	20	200	800	25.0	143,400	125,000	124,300	123,000	122,500	9	17[a]	43
		20	200	800	0	142,800	125,900	125,200	120,200	112,000	13	16[b]	47
		200	200	800	25.0	147,600	132,200	130,900	125,900	121,300	14	19	44
		200	200	800	0	145,700	130,000	128,500	122,500	117,900	12	18	42
K-55	8Mn, O_2 added	20	200	800	25.0	155,800	136,200	132,800	119,000	110,700	15	23	42
		20	200	800	0	154,200	137,000	136,200	129,500	123,000	14	19[a]	44
		200	200	800	25.0	155,500	139,400	135,700	122,500	116,800	8	11	15
		20	200	800	0	150,000	136,800	135,100	121,700	116,000	5	7	11
K-61	6Al-4V, O_2 added	20	200	800	25.0	174,100	158,200	157,700	154,500	150,500	9	15[b]	39
		20	200	800	0	174,900	159,500	158,800	154,000	149,000	10	10[a]	35
		200	200	800	25.0	183,700	–	–	164,000	160,000	9	12[b]	38
		200	200	800	0	182,700	170,000	169,000	162,800	156,700	9	16	35
K-63	4Al-4Mn, O_2 added	20	200	800	25.0	162,400	151,500	150,900	136,800	128,000	13	20[b]	41
		20	200	800	0	163,100	150,000	149,300	142,500	134,500	10	14[b]	35
		200	200	800	25.0	171,700	158,700	157,600	154,000	148,500	13	21[b]	46
		200	200	800	0	171,500	157,500	156,600	151,800	147,200	12	21	36
K-70	2Mn-2Cu	20	200	800	25.0	94,900	69,200	66,800	55,400	42,100	14	23	35
		20	200	800	0	93,200	67,800	66,600	57,500	45,500	17	26	45
		200	200	800	25.0	97,400	65,800	61,700	49,000	42,900	15	19[a]	35
		200	200	800	0	92,800	61,900	55,600	34,800	26,500	16	23	28
K-71	2Mo-2Cu	20	200	800	25.0	96,900	78,900	78,200	75,600	71,800	19	30	53
		20	200	800	0	97,300	79,900	79,600	73,900	69,300	17	24	53
		200	200	800	25.0	96,200	72,300	71,200	61,600	51,900	15	24	48
		200	200	800	0	95,100	73,500	74,200	69,500	60,500	17	26	47
K-73	12Sn-4Mo	20	200	800	25.0	146,200	132,200	129,400	120,200	114,300	10	20	53
		20	200	800	0	146,500	133,900	131,900	124,200	115,000	9	10[b]	44
		200	200	800	25.0	144,800	128,700	124,000	112,900	106,800	8	6[a]	47
		200	200	800	0	145,000	129,700	126,400	112,200	106,000	11	19	50
K-75	12Sn-4Mn	20	200	800	25.0	151,300	136,500	136,300	133,900	130,400	11	15[b]	42
		20	200	800	0	150,700	134,400	134,300	132,600	128,800	11	12[a]	46
		200	200	800	25.0	150,600	140,400	139,700	132,000	126,000	8	12	12
		200	200	800	0	150,000	139,000	138,200	130,500	124,200	10	18	42
K-77	12Sn-4Cr	20	200	800	25.0	158,000	143,200	141,700	136,200	130,900	6	8[a]	16
		20	200	800	0	158,800	143,500	142,200	131,500	120,300	6	9	13
		200	200	800	25.0	156,400	143,900	139,800	126,900	118,000	2	3	6
		200	200	800	0	150,600	145,300	143,800	129,800	111,000	1	0[c]	1
K-79	7Cu, O_2 added	20	200	800	25.0	110,300	94,600	93,100	85,400	76,700	14	18[b]	36
		20	200	800	0	109,500	93,400	91,600	82,300	71,700	16	20[a]	34
		200	200	800	25.0	109,900	88,800	84,600	63,800	51,200	14	18[a]	27
		200	200	800	0	109,600	89,400	86,200	70,200	54,100	16	18[a]	39

(a) Broke outside gage marks.
(b) Broke on gage mark.
(c) Broke in threads.

TABLE 114. RESULTS OF TESTS TO DETERMINE THE HYDROGEN SENSITIVITY OF THE Ti-8Mn ALLOY AS STABILIZED. MEDIUM EQUIAXED ALPHA.

Hydrogen Content, ppm		VHN (10-Kg Load)		Metallographic
Nominal	By Analysis	Hydrogen Content	VHN	Structure, 20 ppm
20	--	20	272	See Figure 21a.
200	--	200	287	
300	--	300	--	

Unnotched Stress-Rupture Tests Using 0.125-In. Round Samples

Nominal Hydrogen	Applied Stress		Rupture Time, hours	Extension, % Between Shoulders	Elongation, % in 4D	Reduction in Area, %
	Psi	% of Ultimate Tensile Strength				
20	120,100	95	22.1	16	28	46
200	126,000	97	2.3	11	21	32
200	123,500	95	235.1	14	--(c)	36
300	124,000	99	0.7	15	25	40
300	121,500	97	1.7	14	--(c)	31
300	119,000	95	4.6	10	--(c)	20

(a) Test discontinued before failure; (b) Broke outside gage mark; (c) Broke on gage mark.

Unnotched Tensile Tests Using 0.125-In. Round Samples

Nominal Hydrogen	Ultimate Tensile Strength, psi	Yield Strength, psi			Proportional Limit, psi	Extension, % Between Shoulders	Elongation, % in 4D	Reduction in Area, %
		0.2% Offset	0.1% Offset	0.01% Offset				
Low Testing Speed - 0.005 In./Min								
20	126,500	107,800	106,600	96,400	88,400	17	26	37
200	130,000	110,600	110,800	105,600	99,200	17	24	44
300	125,300	110,400	110,000	98,700	92,400	15	22(a)	40
High Testing Speed - 0.5 In./Min								
20	125,300					15	29	51
200	127,400					15	27	49
300	126,600					15	27	58

(a) Broke on gage mark; (b) Broke outside gage mark.

Notch-Bend Impact Tests Using Micro Sample

Nominal Hydrogen	Energy Absorbed, in-lb		Conclusion
	At 77 F	At -40 F	
20	33	12	Slow-strain embrittlement at 300 ppm; impact
200	14	10	embrittlement at 200 ppm, but ductility
300	31	10	recovered at 300 ppm

TABLE 115. RESULTS OF TESTS TO DETERMINE THE HYDROGEN SENSITIVITY OF THE Ti-8Mn ALLOY AS SOLUTION HEAT TREATED. MEDIUM EQUIAXED ALPHA.

Hydrogen Content, ppm		VHN (10-Kg Load)		Metallographic Structure, 20 ppm
Nominal	By Analysis	Hydrogen Content	VHN	
20	--	20	256	See Figure 21b.
200	--	200	363	
300	--	300	--	
600		600	--	

Unnotched Stress-Rupture Tests Using 0.125-In. Round Samples

Nominal Hydrogen	Applied Stress		Rupture Time, hours	Extension, % Between Shoulders	Elonga-tion, % in 4D	Reduction in Area, %
	Psi	% of Ultimate Tensile Strength				
200	165,600	99	305.6[a]	9	13	--
200	162,300	97	255.6[a]	--	6	--
200	162,300	97	311.3[a]	4	7	--
300	145,600	99	258.9[a]	9	12	--
600	154,400	99	1.5	11	17	37

(a) Test discontinued before failure; (b) Broke outside gage mark; (c) Broke on gage mark.

Unnotched Tensile Tests Using 0.125-In. Round Samples

Nominal Hydrogen	Ultimate Tensile Strength, psi	Yield Strength, psi			Propor-tional Limit, psi	Extension, % Between Shoulders	Elonga-tion, % in 4D	Reduction in Area, %
		0.2% Offset	0.1% Offset	0.01% Offset				
Low Testing Speed - 0.005 In./Min								
20	140,600	127,600	124,400	108,300	100,900	14	16	58
200	167,400	160,500	160,200	155,100	152,100	12	30	37
300	147,100	138,000	135,800	112,000	106,300	14	18[b]	52
600	156,000	149,000	146,000	117,000	108,000	9	14	36
High Testing Speed - 0.5 In./Min								
20	141,100					12	23	54
200	165,700					6	11	38
300	145,600					11	24	57
600	155,000					9	16	47

(a) Broke on gage mark; (b) Broke outside gage mark.

Notch-Bend Impact Tests Using Micro Sample

Nominal Hydrogen	Energy Absorbed, in-lb		Conclusion
	At 77 F	At -40 F	
20	63	11	Testing was not completed; slow-strain embrittlement 400-600 ppm; impact embrittlement at 200 ppm
20	38	18	
200	9	5	
300	14	9	
600	11	8	

TABLE 116. RESULTS OF TESTS TO DETERMINE THE HYDROGEN SENSITIVITY OF THE Ti-8Mn ALLOY AS SOLUTION HEAT TREATED AND AGED. MEDIUM EQUIAXED ALPHA.

Hydrogen Content, ppm		VHN (10-Kg Load)		Metallographic Structure, 20 ppm
Nominal	By Analysis	Hydrogen Content	VHN	
20	--	20	330	See Figure 21c.
100	--	100	--	
200	--	200	330	

Unnotched Stress-Rupture Tests Using 0.125-In. Round Samples

Nominal Hydrogen	Applied Stress		Rupture Time, hours	Extension, % Between Shoulders	Elonga-tion, % in 4D	Reduction in Area, %
	Psi	% of Ultimate Tensile Strength				
20	157,600	97	5.8	11	20	45
20	154,400	95	311.0[a]	4	10	--
100	161,400	99	0.2	9	--[c]	34
100	159,800	98	262.8[a]	6	9	--
100	158,000	97	260.7[a]	4	5	--

(a) Test discontinued before failure; (b) Broke outside gage mark; (c) Broke on gage mark.

Unnotched Tensile Tests Using 0.125-In. Round Samples

Nominal Hydrogen	Ultimate Tensile Strength, psi	Yield Strength, psi			Propor-tional Limit, psi	Extension, % Between Shoulders	Elonga-tion, % in 4D	Reduction in Area, %
		0.2% Offset	0.1% Offset	0.01% Offset				

Low Testing Speed - 0.005 In./Min

Nominal Hydrogen	Ultimate Tensile Strength, psi	0.2% Offset	0.1% Offset	0.01% Offset	Propor-tional Limit, psi	Extension, % Between Shoulders	Elonga-tion, % in 4D	Reduction in Area, %
20	162,500	148,100	137,300	109,200	97,200	10	14[a]	40
100	163,000	145,500	128,500	102,000	92,900	9	13	34
200	149,300	136,700	134,300	117,000	108,900	7	9	12

High Testing Speed - 0.5 In./Min

Nominal Hydrogen	Ultimate Tensile Strength, psi	0.2% Offset	0.1% Offset	0.01% Offset	Propor-tional Limit, psi	Extension, % Between Shoulders	Elonga-tion, % in 4D	Reduction in Area, %
20	157,500					9	18	49
100	164,400					9	15	36
200	152,500					9	15	37

(a) Broke on gage mark; (b) Broke outside gage mark.

Notch-Bend Impact Tests Using Micro Sample

Nominal Hydrogen	Energy Absorbed, in-lb		Conclusion
	At 77 F	At -40 F	
20	11	9	Slow strain embrittlement at 200 ppm; alloy brittle in impact testing
100	10	8	
200	9	7	

Hydrogen Content, ppm		VHN (10-Kg Load)		Metallographic
Nominal	By Analysis	Hydrogen Content	VHN	Structure, 20 ppm
20	--	20	294	See Figure 21d.
200	--	200	294	
300	--	300	--	

Unnotched Stress-Rupture Tests Using 0.125-In. Round Samples

Nominal Hydrogen	Applied Stress		Rupture Time, hours	Extension, % Between Shoulders	Elonga-tion, % in 4D	Reduction in Area, %
	Psi	% of Ultimate Tensile Strength				
20	112,300	93	262.1[a]	9	--	--
200	120,000	97	64.8	17	--[c]	43
200	115,200	93	283.8[a]	8	--	--
300	117,100	97	8.5	17	22	36
300	114,700	95	14.8	10	12	17
300	112,300	93	287.2[a]	8	14	--

(a) Test discontinued before failure; (b) Broke outside gage mark; (c) Broke on gage mark.

Unnotched Tensile Tests Using 0.125-In. Round Samples

Nominal Hydrogen	Ultimate Tensile Strength, psi	Yield Strength, psi			Propor-tional Limit, psi	Extension, % Between Shoulders	Elonga-tion, % in 4D	Reduction in Area, %
		0.2% Offset	0.1% Offset	0.01% Offset				
			Low Testing Speed - 0.005 In./Min					
20	120,700	93,100	89,000	79,200	74,800	19	30	39
200	123,900	99,000	94,600	78,400	74,700	19	32	45
300	120,700	97,400	92,000	82,000	75,800	16	21[b]	39
			High Testing Speed - 0.5 In./Min					
20	121,500					15	28	48
200	124,200					15	28	47
300	122,200					13	25	48

(a) Broke on gage mark; (b) Broke outside gage mark.

Notch-Bend Impact Tests Using Micro Sample

Nominal Hydrogen	Energy Absorbed, in-lb		Conclusion
	At 77 F	At -40 F	
20	28	12	Slow strain embrittlement at 300 ppm; progressive loss of impact properties
200	22	10	
300	19	8	

Hydrogen Content, ppm		VHN (10-Kg Load)		Metallographic Structure, 20 ppm
Nominal	By Analysis	Hydrogen Content	VHN	
20	--	20	325	See Figure 21e.
200	--	200	348	
400	--	400	--	

Unnotched Stress-Rupture Tests Using 0.125-In. Round Samples

Nominal Hydrogen	Applied Stress		Rupture Time, hours	Extension, % Between Shoulders	Elonga- tion, % in 4D	Reduction in Area, %
	Psi	% of Ultimate Tensile Strength				
20	134,400	93	283.4[a]	2	4	--
200	149,900	97	2.5	9	16	31
200	149,900	97	74.0	7	--[c]	23
200	143,900	93	283.7[a]	1	2	--
400	156,300	99	251.9[a]	3	5	--
400	153,000	97	254.0[a]	1	4	--
400	150,000	95	305.7[a]	1	--	--

(a) Test discontinued before failure; (b) Broke outside gage mark; (c) Broke on gage mark.

Unnotched Tensile Tests Using 0.125-In. Round Samples

Nominal Hydrogen	Ultimate Tensile Strength, psi	Yield Strength, psi			Propor- tional Limit, psi	Extension, % Between Shoulders	Elonga- tion, % in 4D	Reduction in Area, %
		0.2% Offset	0.1% Offset	0.01% Offset				
Low Testing Speed - 0.005 In./Min								
20	144,500	129,400	123,500	108,200	104,200	15	26	36
200	154,700	147,100	143,000	123,000	115,000	9	14	30
400	157,900	151,300	146,700	129,500	118,900	9	14	26
High Testing Speed - 0.5 In./Min								
20	146,300					9	18	42
200	154,000					7	14	35
400	161,500					6	12	34

(a) Broke on gage mark; (b) Broke outside gage mark.

Notch-Bend Impact Tests Using Micro Sample

Nominal Hydrogen	Energy Absorbed, in-lb		Conclusion
	At 77 F	At -40 F	
20	18	10	Testing was not completed; no slow-strain embrittlement at 400 ppm; impact embrittle- ment at 200 ppm
200	9	6	
400	7	4	

Hydrogen Content, ppm		VHN (10-Kg Load)		Metallographic Structure, 20 ppm
Nominal	By Analysis	Hydrogen Content	VHN	
20	--	20	345	See Figure 21f.
100	--	100	--	
200	--	200	357	

Unnotched Stress-Rupture Tests Using 0.125-In. Round Samples

Nominal Hydrogen	Applied Stress		Rupture Time, hours	Extension, % Between Shoulders	Elonga-tion, % in 4D	Reduction in Area, %
	Psi	% of Ultimate Tensile Strength				
20	143,600	93	283.6[a]	4	6	--
100	141,000	97	40.5	1	--[b]	7
200	143,200	93	0.4	1	3	1
200	140,200	91	0.6	1	2	1

(a) Test discontinued before failure; (b) Broke outside gage mark; (c) Broke on gage mark.

Unnotched Tensile Tests Using 0.125-In. Round Samples

Nominal Hydrogen	Ultimate Tensile Strength, psi	Yield Strength, psi			Propor-tional Limit, psi	Extension, % Between Shoulders	Elonga-tion, % in 4D	Reduction in Area, %
		0.2% Offset	0.1% Offset	0.01% Offset				
Low Testing Speed - 0.005 In./Min								
20	154,400	131,900	118,300	97,100	90,200	11	13[b]	23
100	145,500	110,200	100,700	85,700	81,200	6	6[b]	24
200	154,000	141,500	130,800	100,500	92,200	3	4[b]	8
High Testing Speed - 0.5 In./Min								
20	153,700					11	18	29
100	160,300					6	10[a]	22
200	158,700					8	14	23

(a) Broke on gage mark; (b) Broke outside gage mark.

Notch-Bend Impact Tests Using Micro Samples

Nominal Hydrogen	Energy Absorbed, in-lb		Conclusion
	At 77 F	At -40 F	
20	12	7	Slow strain embrittlement at 100 ppm; alloy brittle in impact testing
100	7	6	
200	11	5	

| Hydrogen Content, ppm | | VHN (10-Kg Load) | | Metallographic Structure, 20 ppm |
Nominal	By Analysis	Hydrogen Content	VHN	
20	--	20	--	See Figure 21g.
200	--	200	--	

Unnotched Stress-Rupture Tests Using 0.125-In. Round Samples

| Nominal Hydrogen | Applied Stress | | Rupture Time, hours | Extension, % Between Shoulders | Elonga-tion, % in 4D | Reduction in Area, % |
	Psi	% of Ultimate Tensile Strength				
200	128,700	97	62.6	14	26	44

(a) Test discontinued before failure; (b) Broke outside gage mark; (c) Broke on gage mark.

Unnotched Tensile Tests Using 0.125-In. Round Samples

| Nominal Hydrogen | Ultimate Tensile Strength, psi | Yield Strength, psi | | | Propor-tional Limit, psi | Extension, % Between Shoulders | Elonga-tion, % in 4D | Reduction in Area, % |
		0.2% Offset	0.1% Offset	0.01% Offset				
			Low Testing Speed - 0.005 In./Min					
20	130,000	112,700	109,200	94,400	85,400	19	32	48
200	132,700	115,900	116,400	104,500	98,700	17	27	46
			High Testing Speed - 0.5 In./Min					
20	129,700					15	27	54
200	133,600					16	26	48

(a) Broke on gage mark; (b) Broke outside gage mark.

Notch-Bend Impact Tests Using Micro Sample

| Nominal Hydrogen | Energy Absorbed, in-lb | | Conclusion |
	At 77 F	At -40 F	
20	32	13	Testing not completed; no slow strain embrittle-ment at 200 ppm; impact embrittlement at 200 ppm
200	10	8	

TABLE 121. RESULTS OF TESTS TO DETERMINE THE HYDROGEN SENSITIVITY OF THE Ti-8Mn ALLOY AS STABILIZED. COARSE EQUIAXED ALPHA.

Hydrogen Content, ppm		VHN (10-Kg Load)		Metallographic Structure, 20 ppm
Nominal	By Analysis	Hydrogen Content	VHN	
20	--	20	--	See Figure 21h.
200	--	200	--	
300	--	200	--	

Unnotched Stress-Rupture Tests Using 0.125-In. Round Samples

Nominal Hydrogen	Applied Stress		Rupture Time, hours	Extension, % Between Shoulders	Elonga- tion, % in 4D	Reduction in Area, %
	Psi	% of Ultimate Tensile Strength				
20	116,200	95	105.6	17	--(c)	53
200	118,000	97	29.2	17	--(c)	48
300	118,800	95	218.3	15	16	24

(a) Test discontinued before failure; (b) Broke outside gage mark; (c) Broke on gage mark.

Unnotched Tensile Tests Using 0.125-In. Round Samples

Nominal Hydrogen	Ultimate Tensile Strength, psi	Yield Strength, psi			Propor- tional Limit, psi	Extension, % Between Shoulders	Elonga- tion, % in 4D	Reduction in Area, %
		0.2% Offset	0.1% Offset	0.01% Offset				
			Low Testing Speed - 0.005 In./Min					
20	122,400	100,800	100,100	92,000	85,000	20	31	52
200	121,700	103,700	104,000	96,500	88,500	17	20(b)	47
300	125,000	106,000	103,000	88,400	77,800	20	32	44
			High Testing Speed - 0.5 In./Min					
20	124,000					15	29	54
200	123,800					14	27	48
300	125,000					16	26	50

(a) Broke on gage mark; (b) Broke outside gage mark.

Notch-Bend Impact Tests Using Micro Sample

Nominal Hydrogen	Energy Absorbed, in-lb		Conclusion
	At 77 F	At -40 F	
20	29	10	Slow strain embrittlement at 300 ppm; no impact embrittlement
200	16	8	
300	15	10	

Hydrogen Content, ppm		VHN (10-Kg Load)		Metallographic Structure, 20 ppm
Nominal	By Analysis	Hydrogen Content	VHN	
20	--	20	--	See Figure 21i.
200	--	200	--	
300	--	300	--	

Unnotched Stress-Rupture Tests Using 0.125-In. Round Samples

Nominal Hydrogen	Applied Stress		Rupture Time, hours	Extension, % Between Shoulders	Elongation, % in 4D	Reduction in Area, %
	Psi	% of Ultimate Tensile Strength				
200	118,400	97	On loading	16	--(c)	48
200	116,000	95	29.9	18	--(c)	43
300	118,500	95	28.0	13	24	32
300	117,000	94	30.2	13	19	28

(a) Test discontinued before failure; (b) Broke outside gage mark; (c) Broke on gage mark.

Unnotched Tensile Tests Using 0.125-In. Round Samples

Nominal Hydrogen	Ultimate Tensile Strength, psi	Yield Strength, psi			Proportional Limit, psi	Extension, % Between Shoulders	Elongation, % in 4D	Reduction in Area, %
		0.2% Offset	0.1% Offset	0.01% Offset				
			Low Testing Speed - 0.005 In./Min					
20	123,900	99,700	96,400	87,400	82,800	15	28	41
200	122,100	101,300	96,400	86,900	82,800	16	28	45
300	122,600	102,500	98,400	89,900	82,200	18	26	42
			High Testing Speed - 0.5 In./Min					
20	124,200					15	26	48
200	124,800					16	28	48
300	124,500					14	29	48

(a) Broke on gage mark; (b) Broke outside gage mark.

Notch-Bend Impact Tests Using Micro Sample

Nominal Hydrogen	Energy Absorbed, in-lb			Conclusion
	At 77 F	At -40 F		
20	26	13		Slow-strain embrittlement at 300 ppm; no impact embrittlement
200	33	9		
300	16	8		

TABLE 123. RESULTS OF TESTS TO DETERMINE THE HYDROGEN SENSITIVITY OF THE Ti-2Mo-2Fe-2Cr ALLOY AS STABILIZED. MEDIUM EQUIAXED ALPHA.

Hydrogen Content, ppm		VHN (10-Kg Load)		Metallographic Structure, 20 ppm
Nominal	By Analysis	Hydrogen Content	VHN	
20	--	20	247	See Figure 22a.
200	--	200	245	
300	--	300	--	

Unnotched Stress-Rupture Tests Using 0.125-In. Round Samples

Nominal Hydrogen	Applied Stress		Rupture Time, hours	Extension, % Between Shoulders	Elonga-tion, % in 4D	Reduction in Area, %
	Psi	% of Ultimate Tensile Strength				
20	107,100	95	39.4	15	--(c)	54
20	104,900	93	262.8(a)	8	16	--
200	108,500	95	3.7	16	--(c)	52
200	106,200	93	58.3	16	28	50
300	101,900	93	258.5(a)	10	14	--

(a) Test discontinued before failure; (b) Broke outside gage mark; (c) Broke on gage mark.

Unnotched Tensile Tests Using 0.125-In. Round Samples

Nominal Hydrogen	Ultimate Tensile Strength, psi	Yield Strength, psi			Propor-tional Limit, psi	Extension, % Between Shoulders	Elonga-tion, % in 4D	Reduction in Area, %
		0.2% Offset	0.1% Offset	0.01% Offset				
Low Testing Speed - 0.005 In./Min								
20	112,800	92,200	87,300	71,500	62,200	18	20(b)	51
200	114,200	89,400	84,300	64,600	41,200	19	35	53
300	109,600	82,800	76,400	63,800	57,800	17	25	55
High Testing Speed - 0.5 In./Min								
20	115,100					13	26	58
200	113,500					17	29	56
300	112,000					15	29	57

(a) Broke on gage mark; (b) Broke outside gage mark.

Notch-Bend Impact Tests Using Micro Sample

Nominal Hydrogen	Energy Absorbed, in-lb		Conclusion
	At 77 F	At -40 F	
20	21	12	Testing was not completed; no slow-strain embrittlement or impact embrittlement at 300 ppm
200	13	9	
300	18	8	

TABLE 124. RESULTS OF TESTS TO DETERMINE THE HYDROGEN SENSITIVITY OF THE Ti-2Mo-2Fe-2Cr ALLOY AS SOLUTION HEAT TREATED. MEDIUM EQUIAXED ALPHA.

Hydrogen Content, ppm		VHN (10-Kg Load)		Metallographic Structure, 20 ppm
Nominal	By Analysis	Hydrogen Content	VHN	
20	--	20	348	See Figure 22b.
200	--	200	330	
600	--	600	--	

Unnotched Stress-Rupture Tests Using 0.125-In. Round Samples

Nominal Hydrogen	Applied Stress		Rupture Time, hours	Extension, % Between Shoulders	Elonga-tion, % in 4D	Reduction in Area, %
	Psi	% of Ultimate Tensile Strength				
20	156,300	98	261.9(a)	6	9	--
20	154,700	97	261.0(a)	8	11	--
200	148,000	95	257.4(a)	--	7	--

(a) Test discontinued before failure; (b) Broke outside gage mark; (c) Broke on gage mark.

Unnotched Tensile Tests Using 0.125-In. Round Samples

Nominal Hydrogen	Ultimate Tensile Strength, psi	Yield Strength, psi			Propor-tional Limit, psi	Extension, % Between Shoulders	Elonga-tion, % in 4D	Reduction in Area, %
		0.2% Offset	0.1% Offset	0.01% Offset				
			Low Testing Speed - 0.005 In./Min					
20	159,500	149,000	146,300	132,500	109,500	12	20	45
200	155,800	135,300	121,900	92,100	80,700	13	18(a)	51
600	147,000	139,000	131,000	89,800	81,200	7	12	18
			High Testing Speed - 0.5 In./Min					
20	119,000					14	28	68
200	153,800					9	8(a)	58
600	146,000					9	16	50

(a) Broke on gage mark; (b) Broke outside gage mark.

Notch-Bend Impact Tests Using Micro Sample

Nominal Hydrogen	Energy Absorbed, in-lb		Conclusion
	At 77 F	At -40 F	
20	17	31	Testing was not completed; slow strain embrittlement at 300 to 600 ppm; impact embrittlement at 600 ppm
200	13	6	
600	8	11	

TABLE 125. RESULTS OF TESTS TO DETERMINE THE HYDROGEN SENSITIVITY
OF THE Ti-2Mo-2Fe-2Cr ALLOY AS SOLUTION HEAT TREATED
AND AGED. MEDIUM EQUIAXED ALPHA

Hydrogen Content, ppm		VHN (10-Kg Load)		Metallographic Structure, 20 ppm
Nominal	By Analysis	Hydrogen Content	VHN	
20	--	20	370	See Figure 22c
200	--	200	256	
300	--	300	--	
400	--	400	--	

Unnotched Stress-Rupture Tests Using 0.125-In. Round Samples

Nominal Hydrogen	Applied Stress		Rupture Time, hours	Extension, % Between Shoulders	Elongation, % in 4D	Reduction in Area, %
	Psi	% of Ultimate Tensile Strength				
20	117,300	95	257.5[a]	8	12	--
20	114,800	93	262.7[a]	5	8	--
200	113,700	95	4.8	9	8	45
200	111,200	93	253.3[a]	5	4	--
400	133,100	95	3.9	4	8	7

(a) Test discontinued before failure; (b) Broke outside gage mark; (c) Broke on gage mark.

Unnotched Tensile Tests Using 0.125-In. Round Samples

Nominal Hydrogen	Ultimate Tensile Strength, psi	Yield Strength, psi			Proportional Limit, psi	Extension, % Between Shoulders	Elongation, % in 4D	Reduction in Area, %
		0.2% Offset	0.1% Offset	0.01% Offset				
			Low Testing Speed - 0.005 In./Min					
20	123,500	98,800	91,100	77,300	68,800	14	24	51
200	119,700	99,200	93,300	82,600	76,600	12	7[b]	49
300	140,000	113,000	104,000	80,400	70,800	11	16	22
400	140,100	111,900	98,300	77,100	68,200	10	13	32
			High Testing Speed - 0.5 In./Min					
20	123,000					14	26	57
200	123,800					11	12[b]	45
300	141,000					12	22	34
400	142,200					10	18	37

(a) Broke on gage mark; (b) Broke outside gage mark.

Notch-Bend Impact Tests Using Micro Sample

Nominal Hydrogen	Energy Absorbed, in-lb		Conclusion
	At 77 F	At -40 F	
20	24	13	Slow strain embrittlement at 300; impact embrittlement at 200
200	12	8	
300	10	6	
400	--	--	

TABLE 126. RESULTS OF TESTS TO DETERMINE THE HYDROGEN SENSITIVITY
OF THE Ti-2Mo-2Fe-2Cr ALLOY AS STABILIZED. MEDIUM
ACICULAR ALPHA

Hydrogen Content, ppm		VHN (10-Kg Load)		Metallographic Structure, 20 ppm
Nominal	By Analysis	Hydrogen Content	VHN	
20	--	20	249	See Figure 22d
200	--	200	254	
300	--	300	--	
400	--	400	--	

Unnotched Stress-Rupture Tests Using 0.125-In. Round Samples

Nominal Hydrogen	Applied Stress		Rupture Time, hours	Extension, % Between Shoulders	Elongation, % in 4D	Reduction in Area, %
	Psi	% of Ultimate Tensile Strength				
20	99,800	93	100.6	18	24	40
200	102,800	93	41.1	17	22	38
200	99,500	90	0.1	18	32	50
300	101,700	93	67.1	11	13[b]	20
400	103,500	95	on loading	13	--[c]	38
400	101,400	93	9.2	8	6[b]	13

(a) Test discontinued before failure; (b) Broke outside gage mark; (c) Broke on gage mark.

Unnotched Tensile Tests Using 0.125-In. Round Samples

Nominal Hydrogen	Ultimate Tensile Strength, psi	Yield Strength, psi			Proportional Limit, psi	Extension, % Between Shoulders	Elongation, % in 4D	Reduction in Area, %
		0.2% Offset	0.1% Offset	0.01% Offset				
			Low Testing Speed - 0.005 In./Min					
20	107,400	80,800	75,400	66,200	60,600	17	21[b]	40
200	110,500	79,700	73,600	60,700	56,000	17	28	43
300	109,400	83,300	75,200	53,600	45,200	15	25	36
400	109,000	82,600	76,000	58,800	51,800	13	18[b]	27
			High Testing Speed - 0.5 In./Min					
20	108,500					15	26	42
200	112,500					17	31	53
300	112,200					14	25	45
400	112,800					13	26	41

(a) Broke on gage mark; (b) Broke outside gage mark.

Notch-Bend Impact Tests Using Micro Sample

Nominal Hydrogen	Energy Absorbed, in-lb		Conclusion
	At 77 F	At -40 F	
20	46	42	Slow strain embrittlement at 400 ppm; no impact embrittlement
200	33	30	
300	32	28	
400	33	28	

TABLE 127. RESULTS OF TESTS TO DETERMINE THE HYDROGEN SENSITIVITY OF THE Ti-2Mo-2Fe-2Cr ALLOY AS SOLUTION HEAT TREATED. MEDIUM ACICULAR ALPHA

Hydrogen Content, ppm		VHN (10-Kg Load)		Metallographic Structure, 20 ppm
Nominal	By Analysis	Hydrogen Content	VHN	
20	--	20	294	See Figure 22e
200	--	200	319	
300	--	300	--	
400	--	400	--	

Unnotched Stress-Rupture Tests Using 0.125-In. Round Samples

Nominal Hydrogen	Applied Stress		Rupture Time, hours	Extension, % Between Shoulders	Elongation, % in 4D	Reduction in Area, %
	Psi	% of Ultimate Tensile Strength				
20	115,800	93	262.8[a]	7	11	--
200	133,900	95	65.7	9	16	23
200	131,000	93	262.2[a]	4	5	--
300	117,400	97	296.9	13	17	21
400	126,500	95	52.8	8	--[c]	12
400	126,500	95	10.7	8	12	17

(a) Test discontinued before failure; (b) Broke outside gage mark; (c) Broke on gage mark.

Unnotched Tensile Tests Using 0.125-In. Round Samples

Nominal Hydrogen	Ultimate Tensile Strength, psi	Yield Strength, psi			Proportional Limit, psi	Extension, % Between Shoulders	Elongation, % in 4D	Reduction in Area, %
		0.2% Offset	0.1% Offset	0.01% Offset				
Low Testing Speed - 0.005 In./Min								
20	124,500	96,200	90,200	80,700	76,800	14	20[a]	38
200	140,900	109,500	99,600	81,700	76,000	11	17[a]	26
300	121,000	86,000	77,600	57,300	52,500	16	16	38
400	133,200	102,500	93,000	76,000	65,800	13	15	28
High Testing Speed - 0.5 In./Min								
20	125,500					13	23	54
200	143,600					8	16	30
300	113,800					16	30	57
400	133,300					11	18	39

(a) Broke on gage mark; (b) Broke outside gage mark.

Notch-Bend Impact Tests Using Micro Sample

Nominal Hydrogen	Energy Absorbed, in-lb		Conclusion
	At 77 F	At -40 F	
20	40	18	Slow strain embrittlement at 400 ppm; no impact embrittlement
200	24	11	
300	40	18	
400	25	11	

Hydrogen Content, ppm		VHN (10-Kg Load)		Metallographic Structure, 20 ppm
Nominal	By Analysis	Hydrogen Content	VHN	
20	--	20	297	See Figure 22f
100	--	100	--	
200	--	200	314	

Unnotched Stress-Rupture Tests Using 0.125-In. Round Samples

Nominal Hydrogen	Applied Stress		Rupture Time, hours	Extension, % Between Shoulders	Elongation, % in 4D	Reduction in Area, %
	Psi	% of Ultimate Tensile Strength				
20	122,600	93	264.1[a]	7	10	--
100	136,500	95	128.8	8	12	28
200	121,200	93	0.2	1	1	2

(a) Test discontinued before failure; (b) Broke outside gage mark; (c) Broke on gage mark.

Unnotched Tensile Tests Using 0.125-In. Round Samples

Nominal Hydrogen	Ultimate Tensile Strength, psi	Yield Strength, psi			Proportional Limit, psi	Extension, % Between Shoulders	Elongation, % in 4D	Reduction in Area, %
		0.2% Offset	0.1% Offset	0.01% Offset				
			Low Testing Speed - 0.005 In./Min					
20	131,800	93,400	86,100	72,200	67,700	8	12[a]	15
100	143,700	107,800	93,900	74,800	67,700	9	14	36
200	130,400	95,600	86,700	73,800	69,800	3	4[b]	8
			High Testing Speed - 0.5 In./Min					
20	133,600					9	16	22
100	145,100					8	16	37
200	137,500					4	6	8

(a) Broke on gage mark; (b) Broke outside gage mark.

Notch-Bend Impact Tests Using Micro Sample

Nominal Hydrogen	Energy Absorbed, in-lb		Conclusion
	At 77 F	At -40 F	
20	44	15	Slow strain embrittlement at 200 ppm; impact
100	10	8	embrittlement at 100 ppm
200	9	7	

Hydrogen Content, ppm		VHN (10-Kg Load)		Metallographic Structure, 20 ppm
Nominal	By Analysis	Hydrogen Content	VHN	
20	--	20	--	See Figure 23a
200	--	200	--	
600	--	600	--	
800	--	800	--	

Unnotched Stress-Rupture Tests Using 0.125-In. Round Samples

Nominal Hydrogen	Applied Stress		Rupture Time, hours	Extension, % Between Shoulders	Elonga-tion, % in 4D	Reduction in Area, %
	Psi	% of Ultimate Tensile Strength				
20	134,800	93	260.7[a]	2	3	--
200	145,500	97	1.1	9	--[b]	44
200	142,500	95	203.5	5	17	47
200	139,500	93	260.7[a]	5	6	--
600	144,300	95	1.1	7	8[b]	43
600	141,200	93	25.0	8	16	44
800	146,300	95	20.8	10	14	43

(a) Test discontinued before failure; (b) Broke outside gage mark; (c) Broke on gage mark.

Unnotched Tensile Tests Using 0.125-In. Round Samples

Nominal Hydrogen	Ultimate Tensile Strength, psi	Yield Strength, psi			Propor-tional Limit, psi	Extension, % Between Shoulders	Elonga-tion, % in 4D	Reduction in Area, %
		0.2% Offset	0.1% Offset	0.01% Offset				
Low Testing Speed - 0.005 In./Min								
20	145,000	127,200	126,300	125,400	123,200	8	13	40
200	150,100	132,200	130,000	120,000	100,500	10	17	48
600	151,900	132,000	127,300	108,900	90,600	9	13	42
800	154,000	138,000	133,000	110,000	97,900	10	18	45
High Testing Speed - 0.5 In./Min								
20	146,600					7	10[a]	41
200	150,800					9	17	45
600	152,000					6	8[a]	49
800	156,000					10	20	50

(a) Broke on gage mark; (b) Broke outside gage mark.

Notch-Bend Impact Tests Using Micro Sample

Nominal Hydrogen	Energy Absorbed, in-lb		Conclusion
	At 77 F	At -40 F	
20	36	30	No embrittlement observed through 800 ppm
200	32	26	
600	33	28	
800	28	20	

Hydrogen Content, ppm		VHN (10-Kg Load)		Metallographic Structure, 20 ppm
Nominal	By Analysis	Hydrogen Content	VHN	
20	--	20	--	
200	--	200	--	See Figure 23b
600	--	600	--	
800	--	800	--	

Unnotched Stress-Rupture Tests Using 0.125-In. Round Samples

Nominal Hydrogen	Applied Stress		Rupture Time, hours	Extension, % Between Shoulders	Elongation, % in 4D	Reduction in Area, %
	Psi	% of Ultimate Tensile Strength				
20	134,400	93	259.2[a]			
200	143,500	97	262.5[a]	2	2	--
200	137,500	93	266.4[a]	--	4	--
600	139,800	97	22.2	--	1	--
800	146,500	97	0.8	11	18	48
				12	18	53

(a) Test discontinued before failure; (b) Broke outside gage mark; (c) Broke on gage mark.

Unnotched Tensile Tests Using 0.125-In. Round Samples

Nominal Hydrogen	Ultimate Tensile Strength, psi	Yield Strength, psi			Proportional Limit, psi	Extension, % Between Shoulders	Elongation, % in 4D	Reduction in Area, %
		0.2% Offset	0.1% Offset	0.01% Offset				
				Low Testing Speed - 0.005 In./Min				
20	144,500	--	--	--	--	9	14	41
200	147,900	136,300	134,100	126,500	121,800	8	16	48
600	144,100	117,300	113,100	98,800	86,900	10	11[b]	52
800	151,000	136,000	134,000	124,000	116,000	11	19	35
				High Testing Speed - 0.5 In./Min				
20	143,800					7	15	50
200	154,700					8	14	49
600	148,600					10	19	50
800	152,000					11	21	54

(a) Broke on gage mark; (b) Broke outside gage mark.

Notch-Bend Impact Tests Using Micro Sample

Nominal Hydrogen	Energy Absorbed, in-lb		Conclusion
	At 77 F	At -40 F	
20	26	21	
200	28	26	Both slow strain and impact embrittlement at 800 ppm
600	26	24	
800	12	12	

TABLE 131. RESULTS OF TESTS TO DETERMINE THE HYDROGEN SENSITIVITY OF THE Ti-6Al-4V ALLOY AS SOLUTION HEAT TREATED AND AGED. FINE EQUIAXED ALPHA.

Hydrogen Content, ppm		VHN (10-Kg Load)		Metallographic Structure, 20 ppm
Nominal	By Analysis	Hydrogen Content	VHN	
20	--	20	--	See Figure 23c
200	--	200	--	
400	--	400	--	

Unnotched Stress-Rupture Tests Using 0.125-In. Round Samples

Nominal Hydrogen	Applied Stress		Rupture Time, hours	Extension, % Between Shoulders	Elonga- tion, % in 4D	Reduction in Area, %
	Psi	% of Ultimate Tensile Strength				
20	142,000	93	263.0[a]	3	3	--
200	153,000	97	9.7	8	13	37
200	156,000	95	189.1	8	--[c]	38
200	146,700	93	257.4[a]	2	3	--
400	154,200	97	9.1	6	6	19
400	151,100	95	41.1	3	4	34

(a) Test discontinued before failure; (b) Broke outside gage mark; (c) Broke on gage mark.

Unnotched Tensile Tests Using 0.125-In. Round Samples

Nominal Hydrogen	Ultimate Tensile Strength, psi	Yield Strength, psi			Proportional Limit, psi	Extension, % Between Shoulders	Elonga- tion, % in 4D	Reduction in Area, %
		0.2% Offset	0.1% Offset	0.01% Offset				
			Low Testing Speed - 0.005 In./Min					
20	152,700	--	--	133,700	119,900	8	10[a]	35
200	157,800	143,500	142,200	129,700	117,000	8	16	39
400	159,000	148,000	146,000	129,000	117,000	6	12	33
			High Testing Speed - 0.5 In./Min					
20	153,300					8	15	42
200	159,400					8	16	45
400	169,000					6	12	42

(a) Broke on gage mark; (b) Broke outside gage mark.

Notch-Bend Impact Tests Using Micro Sample

Nominal Hydrogen	Energy Absorbed, in-lb		Conclusion
	At 77 F	At -40 F	
20	32	30	Testing not completed; no embrittlement observed at 400 ppm
200	26	26	
400	24	12	

TABLE 132.   RESULTS OF TESTS TO DETERMINE THE HYDROGEN SENSITIVITY
OF THE Ti-6Al-4V ALLOY AS STABILIZED. COARSE ACICULAR
ALPHA.

Hydrogen Content, ppm		VHN (10-Kg Load)		Metallographic
Nominal	By Analysis	Hydrogen Content	VHN	Structure, 20 ppm
20	--	20	--	
200	--	200	--	See Figure 23d
600	--	600	--	

Unnotched Stress-Rupture Tests Using 0.125-In. Round Samples

Nominal Hydrogen	Applied Stress		Rupture Time, hours	Extension, % Between Shoulders	Elonga-tion, % in 4D	Reduction in Area, %
	Psi	% of Ultimate Tensile Strength				
20	132,000	95	11.6	6	--(c)	23
200	143,500	97	2.3	5	6(c)	28
200	140,600	95	32.3	5	12	29
600	143,100	95	190.9	6	--(b)	18
600	143,100	95	18.5	6	9	18

(a) Test discontinued before failure; (b) Broke outside gage mark; (c) Broke on gage mark.

Unnotched Tensile Tests Using 0.125-In. Round Samples

Nominal Hydrogen	Ultimate Tensile Strength, psi	Yield Strength, psi			Propor-tional Limit, psi	Extension, % Between Shoulders	Elonga-tion, % in 4D	Reduction in Area, %
		0.2% Offset	0.1% Offset	0.01% Offset				
		Low Testing Speed - 0.005 In./Min						
20	139,000	127,300	125,800	115,800	107,800	6	12	24
200	148,000	137,700	136,300	123,800	116,100	6	9(a)	29
600	150,600	136,600	132,900	113,200	97,400	7	11	23
		High Testing Speed - 0.5 In./Min						
20	141,800					6	9(b)	27
200	148,200					6	12	28
600	149,700					6	12	28

(a) Broke on gage mark; (b) Broke outside gage mark.

Notch-Bend Impact Tests Using Micro Sample

Nominal Hydrogen	Energy Absorbed, in-lb		Conclusion
	At 77 F	At -40 F	
20	28	26	Testing was not completed; slow strain embrittle-ment at 600 ppm; no impact embrittlement
200	28	24	
600	22	20	

TABLE 133. RESULTS OF TESTS TO DETERMINE THE HYDROGEN SENSITIVITY OF THE Ti-6Al-4V ALLOY AS SOLUTION HEAT TREATED. COARSE ACICULAR ALPHA.

Hydrogen Content, ppm		VHN (10-Kg Load)		Metallographic Structure, 20 ppm
Nominal	By Analysis	Hydrogen Content	VHN	
20	--	20	--	
200	--	200	--	See Figure 23e
600	--	600	--	
800	--	800	--	

Unnotched Stress-Rupture Tests Using 0.125-In. Round Samples

Nominal Hydrogen	Applied Stress		Rupture Time, hours	Extension, % Between Shoulders	Elongation, % in 4D	Reduction in Area, %
	Psi	% of Ultimate Tensile Strength				
20	126,800	95	14.5	7	9	29
200	134,200	97	2.4	9	8(c)	31
200	131,200	95	258.2(a)	4	7	--
600	139,500	97	0.6	11	18	25

(a) Test discontinued before failure; (b) Broke outside gage mark; (c) Broke on gage mark.

Unnotched Tensile Tests Using 0.125-In. Round Samples

Nominal Hydrogen	Ultimate Tensile Strength, psi	Yield Strength, psi			Proportional Limit, psi	Extension, % Between Shoulders	Elongation, % in 4D	Reduction in Area, %
		0.2% Offset	0.1% Offset	0.01% Offset				
Low Testing Speed - 0.005 In./Min								
20	133,300	118,000	116,200	106,500	102,000	7	8(b)	27
200	138,300	119,200	115,800	101,900	95,300	7	14	30
600	143,800	121,200	116,000	94,000	80,200	7	12	22
800	142,000	116,000	108,000	79,100	65,700	9	12	18
High Testing Speed - 0.5 In./Min								
20	132,700					8	16	30
200	136,300					10	19	32
600	141,000					8	15	31
800	141,000					10	16	21

(a) Broke on gage mark; (b) Broke outside gage mark.

Notch-Bend Impact Tests Using Micro Sample

Nominal Hydrogen	Energy Absorbed, in-lb		Conclusion
	At 77 F	At -40 F	
20	23	31	Slow-strain embrittlement at 800 ppm; no impact embrittlement
200	25	20	
600	20	22	
800	24	21	

TABLE 134.   RESULTS OF TESTS TO DETERMINE THE HYDROGEN SENSITIVITY
OF THE Ti-6Al-4V ALLOY AS SOLUTION HEAT TREATED AND
AGED.   COARSE ACICULAR ALPHA.

Hydrogen Content, ppm		VHN (10-Kg Load)		Metallographic Structure, 20 ppm
Nominal	By Analysis	Hydrogen Content	VHN	
20	--	20	--	
200	--	200	--	See Figure 23f
400	--	400	--	

Unnotched Stress-Rupture Tests Using 0.125-In. Round Samples

Nominal Hydrogen	Applied Stress		Rupture Time, hours	Extension, % Between Shoulders	Elongation, % in 4D	Reduction in Area, %
	Psi	% of Ultimate Tensile Strength				
20	128,800	95	19.0	9	13(b)	37
200	138,200	97	23.5	9	12(b)	36
200	135,400	95	39.7	10	17	36
400	152,000	95	0.7	4	6	6

(a) Test discontinued before failure; (b) Broke outside gage mark; (c) Broke on gage mark.

Unnotched Tensile Tests Using 0.125-In. Round Samples

Nominal Hydrogen	Ultimate Tensile Strength, psi	Yield Strength, psi			Proportional Limit, psi	Extension, % Between Shoulders	Elongation, % in 4D	Reduction in Area, %
		0.2% Offset	0.1% Offset	0.01% Offset				
Low Testing Speed - 0.005 In./Min								
20	135,500	--	--	--	--	12	21	41
200	142,500	128,700	127,800	115,200	108,000	10	16	34
400	160,000	150,200	148,500	132,500	114,100	3	7	15
High Testing Speed - 0.5 In./Min								
20	137,800					10	20	47
200	147,000					9	16	40
400	161,300					3	7	15

(a) Broke on gage mark; (b) Broke outside gage mark.

Notch-Bend Impact Tests Using Micro Sample

Nominal Hydrogen	Energy Absorbed, in-lb		Conclusion
	At 77 F	At -40 F	
20	34	18	Testing was not completed; slow strain embrittlement at 300 to 400 ppm; no impact embrittlement (20 and 200 ppm material showed equiaxed rather than acicular alpha)
200	33	26	
400	21	23	

Hydrogen Content, ppm		VHN (10-Kg Load)		Metallographic Structure, 20 ppm
Nominal	By Analysis	Hydrogen Content	VHN	
20	--	20	--	
200	--	200	--	See Figure 23g
400	--	400	--	

Unnotched Stress-Rupture Tests Using 0.125-In. Round Samples

Nominal Hydrogen	Applied Stress		Rupture Time, hours	Extension, % Between Shoulders	Elongation, % in 4D	Reduction in Area, %
	Psi	% of Ultimate Tensile Strength				
20	124,400	95	107.8	9	--(c)	45
200	129,200	95	on loading	10	21	43
400	128,600	95	31.4	11	--(c)	46
400	128,600	95	252.2(a)	7	12	--

(a) Test discontinued before failure; (b) Broke outside gage mark; (c) Broke on gage mark.

Unnotched Tensile Tests Using 0.125-In. Round Samples

Nominal Hydrogen	Ultimate Tensile Strength, psi	Yield Strength, psi			Proportional Limit, psi	Extension, % Between Shoulders	Elongation, % in 4D	Reduction in Area, %
		0.2% Offset	0.1% Offset	0.01% Offset				
Low Testing Speed - 0.005 In./Min								
20	130,900	114,800	114,800	115,200	111,300	10	10(b)	44
200	136,000	122,500	121,900	115,300	111,700	11	17	51
400	135,400	120,200	118,500	110,500	101,500	11	17(a)	46
High Testing Speed - 0.5 In./Min								
20	135,100					10	16(a)	41
200	138,100					10	16	52
400	139,000					10	19	52

(a) Broke on gage mark; (b) Broke outside gage mark.

Notch-Bend Impact Tests Using Micro Sample

Nominal Hydrogen	Energy Absorbed, in-lb		Conclusion
	At 77 F	At -40 F	
20	34	31	Testing was not completed; no embrittlement observed at 400 ppm
200	33	30	
400	35	30	

TABLE 136.   RESULTS OF TESTS TO DETERMINE THE HYDROGEN SENSITIVITY
OF THE Ti-6Al-4V ALLOY AS STABILIZED. COARSE ACICULAR
ALPHA.

| Hydrogen Content, ppm | | VHN (10-Kg Load) | | Metallographic |
Nominal	By Analysis	Hydrogen Content	VHN	Structure, 20 ppm
20	--	20	--	
200	--	200	--	See Figure 23h

Unnotched Stress-Rupture Tests Using 0.125-In. Round Samples

| Nominal Hydrogen | Applied Stress | | Rupture Time, hours | Extension, % Between Shoulders | Elonga-tion, % in 4D | Reduction in Area, % |
	Psi	% of Ultimate Tensile Strength				
20	142,500	95	43.7	4	3(b)	26
20	139,400	93	259.2(a)	1	2	--
200	125,500	97	0.1	2	-(c)	16
200	123,000	95	20.4	2	2(b)	4

(a) Test discontinued before failure; (b) Broke outside gage mark; (c) Broke on gage mark.

Unnotched Tensile Tests Using 0.125-In. Round Samples

| Nominal Hydrogen | Ultimate Tensile Strength, psi | Yield Strength, psi | | | Propor-tional Limit, psi | Extension, % Between Shoulders | Elonga-tion, % in 4D | Reduction in Area, % |
		0.2% Offset	0.1% Offset	0.01% Offset				
		Low Testing Speed - 0.005 In./Min						
20	149,900	138,400	136,900	130,400	123,800	5	9	18
200	129,600	123,500	122,300	115,000	108,800	4	4(b)	13
		High Testing Speed - 0.5 In./Min						
20	149,900					5	8	23
200	133,700					2	2(b)	14

(a) Broke on gage mark; (b) Broke outside gage mark.

Notch-Bend Impact Tests Using Micro Sample

| Nominal Hydrogen | Energy Absorbed, in-lb | | Conclusion |
	At 77 F	At -40 F	
20	26	26	Slow-strain embrittlement at 200 ppm; no impact embrittlement
200	25	30	

TABLE 137. RESULTS OF TESTS TO DETERMINE THE HYDROGEN SENSITIVITY OF THE Ti-6A1-4V ALLOY AS STABILIZED. MEDIUM ACICULAR ALPHA.

Hydrogen Content, ppm		VHN (10-Kg Load)		Metallographic Structure, 20 ppm
Nominal	By Analysis	Hydrogen Content	VHN	
20	--	20	--	
200	--	200	--	See Figure 23i
400	--	400	--	

Unnotched Stress-Rupture Tests Using 0.125-In. Round Samples

Nominal Hydrogen	Applied Stress		Rupture Time, hours	Extension, % Between Shoulders	Elonga-tion, % in 4D	Reduction in Area, %
	Psi	% of Ultimate Tensile Strength				
200	134,500	95	16.3	6	12	29
400	137,700	97	8.8	8	--(c)	29
400	136,300	96	16.1	6	14	31
400	134,900	95	305.5(a)	4	4	--

(a) Test discontinued before failure; (b) Broke outside gage mark; (c) Broke on gage mark.

Unnotched Tensile Tests Using 0.125-In. Round Samples

Nominal Hydrogen	Ultimate Tensile Strength, psi	Yield Strength, psi			Propor-tional Limit, psi	Extension, % Between Shoulders	Elonga-tion, % in 4D	Reduction in Area, %
		0.2% Offset	0.1% Offset	0.01% Offset				
			Low Testing Speed - 0.005 In./Min					
20	139,400	133,200	132,500	127,500	121,000	7	13	26
200	141,500	136,000	134,300	120,000	111,700	6	13	28
400	142,000	138,300	137,700	131,500	121,000	6	9(a)	31
			High Testing Speed - 0.5 In./Min					
20	139,700					6	12	28
200	142,700					7	13	30
400	144,500					6	13	28

(a) Broke on gage mark; (b) Broke outside gage mark.

Notch-Bend Impact Tests Using Micro Sample

Nominal Hydrogen	Energy Absorbed, in-lb		Conclusion
	At 77 F	At -40 F	
20	21	20	Testing was not completed; no embrittlement observed at 400 ppm
200	20	20	
400	22	22	

TABLE 138. RESULTS OF TESTS TO DETERMINE THE HYDROGEN SENSITIVITY OF THE Ti-4Al-4Mn ALLOY AS STABILIZED. FINE EQUIAXED ALPHA.

Hydrogen Content, ppm		VHN (10-Kg Load)		Metallographic
Nominal	By Analysis	Hydrogen Content	VHN	Structure, 20 ppm
20	--	20	317	
200	--	200	322	
300	--	300	--	See Figure 24a
400	--	400	--	
600	--	600	--	

Unnotched Stress-Rupture Tests Using 0.125-In. Round Samples

Nominal Hydrogen	Applied Stress		Rupture Time, hours	Extension, % Between Shoulders	Elongation, % in 4D	Reduction in Area, %
	Psi	% of Ultimate Tensile Strength				
20	142,500	95	60.5	11	19	44
20	139,500	93	262.3[a]	5	6	--
200	146,300	95	30.1	11	--[c]	43
200	143,300	93	259.8[a]	4	7	--
300	141,200	95	134.0	12	--[c]	42

(a) Test discontinued before failure; (b) Broke outside gage mark; (c) Broke on gage mark.

Unnotched Tensile Tests Using 0.125-In. Round Samples

Nominal Hydrogen	Ultimate Tensile Strength, psi	Yield Strength, psi			Proportional Limit, psi	Extension, % Between Shoulders	Elongation, % in 4D	Reduction in Area, %
		0.2% Offset	0.1% Offset	0.01% Offset				
			Low Testing Speed - 0.005 In./Min					
20	150,000	128,000	127,900	122,900	119,500	12	20	43
200	154,000	135,900	135,500	134,000	131,700	13	16[b]	43
300	148,700	136,100	133,000	125,200	123,500	13	19	47
400	156,000	145,000	132,000	111,000	96,200	10	14	31
600	153,000	138,300	136,200	125,900	116,300	10	15	11
			High Testing Speed - 0.5 In./Min					
20	152,000					11	21	46
200	154,800					11	20	45
300	149,100					10	19	33
400	160,000					9	14	44
600	155,000					7	15	22

(a) Broke on gage mark; (b) Broke outside gage mark.

(Notch-Bend Impact Tests Using Micro Sample

Nominal Hydrogen	Energy Absorbed, in-lb		Conclusion
	At 77 F	At -40 F	
20	22	12	Slow strain embrittlement at 600 ppm; no impact embrittlement
200	13	10	
300	14	11	
400	26	18	
600	11	10	

Hydrogen Content, ppm		VHN (10-Kg Load)		Metallographic Structure, 20 ppm
Nominal	By Analysis	Hydrogen Content	VHN	
20	--	20	319	
200	--	200	333	See Figure 24b
600	--	600	--	
800	--	800	--	

Unnotched Stress-Rupture Tests Using 0.125-In. Round Samples

Nominal Hydrogen	Applied Stress		Rupture Time, hours	Extension, % Between Shoulders	Elonga-tion, % in 4D	Reduction in Area, %
	Psi	% of Ultimate Tensile Strength				
20	144,400	95	309.5[a]	5	7	--
20	141,400	93	262.3[a]	4	6	--
200	149,700	97	85.6	9	13	29
200	146,600	95	256.1[a]	7	11	--
200	143,500	93	259.8[a]	3	5	--
600	145,300	97	192.1	12	--[c]	48
800	147,400	97	2.2	14	18	58

(a) Test discontinued before failure; (b) Broke outside gage mark; (c) Broke on gage mark.

Unnotched Tensile Tests Using 0.125-In. Round Samples

Nominal Hydrogen	Ultimate Tensile Strength, psi	Yield Strength, psi			Propor-tional Limit, psi	Extension, % Between Shoulders	Elonga-tion, % in 4D	Reduction in Area, %
		0.2% Offset	0.1% Offset	0.01% Offset				
Low Testing Speed - 0.005 In./Min								
20	152,000	132,600	132,200	131,800	--	12	20[a]	47
200	154,400	136,800	136,600	134,100	131,000	14	22	48
600	149,800	137,300	135,500	131,300	127,500	14	26	56
800	152,000	138,000	136,000	127,000	109,000	14	22	50
High Testing Speed - 0.5 In./Min								
20	153,000					11	20	48
200	157,300					11	19	50
600	152,700					10	20	52
800	154,000					10	18	44

(a) Broke on gage mark; (b) Broke outside gage mark.

Notch-Bend Impact Tests Using Micro Sample

Nominal Hydrogen	Energy Absorbed, in-lb		Conclusion
	At 77 F	At -40 F	
20	26	16	No embrittlement observed
200	16	12	
600	14	12	
800	16	14	

| Hydrogen Content, ppm | | VHN (10-Kg Load) | | Metallographic |
Nominal	By Analysis	Hydrogen Content	VHN	Structure, 20 ppm
20	--	20	342	
100	--	100	--	See Figure 24c
200	--	200	354	

Unnotched Stress-Rupture Tests Using 0.125-In. Round Samples

| Nominal Hydrogen | Applied Stress | | Rupture Time, hours | Extension, % Between Shoulders | Elongation, % in 4D | Reduction in Area, % |
	Psi	% of Ultimate Tensile Strength				
20	150,800	93	204.8	8	14	28
100	157,000	97	8.6	10	--(c)	36
100	153,700	95	253.9(a)	5	8	--
200	159,200	97	104.7	5	7	10
200	159,200	97	2.5	8	--(c)	21
200	152,800	93	256.1(a)	4	2	--

(a) Test discontinued before failure; (b) Broke outside gage mark; (c) Broke on gage mark.

Unnotched Tensile Tests Using 0.125-In. Round Samples

| Nominal Hydrogen | Ultimate Tensile Strength, psi | Yield Strength, psi | | | Proportional Limit, psi | Extension, % Between Shoulders | Elongation, % in 4D | Reduction in Area, % |
		0.2% Offset	0.1% Offset	0.01% Offset				
			Low Testing Speed - 0.005 In./Min					
20	162,100	135,000	134,000	128,400	124,400	9	14(a)	18
100	161,800	145,000	143,200	131,000	122,100	9	14	30
200	164,300	143,500	141,500	137,400	134,300	10	16	30
			High Testing Speed - 0.5 In./Min					
20	159,600					9	19	34
100	160,500					9	19	40
200	167,200					10	16	37

(a) Broke on gage mark; (b) Broke outside gage mark.

Notch-Bend Impact Tests Using Micro Sample

| Nominal Hydrogen | Energy Absorbed, in-lb | | Conclusion |
	At 77 F	At -40 F	
20	13	9	Slow strain embrittlement at 200 ppm; no impact embrittlement
100	12	10	
200	10	7	

Hydrogen Content, ppm		VHN (10-Kg Load)		Metallographic Structure, 20 ppm
Nominal	By Analysis	Hydrogen Content	VHN	
20	--	20	342	See Figure 24d
100	--	100	--	
200	--	200	387	

Unnotched Stress-Rupture Tests Using 0.125-In. Round Samples

Nominal Hydrogen	Applied Stress		Rupture Time, hours	Extension, % Between Shoulders	Elongation, % in 4D	Reduction in Area, %
	Psi	% of Ultimate Tensile Strength				
20	136,300	95	8.5	6	7	20
20	133,500	93	286.4(a)	4	6	--
100	142,200	97	0.2	6	10	19
100	139,400	95	5.9	7	--(c)	21
200	136,000	97	13.2	5	5	10
200	133,300	95	0.5	4	--(b)	23
200	130,600	93	261.3(a)	3	10	--

(a) Test discontinued before failure; (b) Broke outside gage mark; (c) Broke on gage mark.

Unnotched Tensile Tests Using 0.125-In. Round Samples

Nominal Hydrogen	Ultimate Tensile Strength, psi	Yield Strength, psi			Proportional Limit, psi	Extension, % Between Shoulders	Elongation, % in 4D	Reduction in Area, %
		0.2% Offset	0.1% Offset	0.01% Offset				
Low Testing Speed - 0.005 In./Min								
20	143,500	128,800	127,000	119,000	114,200	6	10	24
100	146,600	131,900	130,000	121,000	117,400	7	9(b)	24
200	140,500	128,600	126,500	116,600	110,200	7	14	14
High Testing Speed - 0.5 In./Min								
20	148,700					8	10	23
100	150,300					7	12	23
200	152,500					6	11	20

(a) Broke on gage mark; (b) Broke outside gage mark.

Notch-Bend Impact Tests Using Micro Sample

Nominal Hydrogen	Energy Absorbed, in-lb		Conclusion
	At 77 F	At -40 F	
20	28	14	Slow strain embrittlement at 200 ppm; no impact embrittlement
100	24	10	
200	23	13	

TABLE 142. RESULTS OF TESTS TO DETERMINE THE HYDROGEN SENSITIVITY OF THE Ti-4Al-4Mn ALLOY AS SOLUTION HEAT TREATED. COARSE ACICULAR ALPHA.

Hydrogen Content, ppm		VHN (10-Kg Load)		Metallographic Structure, 20 ppm
Nominal	By Analysis	Hydrogen Content	VHN	
20	--	20	373	
200	--	200	394	
600	--	600	--	See Figure 24e
800	--	800	--	

Unnotched Stress-Rupture Tests Using 0.125-In. Round Samples

Nominal Hydrogen	Applied Stress		Rupture Time, hours	Extension, % Between Shoulders	Elonga-tion, % in 4D	Reduction in Area, %
	Psi	% of Ultimate Tensile Strength				
20	138,400	93	4.4	5	8	19
20	134,000	90	127	5	--(c)	23
200	138,600	93	26.6	7	11	19
200	134,100	90	261.7(a)	3	5(c)	--
600	137,650	97	22.3	6	--(c)	18
800	147,000	97	1.2	9	9	21
800	144,400	95	3.1	8	--(c)	25
800	141,400	93	279.9(a)	7	8	--

(a) Test discontinued before failure; (b) Broke outside gage mark; (c) Broke on gage mark.

Unnotched Tensile Tests Using 0.125-In. Round Samples

Nominal Hydrogen	Ultimate Tensile Strength, psi	Yield Strength, psi			Propor-tional Limit, psi	Extension, % Between Shoulders	Elonga-tion, % in 4D	Reduction in Area, %
		0.2% Offset	0.1% Offset	0.01% Offset				
		Low Testing Speed - 0.005 In./Min						
20	148,800	133,800	133,200	127,400	125,100	8	12(b)	22
200	149,000	--	--	--	--	5	4(b)	22
600	142,000	135,400	133,300	123,000	117,000	5	7(b)	16
800	152,000	141,000	140,000	130,000	126,000	8	12	24
		High Testing Speed - 0.5 In./Min						
20	149,300					7	12	23
200	155,000					8	9	29
600	153,000					6	9	22
800	158,000					7	11	24

(a) Broke on gage mark; (b) Broke outside gage mark.

Notch-Bend Impact Tests Using Micro Sample

Nominal Hydrogen	Energy Absorbed, in-lb		Conclusion
	At 77 F	At -40 F	
20	28	24	No embrittlement observed
200	32	17	
600	22	13	
800	24	10	

Hydrogen Content, ppm		VHN (10-Kg Load)		Metallographic Structure, 20 ppm
Nominal	By Analysis	Hydrogen Content	VHN	
20	--	20	360	
100	--	100	--	See Figure 24f
200	--	200	390	

Unnotched Stress-Rupture Tests Using 0.125-In. Round Samples

Nominal Hydrogen	Applied Stress		Rupture Time, hours	Extension, % Between Shoulders	Elonga-tion, % in 4D	Reduction in Area, %
	Psi	% of Ultimate Tensile Strength				
20	148,100	93	133.3	-	6	9
100	154,600	95	0.3	5	_(b)	21
100	151,400	93	27.0	4	-	16
100	138,500	85	259.3(a)	2	3	--
200	155,500	93	1.0	1	3	2

(a) Test discontinued before failure; (b) Broke outside gage mark; (c) Broke on gage mark.

Unnotched Tensile Tests Using 0.125-In. Round Samples

Nominal Hydrogen	Ultimate Tensile Strength, psi	Yield Strength, psi			Propor-tional Limit, psi	Extension, % Between Shoulders	Elonga-tion, % in 4D	Reduction in Area, %
		0.2% Offset	0.1% Offset	0.01% Offset				
Low Testing Speed - 0.005 In./Min								
20	159,300	137,100	134,900	126,400	120,400	6	10	18
100	162,800	145,100	142,500	135,000	129,800	5	9	12
200	167,200	161,200	156,900	141,400	136,100	2	3	1
High Testing Speed - 0.5 In./Min								
20	161,300					5	8	14
100	161,900					5	8	18
200	174,900					3	6	13

(a) Broke on gage mark; (b) Broke outside gage mark.

Notch-Bend Impact Tests Using Micro Sample

Nominal Hydrogen	Energy Absorbed, in-lb		Conclusion
	At 77 F	At -40 F	
20	24	12	Slow strain embrittlement at 200 ppm; impact embrittlement at 100 ppm
100	12	11	
200	10	9	

TABLE 144. RESULTS OF TESTS TO DETERMINE THE HYDROGEN SENSITIVITY
OF THE Ti-4Al-4Mn ALLOY AS STABILIZED. MEDIUM EQUIAXED
ALPHA.

Hydrogen Content, ppm		VHN (10-Kg Load)		Metallographic Structure, 20 ppm
Nominal	By Analysis	Hydrogen Content	VHN	
20	--	20	--	See Figure 24g
200	--	200	--	
300	--	300	--	

Unnotched Stress-Rupture Tests Using 0.125-In. Round Samples

Nominal Hydrogen	Applied Stress		Rupture Time, hours	Extension, % Between Shoulders	Elonga- tion, % in 4D	Reduction in Area, %
	Psi	% of Ultimate Tensile Strength				
200	134,000	97	1.3	11	21	36
200	131,300	95	10.3	12	19	40
300	140,500	95	2.5	7	12	17
300	140,500	95	17.9	7	12	20

(a) Test discontinued before failure; (b) Broke outside gage mark; (c) Broke on gage mark.

Unnotched Tensile Tests Using 0.125-In. Round Samples

Nominal Hydrogen	Ultimate Tensile Strength, psi	Yield Strength, psi			Propor- tional Limit, psi	Extension, % Between Shoulders	Elonga- tion, % in 4D	Reduction in Area, %
		0.2% Offset	0.1% Offset	0.01% Offset				
			Low Testing Speed - 0.005 In./Min					
20	134,500	113,000	112,700	107,300	101,600	13	24	36
200	138,200	118,000	117,400	112,300	108,700	12	22	40
300	147,900	136,400	134,600	126,700	121,900	8	11	20
			High Testing Speed - 0.5 In./Min					
20	137,300					10	20	42
200	140,800					11	22	41
300	147,500					6	13	23

(a) Broke on gage mark; (b) Broke outside gage mark.

Notch-Bend Impact Tests Using Micro Sample

Nominal Hydrogen	Energy Absorbed, in-lb		Conclusion
	At 77 F	At -40 F	
20	15	8	Testing was not completed; no embrittlement at 300 ppm
200	16	9	
300	16	10	

TABLE 145. RESULTS OF TESTS TO DETERMINE THE HYDROGEN SENSITIVITY OF THE Ti-4Al-4Mn ALLOY AS STABILIZED. COARSE EQUIAXED ALPHA.

Hydrogen Content, ppm		VHN (10-Kg Load)		Metallographic Structure, 20 ppm
Nominal	By Analysis	Hydrogen Content	VHN	
20	--	20	--	See Figure 24h
200	--	200	--	

Unnotched Stress-Rupture Tests Using 0.125-In. Round Samples

Nominal Hydrogen	Applied Stress		Rupture Time, hours	Extension, % Between Shoulders	Elongation, % in 4D	Reduction in Area, %
	Psi	% of Ultimate Tensile Strength				
20	126,200	95	149.3	11	14	37
200	120,900	95	0.3	6	12	23
200	119,500	94	4.0	5	10	9
200	118,300	93	259.1[a]	2	3	--

(a) Test discontinued before failure; (b) Broke outside gage mark; (c) Broke on gage mark.

Unnotched Tensile Tests Using 0.125-In. Round Samples

Nominal Hydrogen	Ultimate Tensile Strength, psi	Yield Strength, psi			Proportional Limit, psi	Extension, % Between Shoulders	Elongation, % in 4D	Reduction in Area, %
		0.2% Offset	0.1% Offset	0.01% Offset				
			Low Testing Speed - 0.005 In./Min					
20	132,800	112,200	111,800	107,100	102,300	12	16[b]	39
200	127,200	117,500	115,300	106,800	100,300	5	9	18
			High Testing Speed - 0.5 In./Min					
20	137,400					11	21	44
200	136,000					3	2[b]	30

(a) Broke on gage mark; (b) Broke outside gage mark.

Notch-Bend Impact Tests Using Micro Sample

Nominal Hydrogen	Energy Absorbed, in-lb		Conclusion
	At 77 F	At -40 F	
20	8	11	Testing was not completed; slow strain embrittlement at 100-200 ppm; no impact embrittlement
200	26	8	

TABLE 146. RESULTS OF TESTS TO DETERMINE THE HYDROGEN SENSITIVITY OF THE Ti-4Al-4Mn ALLOY AS STABILIZED. FINE ACICULAR ALPHA

| Hydrogen Content, ppm | | VHN (10-Kg Load) | | Metallographic Structure, 20 ppm |
Nominal	By Analysis	Hydrogen Content	VHN	
20	--	20	--	
200	--	200	--	See Figure 24i
300	--	300	--	

Unnotched Stress-Rupture Tests Using 0.125-In. Round Samples

| Nominal Hydrogen | Applied Stress | | Rupture Time, hours | Extension, % Between Shoulders | Elongation, % in 4D | Reduction in Area, % |
	Psi	% of Ultimate Tensile Strength				
200	148,100	97	3.2	8	12	18
200	145,000	95	8.5	9	13	23
200	142,000	93	97.5	6	10	18
300	148,200	95	2.1	9	10	17
300	145,100	93	146.5	7	--(c)	16

(a) Test discontinued before failure; (b) Broke outside gage mark; (c) Broke on gage mark.

Unnotched Tensile Tests Using 0.125-In. Round Samples

| Nominal Hydrogen | Ultimate Tensile Strength, psi | Yield Strength, psi | | | Proportional Limit, psi | Extension, % Between Shoulders | Elongation, % in 4D | Reduction in Area, % |
		0.2% Offset	0.1% Offset	0.01% Offset				
			Low Testing Speed - 0.005 In./Min					
20	148,700	131,600	129,000	117,000	109,100	8	13	19
200	152,700	139,000	137,000	124,000	117,400	8	12	20
300	156,000	144,000	142,000	132,000	127,000	8	10	19
			High Testing Speed - 0.5 In./Min					
20	150,500					9	14	20
200	156,400					8	13	21
300	157,000					7	12	26

(a) Broke on gage mark; (b) Broke outside gage mark.

Notch-Bend Impact Tests Using Micro Sample

| Nominal Hydrogen | Energy Absorbed, in-lb | | Conclusion |
	At 77 F	At -40 F	
20	26	14	Testing was not completed; no embrittlement observed at 300 ppm
200	14	12	
300	22	12	